

THOMAS LUNDQVIST

PRECAMBRIAN GEOLOGY OF
THE LOS-HAMRA REGION
CENTRAL SWEDEN

WITH ONE MAP



STOCKHOLM 1968

SVERIGES GEOLOGISKA UNDERSÖKNING

SER. Ba

ÖVERSIKTSKARTOR MED BESKRIVNINGAR

NR 23

THOMAS LUNDQVIST

PRECAMBRIAN GEOLOGY OF
THE LOS-HAMRA REGION
CENTRAL SWEDEN

WITH ONE MAP
(SCALE 1:100,000)

STOCKHOLM 1968

Editor: Per H. Lundegårdh
C. DAVIDSONS BOKTRYCKERI AB, VÄXJÖ 1968

THIS PAPER IS DEDICATED
TO MY FATHER, THE LATE
PROFESSOR G. LUNDQVIST

CONTENTS

Abstract, sammanfattning	6
1. Introduction	7
2. Earlier work	8
3. Methods of investigation	12
4. Outlines of the Precambrian geology	13
5. Petrographic descriptions	14
5.1. Orogenic complex	14
5.1.1. Supracrustal rocks	14
5.1.1.1. Meta-argillites	14
5.1.1.1.1. Slate, phyllite and mica-schist with subordinate layers of metasiltstone ..	15
5.1.1.1.2. Graphite phyllites	21
5.1.1.1.3. Hornfelses of argillitic composition and related gneisses	22
5.1.1.1.4. Skarn-bearing meta-argillites	24
5.1.1.1.5. Gneisses and migmatites of mainly argillitic origin	31
5.1.1.2. Meta-arenites: quartzite sandstones, quartzites and meta-arkoses	33
5.1.1.3. Crystalline limestone and dolomite	37
5.1.1.4. Skarn and associated magnetite deposits	39
5.1.1.5. Eulysite	46
5.1.1.6. Acid metavolcanics (metarhyolites)	47
5.1.1.7. Basic metavolcanics and metatuffites	51
5.1.2. Primorogenic (synkinematic) intrusions	58
5.1.2.1. Acid primorogenic intrusions	60
5.1.2.2. Intermediate primorogenic intrusions	64
5.1.3. Mainly serorogenic (late-kinematic) intrusions and alterations	66
5.1.3.1. Pegmatite, aplite granite and aplite	66
5.1.3.2. Serorogenic granite	68
5.2. Post-orogenic complex	69
5.2.1. Older post-orogenic granite (Råtan granite)	69
5.2.2. Sub-Jotnian complex	76
5.2.2.1. Dala Volcanics Formation	77
5.2.2.1.1. Basal layers of the Dala volcanics	79
5.2.2.1.2. Dala porphyrites	88
5.2.2.1.3. Breccia, agglomerate, conglomerate and tuff(ite) in the Dala porphyrites ..	92
5.2.2.1.4. Dala porphyries	94
5.2.2.1.5. Breccia and layered tuff(ite) in Dala porphyries	111
5.2.2.2. Dala granites and associated dikes	114
5.2.3. Jotnian complex	120
5.2.3.1. Dala Sandstone Formation	121
5.2.3.2. Dolerite with differentiates	123
5.3. Sulphide occurrences	130
6. Structure and stratigraphy	134
7. Morphology	143
8. Alkali feldspars	145
9. Summary and conclusions	156
Acknowledgements	166
References	168
Tables	175
Index	239

ABSTRACT

The present work deals with the petrology, tectonics and chronology of the Precambrian of the Los-Hamra region in central Sweden. Chemical, mineralogical, textural and structural data are given for the various rock types. The chronological subdivision arrived at is presented in the scheme on p. 156. Two major complexes are distinguished: one orogenic (Svecofennian) and the other post-orogenic. The sub-Jotnian Dala porphyries and granites of the latter complex may be considered to have been formed from anatectic magmas generated during the Svecofennian orogeny. A similar origin is also possible for the (somewhat older) Småland-Värmland granites and Småland porphyries of southern and central Sweden, and for the Rätan granite.

SAMMANFATTNING

Föreliggande arbete behandlar petrologi, tektonik och åldersförhållanden i Los-Hamraområdets prekambrika berggrund i Mellansverige. Kemiska, mineralogiska, textur- och strukturdata ges för de olika bergartstyperna. Den kronologiska indelningen framgår av följande schema:

	(yngst)	
Postorogena komplexen	Jotniska komplexen	{ Diabas med differentiat Dalasandstensformationen
	Subjotniska komplexen	{ Dalagraniter Dalavulkanitformationen
	Rätangranit med differentiat	
<hr/>		
	Serorogena intrusioner och omvandlingar samt veckning	
Orogena komplexen	Intrusion av primorogen magma samt veckning	
	Avsättning av sediment och vulkaniter (Losformationen)	
	(äldst)	

Två huvudkomplexer urskiljs: en orogen (svekofennisk) och en postorogen. De subjotniska Dalaporfyryrerna och Dalagraniterna kan uppfattas som bildade ur anatektiska magmor, alstrade genom den svekofenniska orogenesen. Ett liknande ursprung är också möjligt för de (något äldre) Smålands-Värmlandsgraniterna och Smålands-porfyryrerna i södra och mellersta Sverige, samt för Rätangraniten.

1. INTRODUCTION

The present work describes the Precambrian geology of the westernmost parts of Gävleborg County (Gävleborgs län, see Plate 1). The area is named the Los¹-Hamra region. Its western part, west of the river Voxnan, forms Orsa Finnmark.

The Los-Hamra region attracts considerable petrological interest because of its wide range of rock types. Important information about the Precambrian evolution in central Sweden can be obtained in the area. In the south-south-east and south-east there occur migmatized supracrustal rocks and primorogenic (synkinematic) intrusions belonging to the Svecofennian orogenic belt (see Magnusson et al. 1960 and 1962, Hjelmqvist 1966 and Lundegårdh 1967). In the Los-Hamra region, the migmatites pass into rocks of lower metamorphic grade, in which pre-metamorphic textures and structures are well preserved. The westernmost part of the area is made up of post-orogenic, sub-Jotnian Dala volcanics and granites associated with these. The north is dominated by the southern margin of the vast Rätan granite massif.

Particularly interesting are the abundant low grade metamorphic supracrustal rocks of sedimentary and volcanic origin. They have been considered to represent accumulation in the supposedly long interval between the formation of the migmatites and the extrusion of the sub-Jotnian volcanics (von Eckermann 1936).

The aim of the present investigation has been to study the petrology, tectonics and age relationships of the different Los-Hamra rocks in order to throw some light on the geological evolution. Special emphasis has been laid on the genesis and metamorphism of the supracrustal rocks.

The work is based on field mapping followed by optical, chemical and X-ray investigations of rocks and minerals. Mineralogical, petrological and chemical data are presented at the end of this paper (pp. 175-238).

In the concluding chapter (p. 156 ff.) some general ideas on the Precambrian evolution of central and southern Sweden are presented, these being critically dependent upon the conclusions reached in the Los-Hamra region.

¹ The modern spelling of Los (instead of Loos) has been adopted in the present work.

2. EARLIER WORK

Before the 1880's geological observations in the Los-Hamra region were for the most part limited to the immediate surroundings of small magnetite and sulphide ores. Östberg (1838) gave short accounts of these occurrences, e. g. the cobalt deposit at Los. Some of the most important rock types of the region were also mentioned.

In the 1880's, the first general surveys of the bedrock of this part of Sweden were undertaken, resulting in a 1:500,000 map with accompanying description (Svedmark 1891).

Continued survey of the region led to a paper entitled "Orsa Finmarks geologi" (Svedmark 1895), which was accompanied by a map to the scale of 1:250,000. Mention was there made of porphyry, quartzite and different kinds of granites, including, for example, the "sphene granite". This was the early name for the Rätan granite. The occurrence of dolerite was also noted.

During the years 1889–1894, a general geological investigation was made of the natural resources of Gävleborg County. The work was carried out at the Geological Survey of Sweden and resulted in a map (1:500,000) and description (Blomberg 1895). With regard to the Los-Hamra region, the works of Svedmark mentioned above were included, with some new information added. Descriptions were given of several small occurrences of ore in the area. Among these, the account and sketch-map by Löfstrand of the old cobalt mines at Los are especially noteworthy.

Magnetite and sulphide deposits within the Los-Hamra region were examined in 1908 in connection with an inventory of natural resources along the planned inland railroad (Tegengren 1911). The descriptions include two occurrences of sulphides near Hamra, magnetite in two localities at Björkberg (south of Hamra), and nickeliferous pyrrhotite near Rullbo (15 km WNW of Los). All these deposits were considered to lack economic interest.

With regard to the regional geology, Looström (1916) was of the opinion that two complexes (other than the Dala sandstone and dolerite dikes) existed in the region between the south-western part of the map area of Plate 1 and Orsa in the south. An older, folded and metamorphosed Archean complex, made up of i. a. "hällefrinta" (metarhyolite), quartzite and phyllite, was described to be overlain by gently dipping sheets of "Elfdalgesteine" (= Dala volcanics). Looström considered the older rocks to be deeply eroded before the deposition of the volcanics of the younger complex. The unconformity was placed between the "hällefrinta" at Noppikoski (about 30 km SW of Los) and the Dala volcanics in the west (cf. p. 139).

The occurrence of crystalline limestone on Mansjöberget, about 15 km

south-southeast of Los, was made the subject of a detailed study by von Eckermann (1922). Of particular interest is the abundant formation of skarn minerals at the contact between the limestone and pegmatitic intrusions (see p. 38).

After more than ten years' investigations von Eckermann (1934) published a preliminary report on the petrology of the Los-Hamra area. Two years later the final work appeared, a monograph entitled "The Loos-Hamra Region" accompanied by a 1:100,000 map (von Eckermann 1936). The area covered by von Eckermann's investigation was c. 4,000 sq. km, i. e. larger than that of the present work (cf. Plate 1). However, the name "Los-Hamra region" has been retained for the present study, as this shows all the essential features of its predecessor.

von Eckermann's work of 1936 presented a complicated picture of the geological evolution. A short summary of this is given below.

The oldest ("Old Archaean") rocks of the Los-Hamra region were thought to be strongly migmatized "leptites" of supracrustal origin. They were considered to parallel in age the leptites with intercalations of iron ore and crystalline limestone that occur in the Bergslagen region of central Sweden. The formation of the so-called Mansjö granite was thought to be intimately connected with the migmatization.

On this migmatized complex and separated from it by an unconformity rested the sub-Loos Series. This included cordierite-, andalusite- and anthophyllite-schists, partly feldspar-bearing ("sparagmitic") quartzites and conglomerates.

von Eckermann considered that a period of denudation, represented by talus breccias, separated the sub-Loos from the overlying Lower Loos Series. In the latter were included metamorphosed basic and acid volcanic rocks. The former were altered to amphibolites, and represented original amygdaloidal lavas and agglomerates. The acid metavolcanics were mostly quartz porphyries. Tuffitic metasediments were considered to form from both types of volcanic rocks. The Lower Loos Series was recorded to be intruded by the Risberg granite. A less certain age position was obtained for the Dåasen granite, which was either related to, or older than the Risberg granite. It was, however, considered to be younger than the Lower Loos Series.

The sub-Loos and Lower Loos Series were included in the "Upper Archaean".

After a new period of denudation, an extensive deposition of clay and sand took place, forming the Upper Loos Series. These sediments were little metamorphosed, and original structures and textures well preserved. Slates and metagreywackes formed the middle part of the series, overlain and underlain by quartzites.

The Noppi Series rested on the Upper Loos Series, separated from it by an

unconformity. The following stratigraphy was given for the Noppi Series: (oldest) basal conglomerate – quartz porphyry – tuffitic greywackes – greywackes – quartz-banded slates – quartzites (youngest). The Rätan granite was considered to be connected with the quartz porphyry, somewhat younger than the latter, but older than the Dala porphyries and porphyrites (see below).

The Upper Loos and Noppi Series and the "Hoglandian" basal conglomerate of the Dala Series together formed the sub-Jotnian in the sense of von Eckermann.

The youngest supracrustal rocks of the region formed the Dala Series of Jotnian age. Overlying the basal conglomerate there followed acid volcanics (Dala porphyries) of two generations, more basic volcanics (Dala porphyrites), tuffitic sedimentary rocks and sandstones with conglomerates and shales. Granites of rapakivi type were considered to correspond to the Dala porphyries. Further, three generations of dolerite were mentioned ("Åsby dolerite"). The "Öje dolerite" was the effusive counterpart to one of these. It forms an intercalation in sandstone in Kopparberg County, south-west of the Los-Hamra region (cf. Hjelmqvist 1966). Monzonitic differentiates of dolerite were noted.

As to the tectonics of the region, von Eckermann (1936) arrived at the following conclusions. The oldest, strongly migmatized complex, underwent a regional folding leading to dominating NNW–SSE strike directions. Deformations of the younger series seemed to be more restricted. They were considered to be connected with the different periods of igneous activity. An example of such deformation was constituted by the east-west strikes of the supracrustal rocks in the northern part of the Los-Hamra region. This structure was interpreted to be caused by the intrusion of the Rätan granite.

Tectonic zones, some of which were traceable over several tens of kilometres, were noted by von Eckermann. A common direction of these zones was recorded to be NNW–SSE.

Establishment of the stratigraphic scheme outlined above seems to have been based on the concept that degree of metamorphism could be considered as a function of age. High grade metamorphism was taken to indicate high age. In this way an isolated occurrence of supracrustal rocks, with unknown relations to the surroundings, could be ascribed to one of the above series.

The unconformities between the different series in some localities were marked by horizons of conglomerate or breccia, in others, by small differences in strike. In many cases, however, no unconformity can be observed. An example of this is a north-south section along Västerhocklan (c. 7 km west of Los). From south to north von Eckermann's map here shows sub-Loos schist, Lower Loos basic metatuffite and Upper Loos slate, all conformable with each other. (Cf. also Plate 1 of the present work.)

At the end of the monograph, von Eckermann made tentative correlations between the Los-Hamra rocks and other parts of the Precambrian in Fennoscandia.

von Eckermann's interpretation of the stratigraphic relations in the Los-Hamra region was generally accepted, although some of the terms (sub-Jotnian and Jotnian) have been used in another sense. (See e. g. Magnusson et al. 1960 and Geijer 1963.) A. Högbom (1933), however, criticized the detailed subdivision into different series separated by unconformities. He maintained that most of the conglomerates, which were taken to indicate the unconformities, were of intraformational character. Högbom accepted only two of the occurrences of such rocks as representing important denudation surfaces. One of them was said to be situated about 15 km north of Orsa, outside the region of Plate 1 of the present work. It may be noted that conglomerates in the approximate position of this locality later have been interpreted as so-called Digerberg sediments, forming intercalations in the Dala porphyries and porphyrites (Hjelmqvist 1966). The other occurrence, 3 km south-southeast of Los, is discussed on p. 142.

The occurrence of sulphide and magnetite deposits in the Los-Hamra region has given rise to prospecting activity. At the beginning of the 1930's several small sulphide concentrations around Los were investigated by the Bolidens Gruv AB. (See Grip 1961: p. 70 and von Eckermann 1936: p. 201.) The work was continued at the end of the 1950's and the beginning of the 1960's. During this period, prospecting for iron ore was also carried out by the Korsnäs AB and Ställbergsbolagen AB. Results from all these investigations have been made available to the author through the courtesy of the companies mentioned.

Welin (1966a) has studied the mineralogical composition of specimens from the old cobalt mines at Los. This work formed part of investigations of Swedish uranium deposits.

In 1955 the preparation of a new map of the solid rocks of Gävleborg County began at the Geological Survey of Sweden. This work was carried out under the direction of P. H. Lundegårdh, who has recently (1967) published the map with a description. In connection with this mapping a revision was also planned for the Los-Hamra region. The present author was charged with this work, which started in 1958. However, difficulties soon arose when it was found impossible to fit the new observations into the existing map of the region (von Eckermann 1936). It was therefore decided to remap the Los-Hamra area. This was particularly necessary, as an extensive network of roads had provided many new outcrops since the time of the older mapping.

3. METHODS OF INVESTIGATION

During the field work the following have been used for plotting the geological data: aerial photos (scale 1:20,000), photographic maps (scale 1:10,000) and topographical maps (scale 1:50,000). Unfortunately, only old map material [1:50,000 draft map-sheets of the official (Generalstab) map of Sweden] has been available for the topographical base of the petrological map (Plate 1). Modern topographical maps of this scale cover only the easternmost parts. The old maps have been corrected in several instances and all new roads up to 1965 have been added.

The map, Plate 1, is mainly based on studies of the outcrops. In some regions (e.g. c. 5 km NNW of Los), important information has been obtained from magnetic maps kindly put at the author's disposal by different companies (see acknowledgements). Unfortunately, no aeromagnetic measurements covering the whole Los-Hamra region have been carried out. It is at present not possible to adopt geophysical methods for non-economic projects at the Geological Survey of Sweden. Valuable information would in this way probably have been obtained e. g. on the extension of the dolerite dikes of the western part of the Los-Hamra region.

In areas of poor exposure the study of large (local) moraine boulders has given an indication of the dominant bedrock. This method has been adopted especially where contacts between different units run approximately at right angles to the direction of ice movement, i. e. NE-SW to ENE-WSW (cf. G. Lundqvist 1963).

During the microscopic work, the following manuals have been used: Heinrich (1956), Tröger (1959), Winchell (1961) and Schouten (1962).

Microscopic determinations of plagioclase compositions, axial angles etc. have been carried out on a Leitz' 4-axis universal stage. Most of the plagioclases have been determined according to the zone method. In some cases, however, the position of the indicatrix in relation to cleavage or twin composition planes has been measured. The accuracy is at best $\pm 1-2\%$ An, but may be lowered by zoning, alteration etc.

Refractive indices and other optical data for different minerals are collected in Tables 3-6, pp. 230-232. The refractive indices have been determined for sodium light with the immersion method and a Leitz' micro-refractometer according to Jelley. This method allows an accuracy of about $\pm 0.002-0.003$.

Volumetric analyses (Table 1c, p. 205, and p. 32) have been made with a Swift's automatic point counter. In the petrographic descriptions, the following nomenclature has been adopted to give, in a semi-quantitative way, the estimated volume frequency of minerals:

- > 25 % : main minerals
- 5-25 % : essential minerals
- 1- 5 % : subordinate minerals
- < 1 % : accessories.

The methods and accuracy of optical and X-ray measurements on potash feldspars (Tables 7 and 8, pp. 233-238) are discussed in connection with the presented data (p. 145 ff.).

Unit cell edges of garnets (Table 5, p. 232) have been calculated from X-ray diffraction photographs prepared with a Debye-Scherrer powder camera (diam. = 114.7 mm) and $\text{CuK}\alpha$ radiation. KCl was used as internal standard. The accuracy in these determinations is estimated at $\pm 0.02-0.03 \text{ \AA}$.

Chemical analyses of rocks (sample weights 1-2 kg) are presented in Table 1a, p. 175. If not otherwise stated, they have been carried out as routine team work at the laboratories of the Geological Survey of Sweden. The estimated accuracies, valid for most of the analyses of Table 1a, are given in Table 1d, p. 223. In some analyses, however, the accuracy is higher than stated in this table (nos. 65, 68, 69, 74 and 85). Table 1d is also valid for the feldspar analyses in Table 7.

Petrochemical calculations of the rock analyses (Table 1b, p. 190) have followed Burri (1959).

For the nomenclature and the calculations of suite index and suite type of volcanics and metavolcanics (Table 2, p. 228), see Rittmann (1952 and 1962a).

On the petrological map, Plate 1, a coordinate system has been drawn. The positions of small units (outcrops etc.) in the present paper are given in terms of these coordinates, starting with the horizontal scale. Thus, 150/240 means 150 mm from the western limit of the map and 240 mm from the southern one. Larger geographic units (lakes etc.) can be indicated with a second system, drawn around Plate 1. The positions are then denoted by letters along the x-axis and by figures along the y-axis (e. g. B5, G6).

4. OUTLINES OF THE PRECAMBRIAN GEOLOGY

This re-investigation of the Los-Hamra region has given evidence of two major Precambrian complexes. The older, which is named the orogenic complex, is made up of different supracrustal rocks (comprising the Los Formation) and primorogenic intrusions. It is affected by strong folding, recrystallization and partial migmatization. However, in large areas (the central parts of the region) the grade of metamorphism is lower, and primary structures and textures well preserved.

The rocks of the younger, post-orogenic complex are mainly restricted to the western parts of the region. They are dominated by rhyolitic volcanics (Dala porphyries) with subordinate more basic volcanics (Dala porphyrites), and granites comagmatic with the porphyries. The volcanics (the Dala Volcanics Formation) form sheets covering the orogenic complex. Reddish sandstones with conglomerates (the Dala Sandstone Formation) also belong to the post-orogenic complex, along with the youngest rocks of the region, the dolerites. The latter form dikes occurring mostly in post-orogenic rocks but also cutting the orogenic complex.

The Rätan granite in the northern part of the Los-Hamra region occupies a somewhat uncertain position with respect to the above two complexes. However, most of the observations point to a post-orogenic age.

There follow below petrographical descriptions of the different rock types of the region. They comprise field data, general structural and textural features, and mineralogical and chemical compositions.

5. PETROGRAPHIC DESCRIPTIONS

5.1. OROGENIC COMPLEX

5.1.1. SUPRACRUSTAL ROCKS

5.1.1.1. META-ARGILLITES

Meta-argillites with subordinate layers of metasiltstone are the dominating supracrustal rocks of the orogenic complex. They show a wide range of metamorphism. Thus, there are found transitions from slates via phyllites and mica-schists to gneisses, the latter being largely migmatized. In the north, in the contact with the Rätan granite, argillitic hornfelses occur.

In the areas of lower metamorphic grade, primary features are well preserved and the argillitic character is evident. However, in the strongly migmatized regions, it is often difficult to establish the nature of the original rocks. The conclusion that argillites form the majority of the migmatites is based on the occurrence of better preserved rocks of this character within these regions. This is particularly the case in the region south of Hamra (F1-F3 and E3-E4) and between Dåasen (I7) and Acksjön (J3). However, it cannot be excluded that sediments of e. g. greywacke character are among the supracrustal rocks transformed to migmatites.

Graphite phyllite occurs occasionally in the meta-argillites. Skarn-bearing meta-argillites are also present and represent an original admixture of carbonate(s) and/or iron silicate(s). In the latter case transitions to metamorphosed sedimentary iron ores are found.

Descriptions of the different kinds of meta-argillite occurring in the Los-Hamra region are given below.

5.1.1.1.1. SLATE, PHYLLITE AND MICA-SCHIST WITH SUBORDINATE LAYERS OF METASILTSTONE

The lowest degree of metamorphism in the meta-argillites is represented by slates with a regular cleavage. Such rocks occur in a region from Ryggskog (G7) towards the Västerhocklan brook in the west and north-west. They are also found in the vicinity of Romberg (H8–I8).

Not far west of Ryggskog (c. 340/312) small quarries have been opened in the slate for the production of whetstones. On the waste-dumps, the slate here sometimes shows a weakly developed bedding with layers of a thickness of some millimetres to centimetres. The slaty cleavage can be seen to cut the bedding at different angles. It has, however, not been possible to measure the bedding in solid outcrop, the impression gained being that it varies in strike and dip, whereas the slaty cleavage is approximately constant in orientation.

The slates have a microcrystalline, blastopelitic texture, the grain size being around or somewhat over 0.01 mm. Main and essential minerals are quartz, chlorite and sericite (muscovite). Small amounts of sodic plagioclase occur. Further, the slates contain scattered grains (size ≤ 0.1 mm) of brownish green biotite. They are therefore just above the biotite isograd of metamorphism. Similar grains (with porphyroblastic character) are also formed by chlorite. As subordinate or accessory minerals occur oxides, and, as a characteristic constituent, small (< 0.05 mm) needles of tourmaline (cf. below, page 21). Other accessories are apatite, zircon, leucoxene, and sometimes also epidote.

The slates grade into phyllites, which are somewhat coarser and less regularly cleaved than the slates. The phyllites frequently contain thin fissures filled with quartz. They are mainly found along Voxnan between Rullbo (237/330) and Storlugnet (275/273), south of Tandsjöborg (D5) and in the Noppikoski–Tallsjön region (E1–D2). In the last-mentioned occurrence, they are interbedded with skarn-bearing quartzites. Ripple-marks are found in the phyllites near Noppikoski (at 210/035).

Mineralogically, the phyllites differ from the above described slates in that biotite is often quantitatively more important than chlorite.

Further recrystallization and decrease in cleavage perfection characterize the appearance of the mica-schists. The first step in the transition from phyllite to mica-schist is represented by a meta-argillite at Västerhocklan (309/297, see Table 1a–c: no. 5). Millimetre-sized, poikilitic, randomly oriented porphyroblasts of chlorite have here formed in a lepidoblastic quartz-muscovite-biotite-chlorite matrix (Fig. 1). The chlorite shows strongly anomalous interference colours. The optical data are given in Table 6: no. 1. According to Tröger (1959) the chlorite is a diabantite.



Fig. 1. Chlorite porphyroblasts (dark) in a phyllite transitional to mica-schist. 2 nic., 31 x. Västerhocklan (309/297). Photo I. Signorelli.

The alteration to mica-schists has generally been accompanied by a formation of cordierite and/or andalusite. North of Laxtjärn (around 309/289) typical cordierite-andalusite mica-schists outcrop. They occur here in an aureole around the primorogenic granite in the south, and represent the highest grade of a metamorphism, which has probably been caused by the intrusion of this granite (cf. p. 138).

Mica-schists occur in several other localities, e. g. east of Tenskog (I4). A mineralogically similar rock to that described above is also found near the Rätan granite, with which it has a clear genetical connection. Here the schistosity is weak or absent (decussate texture). The rock has been grouped together with the normal mica-schists and is found close to the granite contact at Svartån (c. 243/298), and to the west of Krovvattnet (241/361). The most important area where such rocks can be found is, however, between Hästberget (c. 340/390) and the southern end of Kolarsjön (280/370). The mica-schists here form structural and mineralogical transitions between the slates and phyllites in the south and the hornfelses in the north. Their metamorphic grade is that of the hornblende-hornfels facies of contact metamorphism (Winkler 1967).



Fig. 2. Andalusite-cordierite mica-schist, Västerhocklan (308/288). (Length of penknife 9 cm.) Photo Th. Lundqvist.

The normal mica-schists are grey in colour and fine-grained. The texture is lepidoblastic. A small-scale folding (amplitude < 1 cm) of the *s* surfaces can sometimes be seen. Main and essential minerals are brown biotite, muscovite and quartz. Poikilitic porphyroblasts (≤ 1 cm) of cordierite and/or andalusite are characteristic constituents of the mica-schists, and give the rock a spotty appearance on weathered surface (Fig. 2). Both these minerals show a varying degree of alteration to sericite (pinite). In the case of an alternation of argillitic and silty (quartz-feldspar-rich) layers, cordierite and andalusite are concentrated in the former.

At Västerhocklan (c. 309/289), there occurs in the lepidoblastic matrix of the mica-schist a second generation of mica (mainly biotite), which lacks a preferred orientation. This mica has probably been formed (together with andalusite and cordierite and the above mentioned chlorite porphyroblasts) by the influence of the primorogenic granite in the south (cf. p. 138).

Subordinate constituents include chlorite (alteration of biotite), sometimes also plagioclase (albite or oligoclase). Accessories are albite, opaque minerals (magnetite etc.), tourmaline, zircon, epidote and apatite. In mica-schists devoid of cordierite and andalusite, scattered microcline grains may occur.



Fig. 3. Alternating layers of quartzite and mica-schist with cordierite porphyroblasts. 2 nic., 5 x. Kolarsjöbäcken (281/367). Photo I. Signorelli.

Sillimanite (strongly sericitized) has been found in one locality (408/158). Anthophyllite is rare, but occurs in a cordierite mica-schist north of Dåsberget (416/333). Optical determination indicates an *mg* value of 0.7 (Table 3: no. 1).

A special variety of cordierite-andalusite mica-schist occurs in the region south-west of Tenskog in an old excavation for iron ore at 379/147 (the "Lakisberget mine"). It contains bands of magnetite, which can be followed on the magnetic anomaly map to Kvarnberg (401/131, see below, p. 33), where a magnetite-bearing anthophyllite-cordierite gneiss occurs. Similar rocks are encountered east of Tenskog in a position which makes it possible to interpret them as metasomatically altered metarhyolite (pp. 51 and 142). The genesis of the cordierite- and anthophyllite-bearing rocks at 379/147 and 401/131 is obscure, especially as the magnetite concentrations in them are of a type not otherwise encountered in the region. They are, however, tentatively placed among the meta-argillites, although an interpretation as metasomatic derivatives of other supracrustal rocks is possible.

The meta-argillite mentioned above, occurring in connection with the Råtan granite, has the same mineralogical composition as the normal mica-schists.

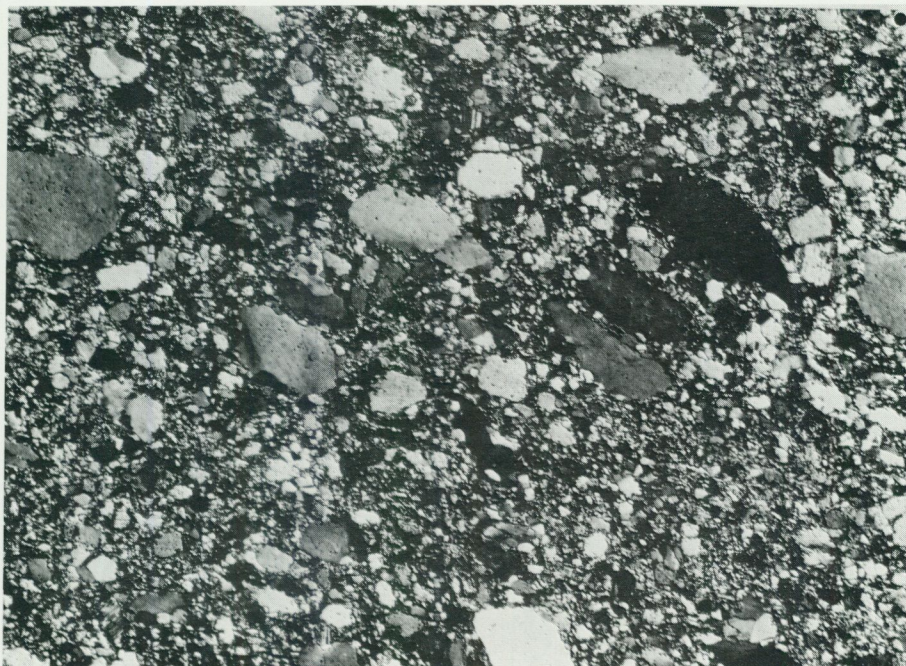


Fig. 4. Metasilstone, consisting of phenoclasts of quartz (and albite) in a matrix of quartz, sodic plagioclase, chlorite and sericite. 2 nic., 47 x. Västerhocklan (294/341).
Photo I. Signorelli.

Main and essential minerals are brown biotite, muscovite and quartz, forming a decussate or weakly lepidoblastic texture. Cordierite and/or andalusite in notably poikilitic porphyroblasts occur in varying amounts (Fig. 3). They may attain a size of a few millimetres, but are on the average smaller than in the normal mica-schists. The cores of the andalusite porphyroblasts occasionally show a pleochroism from pink to colourless. In varying but usually subordinate amounts occur plagioclase (oligoclase to albite, seldom andesine) and chlorite. Accessories are opaque minerals, zircon, apatite, tourmaline and sometimes also sulphides. In the immediate vicinity of the hornfels described below (p. 22), microcline of film perthite type (Andersen 1928) may form a subordinate constituent (see Table 1: no. 7).

As mentioned above, the meta-argillites contain subordinate layers of a more quartz-feldspar-rich composition, indicating a siltstone origin. In these, quartz and plagioclase (\leq c. An_{30} , usually albite) form main minerals. As essential or subordinate constituents occur sericite, chlorite (mainly in slate and phyllite regions) or biotite (in phyllite and mica-schist regions). Accessories are opaque minerals, zircon, tourmaline and apatite.

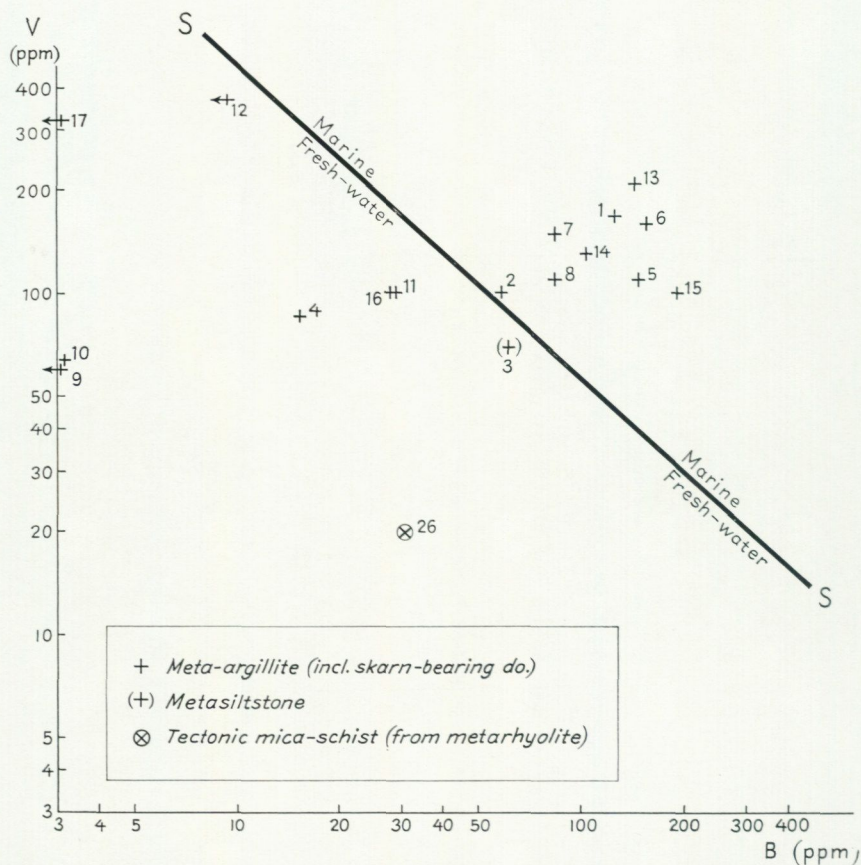


Fig. 5. Logarithmic plot of vanadium against boron for metasediments (and one tectonic mica-schist) from the Los-Hamra region. Numbers correspond to those of Table 1. S - S is the line of separation between marine and fresh-water argillites (Potter et al. 1963). A cross with arrow indicates that the point is situated between the cross and zero in the direction of the arrow (maximum value).

Especially where the metasiltstones form layers in slate, the clastic texture is well preserved. Thus, in some samples there occur generally angular phenoclasts (size 0.2–0.3 mm) of quartz and plagioclase in a fine-grained (c. 0.01 mm) matrix of quartz, plagioclase, sericite and chlorite (Fig. 4). On Håstberget (335/390) there have also been found c. 0.1–0.3 mm diameter fragments of a keratophytic rock mainly consisting of lath-shaped albite crystals.

In connection with the transition from slate via phyllite to mica-schist, the quartz-feldspar-rich layers have usually been recrystallized to a granoblastic texture.

Chemical and modal analyses of the above types of meta-argillite are given in Table 1a-c: nos. 1-2 and 4-8. No. 3 represents a metasilstone. The argillitic character of the first-mentioned rocks is expressed by high Niggli T and t values (Al excess over alkali and alkali + calcium, respectively), and high k values. Relatively high boron contents (caused by the presence of tourmaline, see above) have also been noted. They indicate, together with the values for vanadium, a marine environment of deposition for the meta-argillites. Potter et al. (1963) have developed a method to distinguish between marine and fresh-water argillites from their contents of boron and vanadium. The discriminating line between the two types of argillites has been plotted in Fig. 5, in which also the positions of meta-argillites (together with some other rocks) have been marked. Samples 1-2 and 5-8 as well as two skarn-bearing meta-argillites (nos. 13 and 14) and one argillite gneiss (no. 15) fall in the field of marine deposition. The phyllite no. 4, having a relatively low t value, falls outside the marine field in the same way as the metasilstone no. 3 and a skarn-bearing meta-argillite (no. 12).

From Fig. 5 it is also evident that the alteration to hornfelses and gneisses generally reduces the boron content, whereas vanadium is not changed much. This is consistent with the observations of tourmaline-bearing granitic dikes and schlieren in these meta-argillites (pp. 22 and 69).

For comparison, the position of a mica-schist, interpreted as a strongly tectonized metarhyolite (no. 26 of Table 1), has also been plotted in Fig. 5. It differs from the meta-argillites etc. in being low in both boron and vanadium.

Other trace elements of interest in the analyses 1-2 and 4-8 of Table 1a are barium and rubidium. BaO ranges between 700 and 1,000 ppm and Rb₂O between 160 and 270 ppm. The BaO analyses indicate somewhat higher values than reported by Sahama for Al-rich schists in Finnish Lapland (see Rankama and Sahama 1952: p. 482). For all analysed metasediments in the Los-Hamra region, barium and rubidium are roughly proportional to potassium, in agreement with the diadochy relations between these elements (see e. g. Rankama and Sahama 1952).

5.1.1.1.2. GRAPHITE PHYLLITES

Black, graphite-bearing, generally phyllitic meta-argillites occur in some localities as intercalations in normal meta-argillite or skarn. They have been found at Risåsen (238/361), where they are strongly brecciated in a matrix of pyrrhotite (p. 133). The latter also contains fragments of quartzite (p. 36). About 1 km south-east of the locality mentioned, graphite phyllites, crystalline limestone and quartzite form intercalations in a grunerite-magnetite ore

(p. 40). Drillings have here revealed graphite phyllite layers of thicknesses between a few dm and about 10 m. On Storkullen (263/362) graphite phyllites occur associated with skarn-bearing meta-argillite (p. 28) and metaspilite. Finally, graphite-bearing and quartzitic layers in phyllite are exposed in two small excavations for pyrrhotite south-east of Rullbo, at 242/311 and 241/312 (see p. 133). In the vicinity occur amphibolitic metavolcanics.

The graphite phyllites are fine-grained, sometimes microcrystalline, and have a blastopelitic to lepidoblastic texture. According to chemical analyses the graphite content generally does not exceed 10 weight percent. In addition to graphite the following minerals occur in varying combinations and proportions: biotite, quartz, sodic plagioclase, chlorite and muscovite (sericite). Accessories are tourmaline and zircon, and sometimes also common hornblende and cummingtonite. The latter mineral forms aggregates of radiating crystals at 242/311. Optical determination indicates an *mg* value near 0.8 (Table 3: no. 2). According to Tröger (1959) there should, however, be a gap in composition between $mg = 0.60$ and 0.85 in the cummingtonite series.

The graphite phyllites contain varying amounts of pyrrhotite as narrow veinlets or scattered grains. However, this mineral sometimes forms compact masses, containing fragments of the black phyllites. This is the case in the above mentioned small excavations at Risåsen and south-east of Rullbo, which will be treated below (p. 133). From the observations made it seems most likely that the pyrrhotite is genetically connected with the deposition of the graphite-bearing phyllites. The breccia phenomena should then be caused by metamorphic processes.

5.1.1.1.3. HORNFELSES OF ARGILLITIC COMPOSITION AND RELATED GNEISSES

Argillites altered to hornfels are found in a zone of at least 2 km width near the Råtan granite north of Los. From their mode of occurrence it can be concluded that they have been formed by contact metamorphism caused by the intrusion of the Råtan granite magma (see p. 74). Further, the hornfels contain scattered dikes and schlieren, which have emanated from the Råtan granite.

The typical hornfels are grey in colour. Grain sizes are around 0.1 mm but coarser (c. 0.5 mm) bands and schlieren occur. The texture is granoblastic and the schistosity weak or absent. In the latter case the biotite of the rock shows no preferred orientation. Main and essential minerals are quartz, microcline (film perthite, Andersen 1928), and dark brown biotite. Plagioclase (mostly oligoclase) and cordierite are essential or accessory constituents. The proportions of the above minerals vary greatly, due to a layering which is often visible in thin section. Thus, e. g., there may be found bands consisting almost exclusively of microcline.

Accessories are zircon, tourmaline, apatite, opaque minerals (often magnetite) and muscovite. The latter two may also form subordinate minerals.

In a sample from Össjön (305/396) poikiloblastic andalusite together with accessory sillimanite has been found in a hornfels containing cordierite and microcline.

Anthophyllite has been found in one locality, viz. Brännberget (358/411), where it forms aggregates of radiating needles in a quartz-poor meta-argillite with dominating cordierite and biotite.

In texturally transitional types between the hornfelses and the mica-schists (p. 18) on Brännberget (c. 358/411), the cordierite forms porphyroblasts. Muscovite is here found in subordinate amounts, although cordierite and microcline apparently form a stable association.

The parageneses described above together with the alteration of basic metavolcanics to orthopyroxene-plagioclase rocks (p. 57) show that the potash feldspar-cordierite hornfels facies of contact metamorphism has been attained (Winkler 1967). This in turn indicates temperatures within the "magmatic" range for the Rätan granite (see p. 74).

In some localities skarn schlieren (cf. p. 30) have been observed in the hornfelses. They consist of epidote, actinolite and diopside, and indicate an original content of calcium(-magnesium)-carbonate. As epidote is not stable in the potash feldspar-cordierite hornfels facies (cf. Winkler 1967), its occurrence probably depends either on an earlier metamorphic condition, or is due to retrograde metamorphism, of which there is evidence in the basic metavolcanics (p. 58).

Similar rocks to those described above have been reported by Magnusson (1925) from the Persberg region of central Sweden. They are there found close to the post-orogenic Filipstad granite. The appearance of cordierite together with microcline was interpreted by Magnusson to indicate a deficiency in water. This question will be discussed further on p. 74.

Chemical and modal analyses of hornfelses are presented in Table 1 a-c: nos. 9 and 10. These two rocks have a less pronounced argillitic character (higher SiO_2 and lower t) than the typical meta-argillites (e. g. no. 1). Boron contents are low (Fig. 5, p. 20), which may in part be a consequence of the initial composition. However, from field observations it is evident that boron has been driven off, as black tourmaline is found in granitic dikes and schlieren in the hornfelses.

In some localities in the Johannisberg-Pajkölen region (H9-H10) there occur, between the above described hornfelses and the Rätan granite, meta-argillites which have been transformed to greyish black or grey gneisses. They are treated here because of the field connection with the hornfelses. The gneisses differ from the latter in having coarser grain sizes, a well-developed schistosity and by generally lacking microcline. Their origin seems to be con-

nected with local shearing in the granite contact, permitting retrograde alteration.

The argillite gneisses in the above region have very variable grain sizes (c. 0.05–1 mm). The coarser grains are found in irregular bands and schlieren, in which quartz plays a dominating role.

Main and essential minerals are quartz, dark brown biotite and cordierite. Plagioclase (An-rich oligoclase) in a more or less sericitized state occurs in varying but generally essential amounts. Muscovite (sericite, pinite) forms an alteration product of plagioclase and cordierite. Accessories are opaque minerals, zircon, apatite, tourmaline, chlorite, leucoxene, and sometimes also microcline.

Somewhat west of the hornfels region (at Kolarsjön, 276/371) is a local occurrence of argillite gneiss (not marked on Plate 1) of the above type. In addition to quartz, biotite, cordierite and sericite, the gneiss also contains poikiloblasts of almandite (Table 5: no. 1). The presence of the latter points to a higher pressure of formation than for the hornfelses (Winkler 1967).

In Table 1: no. 11 chemical and modal analyses of an argillite gneiss of the above described type are given.

5.1.1.1.4. SKARN-BEARING META-ARGILLITES

Skarn-bearing meta-argillites and layers and schlieren of skarn¹ in normal meta-argillite occur mainly in three regions. These are between Lillskog (K6) and the north-western slope of Dåasberget (H7), north of Öv. Hamravallen (E6), and between Kolarsjön and Risåsen (F8). The anthophyllite gneiss on Fetingsklacken (J5) possibly also belongs to this group. It is treated below (p. 32).

At Lillskog (K6) the skarn-bearing meta-argillites are interlayered with quartzites and conglomerates, themselves often also skarn-bearing (p. 34). They are transitional to normal meta-argillite and metasiltstone, which occur subordinately. At c. 502/234, large moraine boulders of similar rocks can be studied. Numerous such boulders are also found between the northern end of Dåasen (429/326) and the northern slope of Dåasberget (392/326). (The direction of ice movement in the Los-Hamra region has been from the north-west or north-northwest, cf. G. Lundqvist 1963.)

Cores from diamond drillings in the skarn iron ore horizon north of Dåasberget (H7-I7) show an interstratification of skarn-bearing meta-argillite, tremolite-phlogopite skarn, iron ore and amphibolitic metavolcanics (p. 41).

¹ The term skarn in this paper is used for lithologies dominated by silicates (mainly pyroxenes and amphiboles) of calcium, magnesium and iron. These have generally been formed through reactions with carbonates; sometimes also from iron silicate(s).

The supracrustal rocks of east-west strike north of Dåasberget and those around Lillskog are evidently closely related. The two occurrences of similar rocks have been separated by dextral movement in a north-northwest-striking fault (see Plate 1 and p. 141).

The skarn-bearing meta-argillites in the Dåasberget-Lillskog region vary in colour from grey (quartz + plagioclase) or reddish grey (with microcline) to greyish green (with epidote) and dark green (with hornblende). They are generally fine-grained, sometimes microcrystalline, but medium- to coarse-grained bands and schlieren of skarn minerals, quartz and microcline also exist. In these, crystals of hematite of up to 1 cm diameter may be found (e. g. at 429/326).

The texture of the actual skarn-bearing meta-argillites is xeno- to hypidioblastic, in hornblende-rich layers it is nematoblastic or decussate. Mineralogically, the rocks display great variations. They are characterized by the skarn minerals epidote, common hornblende, actinolite and diopside¹ in varying combinations and proportions. A sample from 435/333 contains diopside with an *mg* value of 0.7 (Table 4: no. 1). In some cases also garnet forms an important constituent. In a moraine boulder from the region south of Lillskog the mineral occurs in 1 cm thick bands. The composition is here andraditic (Table 5: no. 2).

In addition to the above minerals the skarn-bearing meta-argillites contain quartz, microcline and plagioclase (oligoclase or albite, often strongly sericitized) as important constituents. The different layers in the rocks show variations in quartz, feldspar and skarn contents between 0 and > 25 %.

Biotite and chlorite are usually subordinate or accessory minerals, but may be concentrated in certain layers. Biotite-rich rocks contain little or no skarn and are transitional to normal meta-argillites.

Other subordinate or accessory minerals are sphene (with leucoxene), magnetite, hematite (see above), sericite, zircon, apatite, orthite and tourmaline.

The chemical composition of a layered skarn-bearing meta-argillite (average of 1 m² surface) is given in Table 1a: no. 14. A similar distribution of elements would be obtained if CaO and some CaMgO are added to a normal meta-argillite. (CO₂ is, of course, expelled in the skarn-forming reactions). The layering of this rock probably represents an original bedding, although a high mobility of the elements during metamorphism must be assumed because of the concentration of skarn in schlieren and along fissures (cf. also below, p. 45).

The second occurrence of skarn-bearing meta-argillite in the Los-Hamra region is situated north of Öv. Hamravallen (E6). Only very few outcrops

¹ This name is here and below used to embrace all members of the diopside-hedenbergite series.

have been found here, and the mapping is largely founded on observations of moraine boulders. Studies of such boulders along the road east to south-east of Ahkiolampi (E6-F6) have shown that skarn-bearing meta-argillites here have passed over into normal, quartzite-banded meta-argillites. Only very subordinate skarn-bearing rocks seem to exist in this area.

The skarn-bearing meta-argillites of the region north of Öv. Hamravallen are similar to those described above at Lillskog and Dåasberget. They contain intercalations of iron ore (p. 45) and quartzite. The colour is grey with various shades of pink or green. The rocks are fine-grained, and sometimes microcrystalline. Xenoblastic textures prevail in quartz-feldspar-rich layers, whereas hornblende-rich and biotite-rich layers usually have a nematoblastic and lepidoblastic texture, respectively.

In all samples examined of skarn-bearing meta-argillites from this region, plagioclase (albite or oligoclase) and/or microcline form important constituents of the rock. Common hornblende, biotite, epidote, quartz, diopside, tremolite and garnet show a wide range of modal variation. An optical determination of almost pure tremolite (also identified by X-ray powder analysis) is given in Table 3: no. 3. The sample is from a small excavation for iron ore at 236/256. A determination of a dark brown, andraditic garnet has also been carried out (Table 5: no. 3).

Chlorite and muscovite may occur in small amounts. Sphene is found as a subordinate mineral; zircon, apatite and opaque minerals as accessories.

The above two occurrences of skarn-bearing meta-argillites (the Lillskog-Dåasberget and Öv. Hamravallen regions) are interpreted as representing original argillites with an admixture of calcium- and/or calcium-magnesium-carbonate, the latter during metamorphism having reacted to give the skarn. For a geologist who has worked in the ore-bearing region of Bergslagen in central Sweden, it would perhaps be natural to regard the above rocks as skarn-bearing acid metavolcanics (leptites and hälleflintas, cf. Geijer and Magnusson 1944: p. 20). The resemblance to the leptites is strengthened by the circumstance that microcline (instead of biotite) is the potassium-bearing mineral. This is a consequence of the skarn reactions, which have consumed iron and magnesium, whereas potassium is not incorporated but enters the feldspar.

An interpretation of these Los-Hamra rocks as skarn-bearing acid metavolcanics has been considered unlikely for the following reasons. As mentioned above, there are transitions to skarn-poor and skarn-free meta-argillites of normal type. Further, textures are seldom found, which may be interpreted as indicating a volcanic origin. A sample from the region north-west of Dåasberget (393/327), however, shows tabular albite crystals (0.1–0.5 mm) in a finer grained matrix of quartz, albite, microcline and hornblende. This might be regarded as a relict crystal tuff texture, but to the

present author it seems more likely that the rock is an original carbonate-bearing siltstone (cf. above, p. 19). Nevertheless, a volcanic origin cannot be excluded.

In this connection it is useful to consider the possibility of the occurrence of skarn-bearing meta-argillites similar to those of the Los-Hamra region in the leptite formation of central Sweden. Such an interpretation may e. g. be valid for some skarn-bearing "hällflintas" on the island of Utö in the archipelago of Stockholm (cf. Holmquist 1910). Pilava-Podgurski's (1956) investigation of diamond drill cores from the iron ores of Utö pointed in this direction. He found no proof of volcanic products among the rocks surrounding the ores. Further, Gavelin (Gavelin and Lundegårdh 1960) has interpreted the supracrustal rocks on the south-eastern shore of northern Utö as metamorphosed sediments of greywacke type. Metasediments thus seem to play an important role on Utö.

In some of the rocks interpreted as metamorphosed marls (argillites with an admixture of carbonate), plagioclase forms the only feldspar. As biotite and muscovite are also lacking, the rocks in question must show a low k value, which is not a feature of normal argillites. In some cases this may be explained as due to an originally low clay mineral content (metasiltstone). In others, however, which have a lower SiO_2 content than the latter rock type, metasomatic processes may have affected the composition. An interesting possibility of metamorphic differentiation of a layered marly sediment has been proposed by Orville (1963): it is reasonable to assume that during moderate to high grade metamorphism the calcium content of carbonate is incorporated in plagioclase and that at least part of the potassium forms microcline. Laboratory experiments indicate that a metamorphosed sedimentary series composed in this way of alternating anorthite- and microcline-rich layers in equilibrium with an alkali-bearing gas-phase will undergo metamorphic differentiation. There will be a tendency for anorthite-rich layers to be depleted in microcline but enriched in albite, and vice-versa for the anorthite-poor layers. Similar processes may have operated in the Los-Hamra rocks to give the plagioclase-rich compositions mentioned above. An alternative possibility would be to assume that volcanic material of keratophyric composition has been included during sedimentation. The general absence of keratophyres (cf. p. 50 below) does not favour this interpretation.

In the third region with skarn-bearing meta-argillites, between Kolarsjön and Risåsen (F8), there occur rocks of a character different from those described above. In addition to calcium-rich minerals, a magnesium-iron skarn almost devoid of calcium is characteristic of these rocks. The latter type of skarn consists of minerals belonging to the cummingtonite-grunerite and anthophyllite series. The calcium-rich skarn is also found as subordinate bands and schlieren in the adjoining normal meta-argillites.

The skarn-bearing meta-argillites in the Kolarsjön-Risåsen region grade to the west-southwest into a grunerite skarn with magnetite ore at Risåsen (E8-F8). To the south occur normal phyllites and mica-schists. North of the skarn-bearing meta-argillites is a region with spilitic metavolcanics (cf. map, Plate 1).

The skarn-bearing meta-argillites have colours between grey, green and black. They are often bedded with layer thicknesses between one millimetre and some decimetres. Usually they are fine-grained, in part microcrystalline, the notable exception being the calcium-rich skarn, which is often coarser. Amphibole-rich layers generally show decussate textures even if nematoblastic features occur. The calcium-rich skarn is a hypidioblastic intergrowth of diopside, common hornblende etc. Probably the crystallization in these rocks at least in part occurred under the influence of the Råtan granite magma.

The bedding is mainly formed by an alternation of calcium-rich and calcium-poor layers. The latter consist of two types. One is rich in quartz with subordinate amphiboles and biotite. Because of the microcrystalline texture it is interpreted as a somewhat recrystallized precipitate of silica. The layers are often disrupted. In the second type, cummingtonite and greenish brown or brown biotite dominate. The cummingtonites have been optically determined in five samples (Table 3: nos. 4-8). The *mg* values for these range between 0.3 and 0.5.

In a sample from 271/365, layers rich in cummingtonite alternate with those dominated by anthophyllite. The latter is weakly pleochroic in green colours. It has an *mg* value of only 0.3 (Table 3: no. 9), whereas the cummingtonite of the same sample (Table 3: no. 6) has *mg* = 0.4.

In some layers cordierite occurs. Small grain sizes make optical identification difficult. Its presence has been verified by X-ray powder analysis. High alumina contents (Table 1a: no. 13) also point to the presence of cordierite.

In the cummingtonite-biotite-rich layers quartz is found as a subordinate or essential mineral. Plagioclase (oligoclase to andesine) is subordinate or accessory but seems to be lacking in some samples. Distinguishing between plagioclase and cordierite is, however, difficult due to the small grain sizes.

Accessories are sphene, apatite and chlorite. Pyrrhotite is a subordinate constituent at 275/370. It occurs here in a quartz-cordierite-cummingtonite-almandite rock. Data for the latter mineral are given in Table 5: no. 4. Otherwise garnet is rare in the calcium-poor layers. It is somewhat commoner in the calcium-rich skarn (see below, p. 30).

Magnetite is usually a subordinate or accessory constituent. In some localities, however, the mineral is concentrated in certain layers. At 276/371 there occurs a magnetite quartzite (Fig. 6) with subordinate cummingtonite, diopside and common hornblende (cf. Table 3: no. 7 and Table 4: no. 3). This rock is interpreted as a recrystallized jaspilite (skarn-bearing). Better

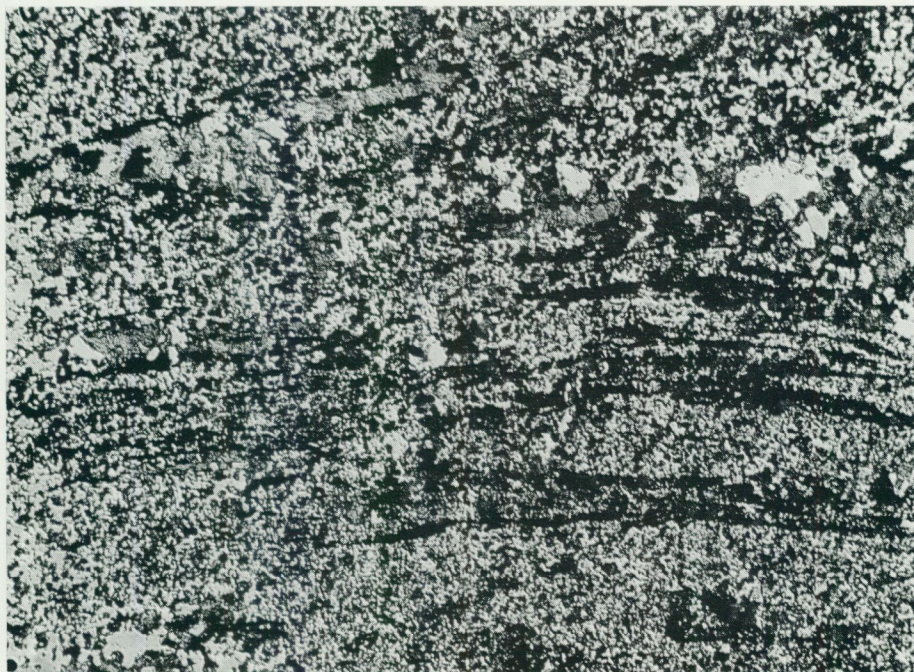


Fig. 6. Magnetite (black) in quartzite with streaks of skarn minerals (common hornblende and cummingtonite). 1 nic., 47 x. Kolarsjön (276/371). Photo I. Signorelli.

preserved, red jaspilite (hematite-stained quartzite) has been found in the iron ores at Risåsen (p. 40). From the iron ore region in central Sweden (Bergslagen) it is known (Magnusson 1953: p. 203) that recrystallization of jaspilite is usually connected with a reduction of hematite to magnetite. A leaching of quartz may also take place, leading to an enrichment of the ore mineral. Small dikes and lenses of vein quartz at 276/371 indicate that such processes have operated here.

Magnetite-rich layers also occur at 269/364. They are here found in a cummingtonite-magnetite-quartz rock with bands of common hornblende and garnet. (See Table 3: nos. 8 and 11.)

The existence of magnetite-quartz-rich layers and the modal composition of the magnesium-iron skarn show that there is a genetical connection between the skarn-bearing meta-argillites of the Kolarsjön-Risåsen region and the skarn iron ores at Risåsen (see below, p. 39). This connection is essential for the interpretation of the rocks described above (p. 30).

The calcium-rich layers are primarily characterized by common hornblende and diopside. A zoning is often developed with diopside in the central parts and hornblende next to the cummingtonite-biotite-rich layers. The contact

towards the latter is usually transitional, with minerals belonging to both the calcium-rich and calcium-poor parageneses. Common hornblende and cummingtonite thereby often form oriented intergrowths.

In two of the samples examined the common hornblende shows *mg* values of 0.7 and 0.5, respectively (Table 3: nos. 10 and 11). The cummingtonites of the same samples (Table 3: nos. 6 and 8) are characterized by $mg = 0.4$ and 0.5, respectively. Refractive indices of two diopsides are given in Table 4: nos. 2 and 3. The *mg* values are 0.4 and 0.3, in good agreement with the *mg* values determined for cummingtonites in the same samples (Table 3: nos. 6 and 7, respectively).

Epidote and quartz are found in very variable amounts in the hornblende-diopside layers. Subordinate or accessory minerals are garnet, sphene, colourless mica, actinolite, calcite and opaque minerals. The colourless mica forms aggregates of small crystals. Probably it is a sericite (muscovite) formed by alteration of plagioclase, although this feldspar has never been identified with certainty in connection with the mica aggregates.

Chemical and modal compositions of two skarn-bearing meta-argillites from the Kolarsjön-Risåsen region are given in Table 1: nos. 12 and 13. In comparison with normal meta-argillites, iron, calcium and sodium contents are high and potassium low. In accord with the relations between calcium and potassium, strontium is higher and barium lower than in the normal meta-argillites. The high Al_2O_3 percentage in no. 13 is somewhat unexpected from the microscopic studies. Cordierite has evidently been more abundant in the material used for chemical analysis than in the thin sections, the rock showing notable variation in compositional banding (cf. also above, p. 28).

It can be concluded from the above description of the skarn-bearing meta-argillites in the Kolarsjön-Risåsen region and the probable genesis of the iron ore at Risåsen (p. 40), that the former originated as a mixture of normal argillitic material with calcite (dolomite) and iron-rich minerals such as greenalite and siderite.

In addition to the occurrences described above of skarn-bearing meta-argillites, there are found in some regions subordinate schlieren of calcium-rich skarn in rocks of argillitic composition. Between Hästberget and Silleråsen (G8-G9) the skarn consists of actinolite, diopside and epidote together with quartz. It occurs here in hornfels (p. 23) and mica-schist. In the phyllites of the Noppikoski-Tallsjön region (E1-D2) layers containing epidote and calcite occur, together with intercalations of skarn-bearing quartzites (p. 36). Similar phyllites with epidote occur east of Vallåsen (D5) and on the western slope of Risberget (G5).

The argillite gneisses described below rarely contain skarn minerals. West of Karlsberg (403/233), however, such an occurrence has been noted. The skarn layers here consist of quartz, microcline, common hornblende and

saussuritized plagioclase. Subordinate and accessory minerals are sphene, apatite and tourmaline. Another occurrence has been observed in a road-cutting at 459/219. Diopside (Table 4: no. 4), hornblende, plagioclase (An_{45}), quartz and sphene here form schlieren in a grey gneiss of sedimentary origin. Cf. also von Eckermann 1936: p. 186.

The anthophyllite gneiss on Fetingsklacken (J5) has been denoted in the same way as the skarn-bearing meta-argillites on Plate 1. Its genesis will be discussed below (p. 33).

5.1.1.1.5. GNEISSES AND MIGMATITES OF MAINLY ARGILLITIC ORIGIN

Argillite gneisses, by comparison with the mica-schists, are characterized by more extensive recrystallization. They are as a rule strongly schistose (lepidoblastic) but possess a less regular cleavage than the mica-schists. The gneisses are fine- to medium-grained. Primary bedding structures are usually obliterated.

The dominating minerals in the argillite gneisses are quartz, biotite and plagioclase (oligoclase or andesine). Muscovite and microcline occur in varying amounts. Accessories are apatite, zircon, tourmaline, chlorite and opaque minerals. In addition, sillimanite, garnet, cordierite and anthophyllite occur in some regions. (For the distribution of garnet, see Plate 1.)

Sillimanite is an important constituent in the region Dåsen-Hedbäcken-Fetingsberg (I5, I6, J6), but may occur sporadically in other localities also. Where it is most abundant it forms compact aggregates (≤ 1 cm), from which single needle-like crystals branch out. Sillimanite also forms inclusions in quartz. It may show an alteration to muscovite. Together with the sillimanite a microcline of film perthite to string perthite type (Andersen 1928, cf. also p. 146 of the present work) is often found.

The association microcline-sillimanite places these sillimanite-bearing gneisses in the upper amphibolite facies of metamorphism (Winkler 1967). The lack of cordierite in the paragenesis microcline-sillimanite-biotite-plagioclase-quartz of the gneisses in question (cf. Table 1c: no. 16) indicates that the pressure has been high enough to prevent the appearance of this mineral (Winkler 1967; Hietanen 1967).

Chemical and modal analyses of two argillite gneisses are given in Table 1: nos. 15 and 16. The chemical composition is closely comparable with that of the lower grade meta-argillites, in spite of the strong metamorphism which has particularly affected the sillimanite gneiss no. 16.

For a description of the argillite gneisses occurring close to the Råtan granite, see p. 23.

The quartz-feldspar-rich (silty) layers in the meta-argillites have xenoblastic

textures. The following point-count analysis gives the modal composition of a typical representative of a metasiltstone transformed to gneiss (from 455/248):

quartz	46
plagioclase (An ₃₁)	44
biotite	7
almandite	1
opaque minerals	1
chlorite	1
zircon, epidote, apatite	< 1
	<hr/> 100

The majority of the argillite gneisses in the Los-Hamra region have a migmatitic character and contain granite or pegmatite as veins, schlieren etc. ("Migmatite" in this work is used as a purely descriptive term according to Sørensen 1961.) On the map, Plate 1, two types have been distinguished on the basis of the structure and the proportion of granitic material (metatect, cf. Sørensen 1961). In one type the latter occurs as conformable veins or more irregular schlieren (veined gneisses). In the other type, the metatect is continuous and forms the larger part of the migmatite. It contains fragments (often lens-shaped) of quartz-feldspar-rich rocks and biotite-rich schlieren, the latter representing the argillitic layers. The quartz-feldspar-rich layers have evidently been broken as a consequence of their relative competency during folding. Microcline augen (porphyroblasts) may occur, particularly in the metatect.

Some special features of these gneisses will be described below. The occurrence of skarn minerals in some localities has been mentioned earlier (p. 30) and indicates an original calcite or dolomite content. Graphite in migmatized paragneisses has been noted at Svensbo, about 10 km south-east of the region of Plate 1 (von Eckermann 1927).

The most important area with gneisses deviating in composition from normal argillites and siltstones is Fetingsklacken (J5). The gneisses occurring here are grey in colour and contain scattered granitic veins. They are characterized in particular by the presence of anthophyllite and almandite.

Primary bedding structures have been largely wiped out, but variations in composition (see below) may reflect an original layering. The texture is xenomorphic or hypidioblastic. Quartz, plagioclase (c. An₃₅) and brown biotite are normally main and essential minerals. Essential or subordinate constituents are usually almandite (Table 5: no. 5), macroscopically black anthophyllite, and sometimes also magnetite and cordierite. All these four minerals may be concentrated in certain layers with crystals sometimes attaining 1 cm in diameter. Accessories are mostly apatite, opaque minerals (cf. above), microcline, serpentine (alteration of anthophyllite) and zircon, rarely also cummingtonite.

An unusually anorthite-rich plagioclase (An₇₀) may occur together with anthophyllite in some layers.

The anthophyllite is weakly pleochroic (γ = green) in thin section. Optical determinations indicate that the mineral contains alumina and has an mg value of 0.4–0.5 (Table 3: nos. 12 and 13).

The chemical composition of a sample of anthophyllite gneiss from Fetingsklacken (Table 1a: no. 17) shows an intermediate alumina excess ($t = 18$). The k value is low (0.33) in comparison with normal meta-argillites. The Fe, Mg, Ca, Cr, V, Ni and Sr contents are higher than in the latter, but Ba is lower.

It does not seem possible to predict the character of the pre-metamorphic rock(s) that has been transformed to anthophyllite gneiss. The metamorphism is very strong and primary structures have been almost completely obliterated. The possibility exists that the original composition has been radically altered. If, however, it is assumed that the present composition is approximately the pre-metamorphic one and that better preserved counterparts to the anthophyllite gneiss occur in other parts of the Los-Hamra region, two possible interpretations exist. The gneiss may have originated as an argillite mixed with basic tuff material. The distribution of trace elements seems to favour this explanation (cf. Table 1a: analyses nos. 27–31), although CaO is relatively low and SiO₂ high. Alternatively, the anthophyllite gneiss was an original argillite relatively rich in iron(-magnesium) silicate (cf. p. 30) and containing small amounts of calcium-magnesium carbonate. The occurrence of bands rich in almandite, anthophyllite and magnetite favour this interpretation.

These interpretations are tentative, and the origin must be regarded as obscure. On the map, Plate 1, the anthophyllite gneiss has been marked as a skarn-bearing meta-argillite (second interpretation).

Above (p. 18) has been mentioned the occurrence of cordierite-anthophyllite gneiss with a relatively high magnetite content at Kvarnberg (401/131). The anthophyllite is richer in magnesium than on Fetingsklacken (Table 3: no. 14). Although this rock has been denoted as an argillite gneiss on Plate 1, a metasomatic origin is also possible (cf. p. 51).

5.1.1.2. META-ARENITES: QUARTZITE SANDSTONES, QUARTZITES AND META-ARKOSES

Meta-arenites, mainly representing original quartz sands, form the second important group of metasediments in the Los-Hamra region. Large areas with such rocks are found north of Noppikoski (D2-D4, E1-E3) and around the amphibolites of the Tenskog-Los-Faxen region (H3-H6-17). Further, they occur as intercalations in meta-argillite (e. g. F6).

Two groups of meta-arenites have been distinguished. One comprises rocks which have been only slightly recrystallized (quartzite sandstone) or show a more advanced recrystallization but still a preservation of clastic textural features (well preserved quartzites). The second group includes quartzites affected by strong recrystallization, which has obliterated the original clastic texture. These quartzites are particularly found in areas with migmatites and primorogenic intrusions.

In the first group some quartzites have also been included, which are interpreted as non-clastic sediments (chemical precipitates of silica). They are found in the Risåsen area (E8).

Quartzite sandstones and well preserved quartzites are greyish white or grey in colour. A bedding is sometimes well developed. It arises from variations in content of mica, feldspar, iron oxide etc. Discordant bedding has been noted in some cases, and is the most important way-up structure (cf. pp. 135 and 136).

Conglomerate horizons with pebbles up to c. 1 dm in diameter occur in some localities. West-northwest of Noppikoski (204/036) and around Ö. Råberget (E2) the pebbles are mostly quartzite sandstone, vein quartz, phyllite, acid metavolcanics with sericitized feldspars and brownish red, jaspilitic quartzite stained with hematite. Local moraine boulders of similar conglomerates have been found south-west of Ö. Råberget (c. 220/049).

Among the skarn-bearing metasediments west of Lillskog (K5-K6, cf. above, p. 24) quartzites and conglomerates also occur. The latter contain pebbles of quartzite, vein quartz and brownish red to black hematite quartzites (jaspilites). Cf. below, p. 45. The matrix between the pebbles is a parti-coloured intergrowth of actinolite, epidote, quartz, microcline, diopside, iron oxide and sphene in strongly varying proportions.

At Ryggskog (348/307) scattered quartzite and vein quartz pebbles occur in the quartzite sandstone.

At Tallsjöbäcken (198/061) is a small outcrop of quartzite sandstone with numerous fragments of quartz-porphyritic metarhyolite. These fragments cannot be derived from the metarhyolite to the west, shown on Plate 1, as discordant bedding indicates that this metarhyolite overlies the quartzite sandstone (p. 136). They must therefore have been eroded from an underlying metarhyolite not exposed in the area. (Cf. also the similar conglomerate pebbles at 204/036 and E2 described above.)

West of Noppikoski (201/031) is a small occurrence (not shown on Plate 1) of quartzite sandstone crowded with reddish brown metarhyolite fragments. It is completely surrounded by a rock similar to that of the fragments. Together with the above observations it testifies to contemporaneous volcanicity and sedimentation during the deposition of the supracrustal rocks now exposed in the region.

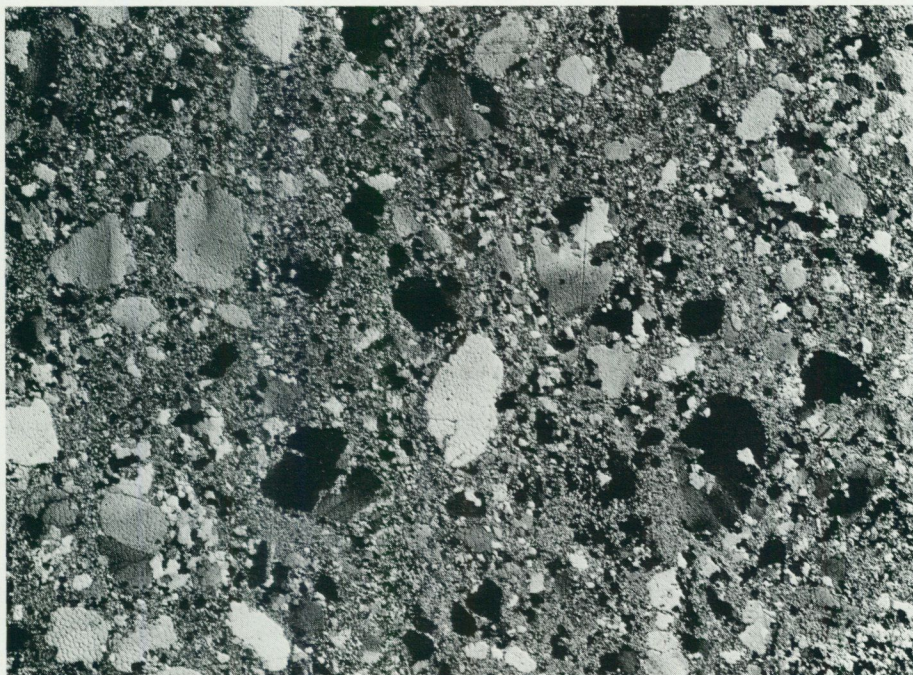


Fig. 7. Quartzite sandstone, consisting of more or less granulated quartz grains in a matrix of quartz and sericite. 2 nic., 13 x. Ryggskog (348/307). Photo I. Signorelli.

Quartz is the dominating mineral of the quartzite sandstones and well preserved quartzites. It occurs mostly in grain sizes between c. 3 and 0.05 mm. Larger, sometimes granulated quartz grains of sand size are often embedded in a more fine-grained quartz-mica(-feldspar) matrix (Fig. 7). The latter is usually subordinate to the larger quartz grains, but predominates in some samples. In the least recrystallized rocks the sand-sized quartz grains are generally well rounded (blastopsammitic texture), often with thin secondary overgrowths. Quartz is, in addition, also found in fissures. Sericite (muscovite) usually occurs as a subordinate or essential mineral in the matrix between the larger quartz grains. Subordinate or accessory minerals are biotite, plagioclase (albite or oligoclase), opaque minerals (iron oxides), sometimes also chlorite and microcline (cf. below). The plagioclase usually occurs in the interstices between sand-sized quartz grains and relatively seldom shows detrital grain shape. A concentration of the opaque minerals is sometimes observed in heavy mineral layers. Accessories are zircon, tourmaline, apatite, epidote, rutile, leucoxene, and occasional calcite. In the quartzites north of Noppikoski (D2-D4, E1-E3) small amounts of limonite and hematite give the rock a brownish violet tint.

Like the earlier described meta-argillites, the meta-arenites are usually very mature sediments, testifying to extensive chemical weathering. Exceptions are formed by the relatively rare reddish grey meta-arkoses, which are found in some localities, e. g. Noppikoski (210/033), Risberget (347/206) and north-west of Storlugnet (272/278). They contain clastic microcline as an essential mineral. At Noppikoski (210/033) this mineral has a weakly developed cross-hatching (cf. pp. 34 and 145). In addition, the quartzite sandstone here contains rare grains consisting of graphic intergrowths of quartz and alkali feldspar. These probably derive from acid metavolcanics (p. 48). On account of the small sizes of the grains, however, it cannot be excluded that they represent granophyric hypabyssal rocks. With this possible, though unlikely, exception, only material from supracrustal rocks has been identified in the meta-arenites.

Some meta-arenites of the Los-Hamra region have evidently contained small amounts of carbonate(s), which has been transformed to skarn. Thus, there occur, west of Lillskog (K5-K6) skarn-bearing, partially conglomeratic (see above) quartzites, together with the earlier described skarn-bearing meta-argillites. Among the skarn minerals epidote is especially important. Some grains are manganiferous (piedmontite). In the phyllites at Noppikoski (E1) occur thin layers of yellow-green epidote quartzite. Further to the east (227/033) a quartzite has been found with rounded quartz grains, up to some millimetres in diameter, embedded in a matrix of fibrous tremolite (Table 3: no. 15) and epidote (Fig. 8).

The strongly recrystallized quartzites are xenoblastic and more coarse-grained than the well preserved meta-arenites. The mineral content is similar to that of the latter, but in addition to the minerals mentioned above cordierite, sillimanite and andalusite also may occur. The presence of these indicates an original admixture of argillitic material. On the eastern shore of Dåasen (450/297), e. g., a medium- to coarse-grained sillimanite quartzite has been observed. On Hammarkesen (299/090) occurs a cordierite-sillimanite quartzite. Only in one case (south of Tenskog, 388/154) cordierite and andalusite have been met with in a quartzite showing relict clastic features.

In migmatite terrains (e. g. at Kvarnberg, 405/126) the quartzites may contain diffuse granite schlieren. In general, however, the quartzites have resisted the migmatization better than the meta-argillites.

The above descriptions concern the quartzitic metasediments of clastic origin. As mentioned above, there also occur quartzites which have been interpreted as chemical precipitates of silica. They occur associated with graphite phyllites and metaspilites at Risåsen. Cf. also p. 28.

The non-clastic quartzites are fine-grained, sometimes microcrystalline, and greyish white or dark grey (graphite) in colour. Thin sections show a xenoblastic texture with greatly varying grain sizes (c. 0.01–0.5 mm). In

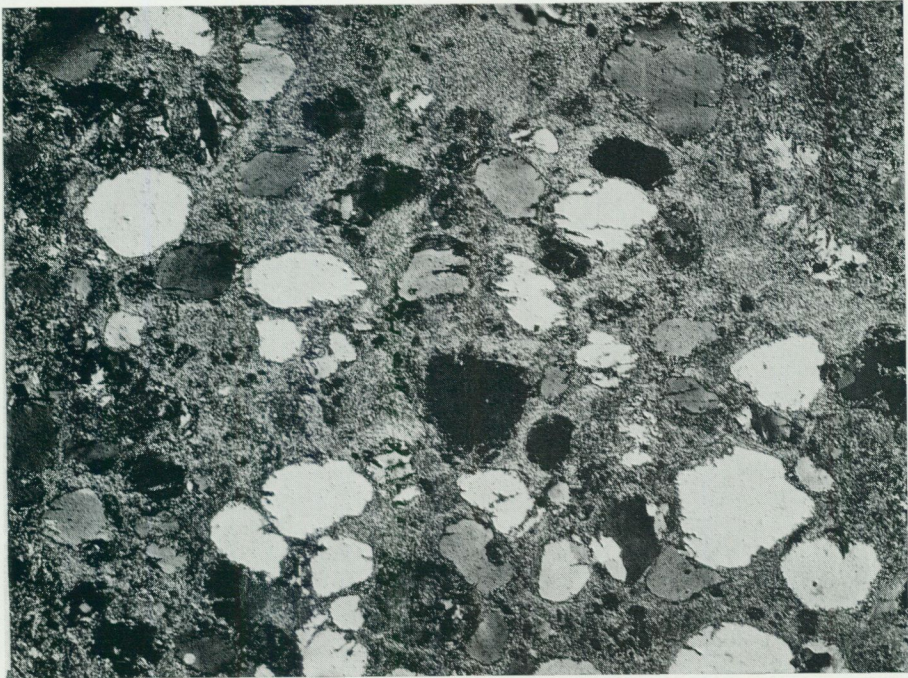


Fig. 8. Metamorphosed calcareous sandstone, consisting of quartz grains embedded in a tremolite matrix. 2 nic., 13 x. Oreälven (227/033). Photo I. Signorelli.

addition to quartz, which is the dominating mineral, the following constituents may be found in subordinate or accessory amounts: graphite, cummingtonite (Table 3: no. 16, cf. p. 22), iron oxides, diopside(?), calcite and apatite.

Quartzitic layers in the grunerite iron ores of Risåsen (E8-F8) also belong to the non-clastic quartzites. In rare cases they contain a hematite pigment (jaspilite).

5.1.1.3. CRYSTALLINE LIMESTONE AND DOLOMITE

Crystalline limestone and dolomite are relatively rare in the Los-Hamra region. However, sedimentary deposits containing carbonate(s) have originally been more abundant, as many occurrences of skarn represent a primary admixture of such minerals in epiclastic sediments. (See pp. 26 and 30.)

The largest occurrence of crystalline limestone is situated on Mansjöberget (448/135). It has earlier been made the subject of a detailed mineralogical-petrographical study (von Eckermann 1922). In connection with this, diamond drilling was carried out and the bedrock exposed through digging.

For the present investigation no new detailed work has been made in this locality. The description below is essentially based on the one given by von Eckermann (1922).

The Mansjöberget crystalline limestone is situated in a strongly migmatized region (cf. Plate 1). The migmatites have been formed from supracrustal rocks, the character of which was probably mainly argillitic. Fine-grained amphibolites (basic metavolcanics) are also found. The limestone is contained in a syncline, plunging 20° to the north-west. In this syncline, eulysite, peridotite, pyroxene gneiss, amphibolite, garnet skarn and crystalline schists also occur. For an account of the five latter rocks, the reader is referred to the original work of von Eckermann.

The crystalline limestone, which is mainly exposed in old quarries, is about 100 m long and ≤ 3 m wide. It is situated in the southern limb of the syncline. The limestone is white in colour and medium-grained (grain sizes c. 2 mm), though coarser near pegmatite intrusions. A sample containing calcite, biotite, diopside, phlogopite(?) and pyrite gave 96.00 % CaCO_3 (von Eckermann 1922: p. 319).

Of particular interest are the minerals formed in the limestone due to the invasion of pegmatite. The latter is connected with the regional migmatization. In the contact pegmatite-limestone, diopside and phlogopite have crystallized. Other important reaction products are chondrodite, green-blue spinel, grossularite, vesuvianite, amphotelite, wollastonite and blue apatite often in compact aggregates. Reactions with the limestone have resulted in the formation of anorthite and scapolite.

Diamond drill-cores from the Risåsen iron ore (E8) show several thin horizons of crystalline limestone. They occur in a sedimentary formation consisting of magnetite-grunerite rock, quartzite (p. 37) and graphite phyllite. The thickest layer of crystalline limestone is 4.2 m and consists of calcite with thin lenticular bands of graphite phyllite. In a prospecting trench at 246/357 calcite layers of a few centimetres' thickness have been found in a grunerite rock. At the contact between the latter and the calcite, reaction zones of diopside and actinolite (Table 3: no. 17) have been formed.

Diamond drilling in the region north of Dåasberget (H7, I7) has revealed thin (up to 3 dm) layers of crystalline carbonate (dolomite) in skarn iron ore (see below, p. 43).

North of Los, at Olofstorp (c. 372/328) the moraine contains numerous large (up to c. 4 m) local boulders of crystalline dolomite with a strongly brown-coloured weathering crust. On the map, Plate 1, the position of the dolomite has been schematically indicated according to studies of the distribution of the boulders, as no solid outcrop has been found. The dolomite contains irregular, chlorite-rich schlieren, which may represent original basic tuff layers.



Fig. 9. Folded and brecciated iron ore showing relict bedding. Dark is magnetite, light grey mainly grunerite. Risåsen (246/355). Photo Th. Lundqvist.

In one sample from Olofstorp the dolomite shows $n_D = 1.689$, which indicates 10 % of $\text{CaFe}(\text{CO}_3)_2$ (Tröger 1959: p. 26).

Layers, up to 2 dm thick, of pink or white crystalline limestone (calcite) occur in slate at 297/356. Similar layers are noted at Bygget (255/348).

Partially skarn-altered calcite layers have been found in mica-schist at 271/279. The skarn is diopside, epidote and actinolite.

Finally, in some of the skarn occurrences described below, subordinate layers or lenses of calcite or dolomite have been found. Further, in the spilites near Bygget (E8) the calcite may collect to form bodies of some decimetres' diameter (p. 56).

5.1.1.4. SKARN AND ASSOCIATED MAGNETITE DEPOSITS

On the map, Plate 1, have been marked the following occurrences of skarn in association with magnetite: Risåsen (E8), north of Dåasberget (H7-I7), north and east of Björkberg (G4 and G3) and Risberget (G5).

The Risåsen skarn (E8) is a fine-grained, greenish black rock in which grunerite and magnetite are the most important minerals. A more or less distinct compositional banding (primary bedding) can be observed (Fig. 9).

In usually subordinate amounts occur common hornblende, brownish green or brown biotite, plagioclase (andesine to albite) and quartz. They form a matrix between the grunerite crystals. Actinolite-rich layers are also observed. Anthophyllite has been identified, but is difficult to distinguish from grunerite (see below). Accessories are chlorite, garnet, calcite, diopside and graphite. In one thin section a bluish green, fibrous alkali amphibole has been observed. It is oriented with the *c*-axes strictly parallel to the bedding.

In the above skarn-magnetite rocks there are intercalations of graphite phyllite (p. 22), crystalline limestone (p. 38), quartzitic layers (very occasionally jaspilitic, p. 37) and (rarely) amphibolitic metavolcanics. Together these rocks form an association of iron-formation type. In the west and north occurs metaspilite (p. 56).

Rocks transitional between the skarn iron ores of Risåsen and normal meta-argillites occur in the Risåsen-Kolarsjön region (F8). They have been described above (p. 27).

The grunerite of the skarn usually forms fibrous, often radiating aggregates. In the latter the central parts are frequently made up of common hornblende. Intimate intergrowth of thin fibrous grunerite crystals often gives the mineral a seemingly parallel extinction. From studies of larger crystals it is, however, evident that the grunerite is usually twinned on a prism surface [probably (100)]. Anthophyllite has also been identified, but for the above reason it is possible that the content of this mineral has been somewhat underestimated.

The grunerite is colourless in thin section. Optical determinations show *mg* values around 0.2 (Table 3: nos. 18–20). The composition is thus near the border between grunerite and cummingtonite (Tröger 1959: p. 71).

A determination of the common hornblende in the same sample as the grunerite, no. 19 of Table 3, indicates a somewhat magnesium-richer composition than for the grunerite (Table 3: no. 21).

Magnetite is the only ore mineral of the skarn rocks. It is usually very fine-grained (c. 0.002–0.05 mm). The magnetite-rich layers have often been brecciated, the cracks being filled by grunerite, quartz, calcite etc. (Fig. 10).

A sample of iron ore from 247/353 contained 0.46 % manganese and 32 % iron.

From the above description it is evident that the Risåsen skarn ores show great resemblance to some ore types of the Lake Superior region (see e. g. James 1954 and 1955) and of the Pajala-Masugnsbyn district (Geijer 1925). Iron silicate (greenalite) and siderite are considered to be the primary carriers of iron in the metamorphosed sedimentary ores of similar type in the Lake Superior region. It is therefore likely that such minerals also originally contained the iron of the Risåsen ores, although no relics of them can be found in the metamorphic assemblages. Another strong argument favouring a

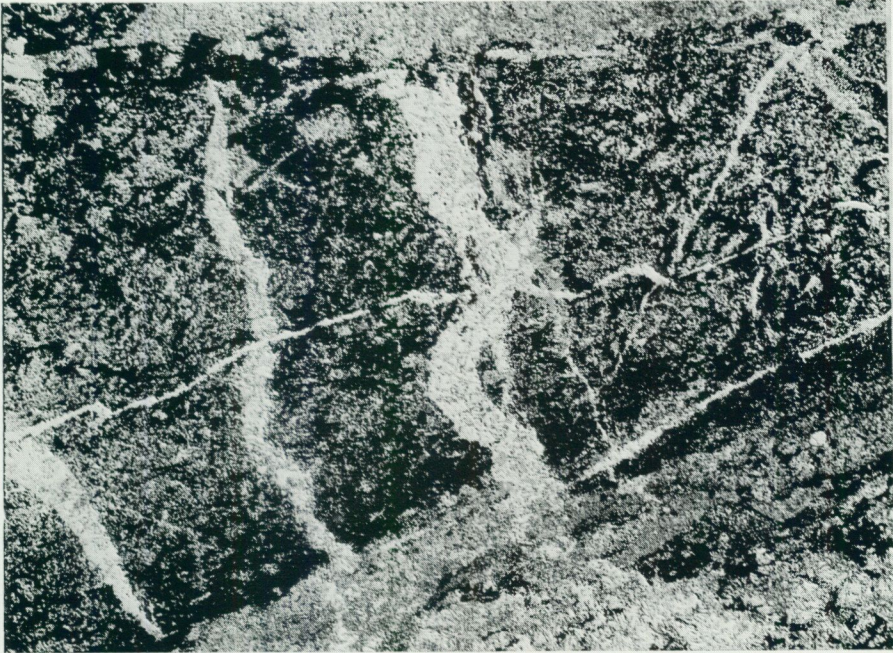


Fig. 10. Magnetite ore. Black is magnetite, white and grey, grunerite. 1 nic., 13 x. Risåsen (247/359). Photo I. Signorelli.

sedimentary origin is the presence of graphite phyllite, crystalline limestone and quartzite (jaspilite), the latter representing recrystallized chert (jasper).

The Lake Superior sedimentary iron ores are considered to be deposited in "restricted basins, which were separated from the open sea by thresholds that inhibited free circulation and permitted development of abnormalities in oxidation potential and water composition" (James 1954).

North of Dåasberget (H7-17), a horizon of skarn iron ore runs in an east-west direction. It is associated with more or less skarn-rich meta-argillites and amphibolitic metavolcanics. Quartzites and graphite-bearing meta-argillites seem to be lacking (cf. above). Jaspilitic layers may, however, have existed (cf. p. 45). The skarn ore is observed to outcrop only in one locality (418/331), but a good knowledge of it has been obtained by diamond drilling.

The outcrop at 418/331 shows a regular interbedding of magnetite and skarn (Fig. 11). In the drill-cores and prospecting trenches bedding structures are also found (Fig. 12), although they are as a rule not so well developed.

The iron ores north of Dåasberget are characterized by a calcium-magnesium skarn, in contrast to the iron-magnesium skarn of Risåsen. They are fine- to coarse-grained and consist of tremolite, phlogopite, olivine (more or less altered to serpentine or chlorite) and magnetite in greatly varying proportions. Also diopside, epidote and common hornblende occur. Acces-



Fig. 11. Folding in skarn-banded iron ore. Black is magnetite, grey and white, skarn (mainly tremolite). North of Dåasberget (418/331). Photo Th. Lundqvist.



Fig. 12. Banded magnetite-skarn ore. The skarn is mainly tremolite and phlogopite. 1 nic., 5 x. North-west of Dåasberget (393/327). Photo I. Signorelli.

sories are leucoxene, sphene, zircon and biotite. A carbonate (dolomite) sometimes forms thin layers or scattered grains in the skarn. Rarely also poor impregnations of pyrite, chalcopyrite and pyrrhotite occur. In some samples a humite mineral (chondrodite) has been noted.

The tremolite is macroscopically pale green to colourless. It forms prismatic crystals. Optical determination of one tremolite indicates a nearly iron-free composition (Table 3: no. 22).

The phlogopite is pale green in hand specimen. In thin section it shows the following pleochroism: $\gamma = \beta =$ pale green; $\alpha =$ pale brown. An optical determination (Table 6: no. 2) points to a small iron content.

According to optical data the olivine is a forsterite (Table 4: no. 5). It may show a complete alteration to serpentine or pale green chlorite. The latter mineral may also occur in the matrix between tremolite needles.

The magnetite is coarser than in the Risåsen ores. Grain sizes are c. 0.05–0.5 mm, but scattered crystals of smaller dimensions occur in the skarn. Aggregate structures in magnetite give grains of several millimetres' size, which, however, usually carry small inclusions of skarn minerals.

Optical data for a diopside ($mg = 0.8$) are given in Table 4: no. 6. The mineral occurs associated with epidote and may show an alteration to uralite.

In a few samples a partially altered mineral of the humite group has been observed. It is pleochroic, from orange to colourless. Only one grain, however, offered possibilities for optical identification. This crystal is probably twinned on (100). With this assumption $\alpha \wedge c \sim 21^\circ$ was obtained; further, $2V_\gamma \sim 74^\circ$. These data indicate that the mineral is probably chondrodite (Tröger 1959). However, the possibility of the presence of other humite minerals can not be excluded.

The genesis of the Dåasberget ore is discussed on pp. 44–45.

North and east of Björkberg (G4 and G3) there are three small excavations for iron ore (at Pajaso and on Kivanhoberget). The deposits are similar in type to that occurring north of Dåasberget. A compositional banding can sometimes be seen arising from variations in the proportions of magnetite and skarn. Generally, however, the distribution between these minerals is irregular giving a patchy rather than banded appearance.

The skarn-magnetite rocks of the Björkberg region are fine- to medium-grained. The skarn consists of olivine (with secondary serpentine), phlogopite, tremolite and pale green chlorite. Magnetite is the only ore mineral. It occurs in rather compact, skarn-poor layers and in varying proportions within the skarn. The magnetite crystals or crystal aggregates range in size from several millimetres in the compact layers down to < 0.01 mm in scattered grains in the skarn.

The olivine is magnesium-rich (Table 4: no. 7). It is often completely altered to serpentine. The phlogopite is colourless or weakly pleochroic from

brown to colourless. In one sample the phlogopite margins are strongly green-pleochroic, probably due to a higher iron content. Optical determinations of three phlogopites are given in Table 6: nos. 3, 4 and 5.

Accessories are apatite, carbonate and zircon.

The genesis of the Björkberg skarn iron "ores" will be discussed below (pp. 44–45).

On the south-western slope of Risberget (G5) skarn-bearing magnetite deposits occur in a north-northeast striking zone, a few metres wide. Several small mining pits have been opened here. The ores are contained in the following stratigraphic sequence (c. 1,000 m thick), starting from the west with the oldest supracrustal rocks: meta-arkose and mica-schist – greyish red to red, quartz-porphyrific, acid metavolcanics (in part breccia) – banded mica-schist – skarn with magnetite – quartzite – quartz-porphyrific meta-rhyolite – mica-schist (brecciated by primorogenic granite). Cf. Plate 1, where, however, the banded mica-schist is not shown.

The skarn-magnetite rocks are fine- to medium-grained. The colour is dark grey, greyish green, dark green or greyish brown. A banding can sometimes be seen caused by varying proportions of magnetite, skarn and carbonate. The most important minerals are phlogopite, dolomite, calcite, magnetite, tremolite and pale green chlorite. Accessories are biotite, apatite, leucoxene and zircon. Blomberg (1895) also mentioned epidote, garnet, chalcopyrite and pyrite.

The phlogopite is weakly pleochroic with $\gamma =$ light brown. For a refractive index determination see Table 6: no. 6.

Grain sizes of magnetite range from c. 0.05 to a few mm. Large crystals or crystal aggregates are poikiloblastic. An incipient oxidation to hematite can be observed along some grain boundaries.

The skarn-magnetite occurrences of Dåasberget, Björkberg and Risberget have very much in common. Magnetite is the ore mineral. The skarn is composed of tremolite, phlogopite, carbonate(s) and chlorite. In addition, olivine and serpentine are present at Dåasberget and Björkberg. In the Dåasberget rocks diopside, epidote and, rarely, chondrodite have also been found. Quartz and feldspar seem to be lacking. In all three cases a compositional banding is sometimes well developed though more irregular variations in mineral composition predominate.

In literature concerning the genesis of Swedish iron ores there has been some discussion as to whether ores of the type described above should be interpreted as formed by (contact) metasomatism of carbonate rocks, or by metamorphism and/or metasomatic alteration of sedimentary deposits. In the former case, ore deposition and skarn crystallization would occur simultaneously, being parts of the same metasomatic process. In the latter case, the skarn minerals would be of a later origin than the ore. Magnusson (1953)

mentioned the following indications of the latter genesis: relics of iron ore containing layers of quartzite and crystalline limestone, and the occurrence of dikes discordant to the ore and containing the skarn minerals. Geijer and Magnusson (1944) considered the presence of humite minerals, ludwigite, fluoborite and axinite to be proof of a contact-metasomatic origin. However, Magnusson (1966: p. 55) after a discussion of the genesis of central Swedish iron ores, stated: "Ich bin deshalb überzeugt, dass beinahe alle phosphorarmen Eisenerze in Mittelschweden Sedimente sind, welche, da sie im vulkanischen Milieu gebildet sind, ihr Eisen durch spätvulkanische Prozesse erhalten haben."

The three actual skarn-magnetite occurrences of the Los-Hamra region are all found within a distance of about 1 km from contacts of primorogenic intrusions. The regional location thus permits a metasomatic origin. The latter may also be favoured by the occurrence of chondrodite north of Dåasberget (cf. above). However, as mentioned in the above descriptions, compositional banding which partially is very regular occurs in all the actual skarn-magnetite deposits. It represents in all probability an original sedimentary bedding and thus points to a syngenetic deposition of carbonate and iron. Later metamorphism may then in part have obliterated the bedding structures. A high mobility of elements during metamorphism is also evident through the occurrence of skarn and magnetite in fissures. The author of this work is therefore of opinion that the actual skarn-magnetite occurrences represent an original sedimentary deposition of calcium-magnesium carbonate(s), some iron compound(s), small amounts of silica(?) and very subordinate argillitic material. The rare occurrence of chondrodite can hardly be regarded as proof of a contact-metasomatic origin.

The nature of the original iron compound(s) is unknown, as no relics of such minerals have been found. Assuming negligible metasomatic alteration it is, however, likely that the iron was primarily bound in silicate(s) and/or carbonate. The occurrence of hematite-bearing quartzites (jaspilites) as pebbles in the conglomerates at Lillskog (see above, p. 34) would indicate that silica was also deposited together with the iron. The Lillskog conglomerates are approximately stratigraphically equivalent to the Dåasberget skarn-magnetite deposits (p. 135). Although jaspilitic layers have not been observed north of Dåasberget, the pebbles may thus be taken as an indication of a sedimentary origin for the Dåasberget ores.

As mentioned above (p. 26), a small skarn-magnetite deposit occurs at Öv. Hamravallen (236/256), intercalated in skarn-bearing meta-argillites. The skarn is composed of diopside (Table 4: no. 8), common hornblende, epidote, tremolite (Table 3: no. 3) and garnet. Accessories are biotite and orthite. The ore mineral is magnetite. Scattered grains of sulphides (pyrite, chalcopyrite and pyrrhotite) also occur.

As the Hamravallen skarn-magnetite deposit forms a concordant layer in supracrustal rocks it is probably of sedimentary origin. However, the small outcrop where it can be studied does not allow more detailed investigations.

The so-called pyroxene gneiss on Mansjöberget (I3, see von Eckermann 1922: p. 313) also belongs to the skarn rocks. It is too small to show on the map, Plate 1. The mineralogy is dominantly hornblende, diopside and plagioclase (bytownite to anorthite).

The special type of skarn, eulysite, which occurs on Mansjöberget (I3), is described separately below.

The so-called iron mines of Mansjöberget (at 447/136, not shown on Plate 1) are mentioned by Blomberg (1895: p. 117) and von Eckermann (1922: p. 294). According to the latter author, the ore mineral is hematite. It occurs in a talc-serpentine-chlorite skarn formed through alteration and oxidation of eulysite. In the latter rock both magnetite and hematite are found (see further below).

The only magnetite deposit in the Los-Hamra region, which does not seem to be associated with skarn, is situated at Lakisberget (379/147). It is connected by magnetic anomalies with a cordierite-anthophyllite gneiss at 401/131, and is possibly of metasomatic origin (pp. 33 and 51).

5.1.1.5. EULYSITE

The only occurrence of eulysite in the region is situated on Mansjöberget (I3, see above, p. 38). A detailed description of the rock was given by von Eckermann (1922: p. 253 ff.), who stated that it was characterized by fayalite, "iron anthophyllite", diopside, grunerite and hornblende in very variable proportions. The "iron anthophyllite" was later shown to be an iron-rich orthopyroxene (Sundius 1932). In subordinate or accessory amounts occur apatite, magnetite, hematite, pyrite and pyrrhotite. Garnet (almandite-spessartite), quartz and biotite are also sometimes present. An increase in magnetite content towards the contacts of the eulysite was noted. Alteration and oxidation were considered to have given rise to hematite concentrations. Chemical analyses of such "ore" show about 50 % Fe_2O_3 and 45 % SiO_2 (von Eckermann 1922: p. 294).

The manganese content of the Mansjöberget eulysite varies up to a maximum of 5 % MnO (von Eckermann 1922: p. 259).

von Eckermann (1922: p. 290) originally interpreted the eulysite as magmatic, formed by "pegmatitic, hydatogeneous and halogeneous residual solutions of basic magmas". Later (1936: p. 165) he changed this opinion: "I have arrived at the conclusion that perimagmatic products are certainly responsible for the origin of the eulysites, but that these products are derived from the Mansjö granite and not from the rest-differentiate of a basic magma.

They do not constitute the sole component of the eulysites, however, but have acted as a metamorphic agent on sediments originally very poor in alkalies and lime but rich in iron, such as quartzitic ore-sediments."

Geijer (1925) described eulysitic iron ores associated with crystalline limestone and dolomite from the Pajala-Masugnsbyn area in northern Sweden. He defined eulysite as an iron silicate rock containing fayalite and lying as a concordant body in a stratified rock series. A high manganese content was sometimes present, but was not an essential feature for the definition. Geijer used the term "eulysitic iron ores" for iron ores with a close relationship to eulysites, whether or not they contained fayalite (thus including, for example, grunerite-magnetite ores). Geijer (1925) mentioned several lines of evidence in support of the view that both eulysitic iron ores and eulysites are metamorphosed chemical sediments, in which the original iron mineral was either a silicate (greenalite) or a carbonate. Later investigations in the Pajala region (Eriksson 1954) have led to the same interpretation. The present author has arrived at similar conclusions for the "eulysitic" Risåsen iron ores of the Los-Hamra region (p. 40). On account of the comparability with the eulysitic iron ores of Norrbotten described by Geijer, it is most likely that the Mansjöberget eulysite represents a metamorphosed iron-bearing sediment. The analysis cited above, showing high Fe_2O_3 and SiO_2 percentages, may possibly indicate an original deposition of silica together with the iron.

The intimate connection between the eulysite on Mansjöberget and the peridotitic rock mentioned by von Eckermann (1922: p. 240 ff.) suggests a similar origin for both rocks. A higher primary content of magnesium (as carbonate) would explain the difference in composition from the eulysite.

5.1.1.6. ACID METAVOLCANICS (METARHYOLITES)

Acid, quartz-porphyritic metavolcanics form an important part of the supracrustal formation. They underlie the amphibolites of the Tenskog-Los-Selingen syncline (H4-H7-J7, cf. p. 136 and map, Plate 1). They are also found in the Lillskog area (K5-K6) in an isolated part of the syncline. West of Lossjön (H6-I6), acid metavolcanics appear to be lacking, although they may exist, in part assimilated by the primorogenic granites.

Isolated areas with acid metavolcanics occur at Sandsjöån (E3), south-east of Rullbo (E6-F7), in the Bygget-Kolarsjön region (F7-F8) and on Brännberget (H9). In the Noppikoski-Sörberget region (E1, D1-D3), quartz-porphyritic metavolcanics are the youngest members of the Los Formation, constituting the basement of the sub-Jotnian Dala volcanics.

The acid metavolcanics are reddish grey, reddish brown or grey in colour. They are almost exclusively porphyritic, with phenocrysts of quartz together with microcline perthite and/or sodic plagioclase. Close to the basal layers

of the Dala volcanics at 191/069, however, the rock is non-porphyrific. In the least recrystallized regions the schistosity is usually very weak or absent. The groundmass in such cases is aphanitic, micro- to cryptocrystalline, and often micropoikilitic, with inclusions of feldspar in quartz. Stronger recrystallization leads to a granoblastic groundmass texture with grain sizes up to c. 0.5 mm. Such a coarsening occurs near primorogenic intrusions and in the migmatite terrains.

Ignimbritic textures and structures, similar to those recorded from the Dala porphyries and described later (p. 101 ff.), occur particularly in the region west and north of Noppikoski. They are also found in other localities, e. g. 256/318. The macroscopically visible structures are formed by pink streaks ("flames") which are generally c. 0.1–1 cm thick and up to c. 10 cm long. These consist of quartz (size \leq c. 1 mm) intergrown with lath-shaped (hypidiomorphic) alkali feldspar, especially towards the margins of the streaks (Fig. 13). The feldspar is usually oriented at approximately right angles to the rims of the streaks. The quartz may show a kind of poikilitic texture, forming a network of equally oriented laths around the feldspar. The textural features of the streaks are similar to those termed axiolitic or pectinate in the literature on Phanerozoic volcanics (see e. g. Ross and Smith 1961).

In addition to the above streaks, which are visible in hand specimen, there may also exist a fragmentation discernible only with the aid of a microscope. The fragments show a distinct preferred orientation (pseudo-fluidal texture). This parallel texture bends around the phenocrysts. In larger fragments an internal parallelism of elongate small quartz grains may be present. Microscopic textures of this type have mainly been found in the Noppikoski-Sörberget region (E1, D1-D3), but have also been recorded in a few other localities (e. g. 374/355).

A comparison of structural and textural features of the Los-Hamra acid metavolcanics with those of Phanerozoic ignimbrites shows many similarities (Ross and Smith 1961). The pseudo-fluidal texture is formed by a parallel orientation of small glass-shards and minute pumice fragments, the original contours of which have been preserved in the least metamorphosed occurrences. The recrystallization has thus mainly taken place within the original particles. Pseudo-fluidal macroscopic structures (streaks, "flames"), on the other hand, reflect larger fragments of (collapsed) pumice. In these, recrystallization has evidently proceeded further than in the smaller fragments and the glass shards.

The considerable lateral extension of the acid metavolcanics (Plate 1) makes an interpretation as lavas unlikely. In view of the structures and textures described above it seems probable that a large part of the Los-Hamra metarhyolites originated as ignimbrites. (For a further discussion of ignimbrites, see p. 103 ff.) It is not clear whether such an interpretation is also



Fig. 13. Thin section of metarhyolite with ignimbrite "flames". One "flame" runs across the centre of the picture, and consists of alkali feldspar laths in relatively coarse-grained quartz. 2 nic., 5 x. Tallsjön (192/073). Photo I. Signorelli.

valid for those metarhyolites that do not show ignimbritic structures and textures (e. g. because of strong recrystallization).

On the south-western slope of Risberget (c. 348/205) occurs a breccia with angular fragments of reddish metarhyolite in a grey matrix of similar composition. Patches of biotite and muscovite are also found there and probably represent original fragments of argillitic rocks in a more or less assimilated state (cf. analyses 20 and 21). At Ryggskog (c. 349/306) similar fragments composed of biotite, tourmaline and opaque mineral(s) occur in metarhyolite.

As already mentioned, the acid metavolcanics are almost exclusively porphyritic. Phenocrysts generally form less than 10 % of the rock. Among them, quartz predominates. It occurs in crystals of approximately one millimetre's size. Occasionally, as on Risberget (352/204), the phenocrysts are larger (5 mm). Their shape is usually rounded, but a tendency towards idiomorphic form has been observed. Corrosion embayments are sometimes present (cf. Rittmann 1962a: p. 202). Micropoikilitic overgrowths in optical continuity with the phenocrysts are a common textural feature, the inclusions

consisting of alkali feldspar. The development of a penetrative schistosity has usually led to a granulation of the quartz. In extreme cases the latter has been drawn out into thin polycrystalline stripes.

Among the phenocrysts, feldspars are usually quantitatively subordinate to quartz. Their maximum size is c. 5 mm. They consist of microcline perthite and/or plagioclase. The latter is usually an albite or sodic oligoclase, but in a few samples the composition reaches andesine (cf. Table 1: no. 22). In such cases microcline phenocrysts are lacking.

Extensive sericitization has sometimes affected the plagioclase and the albite phase of the microcline perthite.

Some aggregates of biotite and opaque minerals occur, perhaps representing altered femic phenocrysts (hornblende, pyroxene).

The bulk of the groundmass is made up of quartz and alkali feldspars. Both microcline and albite occur, but the aphanitic character in many cases makes it impossible to determine the proportions between the two. In samples where an estimate has been possible, both albite and microcline dominance has been noted. However, highly albitic compositions have never been observed (cf. p. 20).

Muscovite (sericite), sometimes accompanied by greenish brown biotite, usually forms an essential or subordinate mineral in the groundmass. Typical accessory or subordinate constituents are opaque minerals (iron oxides). Chlorite occasionally occurs. In addition, the following accessories have been observed: sphene, leucoxene, tourmaline, apatite, fluorite, zircon, epidote, manganese epidote, orthite, rutile and calcite.

Chemical and modal analyses of acid metavolcanics are given in Table 1: nos. 18–25. The majority of these metavolcanics are rhyolites with a Pacific character (Rittmann 1952 and 1962a, see Table 2). However, high Niggli T and t values in some cases indicate a change of the original composition (formation of muscovite). This may be a consequence of contamination with argillitic material (nos. 20 and 21 of Table 1) or of silicification and/or weathering (no. 24, cf. p. 84). In other cases (nos. 18, 23 and 25) the alumina excess can be related to regional tectonic and metamorphic processes, possibly in combination with contamination etc. High k values (cf. Fig. 70, p. 226) may in part be explained by an alteration of plagioclase to muscovite, but in some cases is certainly a primary feature (e. g. no. 23 and von Eckermann 1936: no. 60). From Fig. 70 it is evident that in the acid metavolcanics potassium predominates over sodium. Calcium contents are low.

Of the trace elements, vanadium, chromium, cobalt, nickel, copper, lead and strontium occur in very small amounts. Zirconium analyses lie in the range 200–300 ppm. BaO varies between 450 and 1,700 ppm and Rb₂O between 110 and 270 ppm. There is no clear correlation between potassium, barium and rubidium contents. However, the values recorded may be taken

to indicate a weak negative correlation between BaO and K₂O, and a weak positive one between Rb₂O and K₂O.

Finally, two cases should be mentioned where the composition of acid metavolcanics has been radically altered during deformation.

Along Sandsjöån (E3) occurs a metarhyolite which is largely characterized by bluish quartz phenocrysts (cf. Ljunggren 1954: p. 68 ff.). Especially in the south-eastern parts, it is strongly schistose, with transitions to mica-schist, lacking feldspar. In types with an intermediate mica content, albite (sometimes with moaré twins) is the only feldspar. The mica-schist (Table 1: no. 26) mainly consists of quartz (partly as relict, more or less granulated phenocrysts) and muscovite. In essential or subordinate amounts occur pale brown or greenish brown biotite and strongly sericitized (pseudomorphosed) cordierite or andalusite. Accessories are apatite, zircon, chlorite, sphene, rutile and opaque minerals. Unaltered andalusite porphyroblasts and cordierite pseudomorphs have been found in a similar mica-schist at 228/118.

The second occurrence is situated east of Tenskog (c. 405/155). A normal, quartz-porphyrific metarhyolite is found to the south and south-east of this locality. From this metarhyolite, wedges of tectonic mica-schist seem to project northwards into the quartzites and meta-argillites. The so-called Ställstensberget copper mines (p. 134) are situated in the tectonic mica-schists, which also contain vein quartz bodies associated with the tectonic zones. The mica-schists around the mining pits show relict, more or less granulated quartz phenocrysts in a groundmass of quartz, muscovite and biotite altered to chlorite. Accessories are zircon, tourmaline and opaque minerals. Feldspars seem to be lacking but for a few sericite aggregates which might represent strongly altered plagioclase or microcline.

Around the mining pits at Ställstensberget, a quartzitic rock of uncertain origin is to be found. It may, however, possibly represent another type of strongly metasomatically altered rhyolite, although relict quartz phenocrysts seem to be lacking. In addition to quartz, the rock contains poikiloblastic cordierite and muscovite pseudomorphs after anthophyllite(?). Magnetite forms an essential mineral. Chlorite occurs in subordinate amounts, and accessories are greenish brown biotite and zircon. It is possible that the quartzitic rock is related to the cordierite-anthophyllite gneiss near Kvarnberg and the cordierite mica-schist on Lakisberget (pp. 33 and 18). In all three localities magnetite forms an important constituent of the rocks.

5.1.1.7. BASIC METAVOLCANICS AND METATUFFITES

Basic, usually amphibolitic metavolcanics are quantitatively more important than the metarhyolites. The largest occurrence stretches from the region of Tenskog (H4) through Los (H7) to Selingen (J7). These amphibolites form

the central parts of a large synclinal structure (p. 135). They are also found around Lillskog (K5-K6) in an occurrence isolated from the large syncline by faulting (p. 140).

Amphibolites, in part strongly scoriaceous, form a belt stretching from Bygget to Krokvattnet and Kolarsjön (E7-E8, F8). Relatively thin intercalations of amphibolite in meta-argillite are found in several localities. Further, such rocks are not uncommon in the migmatites and as xenoliths in the primorogenic intrusions.

Generally, the amphibolites have the character of purely volcanic deposits, with little or no admixture of epiclastic material. Frequently they have an amygdaloidal texture and represent original lava flows. However, in some localities amphibolitic rocks occur, which are interpreted as basic metatuffites. In these, a bedding is visible and the mineralogical composition deviates from that of the normal amphibolites, mainly through a higher content of quartz and/or biotite. The most important occurrence of such rocks is situated approximately 10 km north of Los (H8-G8).

Although the majority of amphibolites in the Los-Hamra region are no doubt of supracrustal origin, there are also similarly composed rocks for which an interpretation as basic intrusions is possible. This is especially the case with certain medium- or even coarse-grained amphibolites, found for example south of Romberg (399/348) and in the Storkvarnberget-Tenskog region (H4-I4). The close association with clearly supracrustal, fine-grained amphibolites makes it probable that the coarser varieties either represent a more advanced (original or metamorphic) crystallization in lavas, or subvolcanic intrusions. In other cases, where such an association does not exist (e. g. at 297/050) the coarser amphibolites may represent early primorogenic intrusions. However, since they are subordinate to the metavolcanics and because of the difficulty to distinguish in all cases between supracrustal and intrusive amphibolites no attempt has been made to mark out the coarser rocks on the map, Plate 1.

The amphibolitic metavolcanics are black, dark green or dark grey in colour. They are mostly fine-grained (cf. above). A tendency towards plagioclase- and/or hornblende-porphyritic development is sometimes present. Conspicuous textural features of this kind are, however, relatively rare. For descriptive purposes, two groups of basic metavolcanics may be distinguished: strongly scoriaceous (spilitic) and non-scoriaceous or amygdaloidal.

The amphibolites of the second group display a number of relict primary features. The most common of these is amygdaloidal texture (Fig. 14). Breccias, agglomerates and conglomerates also occur, as well as layered amphibolites of tuff character.

The amygdules of the amphibolites are usually less than 2 cm in diameter and ellipsoidal in shape. Their frequency may vary greatly within a single



Fig. 14. Amphibolite with amygdules filled with quartz. From the cobalt mines at Los (370/303). Scale in inches (above) and centimetres (below). Photo P. H. Lundegårdh 1965.

outcrop. Quartz is the most common mineral of the amygdules, but common hornblende, calcite, plagioclase (generally andesine), epidote, diopside, chlorite and biotite also occur. Small amounts of iron oxide, pyrite and sphene have been found. Zonal amygdules of the following types have been observed (the mineral of the central parts being mentioned first): plagioclase – quartz; sericitized plagioclase – unaltered plagioclase; epidote – plagioclase; quartz – chlorite; calcite – plagioclase; diopside – common hornblende; calcite – diopside. The last mentioned type is evidently the result of a reaction between calcite and the surrounding amphibolite.

Breccias and agglomerates in amphibolite have mostly been found as boulders in moraine. The term agglomerate has here been used for rocks where the fragmental material is somewhat rounded and often shows diffuse contours towards the matrix. Only small variations in composition between fragments and matrix exist. Such rocks may be explained as consisting of pieces of lava which have solidified during or after their ejection, embedded in a matrix of volcanic ash (cf. Pettijohn 1957: pp. 331–332). Auto-brecciated lava flows ("aa lava"), however, may give a similar structure. In the breccias, on the other hand, the fragments are sharp-edged and may be of different rock types. Such fragments are probably torn off from the walls of the volcanic conduit during explosive outbursts.

North of Järperget (H4-H5), a zone of volcanic breccia in amphibolite has been marked on the map, Plate 1. Among the fragments, amphibolites



Fig. 15. Volcanic breccia with fragments of amphibolite and quartz-porphyritic meta-rhyolite (light) in an amphibolitic matrix. Moraine boulder west of St. Tallberget (c. 388/207). Photo Th. Lundqvist.

predominate, but acid, quartz-porphyritic metavolcanics also occur (Fig. 15).

Fragments of meta-argillite in amphibolitic breccia have been observed in moraine boulders at c. 390/348.

North of the church of Los (381/291) is a small occurrence of breccia in amphibolite. The rock fragments consist of albite, common hornblende, magnetite (up to one third of the rock volume) and leucoxene. In the matrix, which shows a relict clastic texture, quartz and albite predominate, whereas hornblende, magnetite, sphene and biotite form subordinate constituents.

Diamond drilling for sulphide ore in the region immediately west of Los (H6) have revealed calcite-rich amphibolite breccias with amygdaloidal fragments. Layered hornblende-bearing rocks of tuff character also occur. The breccias may here in part possibly be of tectonic origin.

Conglomerates are relatively rare in the amphibolites. The pebbles are mostly of amphibolitic composition, but metarhyolites have also been observed. One occurrence is situated at Örnberget, north of Los (H7; polished specimen, collected by H. von Eckermann, in the museum of the Geological Survey of Sweden).

The basic metavolcanics, which do not display a strongly scoriaceous structure, consist mainly of common hornblende and plagioclase. In very varying amounts, but generally subordinate to hornblende and plagioclase, occur brown or greenish brown biotite, opaque minerals (magnetite), chlorite, epidote and quartz. Epidote often forms an irregular network of veins in the amphibolite. The magnetite content may reach 20 % (cf. Table 1c: no. 30). Accessories are apatite, sphene, prehnite, tourmaline, calcite, microcline, pyrrhotite, orthite and zircon. Remnants of clinopyroxene may very occasionally be found in the (uralitic) hornblende, which then shows patches of different absorption intensity (cf. von Eckermann 1936: pp. 198 and 207). The modal composition of amphibolites affected by late alteration is described below (p. 57).

The common hornblende mostly occurs in hypidioblastic, sometimes poikilitic grains. A preferred orientation of the hornblende prisms may exist (nematoblastic texture) or be absent (decussate texture). The mineral further occurs as a filling of fissures or in irregular schlieren in the amphibolites. The pleochroism is generally bluish green (γ) to green (β) and very light brownish yellow to colourless (α), with varying absorption intensity. Optical determinations (Table 3: nos. 23–25) show *mg* values of 0.6–0.8. The common hornblende may show alteration to chlorite, biotite or cummingtonite (see below, p. 57).

The plagioclase is xenoblastic or hypidioblastic and forms equidimensional or tabular [parallel to (010)] crystals. The composition varies greatly: anorthite contents range between 0 and 65 %, although they usually lie between c. 25 and 45 %. Normal zoning, with up to 25 % difference in anorthite content from core to margin, has been observed. Occasionally an inverse zoning may also be found. The central parts of zoned grains are particularly susceptible to sericitization and epidotization with a concomitant albitization. However, almost clear albite (usually in lath-shaped crystals) without evidence of an originally higher anorthite content, has been found in some samples. Such albite occurs in rocks where the hornblende has been largely replaced by chlorite and biotite (e. g. 369/307), but also in association with unaltered common hornblende. An example of the latter case is the volcanic breccia at 381/291, mentioned above, where both rock fragments and matrix contain clear albite. The magnetite-rich amphibolite no. 30 of Table 1 also has an albite-rich plagioclase (An_{15}) coexisting with common hornblende. For other examples, see analyses 31–33 of von Eckermann (1936).

The amphibolites with an albite-rich plagioclase account for a sodic trend, which is evident from the Ca-Na-K diagram of Fig. 70. The chemical analyses of amphibolites will be discussed further below (p. 56).

Those amphibolites which are strongly scoriaceous and contain calcite or skarn minerals in the cavities have been referred to as spilitic metavolcanics

on the map, Plate 1. However, albitic rocks without such a scoriaceous structure occur (see above), and should be classified as spilites (see e. g. Heinrich 1956). These, however, do not form mappable units. They have consequently not been shown on Plate 1.

The most important area with strongly scoriaceous metaspilites lies between Bygget and Kolarsjön (E7-E8, F8). Similar rocks are also found at Pajkölen (364/434) and north of Los (c. 381/345). It should be noted that pillow lava structures have not been observed.

In the southern part of the Bygget-Kolarsjön area, highly calcareous, scoriaceous metaspilites are found as accumulations of large boulders in moraine. In extreme cases, only subordinate fragments of the metaspilite are found in the calcite. In the metaspilite itself, pale green hornblende, albite and epidote form main and essential minerals. In subordinate or accessory amounts occur iron oxide(s), biotite and chlorite. Calcite forms a quantitatively very variable constituent.

In several localities of the Bygget-Kolarsjön area non-scoriaceous amphibolites have been found. Such amphibolites consist mainly of a pale green, aluminous hornblende (cf. Table 1c: no. 31). Subordinate to accessory minerals are opaque minerals, clinozoisite, chlorite, sphene, biotite, sericite (after plagioclase), apatite and fluorite. Small amygdules of quartz, hornblende, calcite or epidote may occur. Rocks of this type probably grade into the strongly scoriaceous metaspilites.

In those parts of the scoriaceous metaspilite, which are situated near the Råtan granite, the calcite has been replaced by skarn minerals. Very heterogeneous schlieren have thus been formed, mainly consisting of diopside, common hornblende, epidote, garnet and plagioclase (oligoclase to andesine). In subordinate amounts occur opaque minerals, sphene, phlogopitic mica, clinozoisite, chlorite and calcite.

The diopside is characterized by an *mg* value of 0.6 in the two samples examined (Table 4: nos. 9 and 10). The garnet contains about equal amounts of andradite and grossularite (Table 5: no. 6).

At Pajkölen (364/434) there occurs a small outcrop of metaspilite with skarn schlieren. The rock is dark green to pale green or grey. The amphibolitic part consists of common hornblende and plagioclase (sodic andesine). In the skarn schlieren diopside with *mg* = 0.5 (Table 4: no. 11), epidote, grossularite (Table 5: no. 7), common hornblende, prehnite, sphene, calcite and microcline are to be found. Vesuvianite also occurs here.

Strongly scoriaceous metavolcanics are also found north of Los (c. 381/345), with calcite as a cavity filling. They contain albite, biotite, chlorite and calcite with minor opaque minerals, leucoxene, quartz and epidote. Gradations to normal amygdaloidal amphibolite occur.

According to the nomenclature of Rittmann (1952 and 1962a), the com-

position of the basic metavolcanics is basaltic to andesitic and the suite type, Pacific to weak Atlantic (Table 2). Chemical and modal analyses are presented in Table 1: nos. 27–31. The trend towards spilitic compositions is evident from Fig. 70 (p. 226), on which the average spilite of Sundius (1930) also has been plotted.

With regard to the trace elements, the basic metavolcanics show a distribution which is common in rocks of this nature. Especially noteworthy is the high chromium content (1,200 ppm) of the SiO_2 -poor amphibolite no. 31. This high value is consistent with the tendency for chromium to become enriched in early crystallates (Goldschmidt 1945; Rankama and Sahama 1952). BaO and SrO contents are a few hundred ppm, usually with somewhat higher values for the former.

The metabasic rocks described above include those where there is little or no evidence of alteration after the crystallization of common hornblende. Below, some cases are described, where the chemical or modal composition of the amphibolites has been subject to alteration. These phenomena mostly occur either in or near shear zones or in contact with the Råtan granite.

A transformation of the common hornblende to cummingtonite has sometimes been noted (e. g. at Selingen, 465/346), and Tenskog, 393/167). In the latter case, the hornblende has been completely replaced by cummingtonite (Table 3: no. 26). The two amphiboles here form oriented intergrowths. At the first locality a transformation to biotite-schist and cummingtonite amphibolite has taken place. In the biotite-schist anthophyllite and minor cummingtonite occur. The *mg* values obtained from optical determinations are 0.6 (cummingtonite) and 0.7 (anthophyllite). See Table 3: nos. 27 and 28. Up to some centimetres large, strongly poikilitic porphyroblasts of black tourmaline have been formed in the cummingtonite amphibolite.

In the tectonic zone along Sandsjöån (F1-F2, E3) occur amphibolites in which the common hornblende has become more or less completely transformed to chlorite. (All these occurrences are not shown on the map, Plate 1.) The plagioclase is strongly altered to epidote, sericite and calcite. Of probably similar origin is a quartz-biotite-chlorite rock at 273/031, which contains magnetite crystals of up to several millimetres' size.

In connection with sulphide impregnations (p. 132) the amphibolites show an alteration of the common hornblende to chlorite and biotite.

An occurrence of a basic metavolcanite in the argillitic hornfels at Östergården (301/412) attracts special interest. The rock consists mainly of plagioclase (An_{30} – An_{35}) and ferrohypsthene (Table 4: no. 12). In essential to subordinate amounts occur strongly poikiloblastic common hornblende and dark brown biotite, the latter showing thin quartz rims towards pyroxene. The hornblende is also found in coarse schlieren. Further, small amounts of cummingtonite and partly poikiloblastic quartz are observed. The textural

relationships seem to indicate that the ferrohypersthene was corroded by the two amphiboles and by the biotite. An alteration of cummingtonite to common hornblende also occurred. In usually subordinate to accessory amounts the following minerals have also been observed: opaque minerals (oxides), chlorite, apatite and carbonate.

The presence of ferrohypersthene shows that the orthopyroxene subfacies of the potash feldspar-cordierite hornfels facies of contact metamorphism has been attained near the Rätan granite contact (cf. Winkler 1967). The mineral paragenesis thus formed [ferrohypersthene-plagioclase(-biotite)] has been partially replaced by retrograde metamorphism to associations of cummingtonite, common hornblende, biotite and plagioclase. Pressure-temperature conditions necessary to attain potash feldspar-cordierite hornfels facies throw some light on the genesis of the Rätan granite (p. 74).

In an amphibolite xenolith in Rätan granite at Tandsjöhallan (C6-D6), up to centimetre-sized, poikiloblastic microcline augen occur at places. These augen, which may be polycrystalline, are sometimes surrounded by (incomplete) oligoclase mantles and contain corroded remnants of plagioclase. The amphibolite in addition to the feldspars also contains common hornblende, quartz and biotite. The growth of the microcline augen is to be ascribed to influence from the Rätan granite.

As already mentioned, basic metatuffites are not common in the Los-Hamra region, in spite of the extensive occurrence of amphibolites. They are mainly restricted to the area north of Los (H8-G8). The rocks show a compositional banding, identified as primary bedding because of interlayered meta-argillites. Pale green (actinolitic) hornblende, quartz, andesine and brown biotite in varying proportions form the major constituents.

In the Lillskog region (K5-K6) some similar metatuffites have been found. The following minerals form the bulk of these rocks: quartz, andesine, chlorite, common hornblende, epidote and biotite.

A high chlorite content of some phyllites has been noted (e. g. at 252/292). This may be due to an original admixture of basic volcanic material.

South of Malungshed (359/153), at the contact between amphibolite and meta-arenite, occur rocks which may possibly represent tuffaceous sandstones.

On the southern slope of Storfaxberget (c. 417/341) occur amphibolitic rocks, the relatively high quartz and biotite contents of which may indicate an admixture of epiclastic material.

5.1.2. PRIMOROGENIC (SYNKINEMATIC) INTRUSIONS

The Los Formation is synkinematically intruded by acid and intermediate primorogenic magmas. The relationship between the intrusions and the supracrustal rocks is mainly concordant. The intrusions form a differentiated



Fig. 16. Primorogenic granite with inclusions of argillitic gneiss. Storlugnet (290/269).
Photo Th. Lundqvist.

suite from quartz diorites to granites, with a predominance of the latter. For the possible occurrence of diorites and gabbros belonging to this suite see p. 52.

Two main types of primorogenic intrusions have been distinguished: acid and intermediate. The former range in composition from normal granite to light granodiorite. The latter have in turn been divided into two groups: granodiorites and quartz diorites to dark granodiorites. The acid intrusions correspond to what has been called "*sura urgraniter*" in Swedish literature, and the two groups of intermediate types to "*intermediära urgraniter*" and "*basiska urgraniter*", respectively.

The acid intrusions in particular show very clearly their intrusive relations to the supracrustal rocks. They thus sometimes contain xenoliths of the latter (Fig. 16) and grade into granophyres and fine-grained, quartz-porphyrific rocks towards the contacts. An alteration of slate to mica-schist has been mentioned earlier (p. 17). It was probably caused by the intrusion of primorogenic granite.

The term "primorogenic intrusions" has been used here, as the rocks in general are regionally schistose and/or lineated. These characteristics imply that they have been intruded before or during orogenic deformation (cf. p.

138). However, particularly the fine-grained marginal facies types, and also some medium-grained rocks, lack a foliation or lineation. This may be partly due to low mica content, but is probably also a function of a protected position during late-orogenic deformation (see below). The latter has been responsible for a schistosity and lineation which generally increase in intensity away from the contacts towards the central parts of the intrusive bodies.

In large areas, the primorogenic intrusions have been affected by serorogenic (late-kinematic) alterations. They have been recrystallized and migmatized to varying degrees. The formation of microcline augen¹ in the granodiorites of the Los-Hamra region geographically seems to be connected with the serorogenic alterations. On the whole, the fine-grained marginal facies varieties have been less affected by the serorogenic alterations than medium-grained types.

Where the process of migmatization has gone furthest, the primorogenic rocks form subordinate remnants in serorogenic pegmatite and granite (cf. above, p. 32). The origin of such migmatites (supracrustal or primorogenic rocks) may be hard to establish. Examples of strongly migmatized primorogenic rocks are e. g. found at Rytarklitten (I3) and east of Tackåsen (G1).

5.1.2.1. ACID PRIMOROGENIC INTRUSIONS

The majority of the primorogenic intrusions are of acid type. They are similar to the "acid oldest granites" ("*sura urgraniter*") occurring in many regions in the Svecofennides (e. g. Vänge granite, cf. Magnusson et al. 1963).

The acid intrusions are reddish grey to red, and occasionally grey in colour. For descriptive purposes they are here divided into medium-grained and fine-grained (marginal facies) types.

In the medium-grained acid intrusions quartz, perthitic microcline and plagioclase form the main and essential minerals. The plagioclase is usually oligoclase, but sometimes albite. Occasionally the composition is sodic andesine. Both microcline and plagioclase may form relict phenocrysts in the form of hypidioblastic or xenoblastic crystals of a larger size than the average of the rock. In such plagioclase, zoning may be present. Another common textural feature is the presence of myrmekite or albite rims on plagioclase, where the latter borders microcline.

Generally, microcline predominates over plagioclase, i. e. the rocks are normal granites. The reverse relationship is, however, sometimes observed,

¹ In Sweden the term "augen" has frequently been used for microcline megacrysts regardless of genesis and shape (tabular or ellipsoidal). This usage is also adopted in the present work.

and the rocks are categorized as granodiorites (Heinrich 1956). The medium-grained acid primorogenic intrusions thus range from normal granites to light (leucocratic) granodiorites.

Microcline augen (porphyroblasts) are much rarer in acid primorogenic intrusions than in intermediate ones, although distinction between porphyroblasts and relict phenocrysts is not always certain. The microcline phenocrysts are, however, much smaller (a few mm) than the porphyroblasts, which have been marked on Plate 1. The latter, which are above one centimetre in size, are mainly found in the migmatite terrains (e. g. 340/033) but do occur also in other regions (Dåasberget, I7). The possibly primorogenic, schistose augen-granites occurring near the Råtan granite at Långberget (E6) are discussed further below.

Essential or subordinate minerals are commonly brown or greenish brown biotite and/or muscovite. In the large tectonic zones (p. 140 ff.), however, an alteration to mica-schist has often taken place. In such mica-schist sillimanite needles have been observed in the muscovite (at 272/032).

The biotite may show an alteration to chlorite and sometimes to prehnite.

In one sample (Table 1c: no. 36) occur small amounts of common hornblende with strong absorption.

Accessories are opaque minerals, sphene, leucoxene, zircon, apatite, almandite, epidote, orthite, fluorite, calcite, rutile and tourmaline.

The contact facies of the primorogenic granites is generally fine-grained. Quartz-porphyritic and granophyric textures are common in such granites. Examples are found near Laxtjärn (G6), east of Noppikoski (E1), on Risberget (H4-H5) and west of Lossjön (H6). Non-porphyritic, fine-grained marginal varieties occur e. g. near Fetingsberg (I5-I6, J5-J6), in the Kvarnberg-Kuttermäki region (I3) and near Öv. Hamravallen (E6).

At 229/032 the contact towards meta-argillite is exposed. The granite is here quartz-porphyritic, with an aphanitic matrix. Approximately 50 m from the contact the groundmass has a grain size of c. 0.01–0.05 mm.

The texture of the fine-grained primorogenic granites is often porphyritic (Fig. 17) with about 1 mm diameter phenocrysts of quartz, microcline perthite and albite (or sodic oligoclase). Quartz phenocrysts are generally rounded and may show corrosion embayment. They are more or less strongly granulated. The feldspar phenocrysts show hypidiomorphic contours. In the groundmass, beautiful granophyric intergrowths between microcline perthite and quartz are often present (Fig. 18). The latter is usually in optic continuity with the quartz in the phenocrysts.

Quartz, microcline and albite predominate also in the groundmass. Micas (muscovite and more or less chloritized biotite) play a quantitatively more subordinate role than in medium-grained granites. Accessories are the same minerals as described for the latter.

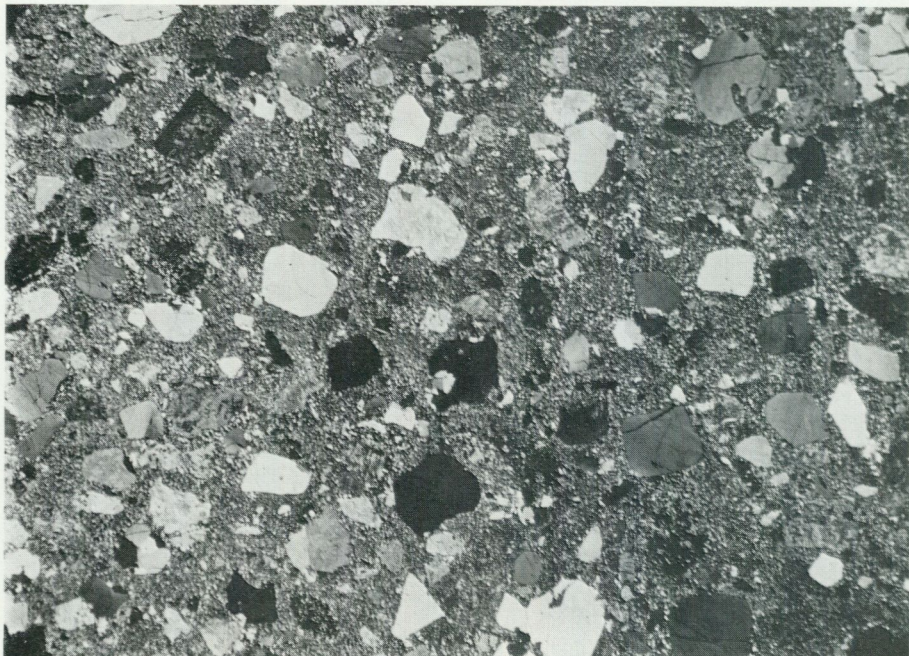


Fig. 17. Porphyritic marginal facies of the primorogenic granite. Phenocrysts of quartz, microcline perthite and albite in a fine-grained matrix. 2 nic., 5 x. Oreälven (229/031). Photo I. Signorelli.

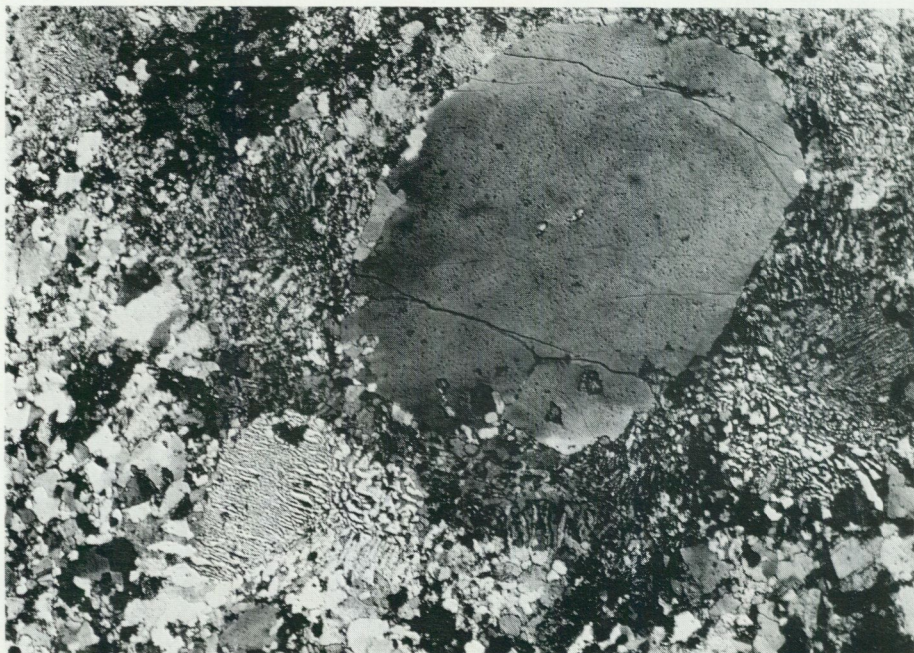


Fig. 18. Marginal facies of the primorogenic granite: phenocryst of quartz in a granophyric matrix. 2 nic., 22 x. South of Laxtjärn (311/277). Photo I. Signorelli.

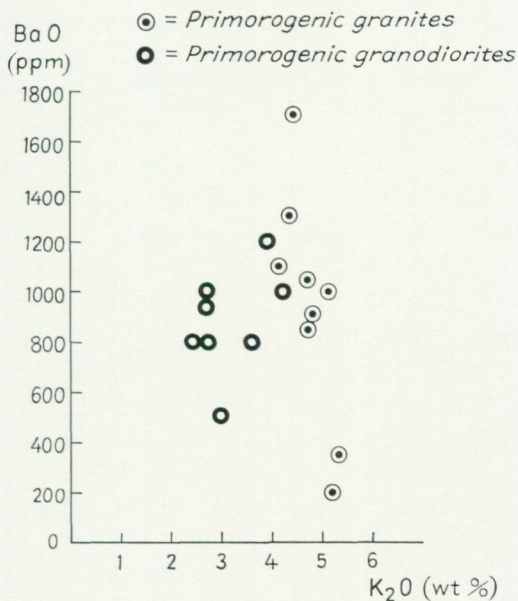


Fig. 19. Plot of BaO against K₂O for primorogenic intrusions in the Los-Hamra region.

Chemical and modal analyses of acid primorogenic intrusions are presented in Table 1: nos. 32–42 and Fig. 70. From the data given there, the acid and salic nature of these rocks is evident. Most of the analysed rocks are normal granites (mineralogical classification). Exceptions are nos. 35 and 37, which are light granodiorites.

Niggli *k* values are usually around 0.5. As to the trace elements, zirconium contents are 100–250 ppm. SrO is low. BaO varies between 200 and 1,700 ppm, and Rb₂O ranges usually from c. 100 to c. 300 ppm. Considering only the primorogenic intrusions with a normal granitic composition, there is a negative correlation between BaO and K₂O (Fig. 19). No correlation between Rb₂O and K₂O seems to exist. The relations between barium and potassium are of a type that would be expected if crystallization differentiation had operated (Rankama and Sahama 1952). For granodiorites, however, no correlation is indicated by the analyses (Fig. 19). The reason for this may be that assimilation of supracrustal material has contributed to the present composition. It is also to be noted that the granodiorites are generally more intensely affected by serogenic alterations than the granites (see further below, p. 65).

5.1.2.2. INTERMEDIATE PRIMOROGENIC INTRUSIONS

The intermediate primorogenic intrusions are mostly grey in colour and medium- or fine-grained. They usually show a schistosity and/or lineation. Porphyroblasts (augen) of microcline occur in large areas. The majority of the intermediate intrusions are found in migmatite terrains. A few observations show that they are cut by acid intrusions (near Storlugnet, 287/267). In the intermediate intrusions fragments of supracrustal rocks (meta-argillite etc.) have been observed. Fine-grained types near the contacts are rare, a character which might be a consequence of secondary recrystallization during serogogenic deformation. Near Storlugnet (288/267) a relict plagioclase-porphyrific texture has been observed (see below).

The modal composition of the intermediate intrusions is, by comparison with the acid types described above, characterized by a higher plagioclase : microcline ratio and a higher content of femic minerals, mainly biotite. The composition is thus granodioritic. A further increase in femic mineral content and decrease of microcline leads to the dark granodiorites and quartz diorites, which are described separately below (p. 65).

Main and essential minerals of the normal granodiorites are plagioclase, quartz, microcline and more or less chloritized greenish brown or brown biotite. Biotite-rich types may appear near the contacts towards meta-argillites (e. g. no. 45 of Table 1). This is probably due to an assimilation of argillitic material. Subordinate and accessory minerals are sericite and epidote (after plagioclase), apatite, opaque minerals, prehnite (after biotite), rutile, calcite, orthite, sphene and zircon, and sometimes also common hornblende. In some regions (e. g. between Nybyn and Hornberget, J3-J4), small amounts of almandite occur (cf. Plate 1).

The plagioclase is usually an oligoclase or sodic andesine. In a few cases occur relict phenocrysts (size c. 1 mm). In these, the cores may be as An-rich as labradorite. Near Storlugnet (288/267, cf. Table 1: no. 45) the relict plagioclase phenocrysts range between An_{62} and An_{17} in composition (normal zoning). The groundmass contains a plagioclase with c. An_{20} .

The plagioclase shows myrmekitic development and albite rims towards microcline in the same way as in the acid intrusions.

As already mentioned, microcline augen are common in the granodioritic intrusions. They are usually 1–3 cm in diameter and pink or greyish white in colour. Their shape is ellipsoidal (longest axes in the schistosity planes) or rectangular. The microcline augen are usually poikiloblastic. A thin mantle of oligoclase grains may surround the augen. An example of such mantling may be studied in moraine boulders near Öv. Lången (at c. 502/175).

Microcline augen are mainly found in the migmatite terrains, but also occur close to the contacts with the Råtan granite (see below, p. 71).

A strong recrystallization in connection with the migmatization may lead to an unfoliated structure and diffuse transitions to serorogenic granite. Alterations of this kind have been studied in the region of Hornberget-Nöningen (J3-J4).

Chemically, the intermediate, granodioritic, primorogenic intrusions, when compared with the acid intrusions, are characterized by higher contents of calcium, iron and magnesium and lower potassium and silicon (Table 1: nos. 43-47). In accordance with this, SrO is higher but Rb₂O lower than in the latter. BaO shows no clear relation to K₂O (Fig. 19, p. 63). A negative correlation between these elements exists for the acid intrusions (p. 63). The intermediate rocks are generally more strongly recrystallized and perhaps also somewhat metasomatically altered in connection with serorogenic migmatization. From the field observations it is evident that assimilation of supracrustal material has occurred. Thus, high biotite contents, e. g. at 288/267, may be referred to reaction with argillitic rocks. Similarly, the relatively hornblende-rich intrusion north-east of Hamra (see below) contains a xenolith of fine-grained amphibolite, and the composition of the intrusive rock is probably influenced by assimilation of the latter. Thus, it might be expected that the effects of crystallization differentiation, resulting in a definite trend in BaO : K₂O ratios, should be less clear in the case of the granodioritic intrusions.

There are in the area relatively rare occurrences of quartz diorite gradational to dark granodiorite. When compared with normal granodiorites these are characterized by a higher content of femic minerals (mainly hornblende). The rocks in question have only been noted to outcrop in two places: north-east of Hamra (F5) and near Västersjön (J5-K5). Observations of moraine boulders at G5 indicate the presence of similar rocks there.

Both at F5 and J5-K5 occur fine-grained amphibolites as xenoliths in the primorogenic intrusions (cf. above).

The quartz diorites and femic granodiorites are dark grey and medium-grained. Plagioclase (c. An₂₆-An₄₇) forms the most important constituent and commonly shows normal zoning. Essential minerals are common hornblende and greenish brown biotite. The quartz content varies (\leq c. 25 %). Microcline forms less than 10 % of the rocks. The higher microcline contents give a granodioritic composition, the lower ones (accessory amounts) a quartz-dioritic (Heinrich 1956).

Sphene forms a subordinate mineral. Accessories are epidote with sericite (after plagioclase), opaque minerals, apatite, zircon, prehnite, chlorite (after biotite) and calcite.

Chemical and modal analyses of a dark granodiorite are given in Table 1: no. 48.

5.1.3. MAINLY SEROROGENIC (LATE-KINEMATIC) INTRUSIONS AND ALTERATIONS

The serorogenic (= late-orogenic) alterations of supracrustal and primorogenic rocks generally are characterized by recrystallization and migmatization of varying intensity. Part of the granitic material formed by the latter process attained a high mobility and intruded the adjacent lithologies. In this way, plugs and cross-cutting dikes of granite, pegmatite, medium-grained aplite granite and fine-grained aplite were formed. These rocks generally lack schistosity, but sometimes a weak parallel orientation of mica may be observed. In several of the migmatite regions microcline porphyroblasts (augen) have been formed. In some areas, however, the growth of such porphyroblasts was probably related to the intrusion of the Råtan granite (p. 69 f.). Likewise, some pegmatites near the latter may be connected with this granite rather than with serorogenic processes (e. g. at 414/356). Granitic dikes and schlieren in the N. Stensjön region (G8-G9) in all probability also derive from the Råtan granite magma.

Pegmatites and aplites are generally associated with the migmatites. Locally, however, dikes and schlieren of this kind may also have formed as differentiates in the primorogenic granites. It is not always possible to distinguish between the two genetically different kinds of pegmatite and aplite.

The migmatites formed from supracrustal and primorogenic rocks have been treated above, in connection with the descriptions of the latter rock types (pp. 32, 36, 60 and 65). For descriptions of the augen-bearing gneisses etc. see pp. 32, 61 and 64. Skarn minerals, formed in crystalline limestone through the invasion of pegmatite, have been described by von Eckermann (1922). See also p. 38.

Only the different granitic (palingenic) products of the serorogenic processes are treated below.

5.1.3.1. PEGMATITE, APLITE GRANITE AND APLITE

Pegmatite, aplite granite and aplite occur in intimate association with each other. The coarse-grained pegmatite usually predominates over medium-grained aplite granite and fine-grained aplite.

The colour of these granitic types is greyish white to pink, and occasionally red. Quartz, microcline perthite and albite (to oligoclase) are the main constituents. In more subordinate amounts occur muscovite, biotite and chlorite. Muscovite is especially abundant where pegmatite has intruded meta-argillites just outside the migmatite regions. Thus, north-west of Storlugnet (279/269) a mica-rich argillitic gneiss has been invaded by pegmatite.

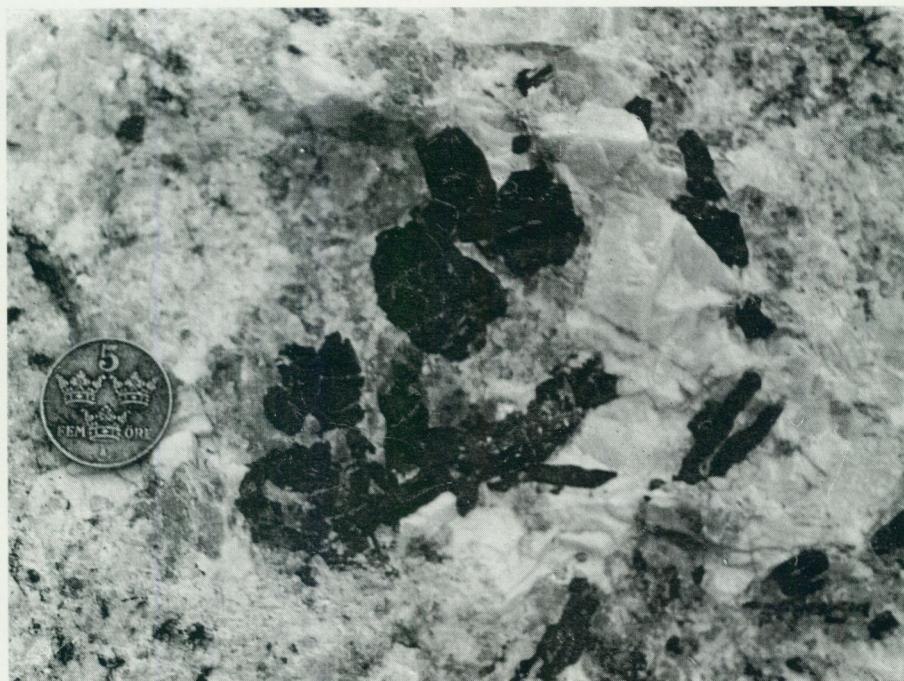


Fig. 20. Black tourmaline crystals in pegmatite. Road-cutting east of Rensjön (287/091). Diameter of coin = 27 mm. Photo Th. Lundqvist.

A series of granitic rocks with strongly varying muscovite contents has been formed in this way. They sometimes contain very muscovite-rich aggregates, which represent incompletely assimilated inclusions of argillitic material.

Chlorite in the pegmatites has mainly been formed through alteration of biotite or garnet.

In addition to the minerals mentioned above, small quantities of black tourmaline, garnet, bluish green apatite, cordierite and sometimes also violet fluorite may be found in the pegmatites. As accessories zircon and opaque minerals also occur.

Tourmaline in particular appears in connection with meta-argillites (and quartzites) which have been migmatized or intruded by serogenic granite or pegmatite. Occasionally, dikes containing this mineral may also occur near primorogenic granite and Råtan granite. At Laxtjärn (c. 307/281) such dikes cut through the granophyric marginal facies of the primorogenic granite. In the dikes and schlieren in the Össjön-Pajkölen area (G9-H9), mentioned above, black tourmaline also occurs.

The most important massif of tourmaline-garnet-bearing pegmatite is situated in the Rensjön-Storhamrasjön region (F2-F4) and is particularly well



Fig. 21. Quartzite breccia with a tourmaline matrix. East of Tenskog (400/158).
Photo Th. Lundqvist.

exposed in road-cuttings immediately east of Rensjön. The tourmaline crystals may attain a few centimetres in length (cf. Fig. 20). They partly form graphic intergrowths with quartz. The pegmatite also contains small quantities of garnet, bluish green apatite and cordierite.

Another locality where tourmaline-bearing pegmatite may be studied occurs near Storlugnet (279/269, cf. above). There, the tourmaline is accompanied by almandite (Table 5: no. 8) and bluish green apatite, and often forms radiating aggregates on joint surfaces. In the surrounding argillitic gneiss occur thin dikes, which mainly consist of tourmaline, quartz and biotite. Accessories are muscovite, opaque minerals and apatite. A similar tourmaline-quartz-biotite rock forms the matrix of a quartzite breccia near Tenskog (400/158, see Fig. 21). In this case, however, no clear relationship to serogenic processes exists (cf., however, p. 142).

5.1.3.2. SEROROGENIC GRANITE

Only small areas with relatively homogeneous, medium- to fine-grained serorogenic granites have been found within or near the migmatite terrains. These granites correspond in their tectonic position to e. g. the Stockholm, Skellefte and Härnö granites of other parts of the Svecofennides (cf. Mag-

nusson et al. 1960). Their colour is reddish grey or grey, and their mineralogical composition is similar to that of the above described pegmatites, i. e. they mainly consist of quartz, microcline and albite-rich plagioclase. Subordinate minerals are biotite and muscovite. The latter, however, forms c. 10–20 % of a granite which is found in large, local boulders at 285/279.

5.2. POST-OROGENIC COMPLEX

5.2.1. OLDER POST-OROGENIC GRANITE (RÄTAN GRANITE)

The northern parts of the Los-Hamra region are occupied by the southern margin of the porphyritic Rätan granite (Högbom 1894: p. 16). The granite extends northwards over an area of 5,000 sq. km (see the map of Magnusson et al. 1960). Only the southern margin of the Rätan granite massif is exposed within the Los-Hamra region.

A southerly outlier of the Rätan granite occurs in the Tandsjön–Svartåvallen–Sandsjö region (C6-D7-E5). It is isolated from the large massif in the north by primorogenic intrusions between Sjöändan and Rullbo (C7-E7).

The relations between the Rätan granite and other rock units in the Los-Hamra region are as follows. The granite is younger than the supracrustal rocks of the Los Formation and the primorogenic intrusions. This is evident from the following observations. In the Bygget–Kolarsjön region (E7-E8, F8) and at Pajkölen (364/434), the calcite of spilitic metavolcanics has reacted to give skarn assemblages close to the Rätan granite contact (p. 56). A transformation of meta-argillites to hornfelses has taken place over large areas of the contact zone (p. 22 ff.). A layer of basic metavolcanite in these hornfelses is characterized by the assemblage orthopyroxene-plagioclase (p. 57). In all the above cases the modal compositions are certainly formed by the influence of the Rätan granite intrusion. Further, in the Össjön–Pajkölen region (G9-H9) microcline-porphyritic granitic dikes and schlieren occasionally occur in the meta-argillites. In all probability they were derived from the Rätan granite.

A fine-grained, somewhat microcline-porphyritic marginal facies of the Rätan granite brecciates meta-argillite at N. Stensjön (339/418, see Fig. 22). The microcline augen are here up to 0.5 cm in size, i. e. smaller than usual. The same trend towards fine-grained groundmass and smaller and fewer microcline augen near the contact has been observed, e. g., at Pajkölen (358/437). However, the Rätan granite may also remain unchanged in grain size and frequency of augen up to the contact, a phenomenon which has been observed *inter alia* near Kolarsjön (269/372).

Metasomatic formation of microcline augen has been observed in an amphibolite xenolith at Tandsjöhallan (C6-D6, see above, p. 58). In addition, small fragments of more or less assimilated amphibolite, sometimes with microcline porphyroblasts, are frequently observed in the Rätan granite.



Fig. 22. Porphyritic marginal facies of the Rätan granite intruding and brecciating meta-argillite. East of N. Stensjön (339/418). Photo Th. Lundqvist.

In moraine boulders north of Rullbo (210/384) unfoliated Rätan granite cuts the schistosity of primorogenic granodiorite. At c. 168/372, poikilitic microcline augen in primorogenic granite seem to be connected with the intrusion of the Rätan granite. Near Svartån (223/306), acid Rätan granite contains sheets of some tens of metres' length of grey, primorogenic granodiorite and sulphide-bearing meta-argillite.

Contacts between the Rätan granite and the migmatites and serorogenic pegmatites and granites have never been observed in the Los-Hamra region. As, however, the Rätan granite has not been affected by the migmatizing processes, it must be regarded as younger than these. It differs from the serorogenic granites in several respects. Pegmatite and aplite seldom occur. No geographical connection with migmatites exists. The Rätan granite is generally unfoliated and lacks linear structures. Resemblance to the Dala granites (p. 114) with regard to these features is greater than to the serorogenic granites. In addition, the Rätan granite shows evidence of differentiation (see below). For these reasons the Rätan granite is here grouped with the post-orogenic rocks. See also p. 158.

The important age relationship between the Rätan granite and the sub-Jotnian igneous rocks is also not known through field observations (cf. p. 114). This relationship can be most suitably investigated by isotope age determination methods (p. 158). Dolerites of Jotnian type cut the Rätan granite. Northwest of the Los-Hamra region, in the County of Jämtland, Jotnian sandstone is known to be younger than this granite (Lundegårdh 1967: p. 36). Thus, from direct field observations, it is only possible to state that the age of the Rätan granite lies somewhere between that of the primorogenic intrusions and that of the Jotnian sedimentation.

Generally, the contacts of the Rätan granite are cross-cutting and sharp. Two important exceptions have, however, been observed, viz. north of Sättnässjön (I8) and around Långberget (D6-E6). In both these cases tectonic movements have affected the bedrock after the intrusion of the granite.

North of Sättnässjön (I8), transitional types between Rätan granite and primorogenic, more or less schistose granodiorite with microcline augen have been observed, mostly in moraine boulders. Deformation in the NNW-striking tectonic zone, which passes through the region (p. 140), makes it hard to establish, whether certain weakly schistose rocks represent Rätan granite or strongly recrystallized (and perhaps metasomatically altered) primorogenic rocks.

Similar conditions prevail in the Långberget region (D6-E6). The bedrock is, however, better exposed here. Non-schistose, augen-rich granites with a higher quartz content than the normal Rätan granite (cf. analysis no. 53 of Table 1) successively pass into similarly composed granites possessing a schistosity. The latter granites have strongly cataclastic textures (cf. p. 141): the quartz is granulated and "rolled out" and the feldspars are marginally crushed ("mortar structure"). Clearly primorogenic granodiorites also occur in the form of medium- to fine-grained, biotite-rich, strongly schistose rocks with scattered microcline augen. On the map, Plate 1, the granites with cataclastic textures mentioned above have been marked as primorogenic. However, two possible interpretations exist for these. They may represent primorogenic granites, in which a schistosity was developed by orogenic deformation. Growth of microcline augen would be related to subsequent intrusion of the Rätan granite, prior to late cataclasis. Alternatively, they may belong to the Rätan granite and have wholly received their parallel structure during the late cataclastic deformation, which also affected the Dala granites to the west (see p. 141). On account of the latter deformation, it does not seem possible to decide whether a pre-cataclastic schistosity existed in the granites in question. The problem is further complicated by the fact that some primorogenic granites in the Los-Hamra region lack a macroscopically visible schistosity.

Lundegårdh (1967: p. 89) mentioned transitions between Rätan granite and

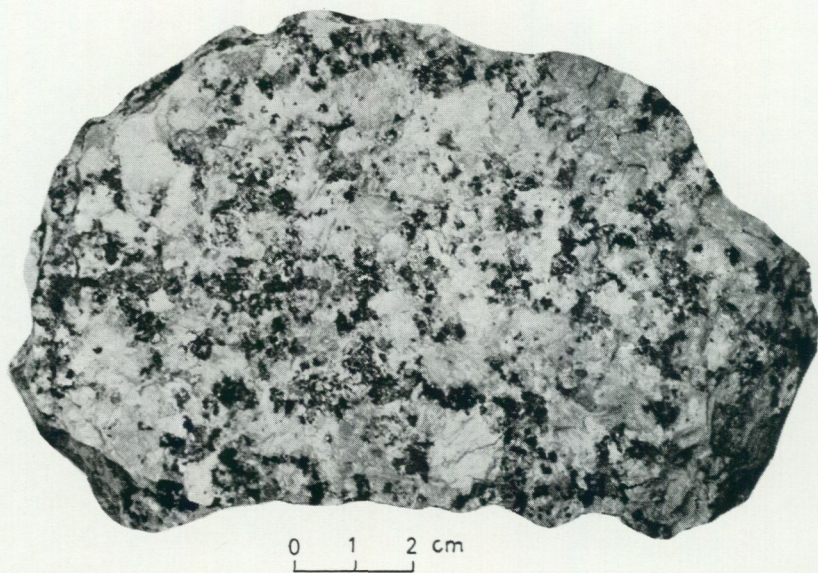


Fig. 23. Specimen of (normal) Rätan granite. Kolarsjön (266/390). Photo Th. Lundqvist.

the older Ljusdal granite in the region of Kårböle. He ascribed these transitions to a regeneration of the latter granite.

The normal Rätan granite of the large, northern massif (Fig. 23) is very homogeneous within the Los-Hamra region, both with regard to mineralogical-chemical and structural features. It is unfoliated and reddish grey to red, occasionally grey in colour. About one fourth of the rock is made up of pink microcline augen (1–2 cm). Contact varieties (cf. above), however, may contain fewer, smaller augen. The microcline augen are roughly tabular parallel to (010) or somewhat ellipsoidal. In detail, however, the contours are generally irregular and the microcline may finger into the groundmass (porphyroblastic character). Karlsbad twinning occurs. The groundmass between the augen is usually medium-grained, but is sometimes fine-grained in the marginal facies (cf. above). The predominating minerals are microcline perthite and plagioclase. The former occurs both in the augen and the matrix. The marginal parts of the augen in particular contain inclusions of plagioclase (oligoclase with albite rims) and biotite. Granophyric intergrowths of quartz and microcline are occasionally present. Sometimes a zonal structure following crystallographic surfaces may be observed in the microcline augen. It is caused by different sizes of the exsolved albite, e. g. an alternation between vein perthite and film perthite (cf. Andersen 1928). Oligoclase mantles of around 1 mm width may surround the microcline augen (rapakivi texture). This is not, however, a typical texture of the Rätan granite. The oligoclase mantle may be in approximate crystallographic continuity with

the microcline and its exsolved albite. The border between microcline and the oligoclase mantle is sutured and gives the impression of corrosion. Graphic intergrowths between quartz and oligoclase occur.

Anti-rapakivi texture (albite mantled by microcline) has been observed, but only rarely. (See also p. 115 f.)

The plagioclase forms up to a few millimetres large crystals, which are often tabular parallel to (010). It is usually zoned (normal zoning). The composition is generally oligoclase (c. An₁₅-An₃₀), but varies in the samples examined between An₁₀ and An₄₇. In addition, thin albite rims may be found between plagioclase and microcline. Myrmekitic intergrowths of plagioclase and quartz are found in a similar position. A strong alteration to sericite and epidote may occur, particularly in the cores of zoned plagioclase crystals.

Essential minerals in the Rätan granite are quartz and brown biotite. The latter may show an alteration to chlorite or prehnite. Subordinate constituents are common hornblende, magnetite and sphene. Wedge-shaped crystals of sphene measuring up to c. 5 mm in length are sometimes found (cf. p. 8). In rare cases remnants of clinopyroxene (augite) occur in the hornblende. The femic minerals of the Rätan granite are frequently clustered in aggregates.

Accessories are apatite, zircon, ilmenite, chalcopyrite, pyrite, fluorite, calcite and orthite.

The typical "rapakivi weathering" (in situ disintegration to gravel) is occasionally observed in the Los-Hamra region. In other parts of the Rätan granite massif, however, it may locally be prominent (cf. Lundegårdh et al. 1964: pp. 32 and 87).

The normal Rätan granite is usually poorly jointed. For this reason, it frequently forms moraine with large boulders (up to several metres in diameter).

The Rätan granite in the isolated occurrence of the Tandsjön-Svartåvallen-Sandsjö region (C6-D7-E5) is less homogeneous than in the northern massif. The frequency, size and shape of the microcline augen are more variable. In some parts the granite is even devoid of augen and medium-grained. The size of the microcline augen ranges between c. 0.5 and 4 cm. In some regions (e. g. east of Nätsjön, 195/240 and south-east of Långberget, 225/255) they show a very pronounced tabular development parallel to (010). Such microcline augen may show a "fluidal" preferred orientation.

Generally, the Rätan granite of the southern outlier is richer in quartz than that of the larger northern massif (cf. below). Further, the plagioclase is of a more albitic composition (oligoclase or albite), and hornblende and sphene are much less important. In the most acid types the biotite content is much lower than in normal Rätan granite. (Cf. Table 1: no. 54.)

This southern massif of the Rätan granite also generally lacks a

schistosity. In tectonic zones (e. g. 223/236), however, it may show a prominent parallel structure due to cataclastic deformation (cf. also p. 141).

The alteration of the meta-argillites at Svartån (c. 243/298), caused by the southern outlier of Rätan granite, corresponds to the hornblende-hornfels facies (Winkler 1967). Thus, the higher-grade potash feldspar-cordierite hornfels facies has not been attained here.

For a mineralogical classification of the whole Rätan granite suite it is necessary to estimate the volume ratios microcline : plagioclase. This can be done for augen-rich types by using chemical whole rock analyses (Table 1a), modal estimates (Table 1c) and determinations of the composition of microcline augen (Table 7: nos. 5-7). Such estimates show that in the normal Rätan granite of the northern massif (Table 1: nos. 49-52) both plagioclase and microcline perthite may be the predominating feldspar. It follows that the composition ranges from quartz-poor granodiorite to quartz-poor granite (Heinrich 1956). In the southern massif (Table 1: nos. 53-54) the rocks are classified as granites. Also the late differentiates (aplite and granite porphyry, cf. below) show a granitic composition (Table 1: nos. 55-56).

From the above description it is evident that the Rätan granite displays many features which may be taken to indicate a magmatic origin. Perhaps the strongest argument for such a genesis is the hornfels contact aureole (p. 22). The argillitic, originally water-rich composition of the hornfels makes it unlikely that the appearance of the cordierite-microcline assemblage has been caused by a deficiency in water (cf. p. 23). The temperature necessary to attain potash feldspar-cordierite hornfels facies is $600 \pm 20^\circ$ at 1,000 bars (3.5 km depth) and $630 \pm 20^\circ$ at 2,000 bars water pressure (7 km depth). See Winkler (1967). Assuming a lower temperature limit for the potash feldspar-cordierite hornfels facies of 620° for a depth of 5-6 km, and a geothermal gradient of about $30^\circ/\text{km}$, an estimate can be made of the magma temperature necessary to cause the appearance of potash feldspar-cordierite hornfels parageneses (see Winkler op. cit.: p. 78 ff.). This gives around 720° , which is a minimum value. The presence of orthopyroxene in a basic metavolcanite (p. 57) indicates that the lower temperature limit of the potash feldspar-cordierite hornfels facies must have been exceeded by c. 100° near the granite contact (Winkler 1967). A minimum magma temperature of about 900° is thus likely. A closer approximation to the magma temperature can be obtained only if the width of the contact aureole and the thickness of the intrusion are known. The hornfels have been located up to c. 2 km from the contact. However, the dip of the contact between the Rätan granite and the hornfels is not known (cf. p. 138), and therefore no further estimate of the temperature of the magma can be made. The calculation carried out for a depth of 5-6 km in any case points to temperatures well within the magmatic range.

The porphyroblastic character of the microcline augen described earlier (p. 72) does in no way contradict a magmatic origin. Such textural features may result from crystallization processes in a late stage of the granite formation (Mehnert 1959).

Acid differentiates in the form of aplite, pegmatite and granite porphyry are rare in the Rätan granite. In the few occurrences where such rocks may be observed, they either form a network of schlieren with gradual transitions to the Rätan granite or cross-cutting dikes with sharp contacts.

The aplites etc. are usually reddish grey to red in colour. They consist mainly of quartz, microcline perthite and plagioclase (albite or oligoclase). In the varieties designated as granite porphyries all these minerals may form phenocrysts in a fine-grained groundmass. The latter sometimes shows granophyric textures. Phenocrysts of quartz are xenomorphic; those of microcline are xeno- or hypidiomorphic and often somewhat poikilitic. Plagioclase phenocrysts are hypidiomorphic (tabular) and show normal zoning. In a sample from St. Acksjöberget (109/452, cf. Table 1: no. 56) they have a composition of c. $(An_{40}-)An_{25}-An_{20}$, while the groundmass plagioclase ranges from An_7 to An_{16} .

Small amounts of biotite, chlorite, common hornblende, sphene, epidote, sericite, apatite, zircon, fluorite and tourmaline may be present in the late differentiates. In a granite porphyry from St. Acksjöberget (109/452), strongly uralitized clinopyroxene has also been found.

Near Garpmyran (190/426) there occur scattered grains of molybdenite, pyrite and pyrrhotite in pegmatite and aplitite belonging to the Rätan granite.

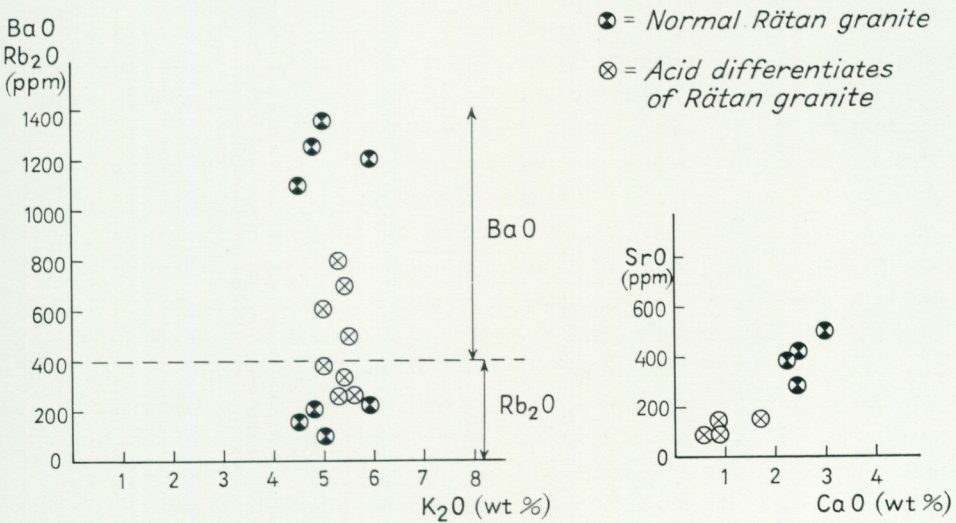


Fig. 24. Plots of BaO and Rb₂O against K₂O, and SrO against CaO for Rätan granite with acid differentiates.

Chemical and modal analyses of the Rätan granite and its late differentiates are given in Table 1: nos. 49–56. (Cf. also Fig. 70 on p. 226.) The relatively low quartz content in the northern massif is expressed by low qz values (c. 30–80). Niggli k values are between 0.43 and 0.50 for normal Rätan granite and usually somewhat above 0.50 for acid types. The analysis no. 73 of von Eckermann (1936), however, shows a lower k value (0.44) for an aplite cutting through Rätan granite.

Among the trace elements, barium, strontium, rubidium and zirconium are of particular interest. The $BaO : K_2O$ ratio is higher in normal Rätan granite than in the acid differentiates (Fig. 24). For the $Rb_2O : K_2O$ ratio the opposite is true. This is in accordance with the tendency for barium to become enriched in early and rubidium in late potassium minerals (Rankama and Sahama 1952). From the relations between the ionic radii of strontium and calcium, the former element would be expected to become relatively enriched in the late differentiates. No such tendency is shown in the diagram of Fig. 24, however. This is probably due to the strontium-potassium diadochy, viz. strontium is captured in early potassium minerals (Rankama and Sahama 1952), which tends to compensate for the enrichment in late differentiates (cf. SrO analyses of Table 7: nos. 6 and 7).

Regarding zirconium, there is a tendency in the analyses 49–56 of Table 1a for somewhat higher contents in normal Rätan granite than in the acid differentiates.

5.2.2. SUB-JOTNIAN COMPLEX

The term sub-Jotnian was introduced by Högbom (1909) for a group of igneous rocks occurring in intimate association with Jotnian (p. 120) sandstones and dolerites and partly underlying the former. Högbom was of the opinion that the Jotnian was separated from the sub-Jotnian by a period of considerable erosion. In the sub-Jotnian Högbom included the igneous rocks of the Nordingrå, Rödö and Ragunda regions in central Sweden, as well as the rapakivi granites in Finland. Regarding the Dala volcanics and granites described here, Högbom (1909) pointed to some features which favour a connection with the sub-Jotnian rocks. However, the abundance of volcanic deposits was not considered characteristic of sub-Jotnian complexes. Högbom therefore hesitated to ascribe such an age to the Dala porphyries etc., and considered the latter to have an undecided position. Later, however, Dala porphyries, porphyrites and granites were included among the sub-Jotnian rocks (Sederholm, in Högbom 1913: p. 24).

von Eckermann (1936) maintained that intercalations of the Dala porphyries and porphyrites and the Dala sandstones occurred in the Los-Hamra region. The concept of a major hiatus between the Dala volcanics and the

Dala sandstones was therefore rejected. The term Jotnian was used for all these rocks.

Hjelmqvist (1966) divided the sub-Jotnian of Kopparberg County (south to west of the Los-Hamra region) into the Dala granites and the Upper and Lower Dala series. The Upper Dala series corresponds to the Dala Volcanics Formation of the present work. In the Lower Dala series Hjelmqvist included some supracrustal rocks which were earlier regarded as Gothian or Dalslandian (cf. map of Magnusson et al. 1960). This series included both volcanic deposits (porphyries and porphyrites) and normal sedimentary rocks (quartzites, schists, conglomerates, arkoses). Hjelmqvist considered the supracrustal rocks around Noppikoski (E1-D1) to belong to the Lower Dala series, which conflicts with the results of the present investigation (see pp. 61 and 163). Such a position for these rocks would give them an age younger than that of the late-Svecofennian granites.

In the Los-Hamra region the sub-Jotnian complex includes Dala granites (Dala-Härdal granites of Lundegårdh 1967) and mainly volcanic supracrustal deposits (Dala Volcanics Formation). Rocks which can be ascribed to the Lower Dala series of Hjelmqvist (1966) are apparently lacking (cf. p. 88).

The rocks of the sub-Jotnian complex have a post-orogenic character in relation to the orogenic complex described above. They are non-schistose and have not been affected by regional metamorphism. The low-temperature alterations which have led to parageneses with chlorite, epidote etc. (cf. below) are probably related to post-magmatic activity, but may also be caused by hydrothermal activity in late faults and fissures. Deformation of the sub-Jotnian complex, which has i. a. given the westerly to south-westerly dips of the supracrustal rocks (cf. below), can be ascribed to block movements (tilting and faulting).

5.2.2.1. DALA VOLCANICS FORMATION

The supracrustal rocks of the sub-Jotnian complex form the Dala Volcanics Formation. In this, volcanic rocks of essentially two types predominate: acid Dala porphyries and Dala porphyrites of mainly basic to intermediate character. Sedimentary deposits are found in the basal layers of the formation and as subordinate intercalations ("Digerberg sandstone"; cf. Hjelmqvist 1966: p. 73) in the porphyrites and porphyries. These intercalations have largely the character of reworked volcanic material (tuffites and conglomerates), but normal tuffs and agglomerates also occur.

The basal layers of the Dala volcanics are made up of sandstones, siltstones, conglomerates and breccias. Pyroclastic material has been observed, but the quantitative importance of this is hard to estimate because of the strong silicification which has affected much of the basal layers.

An unconformity separates the Dala Volcanics Formation from the supra-crustal rocks of the orogenic complex. It is regionally discordant, but may be locally approximately concordant (see further p. 139). No migmatite and granite clasts have been found in the basal conglomerates and breccias. These observations suggest that the orogenic complex was not deeply denudated before the extrusion of the Dala volcanics.

The Dala porphyries of the Los-Hamra region are characterized by phenocrysts of perthitic alkali feldspar and plagioclase, with occasional quartz. In contrast to this, the phenocrysts of the more basic porphyrites are plagioclase and feric minerals but never perthitic alkali feldspar. However, in porphyrites of Kopparberg County, Hjelmqvist (1966) mentioned the subordinate occurrence of potash feldspar and quartz among the phenocrysts.

Dala porphyries, which are the dominating volcanics, are exposed within an area of about 4,000 sq. km, of which only a small part falls in the Los-Hamra region. However, the total extent of such rocks is much larger, as Dala porphyries occur under the cover of Jotnian sandstone in Kopparberg County (cf. Hjelmqvist 1966).

The Dala volcanics dip at low or medium angles to the west or southwest. This is shown by observations of bedding in the layered intercalations within the volcanics and the orientation of the ignimbrite "flames" (see below) in the Dala porphyries. The "flames" generally lie in a surface approximately parallel to the bedding (as is the case in the orogenic complex). From a consideration of the genesis of the "flames" (p. 105), however, they cannot be expected to reflect precisely the bedding orientation. Steep dips of ignimbrite "flames" and band structures in porphyries may be referred to faulting (p. 140) or flow in the ignimbrite sheets (p. 106).

In general the basal layers are overlain by Dala porphyrites, although porphyries appear to be the oldest volcanics in some areas (D4, D5). The relations between the porphyry at Silverknoppen (B6-C6) and the surrounding porphyrites are not clear. It may be an isolated denudated relic of the larger sheets in the south-west and thus be younger than the porphyrites. It may also form an intercalation in the latter. From observations of clasts in intercalated horizons of conglomerate in the porphyrites, it is clear that porphyries have been extruded before or contemporaneously with the porphyrites (see p. 94).

The Dala porphyrites of Kopparberg County show broadly the following stratigraphic succession, which is, however, not the same over the whole area (Hjelmqvist 1966). Conglomerates, tuffites and agglomerates form the oldest deposits, followed by red porphyrites. The latter are overlain by conglomerates etc., on top of which rest grey porphyrites. In the Los-Hamra region the succession may be regarded as roughly similar, although irregularities are numerous.

The main mass of porphyries is younger than the porphyrites. In the former, some trends with decreasing age may be discerned, although a general stratigraphy cannot be established. The oldest porphyry is either phenocryst-rich (e. g. D3) or phenocryst-poor with ignimbrite "flames" (eutaxitic) as e. g. near Sundsjön (D4). The latter type of porphyry is most abundant in the lowest parts of the stratigraphic sequence. In the uppermost (western) parts, the phenocryst-poor porphyry of Bredvad type (cf. Hjelmqvist 1966: p. 96 ff.) predominates. In the Älvdalen region of Kopparberg County, Looström (see Hjelmqvist 1966: p. 73) found that the phenocryst-rich porphyry was the oldest, overlain firstly by a eutaxitic type and then by phenocryst-poor (Bredvad) porphyry. This stratigraphy has been confirmed for some sections in Kopparberg County by Hjelmqvist (op. cit.) and the Los-Hamra region by the present author. Exceptions are, however, present.

It does not seem possible to make a good estimate of the total thickness of the Dala Volcanics Formation. Observations of bedding etc. are too few and variable in dip to allow a regional estimate. However, it seems reasonable to assume that the formation is several thousand metres thick.

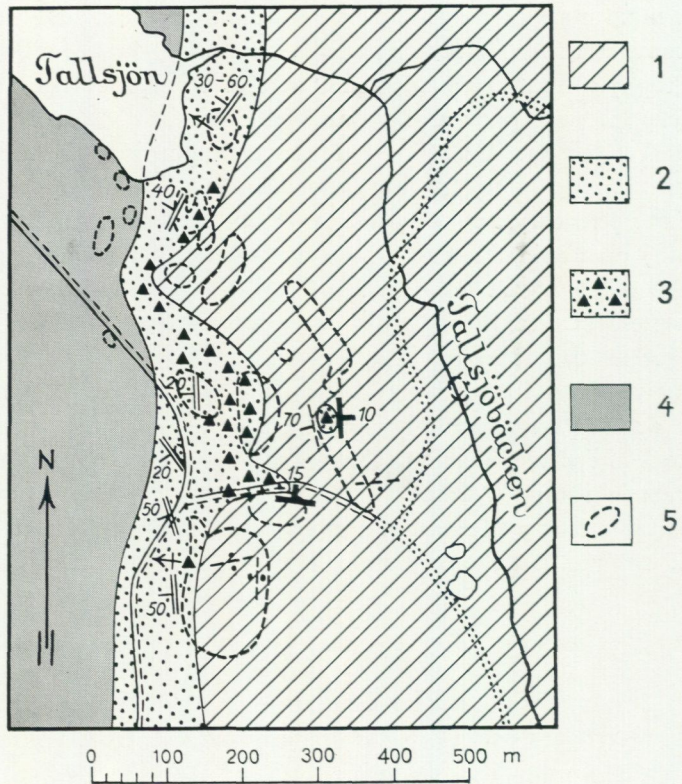
5.2.2.1.1. BASAL LAYERS OF THE DALA VOLCANICS

The basal layers of the Dala volcanics occur in an approximately 100–200 m broad, interrupted belt along the eastern margin of the volcanics. They can be followed from Oreälven at 189/033 via Tallsjön (D2) to Sandsjöberget (192/137). An isolated occurrence is found in a railroad cutting east of Tandsjön (149/273). At 166/206 the basal deposits are missing and Dala porphyry rests directly on quartzite. The thickness of the basal layers is hard to estimate because of variations in dip, but south of Tallsjön (c. 190/072), where the bedrock is well exposed, it seems to be ≤ 70 m. The bedding here dips 20–60° to the west (see Fig. 25).

For a description of the unconformity below the basal deposits, see p. 139.

The basal layers are composed of breccias, conglomerates and more or less tuffaceous sedimentary rocks, often in rapid alternation. A strong silicification (deposition of chalcedony) is characteristic of the larger part of the basal deposits. Fissures in the rocks are filled with quartz (partly rock crystal), chalcedony, hematite and fluorite. Sometimes (south of Tallsjön) the breccias etc. are weakly impregnated with minute sulphide grains.

A large part of the basal layers is made up of sedimentary rocks with clastic material of sand or silt grade (c. 0.03–1 mm). The most fine-grained types are microcrystalline. Vivid colours are characteristic of the basal rocks: dark violet, chocolate brown, reddish brown, pink, greyish white and grey. Bedding may be well developed in the sandstones. Cross-bedding is sometimes observed, as in the area south of Tallsjön (D2). Through observations of such



Scale 1:10000

1. Metarhyolite, mostly quartz-porphyritic
Metarhyolit, mestadels kvartsporfyrisk
 2. Silicified sandstone
Förkislad sandsten
 3. Silicified breccia
Förkislad breccia
 4. Dala porphyrite
Dalaporfyrit
 5. Outcrop (schematically indicated)
Hällyta (schematiskt angiven)
- For structure symbols, see Plate 1
Struktursymboler, se plansch 1

Fig. 25. Petrographic map of the region immediately south of Tallsjön (D2).

bedding it is confirmed that the beds face westwards (Fig. 25). In local moraine boulders in this locality ripple marks and mud-cracks have also been observed (Figs. 26 and 27). The latter are filled with sandstone and cut through sericite-rich layers.

The basal sandstones mainly consist of clastic quartz grains, which are

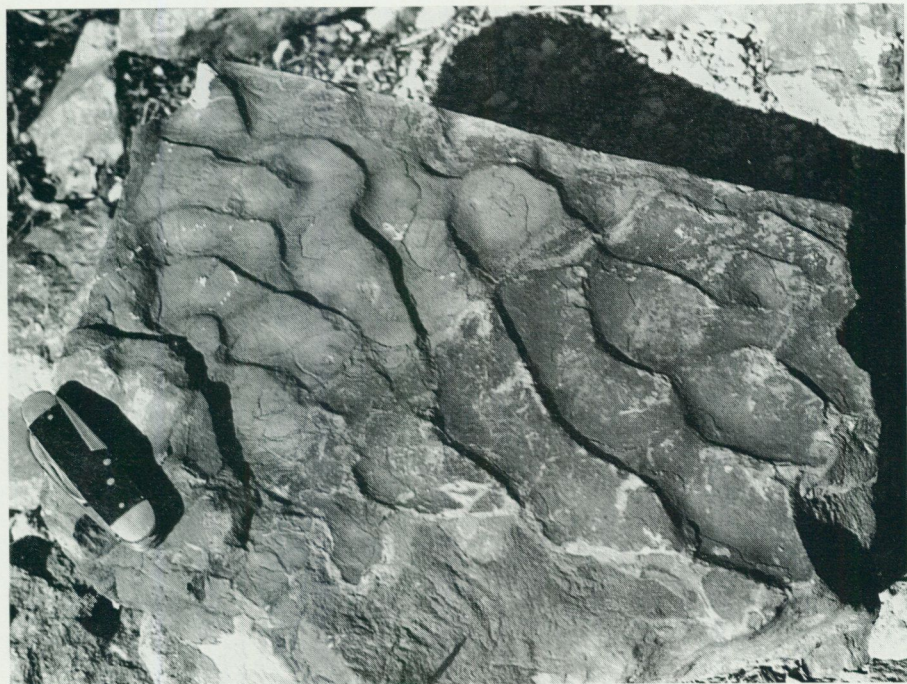


Fig. 26. Ripple marks in the basal sandstone of the Dala volcanics. (Local) moraine boulder south of Tallsjön (190/072). Photo Th. Lundqvist.



Fig. 27. Mud-cracks in a sericite-rich (argillitic) layer in the basal sandstone of the Dala volcanics. The cracks are filled with silicified sandstone. (Local) moraine boulder south of Tallsjön (190/072). Photo Th. Lundqvist.

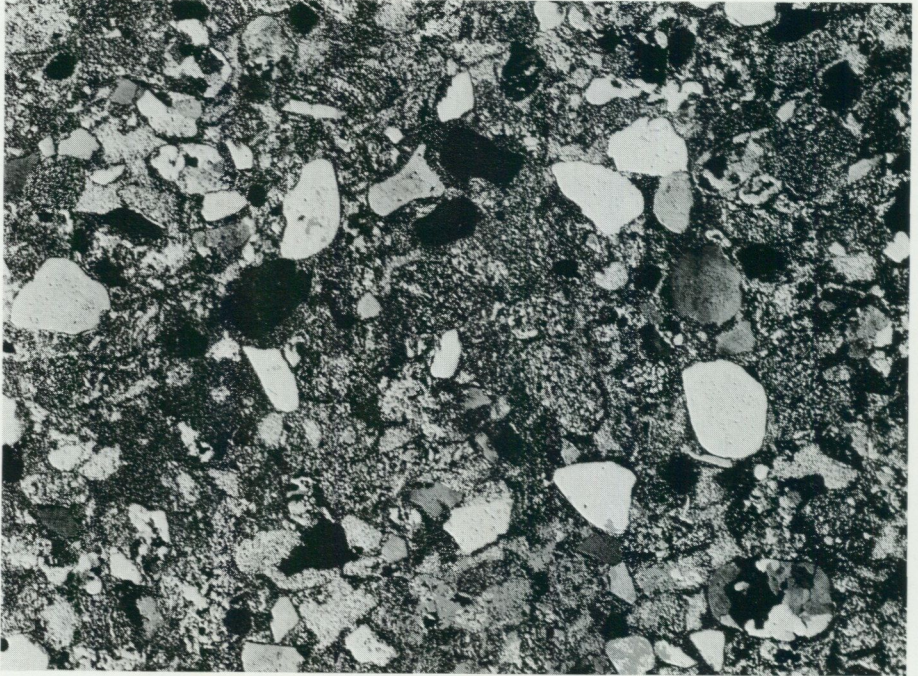


Fig. 28. Silicified basal sandstone of the Dala volcanics. Rounded grains of quartz and sericitized metarhyolite together with feldspar pseudomorphs (sericite) in a matrix of chalcedony. 2 nic., 22 x. South of Tallsjön (191/069). Photo I. Signorelli.

often well rounded (Fig. 28). Sericite pseudomorphs after feldspar are also common. In more subordinate quantities occur grains consisting of a sutured quartz mosaic with scattered small sericite flakes. They are interpreted as sericitized detritus of the metarhyolite, which occurs in the Noppikoski-Tallsjön region (E1-D1-D2). Small grains of cryptocrystalline quartz (chalcedony) are also found in the sandstones. They may be regarded as broken-up layers derived from the basal deposits. In accessory amounts occur zircon, iron oxide (hematite, also magnetite), chlorite, rutile, apatite and biotite. Single grains of unaltered potash feldspar may also be observed. These have escaped the strong alteration to sericite, which has generally affected this mineral (cf. below).

The matrix between the detrital grains in the sandstones is usually chalcedony containing scattered minute sericite grains. The chalcedony may show partial spherulites. It grades into patches of microcrystalline and coarser quartz. A fine hematite pigment can sometimes be observed (jasper). The textural relationships suggest a corrosion of detrital quartz by chalcedony.

In a sample from 189/033, parts of the chalcedony matrix show a diffuse parallel texture, which in all probability represents a relict pyroclastic feature



Fig. 29. Tuffaceous siltstone in the basal deposits of the Dala volcanics. Angular grains of quartz in a chalcedony matrix with relict tuff texture (particularly near the centre of the picture). 1 nic., 73 x. Vassjöån (189/033). Photo I. Signorelli.

(Fig. 29). On account of the strong alteration to chalcedony and sericite which is characteristic of the basal layers, it is, however, not possible to state to what extent the latter contain volcanic ash material.

The most fine-grained microcrystalline basal rocks occur at Tjädermyråsen (193/096) and Sandsjöberget (192/137), in the latter locality partly in the matrix of a quartzite breccia (cf. Fig. 30). They are composed of a mixture of quartz and finer sericite flakes. Scattered larger quartz grains (size up to 1 mm) also occur. Accessories are zircon and opaque minerals. No relict pyroclastic textures have been observed in these localities.

Chemical analysis of a sample of a microcrystalline rock from 192/137 gave 8.0 % Al_2O_3 , 0.2 % Na_2O , 2.4 % K_2O and 0.4 % MgO . Therefore, the mica should be a muscovite (cf. also the analysis of similar mica in a sericitized metarhyolite given by von Eckermann 1936: p. 246).

The occurrence of basal deposits which has been marked on Plate 1 at 195/115 differs from the type described above. The rock is fine-grained (< 0.1 mm), greyish violet in colour, and consists mainly of quartz and sericitized plagioclase (albite). Epidote forms an essential mineral; chlorite is subordinate. It is possible that this rock may be a tuffite associated with



Fig. 30. Basal breccia of the Dala volcanics. Angular pieces of quartzite in a microcrystalline, dark violet-brown quartz-sericite matrix. Sandsjöberget (192/137). Photo Th. Lundqvist.

the Dala porphyrites. In such a case, basal sedimentary rocks would be lacking here.

As mentioned above, breccia and conglomerate horizons occur in the basal layers of the Dala Volcanics. All transitions between breccia and sandstones etc. occur, via scattered fragments in the latter. Only supracrustal rocks have been observed as fragments and pebbles. The material of the breccias is largely derived from the directly underlying rocks, whereas that of the conglomerates indicates a somewhat longer transport.

In the breccia at Sandsjöberget (192/137) almost all fragments are of quartzite (and vein quartz). See Fig. 30. Some fragments similar to the dark violet-brown matrix of the breccia also occur. This rock is microcrystalline as described above (p. 83).

South of Tallsjön (D2) the majority of the fragments in the breccia are of the same types as the underlying, partly eutaxitic metarhyolite (Figs. 31–33). Silicified basal sandstones and compact chalcedony are also observed, as well as very subordinate fragments of quartzite and vein quartz. In the rhyolitic fragments the feldspar has been altered to sericite. Such an alteration has also affected the underlying metarhyolite. Immediately below the basal deposits, the feldspars are completely pseudomorphosed, but further to the



Fig. 31. Basal breccia of the Dala volcanics. Fragments consist mainly of quartz-porphyrific metarhyolite. South of Tallsjön (191/073). Photo Th. Lundqvist.



Fig. 32. Basal breccia of the Dala volcanics, forming a thin remnant on metarhyolite and containing fragments of the latter. South of Tallsjön (192/071). Photo Th. Lundqvist.

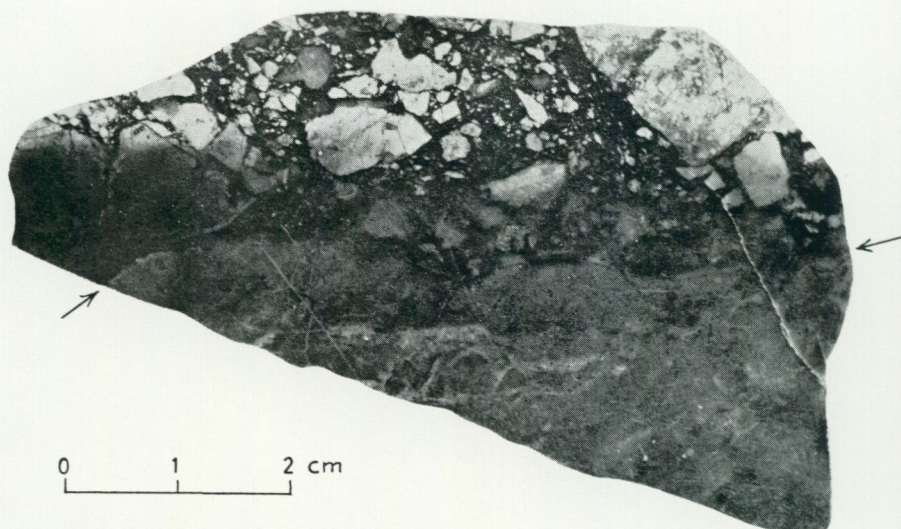


Fig. 33. Polished specimen of the breccia in Fig. 32. The contact towards the underlying quartz-porphyritic metarhyolite is indicated by arrows. Photo Th. Lundqvist.

east only an incipient alteration can be observed. The albite has been attacked first, the potash feldspar evidently being more resistant to sericitization.

Even in strongly sericitized fragments of the breccias, the characteristic structural and textural features of the ignimbrite "flames" are well preserved (cf. p. 48).

South of Tallsjön, a zoning may be observed in metarhyolite fragments of polished specimens of breccia (Fig. 34). The central parts are dark brown and contain a fine pigment of hematite, which is lacking in the pale reddish brown marginal zones.

Beside the road between Noppikoski and Älvho (191/041) is an outcrop with conglomerate belonging to the basal layers. The pebbles are up to some decimetres in diameter. They mostly consist of quartzites and quartzite sandstones (cf. p. 34) of types which are found in the orogenic complex. Some quartzites show the effects of strong cataclasis (undulous quartz). In addition, pebbles of grey, silicified basal siltstones and sandstones, sericitized acid metavolcanics, grey, brownish or reddish chalcedony and red jasper are found. South of this locality (at 191/040) occur transitional types between conglomerates and breccias.

On the basis of the interpretation of the contact between the sub-Jotnian and the orogenic complex as a major unconformity, some chemical weathering of the latter complex would perhaps be expected. Evidence of this is found in the microcrystalline (silt-sized) quartz-sericite rocks at 193/096 and 192/137. However, where a strong silicification has affected the basal layers, as e. g. south of Tallsjön, it is hard to demonstrate pre-sub-Jotnian (pre-



Fig. 34. Polished boulder of the basal breccia of the Dala volcanics. Zoned fragments of metarhyolite (see text) in a silicified, layered matrix. Specimen collected by H. von Eckermann, now in the museum of the Geological Survey of Sweden. From the region south of Tallsjön (c. 191/073). Photo Th. Lundqvist.

silicification) weathering. This is the case because some alteration of the feldspar by hydrothermal deposition of silica would be expected. The sericite pseudomorphs after feldspar, which are frequently found in the basal sedimentary rocks, can hardly have endured transport in their present state. From this it may be concluded that at least part of the alteration has taken place after deposition. The fact that the sericitization of feldspar is in many cases not directly (within a few metres) associated with a deposition of silica can hardly be regarded as proof of a pre-silicification weathering. On the other hand, the fragments in the breccia south of Tallsjön (Fig. 34) may possibly reflect two stages of alteration: an earlier weathering of the whole

fragment followed by a hydrothermal leaching of iron from the marginal parts, the latter taking place in connection with the deposition of silica in the matrix of the breccia.

On the basis of the foregoing discussion, the following interpretation of the genesis of the basal rocks is proposed. The folded and metamorphosed orogenic complex was subject to chemical weathering and erosion. The extent of the former is, however, difficult to estimate. Arkoses, lithic sandstones, siltstones and talus breccias were then deposited. There followed the initial eruptions of the volcanic activity leading to the formation of Dala porphyries and porphyrites. Only small amounts of magma can be related to these early eruptions, although the extent of admixture of pyroclastic material to the basal sediments cannot be estimated because of the silicification, which has later affected the rocks. In such silicification, volcanic glass is especially sensible to replacement. Further erosion and deposition occurred, resulting in the formation of conglomerates and sandstones with well-rounded clasts. In the basal sediments deposition of silica (partly through replacement) as chalcedony and opal took place in connection with the volcanic activity. This hydrothermal activity also caused an alteration of the detrital feldspar grains which had escaped the weathering. Reworking of the sediments during the period of silica deposition is demonstrated by the presence of chalcedony in breccias and conglomerates.

After this sequence the main eruptions occurred and accounted for the extensive formation of Dala porphyrites and porphyries.

The basal deposits of the Dala volcanics may possibly correspond to part of the Lower Dala series of Hjelmqvist (1966). In such a case, these rocks would be the only representatives of the latter series within the Los-Hamra region.

It is interesting to note that the relationship observed in the Los-Hamra region between the sub-Jotnian supracrustal rocks and their basement is similar to those found on the island of Hogland (Suursaari) in the Gulf of Finland (Ramsay 1890; Kranck 1928 and 1929). The basement consists of supracrustal gneisses, metagabbro and granite. It is unconformably overlain by a flat-lying quartzite conglomerate. On the latter rests a sheet of quartz porphyry, considered to be the supracrustal counterpart of the Viborg rapakivi granite (Ramsay 1890; see also Wahl 1947). Porphyrite lava at places underlies the quartz porphyry. A similar stratigraphic position is occupied by tuff breccias and conglomerates, in which clasts from the basement rocks are found. The tuffs may show a silicification (Kranck 1929: p. 188).

5.2.2.1.2. DALA PORPHYRITES

Dala porphyrites generally rest directly on the basal layers. They differ from the porphyries by lacking perthitic alkali feldspar phenocrysts and by



Fig. 35. Dala porphyrite. Phenocrysts of augite and lath-shaped plagioclase in a microcrystalline matrix. 2 nic., 15 x. Börningsberget (080/304). Photo I. Signorelli.

having a more femic character. The normal porphyrites are homogeneous and lack a stratification. Frequently they carry amygdules containing some of the following minerals in varying proportions: epidote, quartz, hornblende, calcite and chlorite. These structures and textures show that the porphyrites largely originated as lava flows. Subordinate intercalations occur of conglomerates, agglomerates, volcanic breccias and tuff(ite)s ("Digerberg sandstone" etc., see Hjelmqvist 1966: p. 73). These intercalations are treated below (p. 92). It should be noted that deposits of this kind in Kopparberg County (Hjelmqvist *op. cit.*) are much more frequent than in the Los-Hamra area.

On the map, Plate 1, two kinds of porphyrite have been distinguished: the one is greenish black, black or dark violet and the other brown, reddish brown or brownish violet. The first group makes up the most basic porphyrites, which are poor in, or lack, potash feldspar and quartz. By contrast, the second group is rich in the latter minerals. A hematite pigment in the potash feldspar accounts for the brown to red colours. It is evident that the porphyrites are strongly differentiated. Chemical analyses show compositions ranging from trachybasalt to quartz latite and even rhyolite (Table 2) according to the nomenclature of Rittmann (1952). The suite type is average Pacific to weak Mediterranean (Rittmann 1962a, see Table 2).

The porphyritic texture (Fig. 35) of the porphyrites is characterized by phenocrysts up to some millimetres in diameter, usually occupying between 10 and 40 % of the rock volume. Two types of phenocrysts predominate: a greyish white or greenish (saussuritized) plagioclase as hypidiomorphic, often lath-shaped crystals, and a femic mineral (probably pyroxene) replaced by epidote, chlorite, pale green hornblende and oxides more or less altered to leucoxene. In the most basic porphyrites, clinopyroxene (augite) in a somewhat uralitized and chloritized state can often be observed (Table 4: nos. 13–14). The augite phenocrysts may be zoned. In one sample (no. 13 of Table 4), values for $2V_\gamma$ were up to 8° higher in the central parts of the crystals than in the margins (cf. p. 124). Pseudomorphs after olivine also occur in some samples of basic porphyrites. They consist of pale green hornblende, green biotite and chlorite in different proportions, surrounded by a rim of iron oxide.

In the most basic porphyrites, plagioclase phenocrysts often show a pronounced normal zoning. The composition is labradorite to andesine. Strong alteration of the plagioclase is frequently observed, resulting in the formation of epidote and sericite; sometimes also prehnite and calcite.

Porphyrites high in SiO_2 and K_2O generally contain plagioclase phenocrysts of albitic composition. Originally, the plagioclase probably was richer in anorthite, epidote often occurring in the albite. However, as the content of epidote is less than in saussuritized plagioclase of the basic porphyrites, the original anorthite percentage was also probably lower than in the latter rocks.

The groundmass of the porphyrites is often aphanitic (microcrystalline), but grain sizes up to c. 0.1 mm may be found. The predominating constituent is plagioclase, which frequently occurs in lath-shaped crystals. In some samples a trachytic texture is present (a parallel arrangement of the plagioclase). In basic porphyrites, the composition of the groundmass plagioclase is mostly andesine or oligoclase. However, optical determination of anorthite content is often impossible due to the small grain size and extensive saussuritization. In samples where measurements have been carried out, the groundmass plagioclase is characterized by a lower anorthite content than the phenocrysts. Thus, at 080/304, the former contains an andesine ($\text{An}_{37}\text{--An}_{45}$), whereas the phenocrysts are labradorite ($\text{An}_{55}\text{--An}_{65}$).

In acid porphyrites, the plagioclase of the matrix is albitic.

In the groundmass, potash feldspar often occurs together with plagioclase. The former is subordinate or lacking in basic porphyrites, but predominates over albite in the acid ones, where quartz also is an important matrix constituent. The quartz is generally micropoikilitic, forming grains of c. 0.5 mm diameter with small inclusions of feldspar(s).

The groundmass of the Dala porphyrites contains strongly varying amounts

of pale green hornblende, chlorite, epidote, sericite, biotite, calcite, prehnite and oxides altered to leucoxene. In the basic porphyrites clinopyroxene (augite) may occur. Apatite is also found, generally near or within aggregates of femic minerals. Small amounts of fluorite have occasionally been observed.

The Dala porphyrites are frequently cut by a network of epidote veins. Sometimes (e. g. on Börningsberget, 083/303), red schlieren also occur, in which strongly hematite-pigmented albite predominates over quartz, potash feldspar and epidote. In the locality mentioned, chalcocite, malachite, calcite and epidote occur as a cavity-filling in a breccia zone in the reddish brown porphyrites (see p. 134).

Near Tallsjön (186/077) a porphyrite is locally impregnated with pyrite. In connection with the impregnation, the rock has become bleached to a pale greyish green colour. Chlorite, epidote and opaque mineral contents are reduced by comparison with the surrounding porphyrite. The sulphide impregnation is probably connected with a dolerite intrusion just west of the locality.

In contrast to the Dala porphyries, the porphyrites have very few intrusive counterparts. However, a dike which is probably related to the porphyrites runs north from Oreälven (201/030) and can be studied in a road-cutting at 204/032. Moraine boulders of the same rock occurring about one kilometre north of this outcrop indicate that the dike extends further northwards. The rock in question was described by von Eckermann (1936: analyses 111 and 112) as an alkaline dolerite. The dike has a porphyritic texture, and the present author favours connection with the Dala porphyrites. However, it is possible that the rock may belong to the Jotnian or post-Jotnian quartz dolerites mentioned by Hjelmqvist (1966: pp. 89 and 155). It is dark greyish green and consists of sericite-stained albite laths, clinopyroxene (augite, see Table 4: no. 15), perthitic alkali feldspar, chlorite and oxides altered to leucoxene. Albite occurs both in the phenocrysts and in the matrix. Subordinate and accessory minerals are carbonate (dolomite according to von Eckermann 1936), apatite, epidote and pyrite. Thus, a notable low-temperature alteration has affected the dike.

A small occurrence of a similar rock has been found at 210/105. Sericite pseudomorphs after plagioclase phenocrysts are embedded in a matrix of opaque minerals, chlorite and quartz with subordinate or accessory amounts of potash feldspar, apatite, epidote, sphene and leucoxene.

Diorite and gabbro referred to the sub-Jotnian occur in some areas in Kopparberg County (Hjelmqvist 1966). They are very subordinate to the Dala granites. In addition, Hjelmqvist (op. cit.: p. 140) mentioned sub-Jotnian dolerite, in part forming composite dikes with granite porphyry.

Chemical and modal analyses of Dala porphyrites are given in Table 1: nos. 57–61. The differentiation towards increasing *si*, *qz* and *alk* and decreas-

ing fm , c and mg is evident from Table 1b. Fig. 71 shows the trend in the direction of lower calcium contents and magnesium : iron ratios. The Ca-Na-K diagram further illustrates the evolution towards k values near 0.5, i. e. ratios characteristic of the Dala porphyries.

The trace elements vanadium, chromium, cobalt and nickel show a decrease with increasing differentiation. This is also the case with the BaO : K₂O and CaO : SrO ratios (see Fig. 51 on p. 110), which is in accord with capture of barium by potassium-bearing minerals and enrichment of strontium in late calcium-bearing minerals (cf. Rankama and Sahama 1952). The rubidium content rises in the acid members of the differentiation suite.

As already mentioned, the Dala porphyrites are classified as trachybasalts to rhyolites. The differentiation trend is thus towards compositions similar to those of the Dala porphyries. However, for reasons given below it does not seem likely that the porphyries have been formed through a crystallization differentiation of basic magma. The geographical association between the two types is indisputable, but considerations of the genetical connection must remain highly speculative.

With regard to the variations in composition displayed by the porphyrites, a simple crystallization differentiation of approximately basaltic magma can hardly explain the abundance of the reddish brown porphyrites, relatively rich in potash feldspar and quartz (cf. the map of Hjelmqvist 1966 and Plate 1 of the present work). Instead, the following hypothesis is tentatively suggested for the genesis of the porphyrite suite. Basaltic magma rose from the lower crust or upper mantle, perhaps as a consequence of crustal deformation in the orogenic complex (Svecofennian orogeny). On its way up, this magma encountered and partially mixed with the parental magma of the Dala porphyries and granites, thus giving rise to compositions characterized by higher K₂O and SiO₂ contents.

5.2.2.1.3. BRECCIA, AGGLOMERATE, CONGLOMERATE AND TUFF(ITE) IN THE DALA PORPHYRITES

Stratified, fragment- and pebble-bearing units are sometimes found as intercalations in the porphyrites. These layered deposits show the same variations in colour as the porphyrites. Dark brownish violet, however, seems to be the predominating colour. The modal composition is also similar to that of the porphyrites. Phenoclasts in the layered rocks contain plagioclase phenocrysts from the latter. Other clastic features are seldom observed because of the strong low-temperature alteration to parageneses with chlorite, sericite and epidote. However, an exceptional case occurs near St. Vassjön (188/105), where the contours of original glass-shards are clearly visible in polarized

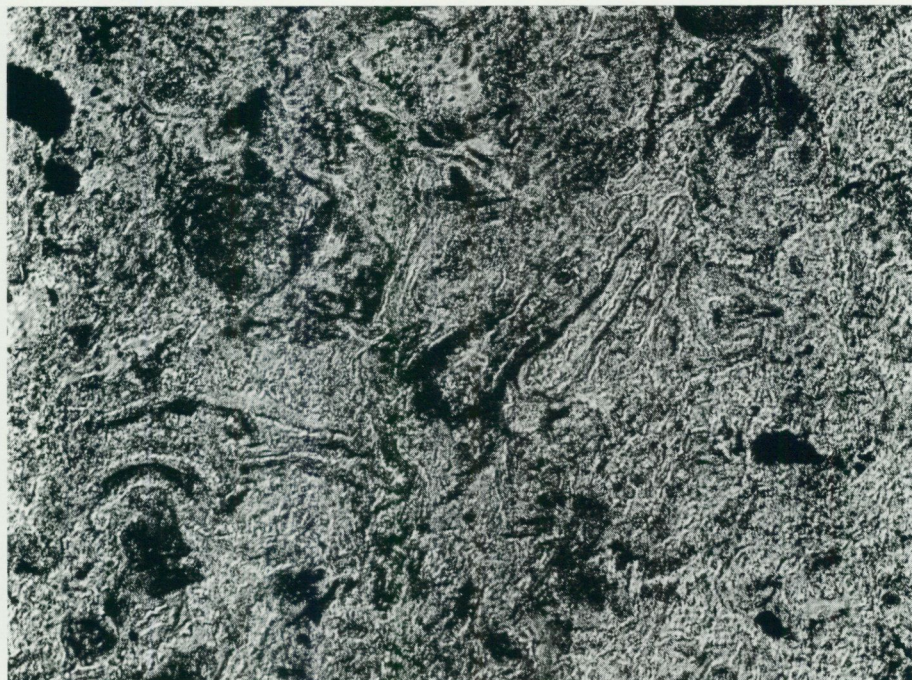


Fig. 36. Glass-shard texture in a tuff layer in Dala porphyrite. 1 nic., 295 x. South-east of Vassjön (188/105). Photo I. Signorelli.

light (Fig. 36). Small fragments of quartz, plagioclase and Dala porphyrite (amygdaloidal) are embedded in the glass-shard matrix.

Porphyrite tuffs and tuffites with layers of breccia and conglomerate can especially be studied in moraine boulders near the railroad at c. 184/154. Here the rocks are reddish brown to dark violet. In the fragments of the breccias porphyrites predominate, but single pieces of eutaxitic Dala porphyry also occur.

Volcanic breccias and agglomerates in the Dala porphyrites are generally closely associated with tuff(ite)s in the same way as in the case just described. In the breccias the fragments are sharp-edged, in the agglomerates more or less rounded and with diffuse borders towards the groundmass (cf. p. 53). The agglomerates are characterized by porphyrite material, other rocks being very rare. Also in the breccias, the fragments as well as the matrix are generally derived from the porphyrites (different types may occur together). Dala porphyry is, however, sometimes observed. On Korsiberget (175/174), pieces of red, fine-grained Dala granite occur as scattered fragments in a breccia with a tuff matrix (see below, p. 114).

Conglomerates in Dala porphyrite contain rounded pebbles up to some decimetres in diameter. Their groundmass is greyish green to dark brown-



Fig. 37. Conglomerate with pebbles of Dala porphyrites. Moraine boulder south-southeast of Vassjön (c. 184/102). Photo Th. Lundqvist.

violet. It consists of mineral and rock detritus including quartz, feldspar (potash feldspar and plagioclase), epidote, opaque minerals, chlorite etc., small fragments of Dala porphyries and porphyrites, and sometimes also jasper. Among the pebbles, different types of porphyrite predominate (Fig. 37). Dala porphyries, mostly phenocryst-poor, and in part eutaxitic, are common. In addition to the normal, feldspar-porphyritic types, some occur with quartz phenocrysts (182/103). Pebbles of Dala granite have not been observed within the Los-Hamra region, but occur in similar conglomerates in Kopparberg County (Hjelmqvist 1966).

In conclusion, the occurrences of agglomerates, volcanic breccias and tuffs show that the porphyrite volcanism was in part explosive. Conglomerates and tuffites testify to an interaction between volcanic accumulation and the contemporaneous erosion.

5.2.2.1.4. DALA PORPHYRIES

Dala porphyries form the main part of the volcanics of the sub-Jotnian complex. They are generally feldspar-porphyritic (both potash feldspar and plagioclase). The composition of the porphyries shows less variation than

that of the porphyrites. However, a differentiation from rhyolites to trachytes is observed, the mineralogical expression of which is a change in frequency of the feldspar phenocrysts.

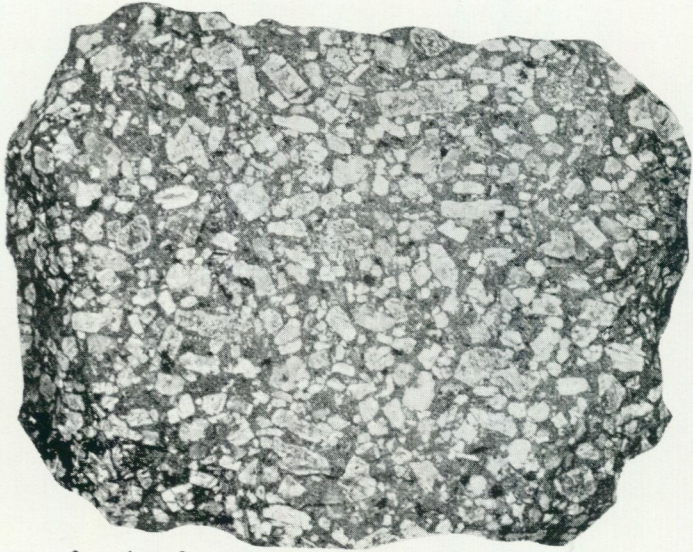
The major types of Dala porphyry have been distinguished on the map Plate 1. Two main groups are phenocryst-rich and phenocryst-poor. In the former, the feldspar phenocrysts occupy $\geq 1/3$ (Fig. 38), in the latter, $< 1/3$ of the total rock volume (Fig. 39). Another feature indicated on the map is the degree of crystallization in the matrix of the porphyries. In one group, grain sizes of the groundmass are above c. 0.05 mm (distinctly phaneritic), in the other, below this size (indistinctly phaneritic or aphanitic). Further, the occurrences of eutaxitic porphyries with macroscopically visible ignimbrite "flames" (see below) have been denoted on Plate 1.

The local names often used for different types of Dala porphyry (Bredvad, Rännås, Blyberg, Orrlok porphyry etc.) have not been adopted in the present paper. For the meaning of such terms, the reader is referred to Hjelmqvist (1966). The local names refer to the different porphyry types which were earlier used as ornamental stones at Älvdalen. The Dala porphyries have provided characteristic boulder types for tracing the movements of the Quaternary land-ice, and in literature dealing with such investigations the local names have also been adopted.

As already mentioned, the Dala porphyries form sheets with a medium to gentle dip to the west or south-west. The thicknesses of the individual units of Dala porphyry are not known, as continuous exposures of the bedrock over long distances do not occur. Because of the cover of lichens on the rocks it is also very hard to trace a boundary between similar porphyries. Changes in the degree of consolidation between different levels in the porphyry units (cf. Ross and Smith 1961) are not preserved. In those types which contain ignimbrite "flames" it may, however, be possible to estimate the thickness of the units. For the belt of such porphyries stretching from Älvho (D1) to Vallknopparna (D2) and Örnberget (D4), a thickness of c. 100 m of apparently uniform porphyry can be calculated. This must be regarded as a minimum value, as a single unit may embrace different structural and textural types.

The contact towards the porphyrites is seldom directly observed. Near Oreälven (175/030), however, it dips below the porphyries at about $75-80^\circ$ towards $N60^\circ W$. This is steeper than would be expected from the general inclination of the Dala volcanics. Local uplift south of Älvho (p. 140) may have affected the dip. South of St. Vassjön (180/110) the contact also appears very steep, although it has not been possible to follow it more than a few cm in a vertical direction.

The Dala porphyries are characterized by red to pink, dark brown, dark violet and black colours. The black types have a nearly vitreous (crypto-



0 1 2 cm

Fig. 38. Dala porphyry rich in phenocrysts. Specimen from Sundsjön (148/191). Photo Th. Lundqvist.



0 1 2 cm

Fig. 39. Dala porphyry poor in phenocrysts. Specimen from the area south-east of Flarksjön (119/203). Photo Th. Lundqvist.

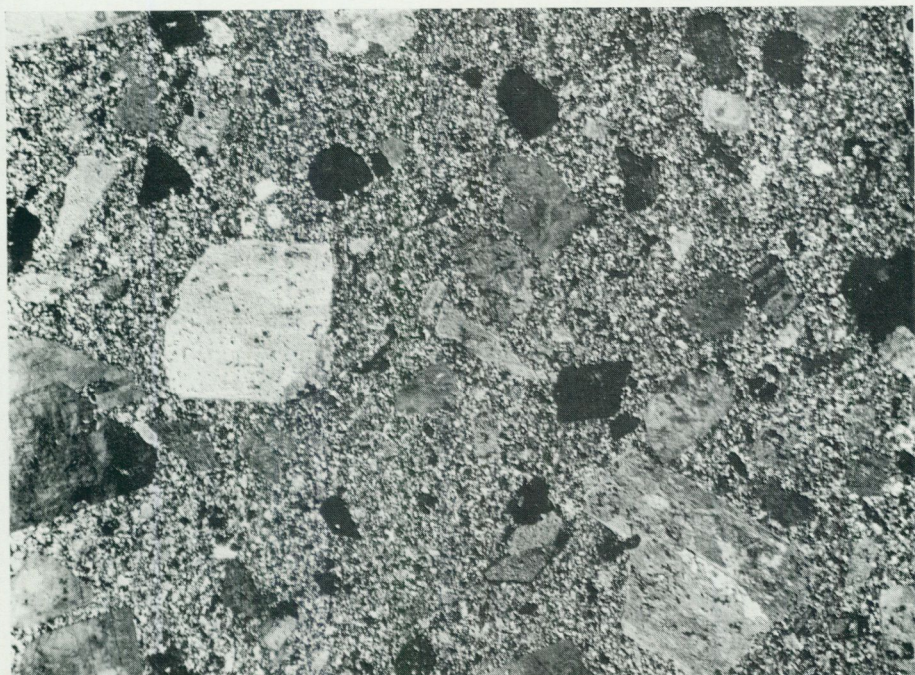


Fig. 40. Phenocryst-rich Dala porphyry. Phenocrysts are perthitic alkali feldspar and plagioclase. Matrix fine-grained. 2 nic., 5 x. Älvho (158/036). Photo I. Signorelli.

crystalline) groundmass. Red, brown and violet colours are caused by a hematite pigmentation occurring especially in the potash feldspar. Phenocrysts of perthitic potash feldspar are red to pink, or sometimes dark grey. The plagioclase in contrast is generally white or greyish green, and, in the latter case, strongly sericitized.

The feldspar phenocrysts make up between c. 5 and 90 percent of the rock volume. In porphyries with a low content of phenocrysts, the latter are usually below c. 5 mm in size. The groundmass of such porphyries is usually aphanitic or just phaneritic. To this group belong most of the porphyries containing ignimbrite "flames". In Dala porphyries rich in phenocrysts, the latter are on the average larger than for phenocryst-poor types, feldspars up to c. 2 cm in diameter having been frequently observed. Such coarsely porphyritic rocks are generally characterized by a distinctly phaneritic groundmass (Fig. 40). Some phenocryst-rich porphyries, however, are crowded with feldspars with a maximum diameter of c. 3 mm, in an aphanitic matrix (e. g. at 173/063, cf. no. 71 of Table 1).

Fragments of supracrustal rocks are most common in Dala porphyries with a high content of phenocrysts. They generally consist of different kinds of supracrustal rocks from the orogenic complex (meta-argillites, chloritized

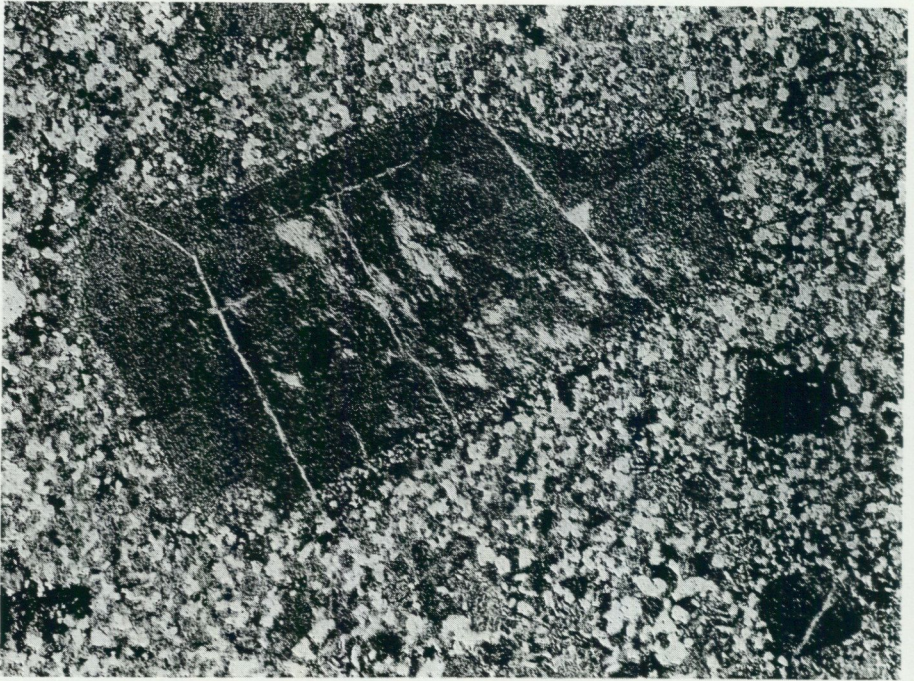


Fig. 41. Phenocryst of perthitic alkali feldspar surrounded by a poikilitic rim. From a phenocryst-poor Dala porphyry (of Bredvad type). Matrix fine-grained, in part granophyric. 1 nic., 31 x. Finnberget (028/165). Photo I. Signorelli.

basic metavolcanics, quartzites) but also of Dala porphyry and porphyrite. At Sundsjön (148/191) fragments of medium-grained Dala granite have been found. Porphyroblasts of alkali feldspar (perthite) may occur in the inclusions. In quartzite fragments at 165/233, this feldspar has replaced the matrix between rounded (relict clastic) quartz grains.

Fragments of older rocks have also been found in the phenocryst-poor porphyries. For example, inclusions of Dala granite have been observed in the black porphyry at 119/203.

The main phenocrysts of the porphyries are perthitic alkali feldspar and plagioclase. Either of these may sometimes be lacking. Subordinate femic minerals (see below) also occur, whilst quartz is rare.

In the perthite phenocrysts, the potash feldspar component is generally microcline, although with a lower triclinicity than for microclines in rocks of the orogenic complex and the Råtan granite (see further p. 145 ff.). The perthite frequently contains corroded inclusions of more or less sericitized plagioclase (generally albite). In addition, it is often surrounded by a thin (usually < 0.2 mm) poikilitic rim of perthite, fingering into the groundmass (Fig. 41). Such textures are common in porphyries characterized by a relati-

vely advanced crystallization in the matrix. Viewed macroscopically, the phenocrysts of perthite as well as those of plagioclase show hypidiomorphic outlines (tabular crystal form). In some cases, zones of pure albite occur within the perthite phenocrysts. Rapakivi texture (albite mantles surrounding the perthite) has occasionally been observed.

Within the perthite phenocrysts are often found crystals of epidote and violet fluorite.

The plagioclase phenocrysts are generally nearly pure albite in the phenocryst-poor porphyries. Oligoclase compositions have, however, also been observed. In porphyries rich in phenocrysts, the plagioclase shows a wide range of anorthite contents. Albite may also occur in such rocks, but frequently the plagioclase shows a normal zoning with margins of albite or oligoclase and cores of oligoclase, andesine, or even (rarely) labradorite.

The plagioclase phenocrysts have frequently been strongly altered to sericite and epidote; sometimes also to calcite or prehnite. Antiperthitic patches of potash feldspar may occur.

As mentioned above, albite is found as corroded remnants in perthite. Another very common texture is a thin mantle of perthite around plagioclase. The relations between these minerals suggest a corrosion of the latter by the perthite. In the case of a glomeroporphyritic arrangement of the plagioclase, the whole aggregate is surrounded by perthite. The mantles are similar to the thin overgrowths on the perthite phenocrysts described above: they have sutured contours towards the matrix and carry inclusions of the latter. Evidently, the mantle textures have arisen in a post-depositional, late- to post-magmatic stage of the evolution of the ignimbritic Dala porphyries. It is likely that they have been formed by crystallization processes caused by the heat content remaining in the porphyry units after deposition (cf. genesis of ignimbrite below). However, albite remnants are found within the perthite phenocrysts of rapidly quenched porphyries with little crystallization in the groundmass, thus indicating that the corrosion of plagioclase started before the eruptions. In such porphyries, mantles of the type just described are lacking. Instead, the feldspar phenocrysts may show corrosion embayments filled by the groundmass mineralogy (Fig. 42). Where a higher degree of crystallization is noted in the matrix, albite remnants may occur in perthite phenocrysts, which are in their turn surrounded by a thin mantle of secondary perthite.

Phenocrysts of quartz are relatively rare in Dala porphyries. Occasionally, a few such crystals may be observed within a thin section. The quartz sometimes shows corrosion embayments. Further, it may be in optical continuity with the quartz of the matrix (cf. p. 49).

According to experimental data (Tuttle and Bowen 1958; Winkler 1967), the early crystallization of quartz from a granitic magma is favoured by high

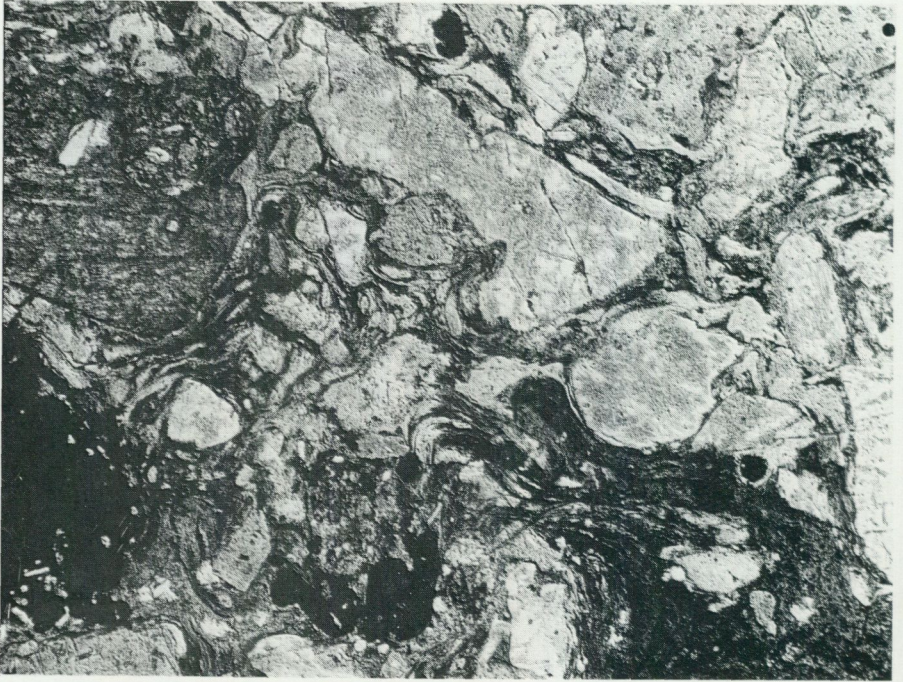


Fig. 42. Phenocryst-rich Dala porphyry. Phenocrysts of perthitic alkali feldspar (partly corroded) and plagioclase in a pseudo-fluidal matrix. To the upper left is an inclusion of an altered volcanic rock. Below this is an opaque mineral (oxide) grain. 1 nic., 22 x. Vassjö-
ån (173/063). Photo I. Signorelli.

water pressure and/or low content of normative anorthite. For the Dala porphyries (and granites), the rare occurrence of quartz phenocrysts thus points to a relatively low pressure (high crustal level), the anorthite percentage being unimportant.

Aggregates of femic minerals usually form less than 5 % of the porphyries. They are made up of epidote, chlorite and oxides more or less altered to leucoxene or sphene. Biotite and pale green (uralitic) hornblende may also occur. In the aggregates are often found a few crystals of apatite and zircon; occasionally also fluorite, prehnite and calcite. Clinopyroxene (augite) in a somewhat uralitized state is relatively seldom observed (see Table 4: no. 16). It is only found in porphyries with little crystallization in the groundmass.

The matrix of the Dala porphyries is mainly composed of quartz and alkali feldspars. In subordinate or accessory amounts occur chlorite, epidote, sericite, hornblende, opaque minerals, leucoxene, sphene, orthite, apatite, zircon, calcite, fluorite and biotite. The latter is especially represented in porphyries with inclusions of meta-argillite (e. g. at 165/233) and has in all probability been formed through assimilation of such material by the por-



Fig. 43. Phenocryst-poor Dala porphyry with pseudo-fluidal glass-shard texture in the groundmass. Note the characteristic Y shape of some shards. Thin fissures are filled with quartz. 1 nic., 24 x. South-east of Flarksjön (119/203). Photo I. Signorelli.

phyry magma. At the locality just mentioned single minute grains of a mineral with high relief, birefringence near 0.010, and very low $2V_{\alpha}$ occur in the porphyry. The mineral is probably corundum, and its origin similar to that of the biotite (cf. also p. 115).

In Dala porphyries with little crystallization in the groundmass a pseudo-fluidal parallel texture has often been observed (with one nicol). The contours of original glass-shards, frequently with the typical Y shape, are marked by differences in crystallinity, minute grains of opaque minerals etc. (see Fig. 43). The pseudo-fluidal texture is represented by a parallel orientation of elongate shards. In the vicinity of phenocrysts, the parallel texture bends in approximate conformity with the borders of the latter. From such features and the occurrence of elongate lenses ("flames") in some types of porphyry (see below), Hjelmqvist (1956) concluded that the Dala porphyries were largely of ignimbrite origin.

In the texturally best preserved porphyries the matrix is cryptocrystalline, with nearly glassy patches (e.g. at 119/203). Spherulitic textures are frequently observed in such rocks. With increasing crystallization the groundmass becomes microcrystalline, often micropoikilitic with quartz "sponges" surround-



Fig. 44. Specimen of phenocryst-poor Dala porphyry with ignimbrite "flames". From a local moraine boulder at Älvho (167/039). Photo Th. Lundqvist.

ing small feldspar grains. These "sponges" are often composed of a network of laths with a uniform optical orientation. Geijer (1913) pointed out the possibility that such "needle quartz" may pseudomorph tridymite.

Granophytic textures may occur in porphyries rich in phenocrysts and characterized by a relatively advanced crystallization in the groundmass. Sometimes, the marginal parts of perthite phenocrysts are granophytic, forming a transitional zone to the matrix. The distinction of such porphyries from intrusive porphyritic granites is not always clear. However, granophyre is much commoner in the latter than in the supracrustal porphyries.

In the porphyries with the highest degree of crystallization in the matrix, the most common texture is made up of small ($< c. 0.2$ mm) tabular crystals of feldspar (mostly perthite) with interstitial xenomorphic quartz.

The macroscopically visible "flames" in the eutaxitic Dala porphyries occur both in rocks with a pseudo-fluidal (micro-)texture and in porphyries where crystallization has wiped out any pre-existing textural features of this kind. A high frequency of such "flames" has been given a special sign on Plate 1. The "flames" have the shape of streaks and lenses showing a pronounced parallel orientation (Fig. 44). Their colour is generally pink or red, and lighter than that of the surrounding porphyry matrix. Usually they are be-

low one decimetre in length, but "flames" up to half a metre long have been observed. The thickness is between one millimetre and a few centimetres. Viewed at right angles to the plane of elongation, the "flames" are approximately equidimensional. Tongue-like off-shoots are characteristic of the ends of these bodies when they are observed parallel to that plane (cf. Ross and Smith 1961). Sometimes there is a tendency for tabular feldspar phenocrysts to be oriented parallel to the "flames".

A microscopic investigation of the "flames" shows the following. In the central parts of these bodies quartz usually predominates. It is much coarser than in the surrounding porphyry matrix. Sometimes the quartz is accompanied by epidote and fluorite. From the marginal parts of the "flames" lath-shaped perthite crystals, embedded in quartz, project towards the centre. Quartz and perthite, or perthite crystals alone, may form intergrowths as relatively coarse partial spherulites along the margins. Complete, cryptocrystalline spherulites are in some cases found to make up a large part of the "flames". (See Figs. 45 and 46.)

Within the flame-like bodies feldspar phenocrysts occur in the same way as in the surrounding porphyry.

The phenomena described above are not always well developed. Thus, the zoning with higher quartz contents in the central parts of the "flames" may be absent. This is especially the case with porphyries showing a relatively high degree of crystallization in the groundmass. Further, the orientation of feldspar laths at right angles to the border of the "flames" does not always exist.

From the above it is evident that the "flames" of the eutaxitic Dala porphyries show the axiolitic and pectinate textures (structures) of Phanerozoic ignimbrites (welded tuffs; ash flow tuffs). They are well-known from the latter and have formed by collapse and flattening of pumice. A later devitrification causes the axiolitic, spherulitic etc. textures (Ross and Smith 1961). Granophyre may also develop in the central parts of ignimbrite units (see e. g. Marinelli 1961). It is evident from the observations of the Dala porphyries that the degree of crystallization within any one thin section is roughly proportional to the size of the fragmental material (pumice, glass-shards, glass "dust"; see also p. 113).

Numerous works have been published on the ignimbrite problem. No attempt is made here to give a complete review, and the interested reader is referred to e. g. Ross and Smith (1961) and the literature cited by Pichler (1963b).

Ignimbrites are considered to be the products of a special type of linear volcanic eruption, viz. the so-called "overflowing glowing clouds" (Rittmann 1962b). The latter are high-temperature, turbulent suspensions of viscous magma (glass shards and pumice), crystals and rock fragments in volcanic



Fig. 45. Phenocryst-poor Dala porphyry with ignimbrite "flames". The latter are relatively coarse-grained (middle part and lower left) or spherulitic (upper right). The matrix between the "flames" is pseudo-fluidal. 1 nic., 13 x. St. Sillakorvamäki (163/043).
Photo I. Signorelli.



Fig. 46. Same as Fig. 45, but with 2 nic. Photo I. Signorelli.

gases. Rittmann (op. cit.) has proposed a possible mechanism for these eruptions, suggesting that the hot gas suspensions arise from degassing of viscous (acid) magma high up in the eruption fissure.

The high temperature in combination with the load pressure of the overlying parts of the ignimbrite sheets causes a welding and flattening of the pyroclastic material. The typical pseudo-fluidal (micro-)texture and the macroscopically visible eutaxitic structure arise in this way. However, particularly the uppermost and basal parts of ignimbrite units may not be welded.

In contrast to acid lavas, the ignimbrites cover vast areas (often thousands of square kilometres) in the form of flat-lying sheets (Rittmann 1958 and 1962a; Ross and Smith 1961). They characteristically level the topographic relief. It has been maintained that a sure diagnosis of ignimbrites can only be founded on observations of their great areal extent, as pseudo-fluidal textures and structures may occur in lava flows as well (Pichler 1963a). In contrast to lavas, the ignimbrites lack a scoriaceous surface.

On the basis of a comparison between ignimbrites of Phanerozoic age (Rittmann 1962a) and those described here, it is possible to make some inference about the evolution of the Precambrian in south and central Sweden (see p. 159).

The above description of the Dala porphyries has mainly concerned general features. However, some relatively rare structures and textures have important bearing on the genesis of the porphyries. They are described below.

Near Korrisjön (143/231) cavity fillings with diameters of about one centimetre have been observed in a phenocryst-poor, weakly eutaxitic porphyry. They consist of quartz and calcite. At Tandhem (165/233), in a phenocryst-rich violet to brown porphyry, aggregates of up to nearly one decimetre in diameter of perthite occur, surrounded by a red, hematite-pigmented zone. The perthite is xenomorphic. In the interstices between the large crystals, and partly as inclusions in the latter, are found smaller perthite grains as well as xenomorphic quartz of sizes ≤ 1 mm. The quartz, which is much coarser than in the surrounding porphyry, may show granophyric intergrowths with perthite.

The quartz-calcite cavity fillings at 143/231 have probably arisen through accumulations of gases remaining in the ignimbrite after its deposition. They are thus vapour-phase minerals, the occurrence of which is (Ross and Smith 1961: p. 27) "commonly a good criterion for ash-flow origin". The genesis of the large feldspars at 165/233 is not so evident, but it seems likely that their crystallization has been promoted by gas accumulations in the porphyry.

The present author agrees with Hjelmqvist (1956: p. 10) in his conclusions with regard to the genesis of the Dala porphyries: "The agreement with characteristic features of much younger welded tuffs is in many cases so

obvious that there seems to be little doubt of the ignimbritic origin of these eutaxitic porphyries. The same is probably true also of porphyries whose eutaxitic character is less evident but whose occurrence together with eutaxitic porphyries is clear." However, in the Los-Hamra region, some rare types of porphyry also give evidence of viscous flow in these rocks. From the literature it is known that there occur transitional types between lavas and ignimbrites. Especially in Russian literature (see Cook 1966), the term tufflava has been used for such volcanics. Another type is the rheoignimbrites (see Rittmann 1958 and 1962a and Marinelli 1961). Tufflavas or foam lavas are thought to represent lava flows, from which the dissolved gases have escaped violently, so as to produce a porous lava froth on the surface. Rheoignimbrites are secondary flows, emanating from ignimbrite sheets deposited on a relatively steep slope.

The most important examples of Dala porphyries formed (at least in part) from viscous flows are found south-east of Flarksjön (at 119/203 and around 123/205). The following features have been noted here. In a black, obsidian-like porphyry at 119/203, the pseudo-fluidal texture shows a small-scale folding. Further, the rock is traversed by numerous thin quartz-filled fissures (cf. Fig. 43, p. 101). Around 123/205, steeply dipping ignimbrite "flames" and regular band structures are observed on weathered rock surfaces (Fig. 47). The banded types may show a folding (Fig. 48). In local moraine boulders, fine band structures may be seen to be broken up to small-scale breccias (Fig. 49). Larger fragments of eutaxitic or banded porphyry in breccia are also observed (Fig. 50). The differences between the various bands in these rocks are due to different degrees of crystallization in the groundmass of the porphyry.

In banded and folded porphyries of the two localities mentioned, the feldspar phenocrysts show undulous extinction and microbrecciation.

The observations described above show that viscous flow movements have occurred in Dala porphyries, which at the same time may display a pyroclastic texture. Strong movements, however, may have obliterated the latter. The band structures have been produced by a laminar flow, which in some cases has also led to a brecciation. Porphyries of this kind may be interpreted as either tufflavas or rheoignimbrites. A distinction between these types can not be made in the present case, as it requires a continuous profile across the porphyries. A criterion for rheoignimbrites would be that types displaying true flow structures without roots pass into ignimbrites (see e. g. Rittmann 1962a).

Evidence of viscous flow is also found in some other localities. For example, in the case at Silverknoppen (c. 098/298), the eutaxitic structure shows varying orientations. In the thin section, a small-scale breccia texture is apparent.

In Table 1: nos. 62-74, chemical and modal analyses of Dala porphyries are presented. In comparison with phenocryst-poor porphyries (nos. 62-70),



Fig. 47. Banded, phenocryst-poor Dala porphyry. Local boulder south-east of Flarksjön (123/205). Diameter of coin = 14 mm. Photo Th. Lundqvist.

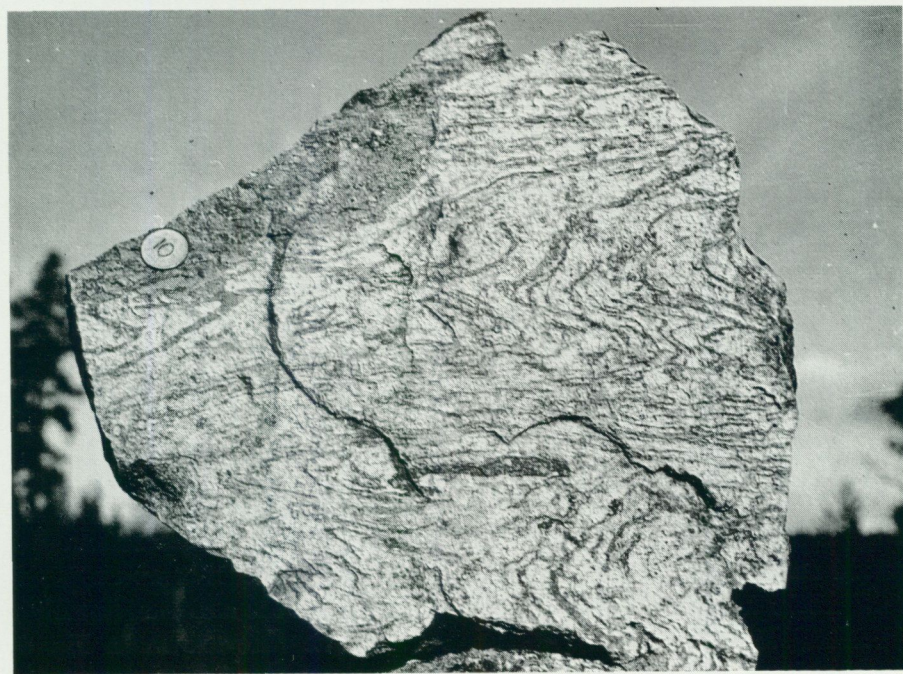


Fig. 48. Small-scale folding in banded, phenocryst-poor Dala porphyry. Local boulder south-east of Flarksjön (123/205). Diameter of coin = 14 mm. Photo Th. Lundqvist.



Fig. 49. Small-scale (auto-)brecciation in banded, phenocryst-poor Dala porphyry. Local moraine boulder south-east of Flarksjön (123/205). Diameter of coin = 14 mm.
Photo Th. Lundqvist.

those rich in phenocrysts (nos. 71–74) are characterized by lower *si* and *qz* values, but higher *fm* and *c*. These differences also follow from the microscopical observations recorded above. The *k* value is for all porphyries near 0.5, i. e. the differentiation has not affected the proportions between sodium and potassium (see below). In Fig. 71 on p. 227, the variations in the Dala porphyries are shown in Ca-Na-K and Fe-Mg-(Na+K) diagrams. In the first, the points fall in the region $\text{Na} : \text{K} \sim 1$ and $\text{Ca} = 0 - 15 \%$. The latter diagram shows a weak tendency for higher ratios of Fe : Mg towards the alkali corner, i. e. in phenocryst-poor porphyries.

The suite type of the Dala porphyries is average Pacific to average Mediterranean (Table 2 on p. 229). Both Dala porphyries and porphyrites (cf. p. 89) thus show a trend towards Mediterranean (potassic) compositions. Such a trend does not exist for the metavolcanics of the orogenic complex.

Of special interest are the variations in trace element contents, notably of zirconium, strontium, barium and rubidium. They are shown in Fig. 51, along with analytical data from Dala granites and porphyrites. From these diagrams it is evident that the granites display the same differentiation trends



Fig. 50. Breccia with fragments of banded and streaky, phenocryst-poor Dala porphyry. Scale 2:3. Local boulder south-east of Flarksjön (123/205). Photo P. H. Lundegårdh 1965.

as the porphyries, which is a good indication of comagmatic origin (see p. 120).

Porphyries and granites which are rich in phenocrysts tend to have somewhat higher zirconium contents than phenocryst-poor rocks. Thus, the differentiation leading to the former has also included the mineral zircon. A tendency for enrichment of apatite in phenocryst-rich porphyries and granites is similarly indicated by the P_2O_5 contents.

The SrO : CaO ratio has been little influenced by the differentiation. This is probably due to the masking effect of the entry of strontium into the early-formed alkali feldspar (cf. p. 76 above).

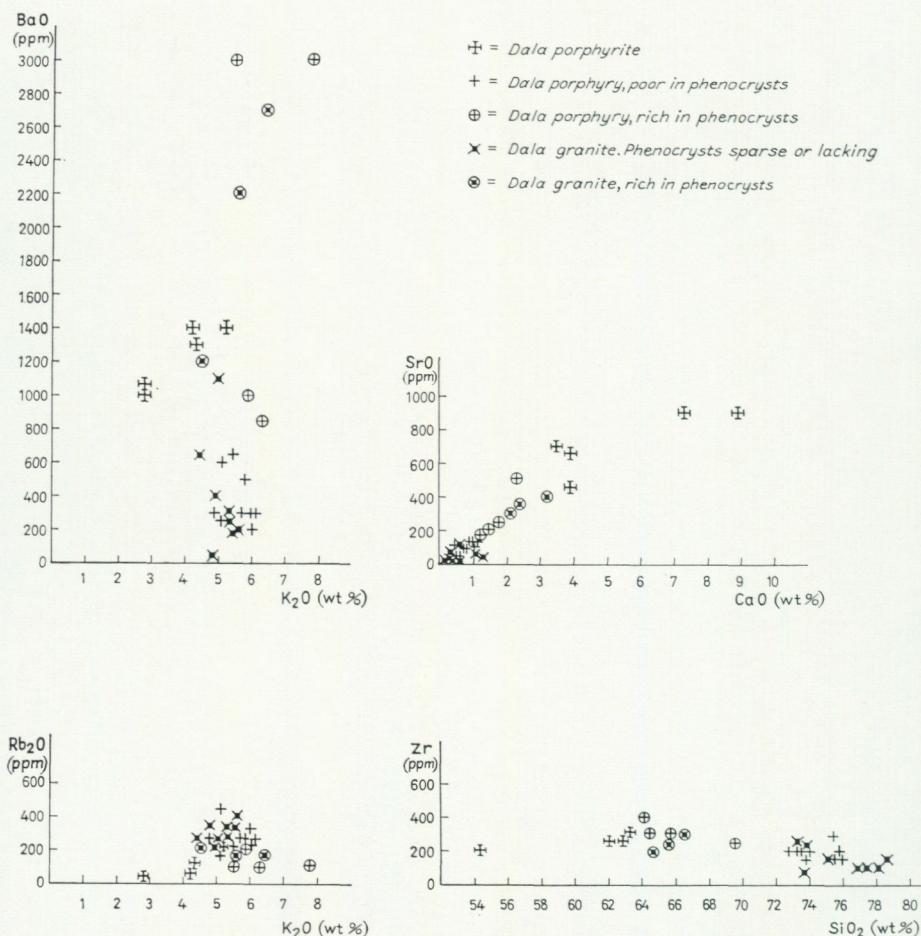


Fig. 51. Diagrams showing the relations between contents of BaO and K₂O, SrO and CaO, Rb₂O and K₂O, Zr and SiO₂ for different sub-Jotnian igneous rocks.

Barium is the element for which the greatest differences have been observed between granites and porphyries rich and poor in phenocrysts. A strong tendency for high BaO : K₂O ratios in the former rocks has been noticed. (cf. also p. 148). It is well-known that barium is captured by early potassium-bearing minerals (Rankama and Sahama 1952), and it is evident that the strongly porphyritic Dala granites and porphyries represent accumulations of early-formed alkali feldspars. This is supported by the distribution of rubidium: phenocryst-rich rocks have a relatively lower Rb₂O : K₂O ratio. This is a consequence of the larger ionic radius of rubidium in comparison with potassium.

From all observations of modal and chemical variations in the porphyries and granites it can be concluded that the strongly porphyritic rocks represent accumulations of minerals crystallizing from the Dala magma (alkali feldspar, plagioclase, feric minerals, zircon and apatite). In addition, xenoliths also seem to have become enriched in the latter rocks (see above). The variations thus have the character of crystallization differentiation. That this operated at some depth, before the volcanic eruptions, is evident from the fact that granites and porphyries show similar variations. For this reason, it can not be expected that the phenocryst-rich porphyries should occupy any special stratigraphic position in relation to those poor in phenocrysts (e. g. from the lower parts of ignimbrite units). Field observations do not support the idea of such a relationship.

It is perhaps somewhat unexpected that the k values have not been influenced by the differentiation leading to phenocryst-rich porphyries. The analysis of perthitic alkali feldspar phenocrysts in a phenocryst-poor Dala porphyry (Table 7: no. 9) in comparison with the whole rock analysis (Table 1: no. 70) shows a higher ratio of potassium to sodium. This is also to be expected from experimental studies of the systems $\text{NaAlSi}_3\text{O}_8\text{-KAlSi}_3\text{O}_8\text{-SiO}_2\text{-H}_2\text{O}$ and $\text{NaAlSi}_3\text{O}_8\text{-KAlSi}_3\text{O}_8\text{-CaAl}_2\text{Si}_2\text{O}_8\text{-H}_2\text{O}$ (Tuttle and Bowen 1958). The approximate constancy of the k values in the Dala porphyries must be due to the fact that both plagioclase and perthite have become enriched in the phenocryst-rich porphyries. The proportions between these minerals in the accumulates must have been such as to keep the k value essentially unchanged.

5.2.2.1.5. BRECCIA AND LAYERED TUFF(ITE) IN DALA PORPHYRIES

Dala porphyries with a variety of inclusions and porphyries with breccia structure have been described above (pp. 97 and 106). They have been interpreted as fragment-bearing ignimbrites and viscous flows (tufflavas or rheo-ignimbrites), respectively. In one locality north of Pilkalampinoppi (156/143) a porphyry breccia occurs, which may be a product of a non-ignimbritic eruption or represent a non-welded part of an ignimbrite sheet (cf. above, p. 105). The breccia is grey and contains numerous angular fragments, up to a few centimetres in diameter, consisting of different types of Dala porphyry. Some of these show a pseudo-fluidal texture. In the matrix of the breccia, contours of original glass-shards can still be discerned. These ash particles lack a preferred orientation. Small angular phenocrysts of feldspar also occur.

Layered, in part somewhat reworked deposits of tuff or tuffite character are rare in the Dala porphyries, but have been observed at Älvho (155/030) and Vassjöän (169/073). The rocks in question have a micro- to cryptocryst-

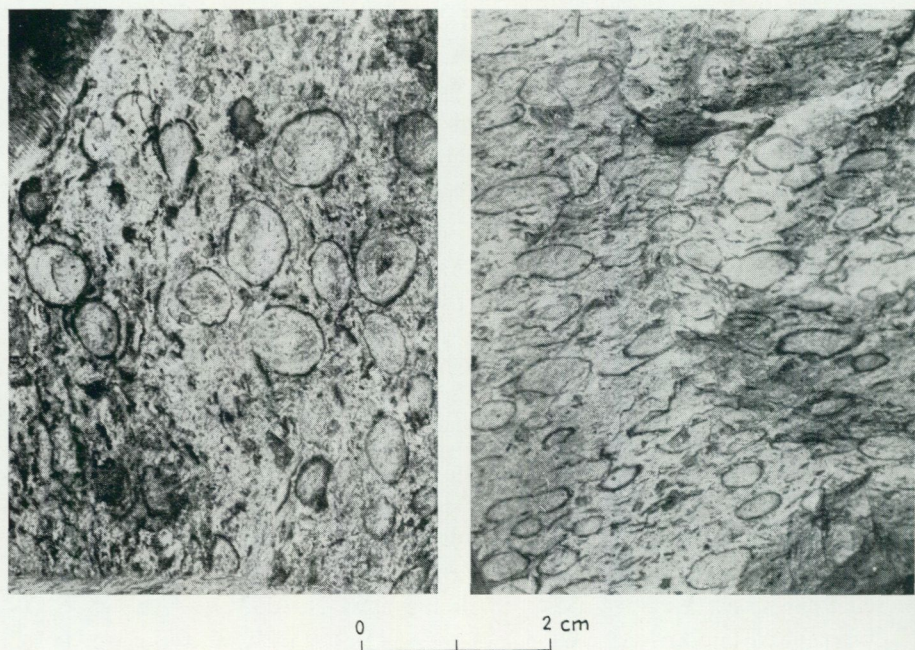


Fig. 52. Pisoliths in Dala porphyry tuff, viewed at right angles (left) and parallel (right) to the plane of bedding. Moraine boulder south-east of Flarksjön (119/203). Photo Th. Lundqvist.

talline matrix of devitrified glass, in which lie angular or somewhat rounded grains of feldspar (potash feldspar and albite) and occasional quartz. Small fragments of volcanic rocks are also met with, as well as scattered crystals of oxide, leucoxene, epidote and zircon.

The layered deposits either represent reworked material from the less consolidated parts of the ignimbrites, or products of separate (non-ignimbritic) explosive eruptions.

South-east of Flarksjön (c. 119/203) interesting boulders of porphyry tuffs have been found in the moraine. They have not been observed in situ and have thus not been marked on the map, Plate 1. One of these boulders shows a bedding, in part graded, represented by differences in content and size of small feldspars and devitrified (micro- to cryptocrystalline) glass-shards and pumice fragments. All these constituents show a strong preferred orientation of their longest axes in the bedding plane. This is probably a depositional feature, which has become further accentuated by compaction (cf. the form of the pisoliths below).

In a moraine boulder from the same locality (119/203), small ellipsoidal bodies are embedded in a weakly layered porphyry tuff. The longest axis of



Fig. 53. Thin section of one pisolith from the specimen of Fig. 52. Note the distinct glass-shard texture both in the pisolith and the surrounding matrix. 1 nic., 17 x.
Photo I. Signorelli.

the ellipsoids is usually ≤ 5 mm and the shortest ≤ 2 mm. The latter is oriented at right angles to the bedding. Sections parallel to the bedding show an almost circular shape of the bodies (Fig. 52). Microscopic examination reveals a glass-shard texture and scattered feldspar phenocrysts both in the ellipsoidal bodies and in the matrix between them (Fig. 53). Devitrification has produced crypto- to microcrystalline quartz-feldspar intergrowths. The zoning visible in hand specimen as a dark rim surrounding a light core (Fig. 52) is caused by differences in particle size and degree of crystallinity. In the marginal parts, the ash particles are smaller and less crystallized than in the cores (cf. p. 103).

On account of their pyroclastic texture, the ellipsoidal bodies are interpreted as pisoliths, i. e. coherent spherules of volcanic ash (Rittmann 1962a: p. 75), which have become flattened by compaction. Such pisoliths constitute a proof of subaerial volcanism.

Pisolithic Dala porphyry tuffs have been observed in situ and in moraine boulders in the regions south-west and north-west of Mora in Kopparberg County (R. Lannerbro, personal communication).

5.2.2.2. DALA GRANITES AND ASSOCIATED DIKES

The Dala granites form an intrusive suite, commonly red to reddish grey, rarely grey in colour. They are intimately associated with the Dala porphyries. This is shown by their geographical distribution and by mineralogical-chemical and textural features. Dala granites are found within or near the regions where the Dala volcanics occur.

At least two generations of Dala granite exist. Fragments of such granites have been observed in Dala porphyry (p. 98) and in a breccia horizon in porphyrite (p. 93). Pebbles of Dala granite also occur in conglomerate overlain by porphyrite (Hjelmqvist 1966: p. 82). On the other hand, porphyritic Dala granite intrudes porphyries which are younger than the deposits which contain granite fragments. Such intrusive relations can be studied at Toreskär (c. 029/180). The granite here generally forms very irregular bodies in a phenocryst-poor porphyry. Towards the contact, the matrix of the porphyritic granite becomes more fine-grained (c. 0.1 mm at the immediate contact). The intrusion has caused little recrystallization of the porphyry, grain sizes of the groundmass being c. 0.05 mm at the contact. The latter is sharp to transitional over about one centimetre. A similar intrusive breccia has also been observed on Granåsen, west of the Los-Hamra region (lat. $61^{\circ} 40' 59''$ N., long. $14^{\circ} 06' 24''$ E.).

The intrusive behaviour of the Dala granites is also demonstrated by the presence of inclusions of Dala porphyry in the granites. Further, in some localities dikes of granophyre and granite porphyry of Dala type cut the porphyries (see below, p. 118 f.).

The age relations between Dala granites and rocks of the orogenic complex have only rarely been observed. This is due partly to the scarcity of outcrops in the critical regions, and partly to the fact that Dala granites only seldom form dikes in the surrounding rocks. At Tallsjöbäcken (202/049), however, a granite porphyry dike cuts the metarhyolite close to the contact towards the underlying quartzite sandstone. A similar dike has been observed near Ned. Gryssjön (c. 053/331).

At Sandsjöån (224/123), a quartz-porphyritic metarhyolite has been intruded by Dala granite. The latter becomes more fine-grained towards the contact and sends apophyses into the older rock.

The age relationship between the Dala granites and the Råtan granite is not clear. A search for dikes of one type of granite in the other along the contact at D5-E5 has not been successful.

The Dala granites have intruded at high crustal levels, as indicated by the predominance of fine-grained, granophyric and porphyritic textures. For this reason, the distinction between them and the supracrustal porphyries is not

always clear. Because of the high level intrusion, the Dala granites have comparatively easily formed xenoliths in volcanic deposits (cf. above). Further, relatively little denudation was needed to expose them.

The Dala granites have been divided into three groups according to grain size and texture: fine-grained (to medium-grained), strongly porphyritic, and medium-grained, weakly porphyritic.

The fine- (to medium-)grained granites mainly consist of quartz and perthitic alkali feldspar. The latter is generally hypidiomorphic and often strongly pigmented by hematite. Some perthite crystals tend to be larger than the average grain size of the rocks, whereby transitional types towards the strongly porphyritic granites arise. Quartz occurs in rounded to hypidiomorphic crystals, in part forming granophyric intergrowths with perthite. Plagioclase (more or less sericitized) is an essential or subordinate constituent. Sometimes it is only represented in accessory amounts (Table 1c: no. 79). The composition is usually albite, but oligoclase may appear in the central parts of the crystals. Albite often forms corroded remnants in perthite or is surrounded by a mantle of the latter mineral. It occasionally contains anti-perthitic patches of potash feldspar.

As a subordinate or accessory mineral in the fine-grained Dala granites occurs muscovite (sericite); in places also biotite and chlorite. Other accessories are sphene (and leucoxene), oxides, epidote, zircon, apatite, orthite, rutile, fluorite and calcite. In a sample from Sandsjö (211/190) scattered grains of strongly sericitized andalusite have been observed. In some other localities occur sericite aggregates which may be pseudomorphs after andalusite and similar minerals. Probably the presence of andalusite is due to assimilation of argillitic material (cf. p. 100).

The strongly porphyritic Dala granites ("Garberg granite", see Hjelmqvist 1966), as already mentioned, are connected with the fine-grained granites by transitional types with an intermediate content of phenocrysts. They are also very similar to certain (supracrustal) porphyries, from which they can not always be distinguished with certainty. Phenocryst percentages range between c. 30 and 90. Thus, these granites correspond to the phenocryst-rich porphyries already considered.

The phenocrysts are mainly feldspar (perthitic alkali feldspar and plagioclase). They are usually hypidiomorphic and ≤ 2 cm in diameter. Granophyric textures prevail in the groundmass. Such intergrowths between quartz and perthite may also occur in the marginal zones of phenocrysts. Plagioclase phenocrysts show a wide range of compositions in the samples examined. Albite and oligoclase predominate, but in the cores of zoned crystals andesine and even labradorite may be found. A strong alteration to sericite, epidote and prehnite is often noted. As in the porphyries, a mantle of perthite around plagioclase (Fig. 54) is a characteristic textural feature. However, the

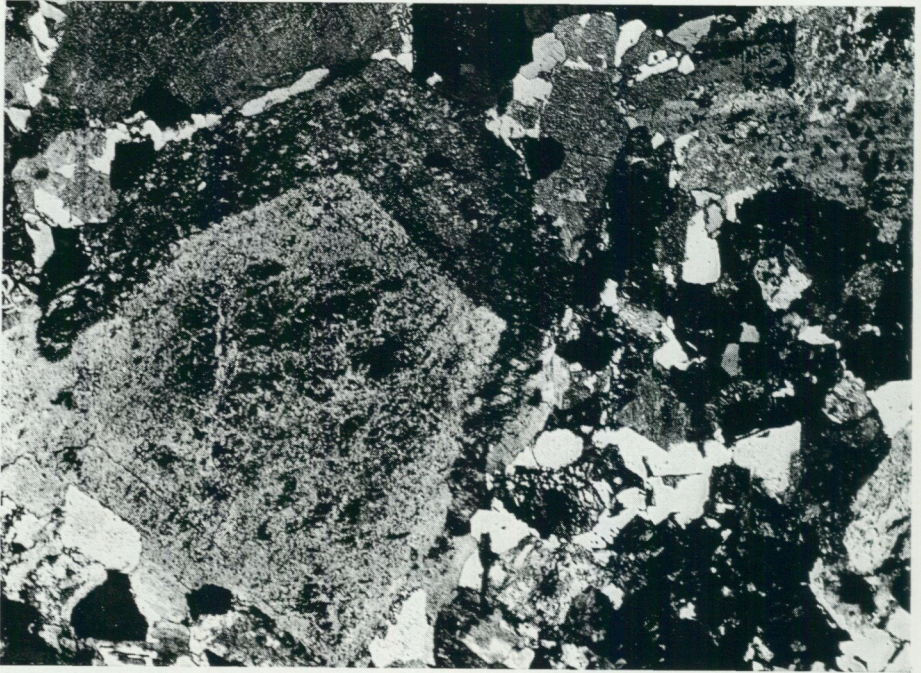


Fig. 54. Mantled plagioclase phenocryst in a porphyritic Dala granite. The mantle consists of potash feldspar (dark) with patches of albite (light). 2 nic., 23 x. Rutimovuo (052/150). Photo I. Signorelli.

mantles on the average are broader than in the porphyries. Variations may be observed from thin mantles to a stage where plagioclase forms small, strongly corroded remnants in perthite. In rare cases albite mantles around perthite have been observed. Stewart and Roseboom (1962) have discussed different possibilities of crystallization at the lower temperature terminations of the three-phase region plagioclase-alkali feldspar-liquid. The disequilibrium shown by corrosion and mantling of the above described anti-rapakivi as well as rapakivi types can be accounted for by a rapid change of the shape of this three-phase region with falling temperature.

The quartz of the porphyritic Dala granites is mainly restricted to the groundmass. Scattered quartz phenocrysts of around one millimetre's diameter have, however, been occasionally observed. They are rounded to hypidiomorphic and often show embayments filled with the matrix minerals. Quartz phenocrysts are sometimes in optical continuity with quartz of the immediately surrounding groundmass.

Phenocryst-like aggregates of uralitic hornblende, chlorite, opaque minerals, sphene etc. occur in the actual granites. They have probably been formed by

alteration of primary pyroxene. Remnants of clinopyroxene in hornblende have been observed in rare cases.

In the matrix of the strongly porphyritic granites, quartz and perthite predominate. Albite occurs in subordinate amounts together with the minerals mentioned above for the fine-grained granites. In addition, common hornblende may occur.

At Toreskär (029/180) mirolitic cavities filled with calcite, quartz and hematite have been observed in moraine boulders of porphyritic Dala granite.

The third type of Dala granite occurs in the massifs immediately east of the region occupied by the Dala volcanics. This granite is characterized by crystals of perthitic alkali feldspar (maximum size one centimetre) and plagioclase (albite or oligoclase), embedded in a medium- to fine-grained matrix. The latter is on the average coarser than in strongly porphyritic Dala granites, and the porphyritic texture therefore less pronounced. Marginal facies types (Sandsjöån, E3, and V. Råberget, E2), however, are fine-grained and have been denoted in the same way as the fine-grained Dala granites described above. The feldspar phenocrysts of the weakly porphyritic granites, although being largely tabular, in detail show sutured or granulated borders (Fig. 55). Perthite grains are often poikilitic. They are further frequently divided into parts of slightly different optical orientation and are traversed by microfissures filled with quartz and feldspar. Granophyric textures are rare.

The plagioclase contains small sericite flakes. Grains bordering on perthite may show myrmekitic intergrowths with quartz, a texture which has not been observed in the strongly porphyritic granites. Corroded remnants of albite in perthite occur, but mantles of the latter plagioclase (cf. above) are incomplete or lacking altogether.

Millimetre-sized, granulated quartz grains occur porphyritically distributed in this type of the granites (cf. Fig. 55).

The matrix of the weakly porphyritic Dala granites is mainly made up of xenomorphic quartz, perthite and albite. Both texturally and mineralogically it is very heterogeneous. Bent twin lamellae of albite and the granulation of quartz and feldspar described above are indications of cataclasis. The textures observed, however, also indicate a recrystallization; e. g., there is comparatively little undulatory extinction in the quartz. It is therefore likely that the cataclastic effects were approximately contemporaneous with the intrusion and crystallization of the granite (protoclastic deformation).

In addition to quartz and feldspars, the weakly porphyritic Dala granites contain subordinate amounts of strongly chloritized biotite, opaque minerals and muscovite; sometimes also common hornblende. Accessories are zircon, fluorite, apatite, epidote, sphene, prehnite, orthite and calcite.

Aplitic and pegmatitic differentiates are restricted to the weakly porphyritic Dala granites (and their fine-grained marginal facies). They occur in the

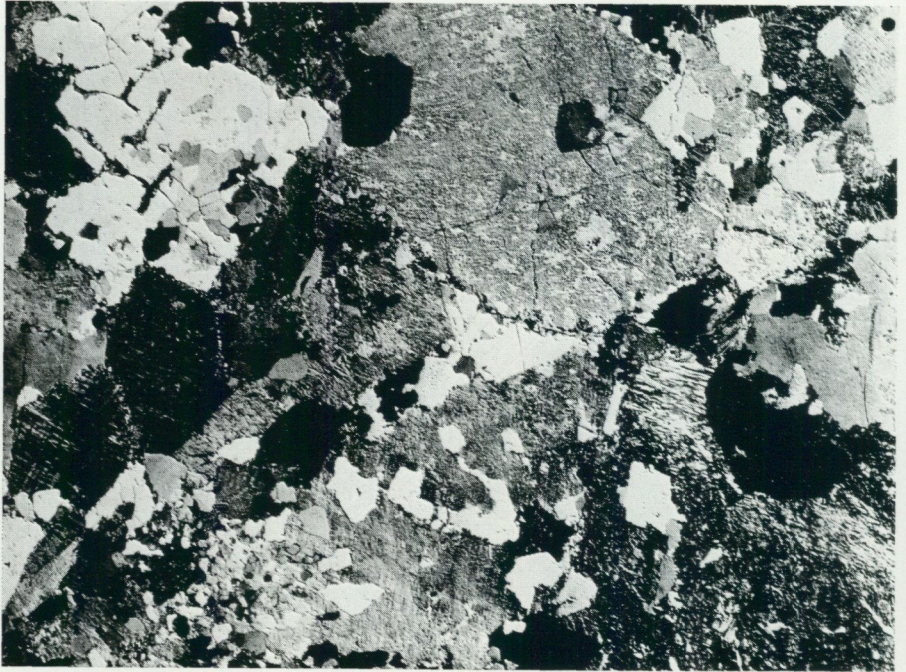


Fig. 55. Weakly porphyritic Dala granite. Note the granulation of the quartz and feldspar margins. 2 nic., 13 x. V. Råberget (214/074). Photo I. Signorelli.

same way as described above for the Rätan granite (p. 75). The rare occurrences of aplite and pegmatite show that the Dala granites have crystallized from relatively "dry" magmas. The highest contents of volatiles evidently occurred in the magma portions originating the weakly porphyritic types.

Xenomorphic quartz and hypidio- or xenomorphic feldspars (perthite and albite) are the dominating minerals of the Dala aplites and pegmatites. Small amounts of chlorite, biotite, muscovite, opaque minerals, zircon and apatite are also met with. Patches of violet fluorite sometimes occur. In one locality (207/178) garnet and sericitized andalusite(?) have been found in extensively assimilated inclusions of meta-argillite (cf. above, p. 115).

Finally, the granitic dikes of Dala type will be described. Some of these dikes are granophyric, with a small percentage of quartz and feldspar phenocrysts. Others are strongly feldspar-porphyritic.

Two narrow dikes of the first (granophyric) type occur at Tandhem (165/233) and one at Sundsjön (148/191). Phenocrysts consist of hypidiomorphic quartz with corrosion embayment, tabular perthite and partially perthite-mantled plagioclase (albite or oligoclase). The groundmass is a granophyric intergrowth of quartz and perthite. A similar rock has also been observed at

Sandsjö (206/192), but its dike character was not possible to verify in the field. The groundmass is only to a small extent granophyric.

Richly feldspar-porphyratic dikes occur at Tallsjöbäcken (202/049), Ned. Gryssjön (c. 053/331) and Tandhem (165/233).

At 202/049 the dike is around seven metres broad and contains tabular phenocrysts of perthite, a centimetre long, and partially perthite-mantled albite in a fine-grained groundmass. The latter is made up of hypidiomorphic perthite with some albite. In the interstices between the feldspar crystals occurs quartz, partly in fine granophyric intergrowths with perthite.

The dike at 053/331 is in part very phenocryst-rich, the groundmass occupying only c. 10 % of the rock volume. Its contacts towards the surrounding rocks (primorogenic granodiorite and Dala porphyrite) are disturbed by shearing (cf. p. 141). The rock consists of phenocrysts of perthite, albite and chlorite-epidote-opaque mineral aggregates embedded in a granophyric or microplitic matrix.

At Tandhem (165/233) the phenocryst-rich Dala porphyry is cut by two dikes of granophyre (see above). In the northern part of the outcrop occurs a granite porphyry, the dike character of which cannot be firmly established because of insufficient exposure. Its contact towards the Dala porphyry is sharp or transitional within a few millimetres. The colour is reddish grey. Numerous approximately (macroscopically) tabular phenocrysts of perthite (≤ 1 cm long) occur. Plagioclase (albite-oligoclase) also forms an important constituent. It is corroded by the perthite. The occurrence of granulated quartz phenocrysts of a few millimetres' diameter as well as macroscopically visible quartz in the groundmass are features which distinguish this rock from the surrounding porphyry. Under the microscope, the porphyritic texture is less distinct. The perthite phenocrysts are strongly poikilitic and pass irregularly into the matrix. The latter is made up of a xenomorphic quartz-perthite-albite intergrowth, in which coarse granophyre is occasionally seen. Considerable textural similarity exists between the granite porphyry in question and the earlier (p. 105) described aggregates containing large phenocrysts in the surrounding porphyry. As for the latter, a reasonable explanation of the texture requires relatively high volatile (water) content during the crystallization, possibly in connection with mild cataclasis.

In this connection, it may be profitable to consider the cause for the general occurrence of distinctly "magmatic" (porphyritic etc.) textures in the Dala granites (cf. also the Råtan granite). This is particularly important in view of the "metasomatic" hypotheses previously entertained (cf. below). The "driest" granites, in which no aplite and pegmatite have been observed, are also those in which such textures have been most perfectly developed. This is in all probability due to the relatively small part played by late- and post-magmatic recrystallization (influenced by volatiles) in such rocks. Where

recrystallization did occur, more or less interlocking, xenomorphic quartz-feldspar textures have been developed.

Chemical and modal analyses of Dala granites are given in Table 1: nos. 75–85. The differentiation into phenocryst-rich and phenocryst-poor granites has led to variations similar to those described above for the Dala porphyries (see p. 106 ff., Fig. 51 and Fig. 71). Thus, the Dala granites range from normal granites to quartz syenites. The latter can be regarded as accumulations of crystals separating from the magma. The comagmatic genesis of porphyries and granites is strongly supported by mineralogical and chemical data and field relations.

The k value of the granites is approximately 0.5 and is thus comparable with that of the Dala porphyries. Plagioclase contents, however, vary greatly. It follows that the granites which have a high content of this mineral are characterized by a low albite content in the perthite (see Table 7: nos. 16 and 19–22 and Table 1: nos. 75–77, 79 and 85). In accord with the microscopic observations, the granites with different plagioclase contents may be regarded as representing different stages of the reaction *plagioclase (albite) + alkali feldspar (Ab-poor) → alkali feldspar (Ab-rich)*.

The differentiation leading to Dala porphyries and granites with varying contents of feldspar phenocrysts has given rise to a negative correlation between normative quartz and feldspar in these rocks. Chayes (1948) made a statistical analysis of Swedish and Finnish sub-Jotnian granites and porphyries to decide whether a replacement origin was possible or not. The background for this was the discussion between von Eckermann (e. g. 1937b) and Backlund (e. g. 1938), in which the former maintained a magmatic genesis for the rocks in question and the latter proposed a replacement origin from Jotnian sandstones. Chayes (op. cit.) found that the hypothesis put forward by Backlund was statistically possible for the Swedish rocks (from the Los-Hamra region) but not for the Finnish rapakivi granites. He therefore rejected this hypothesis as it "does not afford a satisfactory explanation of variations in the bulk chemical composition of the rapakivi granites." Even if it is statistically possible to interpret the sub-Jotnian Los-Hamra rocks as formed by replacement of Jotnian sandstone, this remains a purely hypothetical suggestion. The genesis proposed by Backlund can be maintained only by neglecting the obvious conclusions to be drawn from field and laboratory observations (see also p. 122).

5.2.3. JOTNIAN COMPLEX

The term "Jotnian" was proposed by Sederholm (1895) for non-metamorphic sandstones and associated igneous rocks in the Precambrian of Fennoscandia. Originally, rocks later classed as sub-Jotnian, e. g. the rapakivi granites (cf. p.

76) were also included in the Jotnian (see Sederholm 1897). von Eckermann (1936 and 1937a) followed this usage of the term. In recent accounts on the Precambrian of Sweden (e. g. Magnusson et al. 1960 and Geijer 1963), the division into sub-Jotnian and Jotnian has been generally adopted. In the Jotnian complex are included sandstones with associated siltstones, shales and conglomerates in the Dalecarlia (Dalarna), Nordingrå, Gävle, Mälaren, Svartälven and Almesåkra regions. Similar sedimentary rocks occur in Finland at Muhos and in Satakunta (Simonen 1960; Eskola 1963). The sandstones are intimately associated with dolerites, which are also considered to belong to the Jotnian. The dolerites show intrusive relations to the Jotnian sedimentary rocks (Åsby, Särna and Nordingrå dolerites). An effusive counterpart, the "Öje dolerite", forms intercalations in Jotnian sandstones (see Hjelmqvist 1966). Dolerites, however, also occur in several regions without direct connection with the sandstones (see map of Magnusson et al. 1960).

The problem of the relationship between the sub-Jotnian and the Jotnian is discussed on p. 163 ff.

The Jotnian sandstones etc. in Finland were interpreted by Simonen and Kouvo (1955) as post-geosynclinal sediments of piedmont facies.

In the Los-Hamra region, both sandstones and dolerites of Jotnian type occur. They are most abundant in the region of the sub-Jotnian complex, but dolerite dikes are also met with in the orogenic complex.

5.2.3.1. DALA SANDSTONE FORMATION

The reddish Dala sandstones of the Los-Hamra region occur as outliers and represent the eastern extension of the large sandstone area stretching from the northern parts of Kopparberg County into the province of Härjedalen (see Hjelmqvist 1966 and Magnusson et al. 1960). The sandstone areas shown on Plate 1 of the present work are very schematically drawn. With one exception (c. 048/327), rocks of this kind are never found to outcrop within the Los-Hamra region, and the extension of such deposits has been judged from studies of the distribution of moraine boulders. It is apparent from Plate 1, that there seems to be a close connection between the occurrences of dolerite and sandstone within this narrow region (cf. above and p. 165).

Due to the moraine cover, the contacts between the sandstones and the underlying rocks have not been studied within the Los-Hamra region. The only observation of this relationship was made on a moraine boulder (c. 053/330), where Dala porphyrite contained a fissure filled with sandstone. South of the Los-Hamra region, in Kopparberg County, the contacts between the sandstones and their basement can be studied in outcrop (Hjelmqvist 1966). There, the basal layers were recorded to be conglomerate and breccia. Low angle dips are characteristic of the sandstone formation, except

in the south-west, where steeply dipping strata are found in connection with tectonic zones.

The Jotnian sandstones of the Los-Hamra region are generally arkosic or lithic and red or reddish brown in colour. They contain grey, often ellipsoidal "reduction" patches, elongated in the bedding (cf. Lundegårdh 1967: Fig. 50, p. 102). Conglomerate horizons are common. A distinction between Jotnian sandstones, overlying the sub-Jotnian rocks, and sedimentary intercalations in the latter (see above) cannot be made, as it would require a much better exposure of the bedrock. Included here in the Jotnian are those sandstones and conglomerates, which are characterized by red colours and which do not seem to occur as horizons in the Dala Volcanics Formation.

The pebbles of the Jotnian conglomerates are well rounded and up to some decimetres in diameter. They consist largely of different Dala volcanics (normal types of porphyries and porphyrites), Dala granites, quartzites and vein quartz. Further occur pebbles of chalcedony, jasper and quartz-porphyrific volcanic rocks, which latter belong to the Dala porphyries. The presence of metarhyolites from the orogenic complex is, however, also possible, although such rocks have not been identified with certainty.

In the feldspar-bearing pebbles of the conglomerates, a weathering to sericite, especially of the plagioclase, is frequently observed.

Dala sandstones show well preserved sedimentary structures. These include cross-bedding, ripple marks and mud-cracks (see Hjelmqvist 1966 and Lundegårdh 1967). These structures are also found in the moraine boulders of the Los-Hamra region.

In sandstone boulders may sometimes be observed thin, very fine-grained layers of a red, orange or grey colour. Microscopic investigation shows that they consist of detrital grains of quartz, feldspar etc. (frequently of silt size), embedded in a matrix of chalcedony, jasper, or, occasionally, opal. These siliceous layers have been formed in close connection with the deposition of the sandstones, as they show evidence of erosion. Further, they are sometimes traversed by mud-cracks filled with sandstone.

The Dala sandstones of the Los-Hamra region are mainly made up of detrital quartz, potash feldspar and the same rock types as found in conglomerate pebbles (see above). A silt-sized matrix may fill the interstices between the sand grains. The degree of roundness is very variable. In some layers, rounded or subrounded grains predominate, whereas others are characterized by angular to subangular detrital material (cf. Pettijohn 1957). Thin secondary overgrowths are sometimes noted on quartz grains. The latter may also show evidence of pressure solution (Fig. 56; cf. Gorbatshev and Kint 1961 and Gorbatshev 1962b). Detrital potash feldspar is of two types, either showing a well-developed cross-hatching or lacking microscopically visible twins (cf. p. 145).

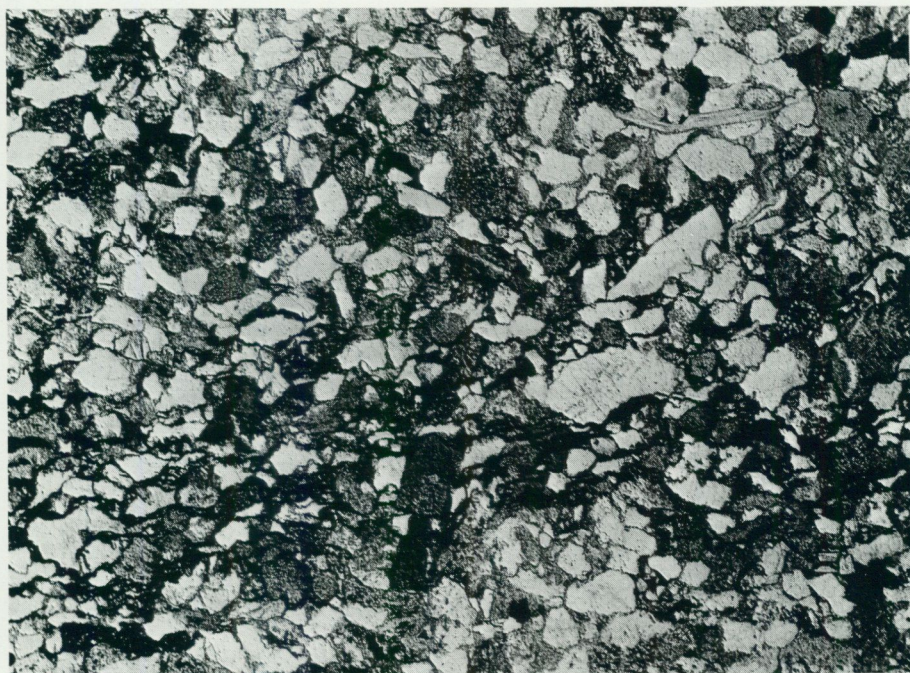


Fig. 56. Dala sandstone (arkosic to lithic). Detrital grains of quartz, microcline, weathered volcanics, muscovite (upper right) etc. Note pressure solution texture in a quartz grain to the right of centre. 1 nic., 22 x. South of Ned. Gryssjön (048/327). Photo I. Signorelli.

Sericite pseudomorphs of feldspar (probably plagioclase) occur in the sandstones. Sericite is also found in subordinate amounts in the matrix between quartz and feldspar grains. Occasionally, large detrital muscovite flakes may also be observed (Fig. 56).

The sandstones contain subordinate or accessory amounts of opaque minerals, biotite, rutile, zircon, apatite and sphene. The latter has been observed to form secondary crystals in the interstices between detrital grains (cf. Gorbatshev 1962a).

5.2.3.2. DOLERITE WITH DIFFERENTIATES

The youngest rocks of the Los-Hamra region are dolerite intrusions ("Åsby dolerite") and associated differentiates. They cut through the orogenic complex and the Råtan granite. Dolerites are, however, most frequent in the sub-Jotnian complex (Dala volcanics and granites). From Kopparberg County (Hjelmqvist 1966) and Jämtland County (P. H. Lundegårdh, personal communication) it is known that similar dolerites also intrude the Dala sandstone.

All dolerite dikes of post-orogenic character are grouped together on

Plate 1. It is possible that different generations of these rocks occur, but there is no evidence of this.

The width of the dolerite dikes varies between < 1 m and c. 200 m (cf. Fig. 57). Normally, the contacts with the country rocks are not exposed, the marginal jointing facilitating erosion (see below). However, two tunnel sections along Oreälven (C1-D1 and E1-F1) give good opportunities for studying the dolerite relationships (Figs. 57 and 58). Widely varying values for strike and dip have been recorded, and suggest a lack of any preferred orientation. It is, however, interesting to note that the low westerly dip of the broadest dike compares closely with the general dip of the great Åsby dolerite dike in Kopparberg County (Hjelmqvist 1966: p. 147). The marginal jointing of the dolerites permits water circulation, an important factor to be considered in tunnel works.

Contact metamorphic phenomena are not conspicuous. They are usually restricted to a faint recrystallization (e. g. at 150/034). However, north of Tallsjön (180/090), extensive epidotization of a conglomerate was probably due to hydrothermal activity related to a dolerite. West of Tallsjön (186/077), pyrite impregnations in Dala porphyrite probably have a similar origin (see p. 91).

The thicker dolerites are medium- to fine-grained, with aphanitic margins. Coarse-grained schlieren, sometimes containing potash feldspar, occur in some localities. The colour of the dolerites is dark grey to black. Ophitic to sub-ophitic textures prevail (Fig. 59), but in some fine-grained dolerites the relationship between plagioclase and pyroxene is sub-doleritic (cf. Krokström 1932b).

Plagioclase is the main mineral of the dolerites. It forms tabular crystals parallel to (010). A pronounced, generally normal zoning is often present, accounting for a variation in the composition, which usually ranges from labradorite to andesine (c. An_{70} – An_{40}). Cores with up to An_{85} have been recorded. In extreme cases, marginal zones may reach c. An_{20} .

Alteration of plagioclase to epidote, sericite, calcite and prehnite is frequently noted.

Clinopyroxene (augite) forms an essential mineral. Particularly in the fine-grained dolerites, it shows brownish violet colours in thin section. A more or less regular zoning is often present. Up to 7° higher values for $2V_\gamma$ have thus been recorded in marginal parts of such pyroxenes when compared to the cores (cf. p. 90). Optical determinations of augites are given in Table 4: nos. 17–22.

The augite may be somewhat altered to brown or green hornblende, biotite and chlorite.

Olivine, opaque minerals and biotite occur in essential to subordinate amounts.

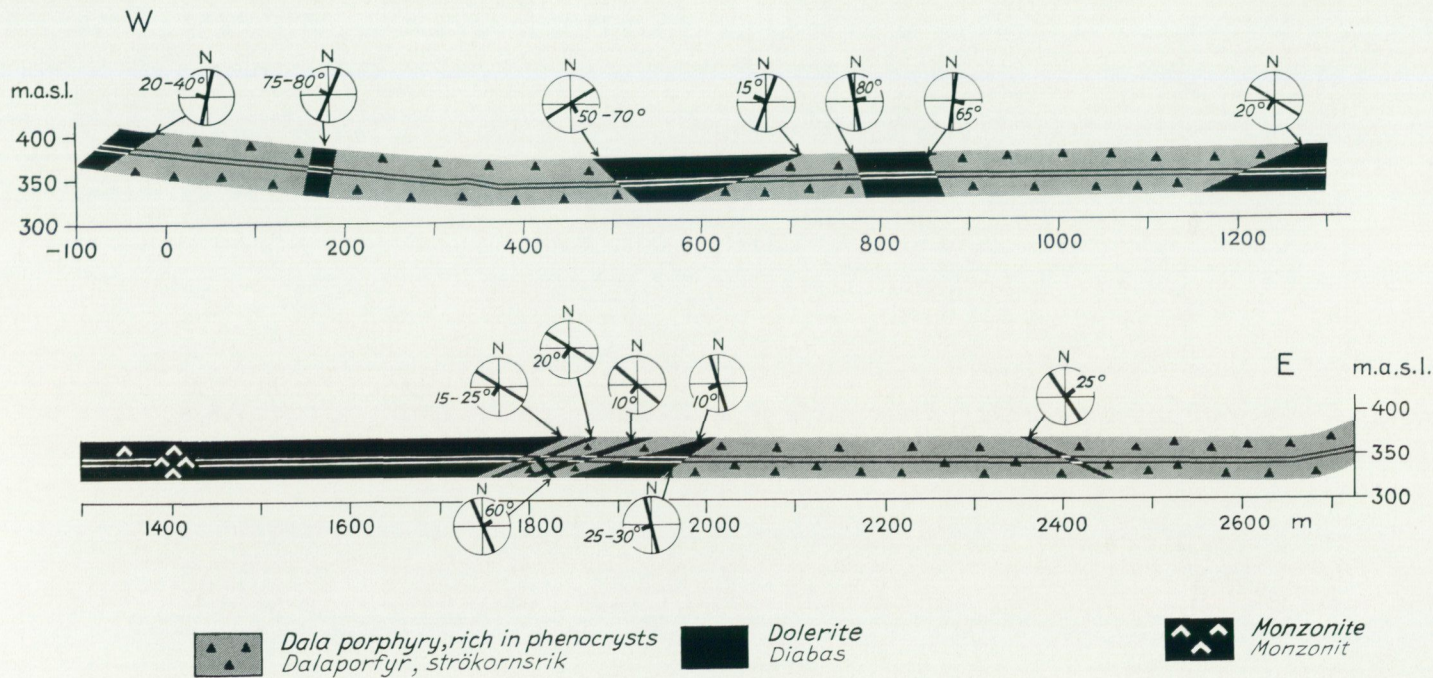


Fig. 57. Cross section along tunnel I, Oreälven. (Position, see Plate 1, C1-D1.) Insets show strike and dip of the dolerite contacts.

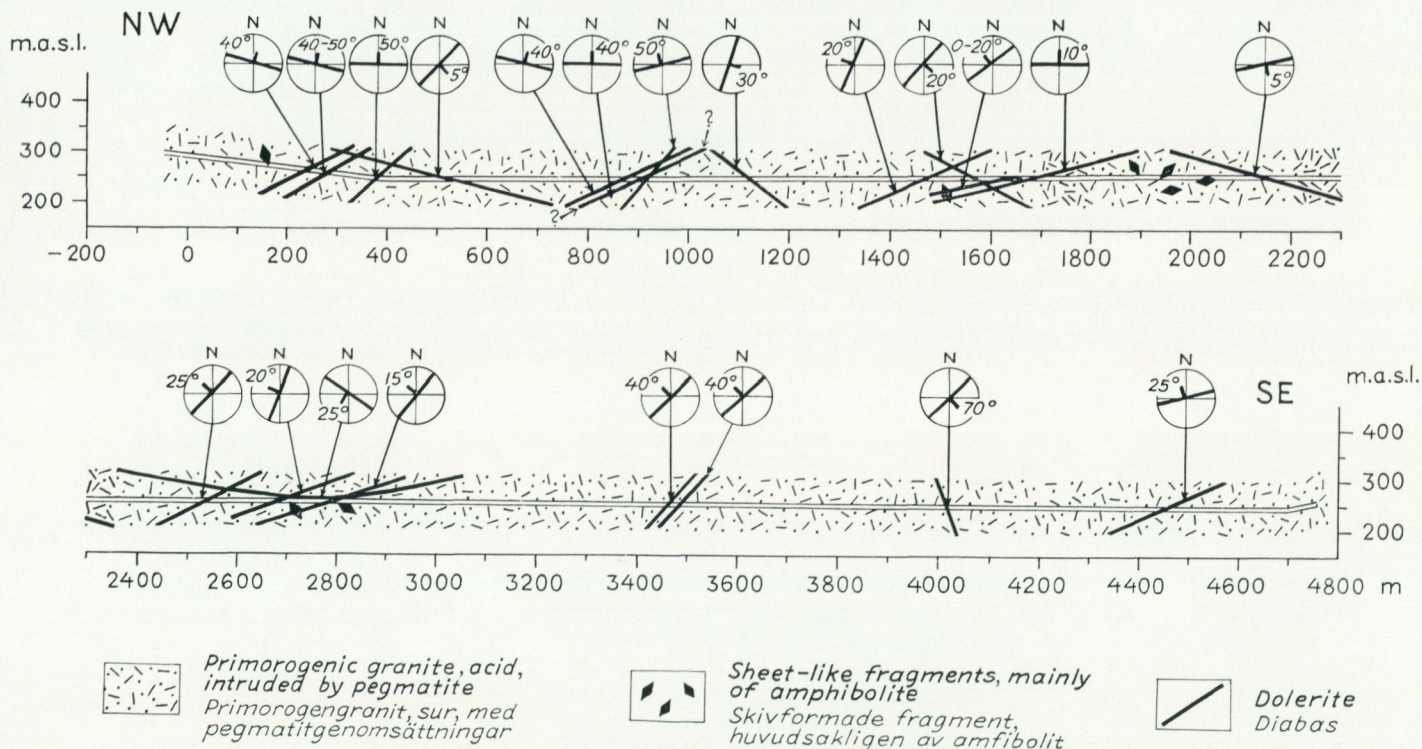


Fig. 58. Cross section along tunnel II, Oreälven. (Position, see Plate 1, E1-F1.) Insets show strike and dip of the dolerite contacts.

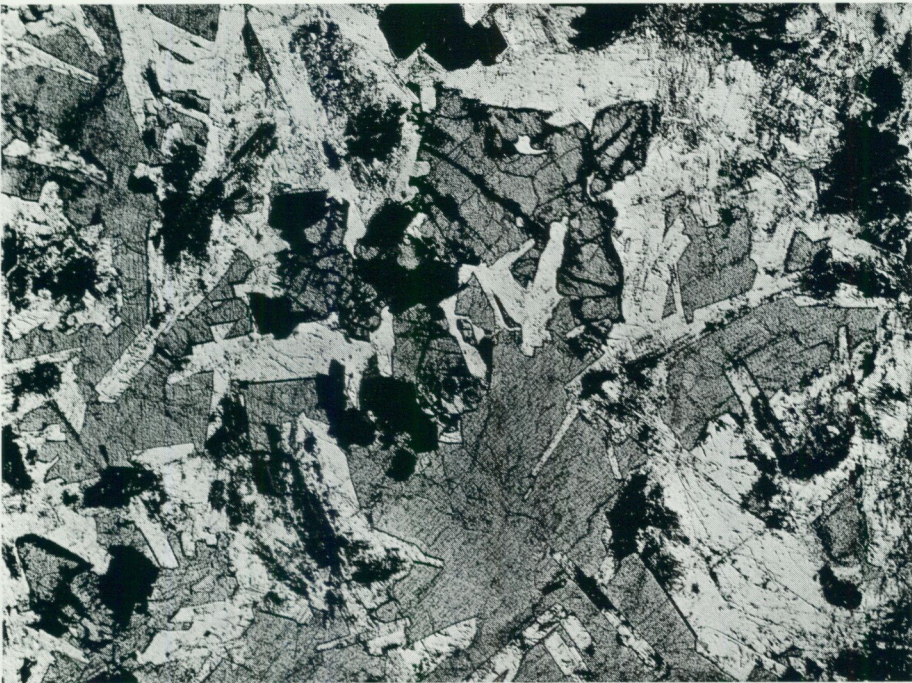


Fig. 59. Dolerite with ophitic texture. Lath-shaped plagioclase crystals embedded in augite (grey crystals showing cleavage). Titanomagnetite-ilmenite grains (black) and olivine (above centre) also occur. 1 nic., 17 x. Naappo (194/226). Photo I. Signorelli.

The olivines of four samples (Table 4: nos. 23–26) show *mg* values between 0.44 and 0.76. The mineral shows an alteration, being pseudomorphosed, in extreme cases, by serpentine, hornblende, biotite-phlogopite, oxides and talc. It may also be corroded by augite.

The opaque minerals are mainly ilmenite and titanomagnetite. They generally form intergrowths, the more or less regular lamellae of ilmenite occurring in the titanomagnetite (Fig. 60). The latter, at high magnifications (>600x), is seen to consist of minute (<1 μ) droplike inclusions of one phase in another. The titanomagnetite is anisotropic in the same colours as ilmenite, although much weaker. Lamellar and patchy textures occur within the titanomagnetite (see Fig. 60), due to variation in crystallographic orientation of the anisotropic phase(s).

Electron probe microanalysis for iron and titanium indicates that the two phases of the titanomagnetite are probably magnetite and ilmenite. Such intergrowths are considered to be formed through oxidation of a magnetite-ulvöspinel solid solution (Buddington and Lindsley 1964).

A rim of dark reddish brown biotite often surrounds the titanomagnetite-ilmenite grains.



Fig. 60. Titanomagnetite-ilmenite grain in dolerite. Ilmenite lamellae black. Titanomagnetite grey to white, patchy. Reflected light, nicols at c. 90° , 104 x. Gäddtjärn (062/234). Photo I. Signorelli.

The biotite of the dolerites is usually dark brown, and occasionally greenish. It is often clearly secondary after augite. Alteration of olivine, on the other hand, seems to have produced a weakly absorbing, phlogopitic mica with pleochroism in green to yellow-brown.

An alteration of biotite to chlorite is often noted.

Quartz and brown-pigmented potash feldspar occur in subordinate amounts, sometimes in granophyric intergrowths. They are located in the interstices between plagioclase and pyroxene crystals. The plagioclase is corroded by potash feldspar.

Accessories are apatite, chalcopyrite and pyrrhotite.

Differentiates rich in potash feldspar occur in several localities in the thick dolerite dikes. They are speckled in black, pink and grey colours. Transitional types link them with the normal dolerites. The composition of the differentiates ranges approximately from monzonite to quartz-poor granite.

The differentiates which have the highest contents of potash feldspar are somewhat heterogeneous both in mineralogical composition and grain size. They are characterized by dominating perthitic alkali feldspar, which mantles and corrodes plagioclase. The perthite may form granophyric intergrowths with quartz. Essential minerals are plagioclase and quartz. The former is

often strongly saussuritized. Its composition ranges from andesine to albite. Normal zoning is frequent.

Common hornblende, often clearly secondary after clinopyroxene, forms an essential or subordinate mineral. Green or brown biotite, opaque minerals and clinopyroxene (augite) are subordinate constituents. Ilmenite predominates among the opaque minerals, but titanomagnetite is also represented (cf. above). Optical determinations of clinopyroxenes from monzonitic to granitic differentiates are given in Table 4: nos. 27–31 (nos. 27 and 28 are from the most granitic rocks). As in the normal dolerites, this mineral may show a zoning with values of $2V_\gamma$ a few degrees higher in the marginal parts of the crystals. The determinations of n_γ suggest a trend towards lower mg values for these augites in comparison with those of the normal dolerites.

Accessories are apatite, leucoxene, sphene, calcite and chalcopryrite. Small amounts of olivine may also be present. This mineral is usually more or less altered to hornblende, oxides, biotite etc. The composition of olivine in a quartz-poor granitic differentiate is fayalitic according to a determination of $2V$ (Table 4: no. 32). In a rock with a lower content of quartz and potash feldspar the olivine is a ferrohortonolite (Table 4: no. 33). The value of $2V_\gamma$ obtained for this olivine seems too high, cf. Tröger (1959).

Fine-grained, cross-cutting granitic veins, a few centimetres wide, may occasionally be observed in the dolerites. They are of two types. One is grey-white in colour and is characterized by quartz and albite, partly in granophyric intergrowths. Subordinate to accessory minerals include biotite, chlorite, opaque minerals, sphene, zircon, apatite, epidote, clinopyroxene and calcite. The second type is pink and may be weakly feldspar-porphyritic. Both perthitic alkali feldspar and albite occur together with quartz. Small amounts of the same minerals as in the veins of the first type are also found. Optical determinations of clinopyroxenes (augites) in dikes of the second type are given in Table 4: nos. 34 and 35.

von Eckermann (1936) also mentioned quartz-porphyritic granitic dikes in the dolerite east of Kroksjön (F4).

Differentiation trends similar to those described above have been found in dolerite associations of the Nordingrå region (Sobral 1913), Södermanland County (Krokström 1932a and 1936; Gorbatshev 1961) and from Kopparberg County (Hjelmqvist 1961).

Chemical and modal analyses of dolerites and their differentiates are given in Table 1: nos. 86–90. The dolerites are somewhat undersaturated in silica (qz negative), in agreement with the presence of olivine. The differentiation towards monzonitic and granitic derivatives has led to an increase of qz , alk and k , and a decrease of fm , c and (generally) mg . (See Fig. 71 on p. 227.) A mineralogical expression of the change in mg is the trend of olivine towards fayalitic compositions. However, two analyses of monzonitic diffe-

renitiates (nos. 107 and 108 of von Eckermann 1936) show a higher *mg* value than the dolerites. The cause for this may be the secondary alterations of femic minerals to serpentine etc.

The trace elements vanadium, chromium, cobalt and nickel decrease in the monzonitic and granitic differentiates. Zirconium, on the other hand, is more abundant in the latter. The ratio BaO : K₂O is lower in the differentiates than in the dolerites, whereas SrO : CaO is somewhat higher.

Two possible interpretations are envisaged for the genesis of the monzonitic to granitic differentiates of the dolerites. Either the parent magma was of dolerite composition, or of dolerite contaminated by assimilation of granitic material. It can not be decided from the present investigation which possibility is the most likely. Observations from Kopparberg County (Hjelmqvist 1966: p. 150), however, indicate that assimilation of granite and porphyry in some localities has caused the appearance of monzonitic varieties of dolerite.

5.3. SULPHIDE OCCURRENCES

Sulphide concentrations are practically limited to the orogenic complex. Different types may be distinguished. Within (and near) the amphibolites around Los (H6-H7), pyrite, pyrrhotite and chalcopyrite occur, sometimes associated with cobalt and nickel minerals etc. In some localities pyrrhotite is found as impregnations and compact masses in graphite phyllites (see above, p. 22). Poor impregnations of pyrite and pyrrhotite are found in two localities near Hamra (F5) and at Svartån (E7). On Ställstensberget, east of Tenskog (I4), chalcopyrite occurs in vein quartz (cf. p. 51). Only two sulphide deposits occur in the post-orogenic complex: the pyrite impregnations in Dala porphyrite at Tallsjön, p. 91, and the chalcocite etc. found in a Dala porphyrite breccia on Börningsberget (cf. p. 91).

The deposition of the sulphides generally has an epigenetic character. As to the pyrrhotite occurring in graphite phyllites it seems, however, likely that it was formed during sedimentation. The intrusive behaviour is then probably due to partial mobilization during metamorphism.

In several localities around Los (see Plate 1) there occur small sulphide concentrations in amphibolites and metasediments. During the eighteenth and nineteenth centuries, some of them were mined for copper and cobalt ("Nätsjö copper mines" at 366/259 and the cobalt mines at Los, 370/303). Subsequently, prospecting activity and diamond drilling carried out by the Bolidens Gruv AB have revealed several new small sulphide concentrations. In no case, however, has the grade of the "ores" been high enough to permit

mining. The description of the occurrences given below is essentially based on observations made in connection with this work. A summary of the main features of the deposits by T. Du Rietz has kindly been put at the author's disposal.

The wall rock is generally amphibolitic metavolcanics (in part amygdaloidal), calcite-cemented amphibolite breccia or tuffaceous metasediments (cf. p. 54). An exception is the occurrence at 352/294, where the sulphides are found in meta-argillites, quartzites and metasiltstones (cf. von Eckermann 1936: p. 232).

In general, the sulphide deposits are approximately lensoid in shape, although irregularities are numerous. They attain a maximum length of 100–200 m and a width of up to a few metres. Frequently, the sulphides are concentrated in folds or shear-zones in the amphibolites.

Among the sulphides, pyrite and chalcopyrite predominate, but copper contents are very variable. Pyrrhotite is a more subordinate constituent. Locally, sphalerite and galena may occur. Arsenopyrite and nickel-cobalt minerals are relatively rare. Banding occurs in the sulphide deposits, due to alternating layers rich in lead, zinc, copper and nickel (Grip 1961). A notably high nickel content has been recorded in a part of a drill-core from 358/316. Cobalt analyses often show around 0.1 ‰. Gold and silver percentages are very low.

The sulphides are accompanied by quartz, which has soaked the wall rocks.

The "Nätsjö copper mines" of similar type to the occurrences above have been described by Blomberg (1895: p. 119) and Tegengren et al. (1924: p. 138). In the 1840's an ore with 4 ‰ Cu was found here and mining commenced. However, this ore body was faulted out, and, when it could not be traced further, mining ceased. The sulphide-bearing zone strikes approximately parallel to the schistosity in the surrounding amphibolite, dipping about eighty degrees to the south-west. The sulphides are pyrite, chalcopyrite and pyrrhotite. The chalcopyrite fills microscopic fissures in the pyrite and contains inclusions of the latter, both indicative of a later deposition of the chalcopyrite. An alteration of pyrrhotite to marcasite has been observed. Small amounts of magnetite and ilmenite also occur.

Vein quartz and calcite accompany the sulphides. The calcite forms crystals up to some centimetres in diameter. Breccia structures are frequently observed, sulphides and calcite forming a network in vein quartz. Intimately associated with the carbonate are common hornblende, epidote and chlorite. In connection with the deposition of sulphides etc., the surrounding amphibolite has locally become brecciated and penetrated by quartz. The rocks so formed are mineralogically heterogeneous. Quartz plays a dominating role, whereas common hornblende, epidote, chlorite and strongly sericitized

anorthite-rich plagioclase are more subordinate. The latter minerals frequently form patches and schlieren.

At present, investigations of the old cobalt mines at Los (370/303) are impeded by the infilling of the pits with water and the overgrowing of the waste-dumps. Further, apparently the cobalt ore has been carefully picked out, so that only insignificant amounts can be found in the waste pieces. The description below is therefore based on older literature (Blomberg 1895; Tegengren et al. 1924) and a modern investigation, mainly of museum specimens (Welin 1966a).

Mining of the cobalt ore at Los was largely carried out around the middle of the eighteenth century. The occurrence is well known due to the discovery of nickel in the ore in 1751 (A. F. Cronstedt). It is situated in a partially amygdaloidal amphibolite. The cobalt ore was mainly found in the upper parts of a steep, north-northwest-striking fissure. It was followed for c. 90 m in this direction. The maximum width of the ore was 30 cm. Ore impregnations also occurred in the vicinity of the fissure.

The gangue of the fissure was largely calcite and quartz, with subordinate tourmaline, fluorite and common hornblende. Baryte formed a rare constituent.

Along the ore-bearing fissure, the wall rock (amphibolite) has been altered, hornblende being replaced by chlorite and plagioclase by sericite. A green biotite has also been formed. In addition, the wall rock is soaked with quartz, calcite, fluorite and tourmaline (Welin 1966a).

The ore-bearing paragenesis consists (in addition to quartz, calcite etc.) of minerals containing iron, cobalt, nickel, copper, bismuth, uranium, arsenic and sulphur. Welin (1966a) identified the following minerals by X-ray diffraction: chalcopyrite, cobaltite, bismuthinite, arsenopyrite, pitchblende (and uraninite), hematite, pyrite, pyrrhotite and marcasite. Tegengren et al. (1924), von Eckermann (1936) and Grip (1961) also mention gersdorffite, chalcocite, sphalerite, galena, niccolite, smaltite, native bismuth and fahlerz. These, however, do not seem to be important constituents of the ore (Welin 1966a). The presence of gersdorffite and native bismuth has later been verified by H. Christofferson (personal communication). According to Tegengren et al. (1924), gersdorffite ("nickelglance") is the mineral in which Cronstedt discovered the element nickel (see above).

Smaltite was originally considered to be the cobalt ore mineral. Welin (1966a) found that all specimens examined by him, which were labelled smaltite or chloanthite, were actually cobaltite. However, the possibility remains that smaltite and chloanthite are present in this association (cf. also Grip 1961).

An isotopic age determination on pitchblende from the Los cobalt ore was interpreted to yield a most probable age of 1690 m.y. (Welin 1966a). This was

considered to indicate that the cobalt mineralization occurred in close connection with the sub-Jotnian igneous activity. There is, however, no geographical association between the ore and the Dala granites. The occurrence of the ore in the amphibolites around Los was held to be due to "structural and chemical wall rock controls" (Welin 1966a: p. 501). Earlier (von Eckermann 1936: p. 200) it had been maintained that the cobalt ore represented late magmatic exhalation products associated with the surrounding metabasalts.

Weak sulphide impregnations occur in several localities in and around Los village, in addition to those shown on Plate 1. Thus, e. g. at 377/301, cubes of pyrite, up to one centimetre in diameter, have been found in thoroughly chloritized amphibolite.

Grip (1961: p. 70) noted that the sulphide deposits of the Los-Hamra region are of two types. One is the cobalt-bearing paragenesis described above (the nickel-arsenic type), the other occurs in some localities in graphite phyllites (disseminated nickel-pyrrhotite type). The second type of deposit is represented in some small mining pits south-east of Rullbo (242/311 and 241/312) and north-west of Risåsen (238/361), cf. p. 22. In the vicinity of these occur amphibolitic metavolcanics. The dominating sulphide is pyrrhotite, with very subordinate chalcopryrite and magnetite. Pyrrhotite shows minor alteration to marcasite. The ore is both compact and disseminated. In the case of the former it may contain fragments of graphite phyllite and quartzite, whilst in the latter it either forms a network of veins or occurs as scattered grains in the graphite phyllite. Quartz and fluorite form a gangue associated with the pyrrhotite. Tegengren (1911) and Tegengren et al. (1924) reported 0.39 % Ni and 0.10 % Cu in a sample from 238/361.

Two unimportant sulphide deposits near Hamra (279/213 and 290/200) have caused the opening of small mining pits. The first-mentioned occurrence is made up of poor pyrite impregnations in quartzite and strongly chloritized amphibolite with pegmatite intrusions. The second deposit (290/200) is situated in chlorite- and biotite-schist with quartzite and amphibolite. The "ore" mineral is pyrrhotite in the form of thin streaks and scattered grains. The pyrrhotite is replaced by marcasite and pyrite. Very subordinate chalcopryrite is also observed. The sulphides are accompanied by a skarn consisting of common hornblende, bytownite, diopside (in several cm large crystals; see Table 4: no. 36), garnet etc. See also Blomberg (1895: p. 126).

Both of the above sulphide occurrences near Hamra seem to be connected with approximately east-west striking schistosity zones, which form a high angle with the general structural trend of the region (cf. Plate 1).

South-east of Rullbo, near Svartån (237/304), a couple of small excavations for sulphides are situated. The bedrock is phyllite, in part graphitic, amphibolite and quartzite. Pyrite is the main sulphide mineral. It forms thin streaks and scattered grains in the phyllite.

An occurrence of pyrrhotite in amphibolite has been reported from the region approximately 1.5 km south of the locality just mentioned ("Ackelamsberget", see Blomberg 1895: p. 127).

The "Ställstensberget copper mines" are situated east of Tenskog (404/155). Mica-schists ("ställsten"), probably formed by shearing of metarhyolite, and a quartzitic rock containing cordierite and anthophyllite(?) pseudomorphs (cf. pp. 51 and 142) outcrop here. Vein quartz is present, associated with the strong tectonic movements in the region, and containing a low percentage of chalcopyrite. The latter also occurs in shear zones and in the surrounding rocks (Blomberg 1895).

A volcanic breccia in Dala porphyrite on Börningsberget (083/303) has been mined for copper on a small scale (cf. Blomberg 1895: p. 127). The ore mineral is chalcocite with secondary malachite. It occurs mainly in the matrix of the breccia together with epidote, calcite, red feldspar and quartz. Hematite is observed in fissures. The presence of chalcopyrite was also mentioned by von Eckermann (1936: p. 290). Copper mineralization in Dala porphyrites has been described from Kopparberg County by Hjelmqvist (1966: pp. 84-85 and 192).

All known sulphide occurrences in the Los-Hamra region lack economic value at present, the metal content and volume of the deposits being too small.

6. STRUCTURE AND STRATIGRAPHY

As already mentioned, the bedrock of the Los-Hamra region is divided into two tectonic units: the orogenic and the post-orogenic complexes. The former is characterized by strong folding, schistosity etc. and a wide range of metamorphic facies. The latter, on the other hand, is unmetamorphosed. Deformation may be related to faulting and tilting rather than folding.

The structural data given on Plate 1 are a representative selection of the observations, it being impossible, on the map, to present all the information acquired during the field work.

The schistosity of the orogenic complex shows dominantly medium to high angle dips (60-90°). Bedding in the supracrustal rocks is found in regions which have escaped alteration to gneisses and migmatites. It is usually concordant with the schistosity, although discordant relationships may locally be observed (p. 15).

Schistosity and bedding strike between north-west and north in the larger part of the region. Such directions are also prevalent to the south and south-east (see Hjelmqvist 1966 and Lundegårdh 1967). In this way, a connection may be traced between the supracrustal rocks of the Los-Hamra region and

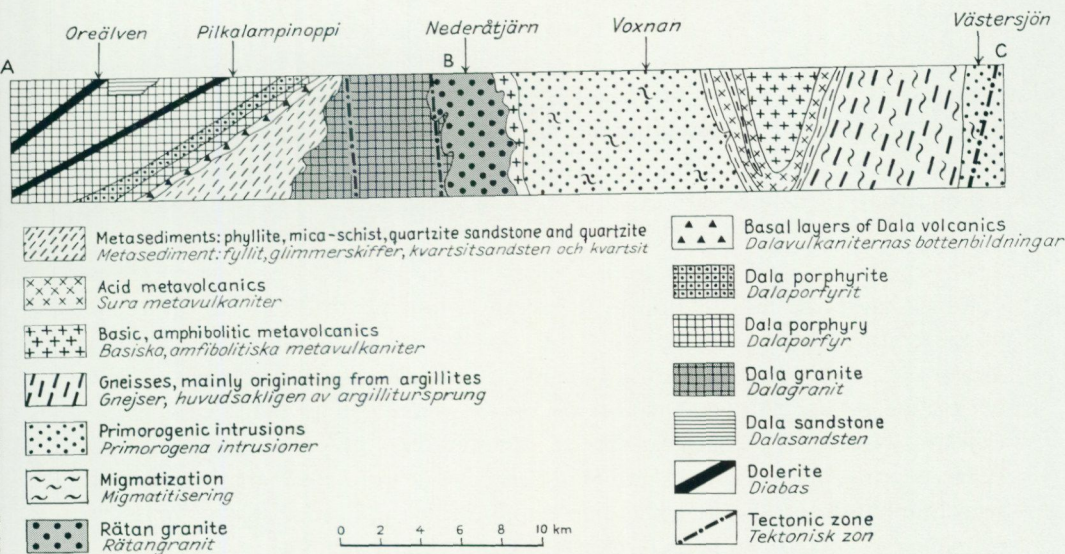


Fig. 61. Schematic cross section through the bedrock of the Los-Hamra region. For position of section, see Fig. 69, pp. 224-225.

those at Hamrånge (Lundegårdh 1956 and 1967). Deviation from the regional strike of the bedding and schistosity occurs in the fold hinges (Tenskog, H3-H4, I3-I4 and Lillskog, K5-K6) and at Noppikoski (E1). In addition, the northern parts of the orogenic complex are characterized by east-west to north-east-south-west strike directions.

The most important structural feature of the orogenic complex is a syncline (see Fig. 61), stretching from the region of Kvarnberg (H3) through Los (H6) to Selingen (J7). The supracrustal rocks at Lillskog (K5-K6) form a part of this syncline, which has been isolated by faulting (p. 140). It is evident that the syncline is broadly symmetrical and folds both bedding and schistosity. From this it follows that the schistosity must have been developed prior to or during the formation of the syncline. In addition, magnetic maps over parts of the syncline show anomalies (due to compositional banding) in agreement with the structures recorded in the field.

Locally, the facing (way-up) of the beds has been determinable. On Risberget (345/206, 351/205) cross-bedding in quartzites indicates younging towards the east. The occurrence of inclusions of metarhyolite in volcanic breccias associated with the amphibolites (p. 53) in the core of the syncline conforms this way-up. Further, cross-bedding in quartzites near Lillskog (511/251) shows that the partly skarn-bearing metasediments here overlie the amphibolites.

Lithological differences exist between the eastern and western limbs of the

syncline. Thus, in the west, two horizons of metarhyolite occur, whereas in the east only one main unit is found. West of Lossjön and around Dåasen (H6-H7, I7, J7) meta-argillites, quartzites and metarhyolites are lacking (cf., however, p. 47). The amphibolites are here in contact with primorogenic granite. In general, the primorogenic intrusions as well as the migmatized supracrustal rocks occupy anticline regions adjacent to the main syncline (Fig. 61).

On the basis of this structural interpretation, the following stratigraphy can be established in a section in the western limb of the syncline, from the vicinity of Ryggskog (G7) to Los (H7): a slate unit overlain by quartzite sandstone, then metarhyolite and finally amphibolitic metavolcanics. South of Romberg (402/350) mica-schist occurs between the quartzite and metarhyolite. North of Dåasberget (H7-I7) and in the Lillskog region (K5-K6), skarn-bearing metasediments (at Dåasberget also iron ores) are found in a stratigraphic position above the amphibolites. The dolomite at c. 372/328 is probably associated with these skarn-bearing metasediments.

The east-west to north-east-south-west strikes in the northern parts of the Los-Hamra region were considered by von Eckermann (1936) to be due to the intrusion of the Råtan granite. In such a case, the deformation would be post-orogenic, involving a folding of older structures. No evidence for such an interpretation has, however, been found. The only indication that the intrusion of the Råtan granite might have been responsible for the deformation is the geographical association of the two. Further, it might be argued that the Råtan granite, because of its size, should be expected to have caused considerable disturbance in the surrounding rocks.

As mentioned above, the stratigraphic relations in the syncline through Los are supported by observations of cross-bedding etc. However, in large parts of the region, the supracrustal deposits are isoclinally folded and only scattered observations on the facing of beds are available. In such cases the stratigraphic sequence has not been obtained. Around and north of Noppikoski (D1-D3, E1-E3), however, cross-bedding occurs in several localities, allowing a determination of the stratigraphy. The oldest supracrustal deposit is a quartzite, which occupies much of the eastern part of this area (Plate 1). Above it follow phyllites with layers of skarn-bearing quartzites. These are overlain by a partially arkosic quartzite (sandstone), which occurs e. g. at the bridge of Noppikoski (210/033). On top of the quartzite rest quartz-porphyrific metavolcanics (ignimbritic).

Lineations have been observed in many localities within the orogenic complex. They are usually formed by a microcorrugation of *s* planes (mica cleavage flakes) or a parallel orientation of prismatic minerals (e. g. amphiboles and sillimanite). In some areas, folding on amplitudes of c. 1 cm to a few metres has been recorded with axes parallel to the linear structures.

Parallelism of lineations and fold axes is known from the ore-bearing region of central Sweden (Geijer and Magnusson 1944: p. 63) and is common in the Caledonides.

The lineations observed in the Los-Hamra region show a varying orientation. Certain main features may, however, be discerned. Thus, in the migmatite region around and south of Hamra (F5 etc.) lineations generally show a medium plunge towards the south to east-southeast. The relations to fold axes are not clear. Because this lineation is regionally associated with migmatites, it may have developed in connection with the formation of the latter (cf. below, p. 138). Further eastwards, within and around the amphibolites of the Los-Tensskog region (H6-H4), similarly oriented lineations also occur, although other directions are also represented. In the synclinal hinge east to south-east of Tenskog (I3-I4) the structure is complex. Here lineations plunging at medium to low angles towards the north-west and north-east predominate. In some specimens two lineation directions at high angles have been observed. Further, the bedrock is cut by north-northwest striking shear zones (pp. 51 and 142), which appear to be later than the main folding of the region. Schistosity and bedding observations in the area indicate a synclinal fold axis plunging approximately $40-70^\circ$ to the north. This is roughly in agreement with the observations of lineation. In this connection it should be mentioned that von Eckermann (1922) recorded an axis of $20-25^\circ$ towards the north-west for a small syncline on Mansjöberget (I3).

Around the southern end of Dåasen (I6-J6), fold axes and lineations have a medium plunge towards the south-east. The lineation arises partly through a parallel orientation of sillimanite needles. Around Fetingsberg (I5-J5), fold axes and lineations generally show a medium to gentle plunge towards the north-west. In the Högsvedberget-Västर्सjön region (K5) the lineation plunges c. $25-50^\circ$ towards the north-west.

Within the isolated supracrustal occurrence at Lillskog (K5-K6), fold axes and lineations are steep; consequently the direction of plunge varies greatly. The constructed fold axis of the syncline hinge at Lillskog is likewise steep.

Within the east-west striking supracrustal belt north and north-east of Los, lineations and fold axes dominantly show a medium plunge towards the east or north-east. Bedding and schistosity dip $70-90^\circ$ towards the north. The fold hinge around 350/350 is not exposed and is located on the basis of the aeromagnetic maps, supported by regional structural and lithological relationships.

In the region dominated by meta-argillites stretching between c. F6 and H9, the lineation generally shows a high or medium plunge in greatly varying directions. The possibilities exist (cf. above) that the variations are due to a rotation of older structures and/or a creation of new lineations in connection with the intrusion of the Råtan granite. More detailed investigations than

have been possible in connection with the present work are necessary to solve this problem.

The axis of the fold in the supracrustal rocks north-west of Noppikoski (D1-E1) plunges c. 60° towards south-west or west-southwest. In this case there seems to be no agreement between the axis and the lineations, the latter usually showing a medium plunge towards the south or east. The cause for this is not clear. Possibly the structure is complicated by later faulting (cf. below, p. 140).

Tectonic zones which cut through the orogenic as well as the post-orogenic complex are treated below (p. 140 ff.).

The generally concordant intrusion of the primorogenic granites etc. can be referred to a later time than the (first) development of a schistosity. Probably these magmas intruded in close connection with folding. In the marginal facies of the granites it is sometimes observed that the latter cut the schistosity of the supracrustal rocks (cf. Fig. 16 on p. 59). From textural relationships it is clear that a second generation of biotite and chlorite (the former accompanied by andalusite and cordierite) formed in an already schistose (lepidoblastic) meta-argillite under the influence of the primorogenic intrusions (cf. pp. 15 and 17). Near Laxtjärn (G6) the mica-schists are strongly schistose, whereas a parallel orientation of the small amounts of mica in the granite is not observed. The contact between the two is not seen. However, the inferred relationship between intrusion and schistosity is supported by the lack of schistosity in the biotite-rich primorogenic rocks in the area. By contrast, within the migmatized primorogenic intrusions, schistosity (and lineation) is usually distinct, even in those cases where marginal facies granites have been altered in this way, as e. g. west of Lossjön (H6-I6). The schistosity has probably developed in close connection with the migmatization. In the serorogenic stage, the marginal facies of the primorogenic granites frequently seem to have occupied a position not affected by recrystallization under directed pressure.

Serorogenic granites, pegmatites etc. may show a weak schistosity.

The possible deformation caused by the Rätan granite has been discussed above (pp. 136 and 137). Little is known of the shape of the Rätan granite intrusion. At Pajkölen (361/448) the schistosity of the argillitic gneiss dips 35° to the west, beneath the granite, suggesting that locally the form is sheet-like, whereas at 269/372, the granite contact is steep.

Lundegårdh (1967: pp. 16–39) has presented a model for the tectonic evolution of central Sweden, embracing both orogenic and post-orogenic deformation. According to this model, the Los-Hamra supracrustal rocks of the orogenic complex were deposited in depressions not far from the southern border of a large geosyncline. The latter successively became filled with sediments of dominantly greywacke character [Härnö formation (series), see

Magnusson et al. 1960]. Deformation in the region south to south-west of the geosyncline was considered to have started with the formation of horsts and grabens. Under the influence of compression and intrusions of primorogenic magma, the supracrustal rocks became folded. The earliest fold axes were oriented in north-south to north-northwest directions. Shearing (imbrication) along steep surfaces striking west-northwest to north-west later took place, in connection with the intrusion of the Revsund and Råtan granites.

The rocks of the sub-Jotnian and Jotnian complexes are, like the Råtan granite, characterized by the absence of schistosity and lineation. Dala porphyries and porphyrites generally dip to the west and south-west (cf. Fig. 61). The tilting of the deposits may e. g. have occurred as a consequence of the igneous activity (emptying of magma chambers in the crust etc.), or in connection with the intrusions of the Jotnian dolerites.

The unconformity under the basal deposits of the Dala volcanics attracts great interest. From the map, Plate 1, it appears that the basal deposits of the Dala volcanics regionally transgress the supracrustal rocks of the orogenic complex at a low angle. The unconformity is marked by differences in schistosity and metamorphism, although there is no very sharp break in these respects. This may be related to two circumstances. The immediately underlying supracrustal rocks of the orogenic complex are only slightly influenced by regional metamorphism. Further they are poor in mica (meta-rhyolites and quartzites) and thus do not easily develop a schistosity. The relations between the Råtan granite and the basal deposits east of Tandsjön (149/272) are not clear.

In general, the supracrustal rocks in the Tallsjön-Noppikoski region (D1-D2, E1-E2) dip approximately $50-70^{\circ}$ to the west, whereas the bedding in the basal layers of the Dala volcanics mainly displays variations between 20 and 60° in the same direction. South of Tallsjön (see Fig. 25 on p. 80) the basal layers are well exposed. The dip of the orogenic metarhyolite, based on the orientation of the ignimbrite "flames", is generally steeply inclined and discordant to the unconformity. However, as the "flames" show great variations in attitude, they may be disturbed and not reflect an original horizontal surface (cf. p. 106). Thin remnants of basal breccia occur as isolated outliers somewhat east of the continuous belt of basal deposits (Fig. 25). From this it is evident that a discordant relationship on the whole prevails between the orogenic complex and the basal Dala deposits. The observations also indicate that the surface on which the basal layers were deposited was somewhat uneven.

There is a general lack of migmatites and other infracrustal rocks in the basal sub-Jotnian conglomerates and breccias. Evidently, the former were not exposed in the provenance areas of the latter.

For a discussion of the stratigraphy of the Dala Volcanics Formation see pp. 78–79.

The regional rather regular medium to gentle dip towards the west or south-west of the Dala volcanics is locally considerably disturbed. It has been mentioned earlier (p. 106) that viscous flow in the porphyries may account for some of the steeper and/or greatly varying dips of the band structures and "flames". Sometimes deviation from the regional dip can also be related to faulting. Such is the case near Älvho (c. 156/030). Bedding and pseudo-fluidal structures here dip c. 70° towards the north-northwest along Oreälven. This is probably due to a fault zone along which dolerite was intruded. Dikes of the latter occur in two narrow "canyons" (cf. von Eckermann 1936: Fig. 17 on p. 270) striking $N80^\circ E$ and dipping 65° towards the north. A similar feature is also found at Grottan (c. 138/028), a gully previously followed by the river Oreälven. A steep jointing approximately parallel to this river is also observed in the eastern parts of Tunnel I (C1-D1).

The regular north-south trend of the western limit of the orogenic complex (see Plate 1) is evidently disturbed along Oreälven. The schists, quartzites and quartz porphyries which outcrop in the Korpmäki-Gråtbäck area south of Älvho (cf. von Eckermann 1936 and Hjelmqvist 1966) would be expected to lie at some depth, covered by Dala volcanics. Their occurrence is probably due to the rising of a horst, the northern limit of which runs along Oreälven.

For the orientation of the dolerite dikes, see p. 124. The geographical association between Jotnian sandstones and dolerites is discussed on p. 165 (cf. also p. 121).

Tectonic zones characterized by faulting, strong cataclastic deformation, formation of mica-schists etc. have been marked on the map, Plate 1. The above described fault along Oreälven belongs to these zones. In addition to the tectonic lines indicated on the map, several others are thought to exist, accounting for various topographic features. As the cataclastic effects have produced a rock that is relatively easily attacked by erosion, such zones tend to form valleys, which become filled with moraine, glacialfluvial deposits etc. In such cases, the mylonitization in these zones may not always be seen in outcrops. On Plate 1 only the central parts of zones, where cataclastic effects have been observed, are indicated.

The most important tectonic lines run in a north-northwesterly direction. The maximum width of clear cataclastic effects is c. 3 km. Thus, in the eastern parts of the Los-Hamra region, a tectonic line runs from L. Öjungen (K3) towards Selingen (J7). It can be traced further north on topographical maps, and seems to continue along the eastern border of the Råtan granite massif (cf. Lundegårdh 1967 and Magnusson et al. 1960). The granite is also affected by the deformation. From the map, Plate 1, it is evident that con-

siderable (up to c. 9 km) dextral movement has occurred along the zone, accounting for the displacement of the synclinal hinge of the Lillskog (K5-K6) supracrustal rocks. The difference in plunge of the fold axes and lineations on each side of the fault and the wide outcrop of the skarn-bearing metasediments at Lillskog suggest some vertical as well as strike-slip movement in the fault zone.

Within the L. Öjungen-Selingen zone the bedrock has been mylonitized and partly altered to mica-schists (e. g. at 485/300). The new schistosity generally shows a medium to high dip towards the west.

The so-called Räkaklitt iron ore, situated about 11 km south-east of Nybyn (Nybyn = 480/125) seems to be connected with the tectonic zone just described by a topographical feature (cf. Blomberg 1895: p. 117 and von Eckermann 1936: p. 136). The ore mineral is hematite. It occurs in a quartz-cemented breccia.

A very pronounced tectonic line runs parallel to the one described above, immediately east of the map region of Plate 1. It is most evident in the valley Skrälldalen and lake Ängratörn (J9-J10, K9-K10).

Another important tectonic zone runs along Sandsjöån via Lillhamra and Tandsjön towards Ned. Gryssjön (F1-D4-C6-A7). An eastern branch seems to follow Kvarnån (E3-F3) and continue via Sandsjö (E4) towards Öv. Hamravallen (E5). The rocks of the orogenic complex (primorogenic intrusions, amphibolites, quartzites etc.) and the Dala porphyrites near Ned. Gryssjön have been strongly brecciated and mylonitized. The primorogenic intrusions and acid metavolcanics along Sandsjöån have often been transformed to mica-schists. An example of this has been described earlier (p. 51), with the alteration of metarhyolite to cordierite or andalusite mica-schist. The Råtan granite and the Dala granites are also affected, the latter, however, relatively weakly (mortar structure etc.). The effects of the tectonic movements on the Dala sandstones and the dolerite north of Lillhamra (D5) are not known. Thin dolerite dikes at Sandsjöån (268/076 and 225/125) are, however, clearly affected and partially altered to low-temperature assemblages. Further, north-west of the map region of Plate 1, the tectonic zone (or zones closely related to it) cuts through Jotnian dolerites (P. H. Lundegårdh, personal communication).

That the cataclastic and recrystallization phenomena in the rocks of the orogenic complex are much more extensive than in nearby Dala granites may be taken to indicate that movements have occurred in the zone before the intrusion of the granites. One phase of deformation is also probably contemporary with the intrusion (p. 117), whilst there is also some evidence of later deformation affecting the dolerites.

From the southern end of Tandsjön (c. 160/250) a tectonic zone runs towards east-northeast (Långberget, E6). It passes through Dala granite,

Rätan granite and primorogenic rocks. The extent of the latter is hard to estimate because of the cataclastic effects, which have produced undulous and granulated quartz and mortar structure in feldspars (p. 71).

East of Tenskog (I4) strong shearing has transformed a metarhyolite to mica-schist (p. 51). A copper mineralization is also connected with the tectonic zone running here (p. 134). The possibility exists that the shearing and the accompanying alterations have occurred as a consequence of deformation in the migmatite region to the south and east.

Around Lossjön (I6) zones with strong deformation have been noted. Probably the whole valley of Loån to the south is an important tectonic line. The bedrock can, however, seldom be studied here as it is covered with thick Quaternary deposits. There may exist a connection between the Loån zone and the north-northwest striking mineralized fissure of the cobalt mines at Los (p. 132).

One locality south-west of Lossjön (397/258) is of particular interest. A breccia occurs there, which was interpreted by von Eckermann (1936: p. 195 f.) as talus deposited on a peneplain cut into the sub-Loos Series. The breccia should thus form the basal layer of the dominantly volcanic Lower Loos Series. Road-work at this locality in 1962 created new outcrops, which show a muscovite-rich quartzite cut by red pegmatite. Extensive deformation has caused a brecciation of both these rocks. In the new outcrops all transitions are to be seen from a pegmatite-intruded quartzite to a breccia with fragments mainly of quartzite and red microcline in a quartz-plagioclase-microcline-muscovite matrix. Such a breccia is also exposed in outcrops examined by von Eckermann. Undulous quartz, bent twin lamellae in plagioclase and curved cleavage surfaces in muscovite together with a crushing of microcline all testify to very strong deformation. Also the surrounding red, fine-grained primorogenic granite shows strong cataclastic effects. The breccia is consequently interpreted as a purely tectonic phenomenon by the present author.

Deformation in north-northwest trending zones has also been observed along Voxnan, north-west of Rullbo (D8-D9) and south-west of Tenskog (H3). Similar zones also occur at Hamra (F5).

With regard to the age of the tectonic lines described above, the following general conclusions can be drawn from the observations. It is clear that some movement occurred in post-dolerite time, i. e. after the formation of the youngest rocks of the region. In some cases it is likely that deformation took place in several stages separated by more quiet intervals. On p. 117 it has been mentioned that tectonic movements probably accompanied the intrusion of the medium-grained weakly porphyritic Dala granite. An independent line of evidence leading to the same conclusion has been obtained from the old cobalt mines at Los. As mentioned on p. 132, the ore was found within and along a north-northwest striking fissure (cf. also above). The mineralization

seems to have occurred in connection with the intrusion of the Dala granites (Welin 1966a). Movement in tectonic zones has evidently also occurred at a time when regional (serotogenic?) recrystallization operated to transform the sheared rocks to mica-schists, sometimes containing andalusite etc. (pp. 51 and 61).

In Kopparberg County, lead mineralization along north-south fissures seems to be of a late sub-Jotnian or Jotnian age (Wickman et al. 1963: p. 239).

It is interesting to note that the major tectonic lines of the Los-Hamra region have the same general strike as similar zones in the western parts of southern and central Sweden. For the most important of these, Magnusson (see Magnusson et al. 1963: p. 162) from potassium-argon data maintained an age of c. 1,240–1,380 m. y. Welin (Welin and Blomqvist 1966: p. 16), however, considered a maximum age of 950–1,050 m. y. more probable. Further, overthrusts with similar strikes in the Dal formation in south-western Sweden are thought to be somewhat older than the Bohus granite (Magnusson et al. 1963: p. 160), the age of the latter being c. 900–1,000 m. y. (Magnusson et al. 1963: p. 163; Welin and Blomqvist 1964).

Quartz dolerite dikes filling north-west fissures occur in Kopparberg County, intersecting the effusive "Öje dolerite" and the Dala sandstones. One of these dikes appears to have intruded after the deformation leading to steep dips in the sandstone (Hjelmqvist 1966: p. 155).

Movements in Phanerozoic time may have occurred in connection with e. g. deformation in the Caledonides. A general uplift of the latter seems to have taken place in Tertiary time (Magnusson et al. 1963: p. 354). A release of stress may consequently have occurred then along older tectonic zones (cf. Lundegårdh 1967: p. 39).

7. MORPHOLOGY

Over large parts of the Los-Hamra region the composition and the structure of the bedrock greatly influence the morphology.

Areas with north-northwest striking schistosity and compositional banding are generally characterized by an elongation of ridges, valleys and lakes in this direction. The effect of the Quaternary land-ice has probably been to emphasize these features, as the common direction of ice movement was approximately parallel to these structures (G. Lundqvist 1963). The tectonic zones described in the preceding chapter also run in the same direction and have clearly had a very strong influence on the morphology. The east-west flow of Oreälven in the Älvho–Noppikoski region (C1-F1) deviates from the general direction of the river courses. This is probably due to faulting connected with the formation of a horst in the south (p. 140).



Fig. 62. Örnberget (c. 170/163), a hill consisting of Dala porphyry (phenocryst-poor, with ignimbrite "flames"). View from the north. The steep scarp to the left (east) contrasts to the gentle dip slope to the right (west). In the foreground occurs Dala porphyrite.
Photo P. H. Lundegårdh 1965.

Within the orogenic complex large differences in mechanical properties and resistance to weathering exist. Thus, quartzites and amphibolites on the whole tend to form ridges with numerous outcrops (e. g. H6-I4), whereas slates and phyllites give a very flat topography with few exposures (e. g. F7). During the mapping of the region, more resistant rocks may therefore have been quantitatively somewhat overestimated.

The sub-Jotnian rocks give a landscape with a relatively broken relief. This is also observed in other regions with similar rocks (e. g. at Nordingrå and Ragunda in northern Sweden). As already mentioned, the Dala volcanics occur in sheets with a medium to gentle dip towards the west or south-west. These rocks tend to split along the bedding planes and the surfaces of the pseudo-fluidal structure. The topographical expression of this is that hills built up of such rocks often have steep eastern scarps and gently westerly dip slopes. Examples of this are Örnberget (D4, see Fig. 62), Korsiberget

(D4) and Pikkalampinoppi (D3). However, the steep eastern limit of the Dala volcanics in the region Lillhamra-Tandsjön (D4-D5, C6) seems to be due to tectonic movements in the Sandsjöån-Ned. Gryssjön zone (p. 141).

8. ALKALI FELDSPARS

A special study has been undertaken on the alkali feldspars of the different igneous rocks from the Los-Hamra region. Even from a rapid survey of thin sections, it is evident that alkali feldspars in sub-Jotnian and Jotnian igneous rocks differ from those of the orogenic complex and the Rätan granite. Further, it is known that in the Finnish rapakivi granites, which have been compared to the Swedish sub-Jotnian granites, the dominating potash feldspar is orthoclase (see e. g. Simonen 1960, Savolahti 1962 and Eskola 1963), in contradistinction to the microcline of the majority of Precambrian rocks. The present investigation has been undertaken with a view to examine whether the alkali feldspars can be of diagnostic value for distinguishing between sub-Jotnian and Jotnian rocks on the one hand and older rocks on the other.

From the microscopic examination of thin sections from all rocks containing potash feldspar in the Los-Hamra region some general features are evident. Microscopically visible twinning according to the albite and pericline laws (cross-hatching) is much rarer in the sub-Jotnian and Jotnian complexes than in the orogenic complex and the Rätan granite. Such twinning has been observed only in a few samples from the former two complexes. It may then appear as very fine lamellae close to minute cracks in the feldspar crystals. From other works it is known that deformation may promote triclinization of an originally monoclinic potash feldspar (see e. g. Karamata 1961 and Dietrich 1962). In connection with this, twinning may also develop.

The acid metavolcanics of the Los Formation contain perthitic alkali feldspar phenocrysts, in which microscopically visible twinning may be absent or sparse. In one sample a zoning has been noted, a cross-hatched margin surrounding a core lacking visible twins.

The potash feldspars are perthitic in all rocks of the Los-Hamra region. Generally, the albite bodies of the perthite are much smaller in sub-Jotnian and Jotnian than in older rocks, occurring as irregular patches with a more or less pronounced tendency for elongation in a plane forming c. 90° with (010) and c. 75° with (001). This plane is near the "murchisonite" cleavage ($\bar{1}502$). However, the central parts of phenocrysts in sub-Jotnian and Jotnian rocks in particular may contain clear patches, which are non-perthitic or perthitic on a submicroscopic scale (cf. below). On the other hand, in the orogenic complex and in the Rätan granite, vein perthite is abundant,

although film (to string) perthite also occurs (cf. Andersen 1928). The latter type of perthite is characteristic of the sillimanite gneisses (p. 31) and horn-felses (p. 22), which represent the highest degree of regional and contact metamorphism, respectively, in the region. It also appears in the Råtan granite together with vein perthite.

Both in the orogenic and post-orogenic complex it can frequently be observed that the albite bodies of perthites have approximately the same crystallographic orientation as the host potash feldspar. The albite component of the perthite is not uncommonly twinned according to the albite law.

X-ray and optical parameters have been determined for potash feldspars from 71 samples of igneous rocks from the Los-Hamra region (Table 8). The X-ray investigation has been carried out with the aid of a Philips diffractometer type PW 1051 to give the triclinicity of the potash feldspars (cf. Goldsmith and Laves 1954a). For porphyritic rocks the powder was obtained by hand-picking from at least ten different phenocrysts. Potash feldspars from even-grained rocks and groundmasses of porphyritic rocks were separated with heavy liquids. Optical determinations have comprised measurements of $2V_\alpha$ on a four-axis universal stage and of extinction angles $\alpha' \wedge (001)$ on (010) and $\alpha' \wedge (010)$ on (001). The latter determinations have been carried out on powdered samples in immersion liquids.

The accuracy in the measurements mentioned above is highly dependent on the character of the material. The minimum error in triclinicity can, however, be estimated at c. ± 0.02 – 0.03 , in axial angle ($2V_\alpha$) at $\pm 1^\circ$ (by measurement of both optical axes) and in $\alpha' \wedge (001)$ on (010) and $\alpha' \wedge (010)$ on (001) at $\pm 0.5^\circ$. In strongly perthitic and hematite-pigmented feldspars the accuracy is necessarily much lower. Further, many of the samples (especially from sub-Jotnian and Jotnian rocks) contain potash feldspars which are very heterogeneous both with regard to optical and X-ray properties (cf. below).

As mentioned above, all potash feldspars are perthitic. The exsolution has been complete or nearly so, according to the method of determining albite in solid solution with potash feldspar proposed by Goldsmith and Laves (1961). From Guinier powder photographs (monochromatic $\text{CuK}\alpha_1$ radiation) the difference Δd in d values between the 220 line for pure silicon metal and the 400 line for potash feldspar was measured. Δd is negative for pure potash feldspar (microcline and sanidine) and passes through zero at c. 10–15 weight percent albite to positive values corresponding to higher albite contents. The determination was somewhat complicated by the appearance of a weak line (also obtained with a sample of almost pure potash feldspar), which could be mistaken for 400 and would correspond to an albite content of c. 20 weight percent. As, however, the photographs prepared all show a line corresponding to albite percentages near zero, this is taken to

indicate complete or almost complete exsolution (Table 7). Samples from sub-Jotnian rocks often show a somewhat diffuse 400 reflection, indicating a somewhat variable composition, with a maximum of a few percent of albite in solid solution. Small amounts of sodium may therefore have remained in the potash feldspar lattice.

The compositions of eighteen samples of perthitic alkali feldspar have been determined by chemical analysis (Table 7: nos. 1–18). In addition, the compositions of four perthites from Dala granites have been calculated from whole rock chemical and point-count analyses, assuming 5 % potash feldspar and 5 % muscovite to be contained in the plagioclase of the rocks (Table 7: nos. 19–22, cf. also p. 115). For the chemical analyses of the feldspars, the phenocrysts have been separated by hand-picking. Heavy liquids ($d = 2.605$) were used for purifying the phenocryst material and for separation of perthite from non-porphyrific rocks. This heavy liquid separation was carried out on material in the fraction 0.1–0.2 mm. It was necessitated by the occurrence of inclusions of corroded albite etc. in the perthite (cf. pp. 99 and 115). Very small inclusions could, however, not be separated by this method. Smaller grain sizes, on the other hand, could not be used, as the separation would then have severely affected the composition of the perthite itself. The accuracy of the method is hard to estimate, as it is dependent on several factors (size of albite bodies, foreign inclusions etc.). However, a good approximation of the true perthite composition will certainly be obtained in this way. Further, the albite percentages of Table 7: nos 1–18 are reasonable with regard to the corresponding chemical whole rock analyses (Table 1a), modal estimates (Table 1c) and rough microscopic estimates of compositions of the coarser perthite types.

The chemical analyses of perthites comprise sodium, potassium, calcium and trivalent iron; in a few samples also barium and strontium. On recalculation to feldspar "molecules" from these analyses, the minimum value obtained was c. 92 %. The deviation from 100 % is caused by errors of determination (Table 1d) and small amounts of minute inclusions (quartz, sericite etc.) in the feldspars.

In Table 7, the analyses have been recalculated to $Ab + Or + An = 100$. Feldspars from Dala granites and porphyries are richest in albite (26–48 mol. %). The Råtan granite augen (phenocrysts) contain 20–26 % Ab and the perthites of two primorogenic rocks show 13 and 17 % Ab, respectively. Pegmatite perthites are relatively low in albite: in two pegmatites connected with migmatization the albite percentages are 11 and 19, in one Råtan pegmatite 17, and in two Dala pegmatites 9 and 16.

Anorthite contents are very low. A maximum of 2 mol. % has been recorded in some sub-Jotnian rocks.

The pigmentation with hematite, which causes an intense red colouring,

is especially prominent in some sub-Jotnian granites and porphyries, e. g. nos. 12 and 15 of Table 7. In comparison with the very red perthite no. 12, the analysis of a pale red coloured perthite from the same outcrop (no. 11) shows a lower Fe_2O_3 content.

The intensity of hematite pigmentation may vary greatly over short distances. Sometimes the colouring can be observed to follow fissures in the rocks. It is, however, intimately connected with the sub-Jotnian porphyries and granites. It seems likely that it belongs to a post-magmatic stage of the igneous activity.

The analyses of BaO and SrO of the alkali feldspars have given values in the range 0.07–0.5 and 0.01–0.06, respectively. A comparison with the corresponding whole rock analyses (see last column of Table 7) shows that there is a greater tendency for barium than strontium to concentrate in the alkali feldspars. This is what can be expected from known substitution relations (see Rankama and Sahama 1952 and Heier 1962). The diadochy between barium and potassium is more pronounced than between strontium and potassium. On the other hand, strontium has a higher tendency than barium to replace calcium and thus enter the plagioclase lattice. Heier (1962) has shown that the ratio between strontium in potash feldspar to strontium in plagioclase is generally close to unity, whereas the corresponding ratio for barium is above unity.

It is also interesting to note that perthite from a phenocryst-poor porphyry (no. 9 of Table 7) has a lower BaO : K_2O ratio than perthites from two phenocryst-rich porphyries (nos. 10 and 12). The phenocrysts of the former porphyry evidently belong to a later stage of differentiation than those of the latter two (cf. p. 110). It is also noted that the fractionation in BaO : K_2O is much more pronounced than that of Na_2O : K_2O , the latter being negligible in the recorded figures.

Data from optical and X-ray measurements are presented in Table 8 and Figs. 63–68. From these it is evident that the perthitic alkali feldspars can be used for distinguishing between two groups of igneous rocks. This division is nearly identical with the one derived mainly from field data, into an orogenic and a post-orogenic complex. An exception is formed by the Rätan granite, which, with regard to the character of its potash feldspar, belongs to the same group as rocks from the orogenic complex. The two groups of perthitic alkali feldspars are thus constituted by those from the orogenic complex and the Rätan granite with differentiates on the one hand (group 1) and those from the sub-Jotnian and Jotnian complexes on the other (group 2).

The distribution of optical axial angles $2V_\alpha$ of potash feldspars within the two groups just mentioned is shown in Fig. 63. Values in group 1 generally fall in the range $81\text{--}85^\circ$, the total variation being c. $73\text{--}88^\circ$. These axial angles are thus those which are characteristic of microcline (cf. Tröger 1959).

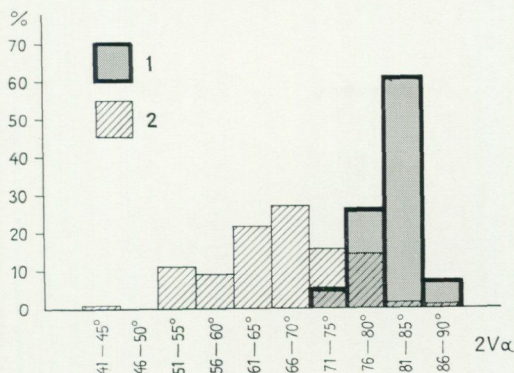


Fig. 63. Distribution of $2V_{\alpha}$ of the potash feldspars in igneous rocks from the Los-Hamra region.

1 = orogenic complex and Råtan granite. Number of measurements $N = 95$.

2 = post-orogenic complex excluding the Råtan granite. Number of measurements $N = 155$.

Group 2, on the other hand, shows a considerable spread in the $2V_{\alpha}$ values: $52-86^{\circ}$. One single determination (no. 68 of Table 8) of low accuracy caused by a high content of albite and strong hematite pigmentation yielded 44° . A range of $2V_{\alpha}$ values of more than 10° is often recorded within one thin section or even within one grain.

The $2V_{\alpha}$ determinations on potash feldspars of group 2 have thus given values characteristic of both orthoclase and microcline (cf. Tröger 1959).

The value of $2V_{\alpha}$ of potash feldspar is essentially a function of the Si-Al order-disorder and of chemical composition. (See e. g. Hewlett 1959 and Marfunin 1961.) The influence on $2V_{\alpha}$ of the small contents of barium, strontium etc. which occur in the Los-Hamra potash feldspars (cf. Table 7) is not possible to evaluate, but the observed spread of values in feldspars from sub-Jotnian and Jotnian rocks (group 2) can hardly be due only to variations in these elements (cf. Winchell 1961: p. 304). As mentioned above, only small amounts of sodium seem to have remained in the potash feldspar lattice. The most probable cause for the great spread in $2V_{\alpha}$ for group 2 therefore seems to be variations in Si-Al ordering. Submicroscopic twinning has been calculated not to exert a great influence on $2V_{\alpha}$ (Marfunin 1961). The existence of cryptoperthite within the potash feldspars may somewhat influence the value of $2V_{\alpha}$. Extinction angles on (010) seem to indicate that such cryptoperthite always contains less than c. 40% Ab (cf. Fig. 64 of the present work and Marfunin 1961: Fig. 7). This might cause a variation of a few degrees in $2V_{\alpha}$, but can hardly account for the large variations observed.

Extinction angles $\alpha' \wedge (001)$ on (010) fall in the range $3.5-7.0^{\circ}$ for feld-

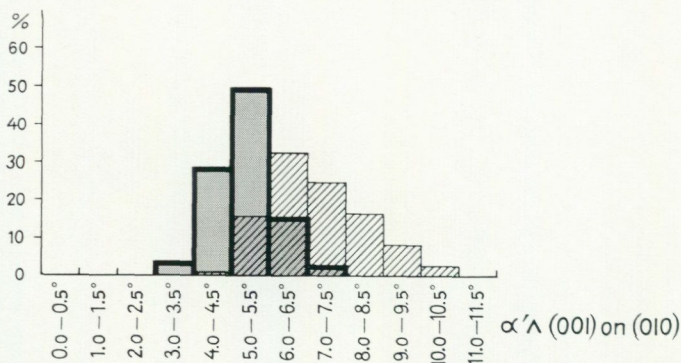


Fig. 64. Distribution of extinction angle $\alpha' \wedge (001)$ on (010) of the potash feldspars in igneous rocks from the Los-Hamra region. For explanation see Fig. 63. Orogenic complex and Rätan granite : N = 160. Post-orogenic complex excluding the Rätan granite : N = 235.

spars of group 1 and between 4.5 and 10.5° for those of group 2 (see Fig. 64). The spread is thus also in this case greater for the latter group. For microcline the extinction angle is 5–6°, and for pure (non-sodic) orthoclase c. 5° (see Tröger 1959).

The small contents of barium, strontium and calcium in the Los-Hamra potash feldspars cannot cause great variations in the extinction angle on (010) . Further, these elements tend to reduce the value of the latter (Ansilowski 1961: p. 35). Another cause must therefore be looked for to explain the high extinction angles. For several samples, some spread can be connected with a low accuracy of measurement because of the high content of exsolved albite, hematite pigment etc. However, even in cases where the feldspar is apparently homogeneous an angle several degrees greater than that of pure orthoclase and microcline has frequently been recorded. In such cases it seems likely that the high extinction angles should be caused by cryptoperthitic albite with approximately the same crystallographic orientation as the potash feldspar host. The integrated optical properties of such an intergrowth of albite and potash feldspar are those of a mechanical mixture of the two minerals. Cryptoperthitic bodies of albite cause a rise in the extinction angle $\alpha' \wedge (001)$ on (010) , see Marfunin (1961: Fig. 7). The values recorded seem to indicate a maximum of roughly 40 % albite in cryptoperthite (cf. Table 7).

An independent indication that cryptoperthitic albite bodies exist is formed by the alkali feldspar no. 9 of Table 7. The albite content (34 mol. %) obtained in the chemical analysis is much higher than would be expected from microscopic examination. Further, X-ray investigation indicates a very low content of sodium in solid solution.

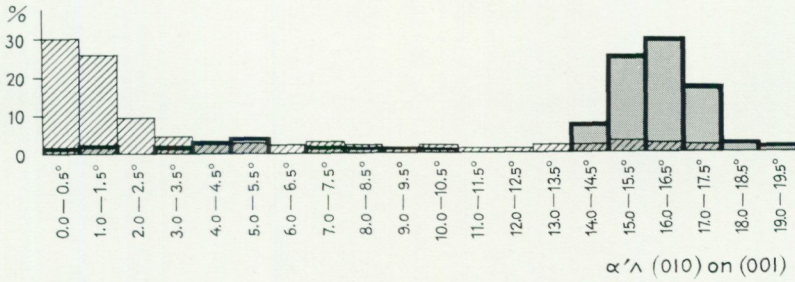


Fig. 65. Distribution of extinction angle $\alpha' \wedge (010)$ on (001) of the potash feldspars in igneous rocks from the Los-Hamra region. For explanation see Fig. 63. Orogenic complex and Rätan granite : $N = 181$. Post-orogenic complex excluding the Rätan granite : $N = 278$.

It should be noted in this connection that the optical measurements on potash feldspars are necessarily limited to microscopically relatively homogeneous parts of the crystals. This may have somewhat influenced the values, e. g. in the following way. Cryptoperthitic patches may have been selected for the determinations instead of those parts of the feldspar where exsolution has produced coarser albite bodies. From what is said above, this will clearly influence the value of the extinction angle $\alpha' \wedge (001)$ on (010) .

The extinction angle $\alpha' \wedge (010)$ on (001) is zero for monoclinic potash feldspars and c. 16° for microcline (Tröger 1959). Fig. 65 shows the distribution of this angle within the two rock groups mentioned above. In addition to "monoclinic" angles near zero and "triclinic" ones near 16° there are also recorded intermediate values. It should, however, at once be noted that the quantitative importance of these intermediate angles has been somewhat exaggerated in relation to the "monoclinic" and "triclinic" angles. This is so because in general a relatively greater number of determinations have been carried out on feldspars with intermediate angles, in order to establish the variation, which is often considerable in such samples (cf. Table 8). As the intention is to give only a qualitative or semi-quantitative idea of the distribution within the two groups, this is, however, not of importance.

Orogenic rocks and the Rätan granite (group 1) show a clustering around 16° . It is often difficult to make exact determinations of the angle, as the microclines are frequently finely twinned. This causes a spread around 16° . However, angles down to zero have also been measured in the acid metavolcanics belonging to this group. The cause for this in some feldspars is the passage from an apparently untwinned state via very fine lamellae to a microscopically visible twinning. In the apparently non-twinned and very finely twinned parts of the crystals values between 0 and 15° have been obtained. This is probably caused by a more or less complete compensation between

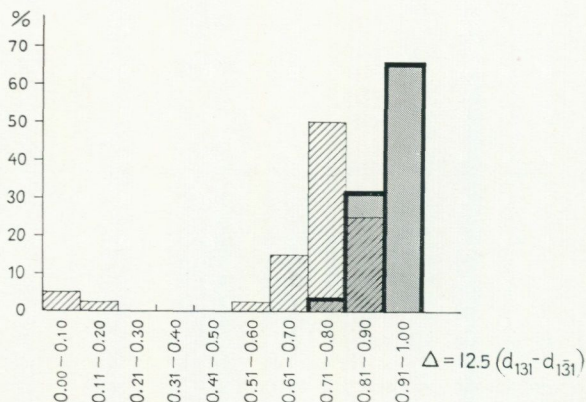


Fig. 66. Distribution of triclinicity Δ of the potash feldspars in igneous rocks from the Los-Hamra region. Samples with variations in Δ greater than c. 0.1 have been omitted.

For explanation see Fig. 63.

Orogenic complex and Rätan granite : N = 32.

Post-orogenic complex excluding the Rätan granite : N = 40.

right- and left-hand twins of mainly submicroscopic size. The axial angles of these feldspars are those of microcline and their X-ray triclinicity is high (Table 8: nos. 1-5).

In sub-Jotnian and Jotnian rocks (group 2) low extinction angles are most abundant, although intermediate and high values have also been recorded. High angles are found in the relatively rare samples in which twinning is visible with the aid of a microscope. The cause for the appearance of intermediate angles is probably similar to that indicated above for some samples of group 1.

The low angles of group 2 are seldom strictly "monoclinic" (zero). They are frequently one or a few degrees. This is in some cases clearly a consequence of the difficulty of measuring (strongly perthitic character etc.), but can probably also be related to an incomplete compensation between right- and left-hand triclinic units of submicroscopic size. Only very seldom do monoclinic (by X-ray methods) potash feldspars occur (cf. below).

It is also evident from X-ray powder investigation that differences exist between group 1 and group 2. Fig. 66 shows the distribution of triclinicity within the two groups. According to Goldsmith and Laves (1954a) the triclinicity is defined as $\Delta = 12.5 (d_{131} - d_{\bar{1}\bar{3}\bar{1}})$. Potash feldspars of group 1 show a great predominance for high triclinicities in the range 0.9-1.0, values down to 0.71, however, being recorded. The 131 and $\bar{1}\bar{3}\bar{1}$ peaks are generally sharp (see Fig. 67). Potash feldspars from group 2 show a maximum at 0.71-0.80. The variation is here much greater than for group 1. A few determinations (all from Dala porphyries) have yielded very low Δ values. Feldspars from group 2 often give diffuse peaks on the diffractometer curves (Fig. 67). It is,

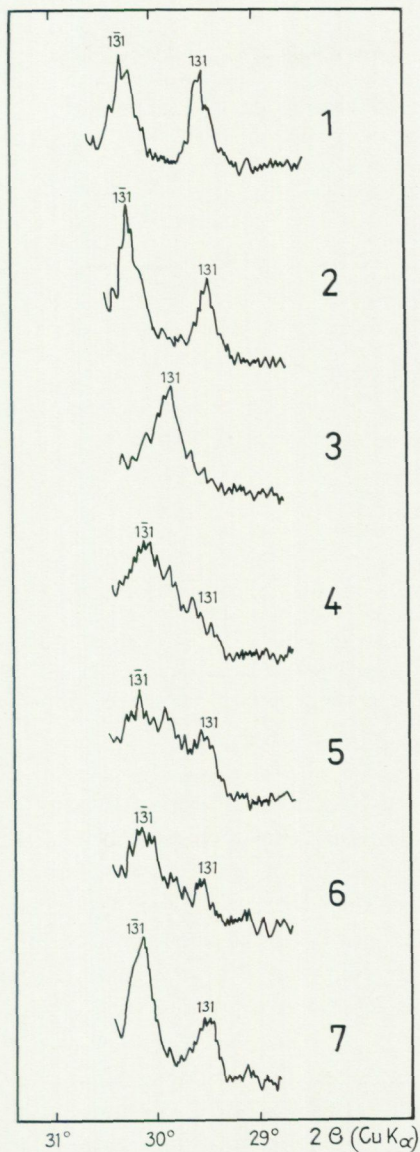


Fig. 67. X-ray powder diffraction curves for potash feldspars from the Los-Hamra region. The samples are from (for localities see Plate 1):

1. Primorogenic light granodiorite, 256/030.
2. Rätan granite, phenocrysts, 106/418.
3. Dala porphyry, big phenocryst, 165/233.
4. " " , phenocrysts, 077/176.
5. " " , " " , 119/203.
6. " " , " " , 158/036.
7. " " , " " , 148/191.

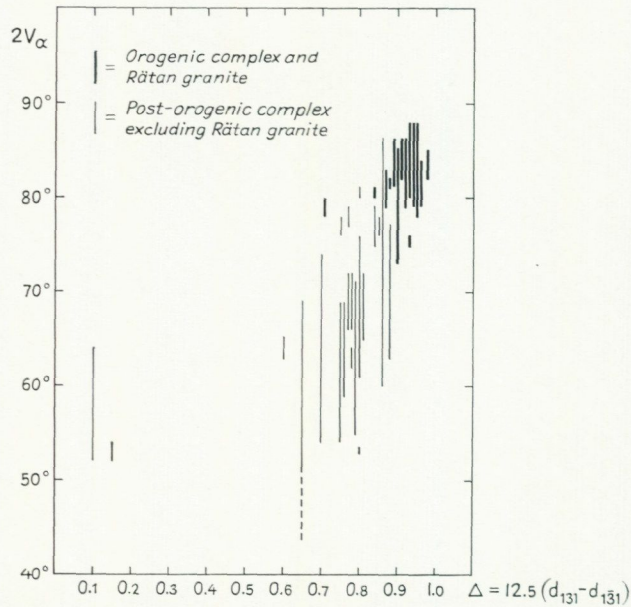


Fig. 68. Plot of $2V_{\alpha}$ against trilineicity Δ for the potash feldspars in igneous rocks from the Los-Hamra region. Broken line indicates uncertain values. Samples with variations in Δ greater than 0.1 have been omitted.

however, not possible to get a quantitative measure of this spread in Δ . Therefore, the values in Table 8, which have been used for the construction of the diagram in Fig. 66, are in many cases averages and the true spread consequently greater than shown in the latter figure. Samples with variations in Δ obviously greater than 0.1 have been omitted in Fig. 66.

From Fig. 66 it is evident that the great majority of potash feldspars in Los-Hamra igneous rocks are microclines with regard to their X-ray properties. Feldspars with a Δ value near zero are rare, but occur in the Dala porphyries. However, the microscopic determinations (see above) have indicated a much higher frequency of optically monoclinic feldspars [low $2V_{\alpha}$ and $\alpha' \wedge (010)$ on (001)]. This is also clear from Fig. 68., which gives the relations between $2V_{\alpha}$ and Δ . There is a tendency for orthoclase axial angles of $50\text{--}60^{\circ}$ to appear in combination with trilineicities of c. 0.65–0.80. In spite of high X-ray trilineicity, optical data in several samples indicate a monoclinic symmetry (e. g. nos. 49 and 55 of Table 8). The explanation for this is probably the different wave-lengths used in optical and X-ray investigations. Visible light has a wave-length of the order of 10^3 times greater than that of the X-rays. Microscopic determinations thus give the integrated properties of much greater volumes than X-ray investigation. Potash feldspars

with monoclinic optics and high X-ray triclinicity probably consist of sub-microscopic triclinic (more or less completely ordered) units or domains, which are large enough to be detected with X-ray techniques. The integrated optical properties are monoclinic in case of a compensation between right- and left-hand units. Goldsmith and Laves (1954b) and Laves (1961) have pointed to the possibility of a potash feldspar being orthoclase optically and microcline by X-ray technique. The suggestion given above for the structural relationships in some Los-Hamra potash feldspars favours a model similar to that proposed by Goldsmith and Laves (*op. cit.*) for orthoclase. The difference from the latter is that the triclinic units of potash feldspars in the Dala porphyries and granites are usually large enough to be detected by X-rays. In three samples (nos. 40a, 40b, and 44 of Table 8), Δ values of c. 0.1–0.2 have been obtained (calculation of Δ according to Dietrich 1962), which are probably due to smaller triclinic units, possibly in combination with a more disordered structure, than in the other samples.

The diffuseness of the peaks of feldspars of group 2 may be attributed to a varying degree of Si–Al order in different "crystal" domains (randomly disordered structures), or to out-of-step domain borders (see Christie 1962).

A comparison between sub-Jotnian and Jotnian igneous rocks on the one hand and similar rock types from the orogenic complex (volcanics and high level intrusions) on the other is of interest. With regard to the characters of these rock types it is safe to assume that their original feldspars were homogeneous and monoclinic both optically and to X-rays (sanidine and orthoclase). Further, Laves (1950) has shown that the twinning of common microcline indicates that it grew originally as a monoclinic modification. It is thus evident that a triclinization and exsolution has occurred in the Los-Hamra feldspars. The triclinization has been more complete in rocks of the orogenic complex and the Rätan granite than in sub-Jotnian and Jotnian rocks. This cannot be assumed to be simply a function of time, as no great difference in age seems to exist (*cf.* p. 157 *ff.*). The cause of it is probably to be sought for in the different evolution of the orogenic and post-orogenic complexes, although the high triclinicity of potash feldspars in the Rätan granite is not explained in this way. Possibly, however, this high triclinicity can be related to the extensive late- or post-magmatic crystallization which has affected this granite.

From the above investigation follows that the type of potash feldspar in igneous rocks of the Los-Hamra region can be used diagnostically to distinguish between sub-Jotnian and Jotnian rocks on the one hand and older rocks on the other.

Finally and parenthetically a special type of potash feldspar should be mentioned, occurring in very thin veinlets e. g. in the phyllites at Noppikoski (212/034). It probably shows the same combination of orthoclase axial angles

and high (X-ray) triclinicity as some feldspars treated above. The crystals are often more or less wedge-shaped, undulous and contain very little microscopically visible albite. Diffuse twin lamellae are sometimes seen. The birefringence is low. At 212/034 the axial angle $2V_{\alpha}$ varies between c. 45 and 60° within one thin section. The veinlets are too narrow to allow separation of enough material for chemical analysis. However, the author has observed similar potash feldspar on the island of Utö in the archipelago of Stockholm. The mineral occurs in thin veinlets in metagreywacke. An investigation of material collected here may be of interest in this connection. Variations in $2V_{\alpha}$ between 65 and 75° were recorded. The triclinicity Δ was determined at 0.8. Only c. 5 mol. % albite was obtained by chemical analysis. Probably the mineral is a highly triclinic (triclinized) potash feldspar of adularia type (cf. Laves 1952: p. 445). Gavelin (1939: pp. 33–34) mentioned the occurrence of a similar feldspar in the Malånäs district, northern Sweden. This mineral, however, was interpreted by him as an anorthoclase.

9. SUMMARY AND CONCLUSIONS

The sequence of main events established within the Los-Hamra region may be summarized in the following scheme:

Post-orogenic complex	(youngest)	
	Jotnian complex	{ Dolerite with differentiates Dala Sandstone Formation
	Sub-Jotnian complex	{ Dala granites Dala Volcanics Formation
	Rätan granite with differentiates	
<hr/>		
Orogenic complex	Serorogenic (late-orogenic) intrusion, alteration and refolding	
	Intrusion of primorogenic magma and folding	
	Deposition of sediments and volcanics (Los Formation)	
	(oldest)	

The scheme differs in several respects from that given by von Eckermann (1936). The different supracrustal series in the latter work appear to have been distinguished largely because of differences in degree of metamorphism (cf. p. 10). For the orogenic complex this is here explained by varying pres-

sure-temperature conditions (both in space and time), affecting a single supracrustal formation. The degree of metamorphism (chiefly observed in the meta-argillites) ranges from greenschist facies (biotite isograd) to upper amphibolite facies or to potash feldspar-cordierite hornfels facies (cf. Winkler 1967). Cordierite in regional-metamorphic rocks is present in the mica-schists and argillitic gneisses, except in the highest-temperature range of the amphibolite facies (cf. p. 31). This points to pressures similar to or somewhat above those of the low pressure Abukuma-type facies series (Winkler *op. cit.*).

The supracrustal Los Formation is essentially made up of metamorphosed marine sediments of a dominantly mature character (argillites and ortho-quartzitic sandstones) together with acid and basic metavolcanics. The stratigraphic succession has been established only for some parts of the region. Thus, in the large syncline passing through Los and in the Noppikoski region, the metasediments in general underlie the metavolcanics. Further, the acid metavolcanics of the syncline were deposited before the basic. However, regionally there appears to be an interbedding of volcanic and normal sedimentary (epiclastic) rocks.

It has been mentioned earlier (p. 138) that the supracrustal rocks of the Los Formation were deposited not far south-west of a geosyncline (geosyncline of central Norrland, see Magnusson *et al.* 1960: p. 6), which became filled with sediments of dominantly greywacke character [the Härnö formation (series)]. Metamorphosed feldspar-quartzites, arkoses and subgreywackes occupy the miogeosynclinal border zone of the geosyncline (Lundegårdh 1960 and 1967). South of the Los-Hamra region, in the ore-bearing district of central Sweden, the supracrustal rocks of the Svecofennides (cf. Ramsay 1909) are mainly composed of acid metavolcanics (leptites and hälleflintas, see Magnusson *et al.* 1960). However, metasediments are also found, e. g. in the Grythytte syncline (Sundius 1923), where there are many lithological features in common with the Los Formation. Acid metavolcanics, however, are more abundant than in the latter, and underlie the metasediments (slates).

After development of a schistosity in the supracrustal rocks of the Los Formation, the latter were intruded by primorogenic magma and refolded. At a later (serorogenic) stage both the supracrustal and primorogenic rocks were affected to a varying degree by folding and migmatization with a concomitant formation of granite, pegmatite and aplite. From the regional field relationships, it appears that this migmatization was late Svecofennian, yielding a potassium-argon age of c. 1,700–1,780 m. y. (Magnusson 1960) and a uranium-lead age of c. 1,810 m. y. (Welin and Blomqvist 1964). Age determinations by the potassium-argon method, carried out on members of the Los Formation, have yielded very different ages: one slate from Ryggskog (c. 340/312) gave 1,730 m. y. (Magnusson 1960), one phyllite from Noppikoski (212/034), 1,480 m. y. (Magnusson *et al.* 1963: p. 195) and one

amphibolite from Dåasen (435/329), 1,600 m. y. (N. H. Magnusson, personal communication). The spread in the age figures is probably due to variable post-crystallization argon loss. The amphibolite from Dåasen shows a low age in relation to the epigenetic uranium mineralization in the amphibolites of approximately equivalent stratigraphic position. This mineralization probably occurred c. 1,690 m. y. ago (Welin 1966a; cf. p. 132 of the present paper). The value 1,600 m. y. for the Dåasen amphibolite is similar to one of the two existing age determinations on the Rätan granite (1,620 m. y., see below), and may, from the position of the sampling locality, be due to influence from the latter granite. In the case of the phyllite at Noppikoski, loss of argon may have occurred in connection with faulting in the Oreälven zone (cf. p. 140).

As mentioned before (p. 71), the relative age of the Rätan granite is uncertain, although post-orogenic intrusion is probable. Two age determinations by the potassium-argon method have been carried out on this granite. One of these samples is from the vicinity of Kårböle, north of the Los-Hamra region, and yielded 1,850 m. y. (Magnusson 1960). The other sample is from a cutting along the road Orsa-Sveg, c. 2 km north of the county border at Acksjön (B9). The result of this determination was 1,620 m. y. (Gerling et al. 1966). The reason for the great difference between the two figures is not known. Further determinations, preferably by different methods, are evidently needed to determine the age of the Rätan granite.

The following considerations may be taken to indicate a relationship between the Rätan granite and the processes giving rise to migmatites and granites in a late stage of the Svecofennian orogeny. Gavelin (1955) arrived at the conclusion that the formation of the augen-bearing Revsund granite in Västerbotten County was intimately connected with late-Svecofennian metasomatic alterations leading to the formation of pegmatites and granites. However, within the vast regions occupied by the Revsund granite (cf. the map of Magnusson et al. 1960) there occur granite types, which appear to lack such a connection and are very similar to the Rätan granite. The present author has studied the Revsund granite in the Björna-Trehörningsjö region of Västernorrland County. The granite is here generally non-schistose and devoid of pegmatite and aplite, although such differentiates are sometimes met along the borders of the massif. Further, the contacts with the surrounding migmatites are cross-cutting. Microcline augen may reach 1 dm in size. Inclusions of a granite similar to the serorogenic Härnö granite are common. The sparse occurrence of pegmatite and aplite is a feature which is not typical for serorogenic granites in the Svecofennides. It therefore appears that within the large Revsund granite massifs there exist different facies, giving rise to transitions between serorogenic and post-orogenic granites: on the one hand there occur types connected with and transitional to migmatites, on the

other, types apparently lacking such a connection. The latter facies may represent magmas which have reached a higher degree of homogeneity and moved from the migmatite milieu where they were formed by anatexis (granitization). The Råtan granite may also belong to this type.

As to the age of the sub-Jotnian igneous activity, three determinations by the rubidium-strontium whole rock method have been carried out on Dala porphyries from the Los-Hamra region (Knoppvägen, 169/061; Gethelvetet, 142/225; Finnberget, 028/165; see Welin et al. 1966). The result of 1,685 m. y. is in agreement with the uranium-lead age (1,700 m. y.) obtained for the Finnish rapakivi granites (Kouvo 1964). Potassium-argon and rubidium-strontium dating of rapakivi granites and related intrusions in Finland and Russia have given somewhat lower ages (cf. Kouvo 1958 and Gerling et al. 1966). A similar age was also indicated by lead isotope investigations (Wickman et al. 1963). Thus, the post-orogenic sub-Jotnian igneous activity seems to have occurred in relatively close connection with the Svecofennian orogeny. With regard to the above figures, the potassium-argon age of the so-called Järna granite, referred to the sub-Jotnian by Hjelmqvist (1966), is remarkably high (1,810–1,880 m. y., see Magnusson 1960 and Gerling et al. 1966).

Considering the relationships in time between the Svecofennian orogeny and the sub-Jotnian igneous activity it is useful to compare similar phenomena elsewhere in the world. It is known from the occurrences of extensive sheets of ignimbrites and related intrusions that they are usually characterized by a connection to orogeny in space and time. Generally, the ignimbrite eruptions occurred in a post-orogenic stage (Rittmann 1958 and 1962a: p. 260; van Bemmelen 1961). (Note, however, that in Rittmann 1962a the term orogenesis refers to the uplift following geosynclinal sinking and tectogenesis.) The cause for the appearance of ignimbrites is thought to be the rise (by buoyancy) of anatectic magmas, formed in the root zones of the sinking geosynclines. These magmas may collect in near-surface chambers, which are opened by high vapour pressure and/or tensional stress in the crust during a post-orogenic stage (Rittmann 1962a: p. 216). Ignimbrites have frequently been deposited in extensively peneplained continental regions (Rittmann *op. cit.*: p. 48). The emptying of magma chambers causes fissuring and faulting by collapse (graben structures; cf. Rittmann 1962a: pp. 144–145 and van Bemmelen 1961).

A great number of ignimbrite occurrences are of a Tertiary or Pleistocene age, and are the products of volcanic activity initiated by Cretaceous–Tertiary orogeny (see e. g. Rittmann 1958 and Ross and Smith 1961: p. 49). Examples include the ignimbrites occurring in the Great Basin District and in the Yellowstone Park area in the U. S. A. (see van Bemmelen 1961: p. 407). In western Tuscany (Italy) ignimbrites of Pliocene–Pleistocene age are post-

orogenic in relation to the Alpine orogeny (Rittmann 1958 and 1962a; Marinelli 1961; Pratesi and Mazzuoli 1961). In Indonesia, three different phases of acid magmatism, in part producing voluminous deposits of ignimbrites, can be distinguished (van Bemmelen 1961: pp. 400–401). They all occurred after Mesozoic geosynclinal subsidence, during which ophiolitic magma was intruded and extruded.

The hypothesis cited above involving the formation of ignimbrites and related intrusions by derivation from anatectic magmas, and the general tectonic position of such igneous rocks may be used to explain the relationship between the sub-Jotnian igneous activity and the Svecofennian orogeny. The analogy would suggest the following: the Dala porphyries and granites formed from (differentiated) anatectic magmas, which originated during the Svecofennian orogeny. Evidently, possibilities were also created in the post-orogenic stage for simatic magma to rise to the surface. Thus the Dala porphyrites and related intrusions were formed (cf. also p. 92).

In the orogenic complex of the Los-Hamra region, there are igneous rocks (acid metavolcanics, cf. esp. p. 48, primorogenic and serorogenic intrusions), the corresponding magmas of which may have been generated by anatectic processes. However, except in the case of the serorogenic intrusions, field evidence of their anatectic origin is lacking. They would thus, similarly to the above discussed Råtan granite, represent formation and rise of acid anatectic magmas in earlier evolutionary phases than the sub-Jotnian igneous activity (cf. evolution in Indonesia cited above).

The concept of a genetical connection between the Svecofennian orogeny and the post-orogenic Dala porphyries and granites raises the question of whether the Småland-Värmland granites and associated supracrustal rocks of south-eastern and central Sweden (cf. map of Magnusson et al. 1960) could be associated with the Svecofennian evolution in a similar way. Småland-Värmland granites cut the Svecofennian structures, usually with sharp contacts (see Magnusson et al. 1960: p. 45), but predate the sub-Jotnian igneous activity (Hjelmqvist 1966). They are essentially non-schistose, in part augen-bearing (porphyritic). Within the granite massifs occur large areas with acid volcanic rocks (Småland porphyries), which are considered to be genetically connected with the granites although somewhat older than these (see Magnusson et al. 1960: p. 44). Further, more or less metamorphosed quartzites and other sedimentary rocks occur within the region of the granites (see below).

For the same arguments as given above for the Dala granites and porphyries, it seems likely that the Småland-Värmland granites and Småland porphyries are also genetically linked with the Svecofennian orogeny. Thus, the belt of Småland-Värmland granites and associated rocks would not represent a separate Gothian orogeny or cycle (cf. Wahl 1936 and Magnus-

son et al. 1963: pp. 1–3), a conclusion which has earlier been drawn by Welin (1966b, c; Welin et al. 1966) on the basis of isotope age determinations. Such dating of Småland granites and sub-Jotnian Dala porphyries has yielded values, which, according to Welin (1966: p. 31), indicate that these rocks should be included in what he calls the Svecofennian period of igneous activity. Lundegårdh (1967: p. 279), however, introduced the term Gothian era as a purely chronological term, embracing the time of formation of these granites, porphyries and associated rocks (c. 1,350–1,780 m. y.). The Svecofennian era he defined to range between c. 1,780 and $> 1,950$ m. y.

With regard to the age of the Småland granites, Welin (Welin and Blomqvist 1966; Welin et al. 1966), from rubidium-strontium whole rock and uranium-lead determinations, maintained a value of 1,745 m. y., whereas Magnusson (1960: p. 421) from potassium-argon data claimed a younger age (1,660–1,420 m. y.). If, however, values from specimens taken near the border between Småland granites and Svecofennian granites are excluded, the age figures fall between 1,560 and 1,420 m. y. (see Magnusson et al. 1963: p. 118). The potassium-argon data mentioned also include the Karlshamn granite (1,420 m. y., see Magnusson 1960: p. 421), which, according to uranium-lead determinations, is 1,455 m. y. (Welin and Blomqvist 1966). Welin (1966b) refers this granite to a separate period of igneous activity, following after the Svecofennian period. The potassium-argon ages for the Småland granites were explained by Welin (Welin and Blomqvist 1966) as due to variable argon loss during the Sveconorwegian regeneration (cf. Magnusson 1960) and during the intrusion of the Karlshamn granite.

The age of the Småland porphyries is probably similar to that of the Småland granites. The age of the metamorphosed sedimentary rocks (quartzites etc.) occurring in the Småland-Värmland granites is not known. Observations of quartzite fragments in Småland porphyries (see Magnusson et al. 1963: p. 115) indicate, however, that the metasediments are older than the latter. The quartzites etc., which occur e. g. in the Västervik, Vetlanda and Råmsberg regions (see map of Magnusson et al. 1960), may be regarded as parts of an (interrupted) extensive belt of similar rocks, which continues through Kopparberg County (Hjelmqvist 1966) and the Los-Hamra region to the northern parts of Gävleborg County (the "Naggen quartzite", see Lundegårdh 1960 and 1967; cf. also the tectonic model of Lundegårdh 1967: Fig. 8 on p. 20). In the last-mentioned region the metasediments are clearly older than the Svecofennian primorogenic intrusions (Lundegårdh 1967: p. 61). A similar relationship also holds for the quartzites etc. of the Los-Hamra region (see the present work). In Kopparberg County, the quartzites have mainly been classified as belonging to the sub-Jotnian Lower Dala series, although some small occurrences were considered to be Gothian (Hjelmqvist 1966). Cf. also p. 163. A Lower Dala age was ascribed to the so-called

Leksand quartzite, conglomerates in which contain pebbles of i. a. Svecofennian primorogenic and serorogenic granites (Hjelmqvist 1966: p. 57). Other quartzites in the Lower Dala series were so classified due to association with volcanic rocks, which were considered to be closely related to dikes cutting both Värmland granites and late-Svecofennian granites (Hjelmqvist 1966: pp. 52 and 54).

The age of the Västervik quartzite is uncertain. To establish this, two main problems remain to be solved. One is whether the so-called Loftahammar granite, which occurs in contact with the quartzite, intrudes the latter or unconformably underlies it. The other concerns the position of this granite in the regional chronological scheme. Magnusson (Magnusson et al. 1963: p. 113) favours an early Gothian age for the Loftahammar granite, and, in addition, considers it probable that it formed the basement on which the Västervik quartzite was deposited.

Quartzites, conglomerates and meta-argillites occur in the Vetlanda region, c. 100 km west-southwest of Västervik. These metasediments are intruded by the Småland granites. In the conglomerates (e. g. in the Malmbäck conglomerate), pebbles of granitic rocks are found (Magnusson et al. 1963: p. 114). The granite pebbles may be eroded from a nearby belt of gneissose granites, for which Magnusson (op. cit.: p. 196) favours an age between that of the Småland-Värmland granites and the late-Svecofennian granites (early Gothian). The assumption of such an age, as well as the similar assumption concerning the Loftahammar granite (above), involves the concept of a Gothian orogeny. However, the possibility exists that both the Loftahammar granite and the gneissose granites in the Vetlanda region are Svecofennian primorogenic intrusions, unrelated to the Småland granites.

Although the relative age of some quartzites in the above mentioned belt is not clear, it appears that the deposition of these sediments has not been contemporaneous within the whole belt. This assumes that the main geological processes such as intrusion and migmatization occurred approximately synchronously over the whole region. From potassium-argon data this seems to be the case at least with regard to the late-Svecofennian migmatization (Magnusson 1960).

The Lower Dala series of Hjelmqvist (1966) occupies a position in the chronological sequence between the intrusion of the Småland-Värmland granites and the deposition of the Upper Dala series. The latter is equivalent to the Dala Volcanics Formation of the Los-Hamra area. Although Hjelmqvist (1966: p. 48) did not find evidence of a great unconformity between the Upper and Lower Dala series, the supracrustal rocks of the latter generally show a steeper dip than those of the former (cf. map of Hjelmqvist 1966). Further, the strikes in the Lower Dala series frequently run in conformity with the structures in the Svecofennian supracrustal rocks (leptites etc.) A

schistosity is often present, and the metamorphic grade in places corresponds to the amphibolite facies (presence of andalusite and cordierite). This may indicate a deformation period, following the deposition of the Lower Dala volcanics and sediments, and affecting both these rocks and the older leptites etc. This deformation should have interrupted the essentially non-orogenic conditions prevailing during the formation of the Småland-Värmland granites, Småland porphyries and the (Upper) Dala volcanics and granites.

It is to be noted, that the above considerations of the Lower Dala series do not include the supracrustal rocks at Noppikoski. The present author does not agree with Hjelmqvist (1966) that the latter should be referred to the Lower Dala series, because primorogenic granite intrudes the meta-argillites east of Noppikoski (p. 61). East of Ö. Råberget (250/064) a similar intrusive relationship has been observed. The quartzite occurring here contains dikes of primorogenic granite and pegmatite. The metasediments east and north of Noppikoski thus belong to the Los Formation. This is probably also the case with the metarhyolites etc., which have been folded together with the granite-intruded metasediments. Indeed it seems likely that most of the supracrustal rocks of the Korpmäki-Gråtbäck area in Kopparberg County belong to the Los Formation (cf. p. 140). From thin sections of rocks from this area, kindly put at the author's disposal by Hjelmqvist, it appears, however, that deposits similar to the basal layers of the Dala volcanics in the Los-Hamra region also occur in the Korpmäki-Gråtbäck area.

From the discussion above (p. 158) it is probable that the position of the Rätan granite in the chronological scheme (p. 156) is similar to that of the Småland-Värmland granites. A comparison with the latter granites was first proposed by Sundius (1921) not only for the Rätan granite but also for the Revsund, Järna and Siljan granites. The latter two have been grouped with the sub-Jotnian Dala granites by Hjelmqvist (1966). The Revsund granite is at present regarded as late-Svecofennian (see e. g. Magnusson et al. 1960; cf. also above, p. 158).

Evidence for a major unconformity separating the Jotnian complex from the sub-Jotnian is difficult to find, as is clear from the following discussion. Angular differences of bedding in the Jotnian and sub-Jotnian supracrustal formations may indicate local tilting and faulting connected with igneous activity rather than a considerable break in the depositional history of the region. Further, the "in situ" weathering of the basement to the Jotnian sandstones, which is observed in some regions (see e. g. Sobral 1913), gives no clue as to what hiatus is involved (cf. also p. 115). From the observations in the Los-Hamra region (von Eckermann 1936 and 1937a, and the present work) and in Kopparberg County (Hjelmqvist 1966) it is evident that denudation and weathering have been active during the time of deposition of the

Dala volcanics (p. 94). The much greater importance of epiclastic sedimentary rocks in Jotnian deposits when compared to sub-Jotnian may be simply a consequence of a cessation of igneous activity. The only method of estimating the length of time separating the deposition of the Jotnian and sub-Jotnian supracrustal formations appears to be radiometric. However, even these determination methods meet considerable difficulties, being dependent on the recognition of authigenic minerals in sedimentary deposits.

Potassium-argon dating of Jotnian sedimentary rocks in Fennoscandia [including slate in the Almesåkra formation (series)] has given ages between 850 and 1,310 m. y. (Magnusson 1960; Eskola 1963). Determinations by the same method on "overwhelmingly authigenic or recrystallized" mica in a sandstone, which may possibly be referred to the Jotnian, has yielded 1,490 and 1,540 m. y. (Gorbatshev 1962b).

Two samples of an Åsby dolerite intrusion in Dala sandstone from Kopparberg County have yielded 1,100 and 1,350 m. y. by the potassium-argon method (Gerling et al. 1966). The former figure was obtained from pyroxene and amphibole near the contact, the latter from pyroxene from the central parts of the dike. Rubidium-strontium dating of a Jotnian dolerite intruding sandstone in the Nordingrå region (Welin 1966c) has given 1,300–1,400? m. y., which is thus a minimum value for the deposition of the sandstone. This would point to a somewhat older age for the latter than the potassium-argon data, although it must be observed that a fairly low accuracy is attached to the determination.

Potassium-argon dating of the effusive "Öje dolerite", forming an intercalation in Dala sandstone, has yielded 814 m. y., and a possibly Jotnian dolerite from southern Dalarna (Dalecarlia), 740 m. y. (Gerling et al. 1966). The former sample was, however, extensively chloritized.

The spread in the age determinations on the dolerites, which, from the field observations, are younger than all or part of the Jotnian sedimentary rocks, is thus c. 740–1,400 m. y. It is uncertain, to what extent these figures reflect different ages of intrusion and how much of the variation is caused by loss (or accumulation) of the daughter isotopes. The same may be said for the determinations of the Jotnian sedimentary rocks: 850–1,310 (–1,540) m. y.

A minimum age of 900–1,000 m. y. (Magnusson 1960; Welin and Blomqvist 1964) is obtained for the Jotnian sandstones, if one accepts the hypothesis of Sundius (1944) that the Jotnian sedimentation was contemporary with the deposition of the Dal formation in south-western Sweden. The former would represent a continental, the latter a marine facies.

From the above age determinations, the question of the age of the Jotnian sedimentation can not be answered definitely. As to the sub-Jotnian igneous activity, however, uranium-lead and rubidium-strontium dating point to

ages of c. 1,700 m. y. (see above). Further age determinations are needed to estimate the length of the possible time interval separating the Jotnian from the sub-Jotnian. The figures available, however, do not exclude the possibility of an interval of a few hundred million years between the sub-Jotnian igneous activity and the deposition of the Jotnian sediments.

The close geographical association between sub-Jotnian and Jotnian rocks in Fennoscandia has been ascribed to faulting caused by the sub-Jotnian igneous activity (Asklund 1931: pp. 278-279). As mentioned above (p. 159), such faulting, leading to the formation of faults and graben structures, is frequently connected with post-orogenic intrusion and extrusion of acid magma. The Jotnian sedimentation has therefore on this hypothesis probably largely been localized in tectonic depressions genetically associated with the sub-Jotnian igneous activity. This does not, however, necessarily mean that the sedimentation started c. 1,700 m. y. ago (cf. above), as the faults may have become re-activated later.

It is interesting to note that the Jotnian Almesåkra formation (series) occurs in a region dominated by Småland granites (see Magnusson et al. 1960: p. 63). According to the interpretation given above (p. 160), both the Småland-Värmland granites and the sub-Jotnian igneous rocks are genetically associated with the Svecofennian orogeny and post-orogenic in relation to the latter. Therefore, it is not unexpected that, for the same reasons as given above, the Jotnian sedimentation should have been localized also in the belt of Småland-Värmland granites.

From the geographical association between the Jotnian sedimentary rocks and the Jotnian (or post-Jotnian) dolerites it appears that the intrusion of the latter has in part been guided by pre-existing fissures and faults, which had originated as a consequence of the sub-Jotnian igneous activity. Faulting accompanying or following the dolerite intrusions and the covering of sandstones with flat-lying, extensive sheets (sills and flows) of dolerite and basalt have apparently contributed to the preservation of the Jotnian sedimentary rocks from erosion.

Chemical and mineralogical investigations of the different igneous rocks of the Los-Hamra region have revealed that crystallization differentiation trends are on the whole much more pronounced in the post-orogenic complex than in the orogenic. This may be related to metamorphic (metasomatic) alteration, which has affected the rocks of the latter complex to a varying degree. The differences in structural states of potash feldspars in igneous rocks belonging to the two complexes may similarly be interpreted as due to different evolutions of the post-orogenic and orogenic rocks (p. 155). The Råtan granite and its acid differentiates, however, belong to the same group as the orogenic rocks with regard to potash feldspar type.

ACKNOWLEDGEMENTS

This study of the Precambrian of the Los-Hamra region has been carried out at the Mapping Department of the Geological Survey of Sweden in connection with the geological mapping of the bedrock in Gävleborg County. The latter work was led by fil. dr. P. H. Lundegårdh, to whom my sincere thanks are due for stimulating discussion during both field and laboratory work, and for critically reading the manuscript.

Prof. S. Gavelin, my academic teacher, has provided much encouragement during the work, and for this the author is most grateful. Prof. O. Mellis has kindly read critically the chapter dealing with the alkali feldspars. I also want to thank fil. dr. E. Welin for discussions of the age determination data.

The following have participated in the field work: fil. lic. R. Gorbatshev (the region around and south of Los), fil. dr. P. H. Lundegårdh (mainly west of Tand-sjöborg and Lillhamra), fil. kand. H. Nairis (at various places during the final checking of the map) and fil. lic. N. B. Svensson (in the Lillskog-Los-Hamra-Rullbo area).

Prof. S. Hjelmqvist has given me the opportunity of studying material collected during the survey mapping of the bedrock of Kopparberg County. Prof. H. von Eckermann has kindly put his own material from the Los-Hamra region at my disposal. Sincere thanks are also due to prof. N. H. Magnusson for several stimulating discussions of problems concerning the Precambrian of Sweden.

I want to thank prof. F. E. Wickman and prof. S. Gavelin for giving me the opportunity to study areas of recent volcanicity during six months in Italy. Sincere thanks are also due to my teacher in volcanology, prof. A. Rittmann, and his collaborators at the Universities of Catania and Pisa for numerous discussions, especially concerning ignimbrites.

Mrs. Elisabeth Björk has drawn the maps and diagrams. Her great experience of such work has contributed greatly to the quality of the latter.

Chemical analyses and most of the X-ray work have been carried out at the laboratories of the Geological Survey, under the direction of fil. lic. A. Danielsson, fil. lic. A.-M. Asklund and fil. mag. B. Rönholm. Important contributions to this work have been made by Mrs. V. Grundulis, Mrs. B. Rajandi, Miss B. M. Eriksson and the late Mr. A. Aaremäe. The electron probe microanalyses have been carried out by fil. mag. J. Malmqvist.

Mrs. S. Nordh at the Institute for Inorganic Chemistry, University of Stockholm, has prepared Guinier powder photographs of alkali feldspars.

Maps of magnetic anomalies, drilling cores and other petrographic information have kindly been put at the disposal of the Geological Survey by the Korsnäs AB (now Korsnäs-Marma AB) through ing. L. O. Martin, and by the Ställbergsbolagen AB through fil. lic. A. Wesslén. A grant in support of some microscopic investigations has also been received from the Korsnäs AB. Thanks are also due to Mr. S. Persson (formerly Korsnäs AB) for information on field data obtained during the prospecting work.

Fil. dr. E. Grip and fil. dr. T. Du Rietz, Bolidens Gruv AB, have given valuable information on geophysical, petrographical and chemical data, especially concerning the sulphide deposits around Los.

Ing. L.-E. Sundwall and ing. E. Saltin, Skånska Cementgjuteriet AB, have given me opportunity to study the two tunnels along Oreälven. By permission of the Korsnäs-Marma AB, the tunnels are shown on Plate 1.

I specially want to express my gratitude for the work done by D. G. Gee, Ph. D., who not only corrected the English of the manuscript, but also critically discussed petrological and tectonic problems. P. Padget, Dr. Phil., has checked the English text on Plate 1.

Mrs. I. Signorelli has taken the microphotos in cooperation with the author. Mrs. I. Smith kindly undertook the typewriting of the manuscript. Some typing has also been carried out by Miss M. Nordström.

I also acknowledge the great help of my wife in compiling the index.

REFERENCES

- GFF – Geologiska Föreningens Förhandlingar
 SGU – Sveriges geologiska undersökning
- ANDERSEN, O., 1928: The genesis of some types of feldspar from granite pegmatites. *Norsk Geol. Tidsskrift* 10: pp. 116–208.
- ANSILEWSKI, J., 1961: The problem of classification of the alkali feldspars. *Archiwum Mineralogiczne* XXIII: pp. 5–59.
- ASKLUND, B., 1931: Fennoskandias geologi (prekambrium). In W. RAMSAY: *Geologiens grunder*, 3rd ed., part II: pp. 139–305. Stockholm.
- BACKLUND, H. G., 1938: The Problems of the Rapakivi Granites. *J. Geol.* 46: pp. 339–396.
- BEMMELEN, R. W. VAN, 1961: Volcanology and geology of ignimbrites in Indonesia, North Italy, and the U. S. A. *Geologie en Mijnbouw* no. 12: pp. 339–411. (Also published in *Bull. Volc.* XXV: pp. 151–173, 1963.)
- BLOMBERG, A., 1895: Praktiskt geologiska undersökningar inom Gefleborgs län. SGU C 152.
- BUDDINGTON, A. F., and LINDSLEY, D. H., 1964: Iron-Titanium Oxide Minerals and Synthetic Equivalents. *J. Petrology* 5: pp. 310–357.
- BURRI, C., 1959: *Petrochemische Berechnungsmethoden auf äquivalenter Grundlage*. Birkhäuser Verl., Basel-Stuttgart.
- CHAYES, F., 1948: A petrographic criterion for the possible replacement origin of rocks. *Am. J. Sci.* 246: pp. 413–425.
- CHRISTIE, O. H. J., 1962: Observations on natural feldspars: Randomly disordered structures and a preliminary suggestion to a plagioclase thermometer. *Norsk Geol. Tidsskrift* 42 (feldspar volume): pp. 383–388.
- COOK, E. F. ed., 1966: *Tufflavas and Ignimbrites, a survey of Soviet studies*. New York.
- DIETRICH, R. V., 1962: K-feldspar structural states as petrogenetic indicators. *Norsk Geol. Tidsskrift* 42 (feldspar volume): pp. 394–414.
- ECKERMANN, H. VON, 1922: *The Rocks and Contact Minerals of the Mansjö Mountain*. (Academical Dissertation.) GFF 44: pp. 203–410.
- 1927: *The Graphite Deposit at Svensbo*. GFF 49: pp. 565–587.
- 1934: *A Preliminary Report on the Geology of the Loos Region*. GFF 56: pp. 341–358.
- 1936: *The Loos-Hamra Region*. GFF 58: pp. 129–343.
- 1937a: *The Jotnian Formation and the Sub-Jotnian Unconformity*. GFF 59: pp. 19–58.
- 1937b: *The Genesis of the Rapakivi Granites*. GFF 59: pp. 503–524.
- ERIKSSON, T., 1954: *Pre-Cambrian geology of the Pajala district, Northern Sweden*. SGU C 522.
- ESKOLA, P., 1963: *The Precambrian of Finland*. *The Precambrian*, vol. 1: pp. 145–263. (K. RANKAMA ed.) Intersci. Publ., Great Britain.
- GAVELIN, S., 1939: *Geology and Ores of the Malånäs District, Västerbotten, Sweden*. SGU C 424.
- 1955: *Beskrivning till berggrundskarta över Västerbottens län. 1. Urbergsområdet inom Västerbottens län*. Summary: Description to Map of the Pre-Quaternary rocks of the Västerbotten County, N. Sweden. With map to the scale of 1:400,000. SGU Ca 37.
- GAVELIN, S., and LUNDEGÄRDH, P. H., 1960: *Development of gneisses and granites in southern Sweden*. Guide to excursions nos. A28 and C23. *Int. Geol. Congr., XXI Session, Norden 1960*.

- GEIJER, P., 1913: On poikilitic intergrowths of quartz and alkali feldspar in volcanic rocks. GFF 35: pp. 51-80.
- 1925: Eulysitic iron ores in northern Sweden. SGU C 324.
- 1963: The Precambrian of Sweden. The Precambrian, vol. 1: pp. 81-143. (K. RANKAMA ed.) Intersci. Publ., Great Britain.
- GEIJER, P., and MAGNUSSON, N. H., 1944: De mellansvenska järnmalmernas geologi. SGU Ca 35.
- GERLING, E. K., LOBAC^V-ZUCENKO^V, S. B., and BORISENKO, N. F., 1966: New Data on the Absolute Age of the Jotnian of the Baltic Shield (title translated from the Russian). Doklady Akademii Nauk SSSR 166: 3: pp. 674-677.
- GOLDSCHMIDT, V. M., 1945: The Geochemical Background of Minor-Element Distribution. Soil Sci. 60: pp. 1-7.
- GOLDSMITH, J. R., and LAVES, F., 1954a: The microcline-sanidine stability relations. Geochim. et Cosmochim. Acta 5: pp. 1-19.
- 1954b: Potassium feldspars structurally intermediate between microcline and sanidine. Geochim. et Cosmochim. Acta 6: pp. 100-118.
- 1961: The Sodium Content of Microclines and the Microcline-Albite Series. Inst. "Lucas Mallada", C. S. I. C. (España). Cursos y conferencias. Fasc. VIII: pp. 81-96.
- GORBATSCHEV, R., 1961: Dolerites of the Eskilstuna region, Eastern Central Sweden. SGU C 580.
- 1962a: Secondary sphene in the Mälarsandstone. GFF 84: pp. 32-37.
- 1962b: The Pre-Cambrian Sandstone of the Gotska Sandön Boring Core. Bull. Geol. Inst. Univ. Uppsala XXXIX: pp. 1-30.
- GORBATSCHEV, R., and KINT, O., 1961: The Jotnian Mälarsandstone of the Stockholm Region, Sweden. Bull. Geol. Inst. Univ. Uppsala XL: pp. 51-68.
- GRIP, E., 1961: Geology of the Nickel Deposit at Lainijaur in northern Sweden and a summary of other Nickel Deposits in Sweden. SGU C 577.
- HEIER, K. S., 1962: Trace elements in feldspars - a review. Norsk Geol. Tidsskrift 42 (feldspar volume): pp. 415-454.
- HEINRICH, E. Wm., 1956: Microscopic Petrography. New York.
- HEWLETT, C. G., 1959: Optical properties of potassic feldspars. Bull. Geol. Soc. Am. 70: pp. 511-538.
- HIETANEN, A., 1967: On the Facies Series in various types of metamorphism. J. Geol. 75: pp. 187-214.
- HJELMQVIST, S., 1956: On the Occurrence of Ignimbrite in the Pre-Cambrian. SGU C 542.
- 1961: The Relation between Diabase, Granite, and Porphyry at Bullberget in Dalarna, Central Sweden. A Proof of Magmatic Granite Formation. Bull. Geol. Inst. Univ. Uppsala XL: pp. 69-80.
- 1966: Beskrivning till berggrundskarta över Kopparbergs län. Summary: Description to map of the Pre-Quaternary rocks of the Kopparberg County, Central Sweden. With map in two sheets, to the scale of 1:200,000. SGU Ca 40.
- HÖGBOM, A., 1933: Diskussionsinlägg med anledning av föredrag av H. von Eckermann över "Loosfältets geologiska byggnad". GFF 55: p. 657.
- HÖGBOM, A. G., 1894: Geologisk beskrifning öfver Jemtlands län. 1st ed. SGU C 140.
- 1909: Precambrian geology of Sweden. Bull. Geol. Inst. Univ. Uppsala X: pp. 1-80.
- 1913: Fennoskandia. Handbuch der regionalen Geologie IV:3. (G. STEINMANN and O. WILCKENS.) Heidelberg.
- HOLMQUIST, P. J., 1910: The Archaean geology of the coast-regions of Stockholm. GFF 32: pp. 789-911.

- JAMES, H. L., 1954: Sedimentary Facies of Iron-Formation. *Econ. Geology* 49: pp. 235–293.
 – 1955: Zones of regional metamorphism in the Precambrian of Northern Michigan. *Bull. Geol. Soc. Am.* 66: pp. 1455–1488.
- KARAMATA, ST., 1961: Einfluss des geologischen Alters und des tektonischen Drucks auf die Art der Alkalifeldspäte. Inst. "Lucas Mallada", C. S. I. C. (España). *Cursillos y conferencias*. Fasc. VIII: pp. 127–130.
- KOUVO, O., 1958: Radioactive age of some Finnish Pre-Cambrian minerals. *Bull. Comm. géol. Finl.* no. 182: pp. 1–70.
 – 1964: Kallioperämme ikäsuhteista. *Geologi* 16, no. 2.
- KRANCK, E. H., 1928: A Stereogram of Suursaari (Hogland). *Fennia* 50, no. 18.
 – 1929: Hoglands berggrund. *GFF* 51: pp. 173–198.
- KROKSTRÖM, T., 1932a: The Breven dolerite dike. *Bull. Geol. Inst. Univ. Upsala XXIII*: pp. 242–330.
 – 1932b: On the ophitic texture and the order of crystallization in basaltic magmas. *Bull. Geol. Inst. Univ. Upsala XXIV*: pp. 197–216.
 – 1936: The Hällefors dolerite dike and some problems of basaltic rocks. *Bull. Geol. Inst. Univ. Upsala XXVI*: pp. 113–263.
- LAVES, F., 1950: The lattice and twinning of microcline and other potash feldspars. *J. Geol.* 58: pp. 548–571.
 – 1952: Phase relations of the alkali feldspars. I. Introductory remarks. *J. Geol.* 60: pp. 436–450.
 – 1961: Discussion after R. V. Dietrich: Comments on the "Two-feldspar geothermometer" and K-feldspar obliquity. Inst. "Lucas Mallada", C. S. I. C. (España). *Cursillos y conferencias*. Fasc. VIII: pp. 19–20.
- LJUNGGREN, P., 1954: The region of Hålia in Dalecarlia, Sweden. Göteborg.
- LOOSTRÖM, R., 1916: Die Unterlage der Elfdalgesteine im Kirchspiel Orsa. *Bull. Geol. Inst. Univ. Upsala XV*: pp. 279–288.
- LUNDEGÅRDH, P. H., 1956: Hamrängesyklinalens ytbergarter och deras metasomatiska omvandling. Summary: The Hamränge Syncline and its Metasomatism. *GFF* 78: pp. 329–344.
 – 1960: The Miogeosynclinal Rocks of Eastern Central Sweden. *SGU C 570*.
 – 1967: Berggrunden i Gävleborgs län. Med separat karta i två blad i skala 1:200 000 samt inhäftad karta i skala 1:75 000. Petrology of the Gävleborg County in Central Sweden. With maps to the scale of 1:200,000 and 1:75,000. *SGU Ba 22*.
- LUNDEGÅRDH, P. H., LUNDQVIST, J., and LINDSTRÖM, M., 1964: Berg och jord i Sverige. Uppsala.
- LUNDQVIST, G., 1963: Beskrivning till jordartskarta över Gävleborgs län. Karta i skala 1:200 000. English summary: Description to Map of the Quaternary Deposits of Gävleborgs län, Central Sweden. *SGU Ca 42*.
- LUNDQVIST, TH., 1962: Ferroan-aluminian anthophyllite from the northern archipelago of Stockholm, Sweden. *Arkiv Mineral. Geol.*, vol. 3: pp. 187–192.
- MAGNUSSON, N. H., 1925: Persbergs malmtrakt och berggrunden i de centrala delarna av Filipstads bergslag. *Dissert.* Stockholm.
 – 1953: Malmgeologi. Jernkontoret, Stockholm.
 – 1960: Age Determinations of Swedish Precambrian Rocks. *GFF* 82: pp. 407–432.
 – 1966: Die mittelschwedischen Eisenerze und ihre Skarnmineralien. *Fortschr. Miner.* 43:1: pp. 47–76.
- MAGNUSSON, N. H., LUNDQVIST, G., and REGNÉLL, G., 1963: Sveriges geologi. 4th ed. Stockholm.

- MAGNUSSON, N. H., THORSLUND, P., BROTZEN, F., ASKLUND, B., and KULLING, O., 1960: Description to accompany the map of the pre-Quaternary rocks of Sweden. With one map to the scale of 1:1,000,000. SGU Ba 16.
- 1962: Beskrivning till karta över Sveriges berggrund. Med karta i skalan 1:1 000 000. SGU Ba 16.
- MARFUNIN, A. S., 1961: The relations between structure and optical orientation in potash-soda feldspars. Inst. "Lucas Mallada", C. S. I. C. (España). *Cursillos y conferencias*. Fasc. VIII: pp. 97–107.
- MARINELLI, G., 1961: Genesi e classificazione delle vulcaniti recenti Toscane. *Atti Soc. Tosc. Sci. Nat.*, vol. LXVIII. Serie A: pp. 73–116.
- MEHNERT, K. R., 1959: Der gegenwärtige Stand des Granitproblems. *Fortschr. Miner.* 37, no. 2: pp. 117–206.
- ORVILLE, P. M., 1963: Alkali Ion Exchange between Vapor and Feldspar Phases. *Am. J. Sci.* 261: pp. 201–237.
- ÖSTBERG, C., 1838: Mineralogisk beskrifning öfver Färla, Ofvanåkers och Woxna Socknar i Helsingland. *Jernkontorets annaler, tjuogoandra årgången*. Pp. 256–274.
- PETTIJOHN, F. J., 1957: *Sedimentary Rocks*. 2nd ed. New York.
- PICHLER, H., 1963a: Zur Problematik der Ignimbrit-Diagnose. *N. Jahrb. Geol. Paläont. Abh.* 118:3: pp. 281–290.
- 1963b: Ignimbrite auf Santorin (Ägäische Inseln). *Annales Géologiques des Pays Helléniques* 14: pp. 408–435.
- PILAVA-PODGURSKI, N., 1956: Nya geologiska undersökningar vid Utö järnmalmsfält. With English abstract. SGU C 541.
- POTTER, P. E., SHIMP, N. F., and WITTERS, J., 1963: Trace elements in marine and freshwater argillaceous sediments. *Geochim. et Cosmochim. Acta* 27: pp. 669–694.
- PRATESI, M., and MAZZUOLI, R., 1961: Guide for the excursion to Mt. Amiata (Tuscany). *Int. Ass. Volc. symposium on "Ignimbrites and Hyaloclastites"*, Sept. 1961. *Ist. di Vulcanologia, Univ. di Catania*.
- RAMSAY, W., 1890: Om Hoglands geologiska byggnad. *GFF* 12: pp. 471–490.
- 1909: *Geologiens grunder*. 1st ed. Helsingfors.
- RANKAMA, K., and SAHAMA, TH. G., 1952: *Geochemistry*. Univ. Chicago Press, U. S. A.
- RITTMANN, A., 1952: Nomenclature of Volcanic Rocks. *Bull. Volcanologique* 12: pp. 75–102.
- 1958: Cenni sulle colate di ignimbriti. *Boll. delle sedute dell'Accademia Gioenia di Scienze naturali in Catania. Serie IV, vol. IV, fasc. 10*: pp. 524–533.
- 1962a: *Volcanoes and their Activity*. 2nd ed. London.
- 1962b: Erklärungsversuch zum Mechanismus der Ignimbritausbrüche. *Geol. Rundschau* 52: pp. 853–861.
- ROSS, C. S., and SMITH, R. L., 1961: Ash-Flow Tuffs: Their Origin, Geologic Relations and Identification. U. S. Geol. Survey Prof. Paper 366.
- SCHOUTEN, C., 1962: Determination Tables for Ore Microscopy. Amsterdam.
- SAVOLAHTI, A., 1962: The Rapakivi Problem and the Rules of Idiomorphism in Minerals. *Bull. Comm. géol. Finl.* no. 204: pp. 33–112.
- SEDERHOLM, J. J., 1895: Några ord om södra Finlands prekvartära geologi. *Fennia* 12, no. 3.
- 1897: Über eine archaische Sedimentformation in südwestlichen Finland und ihre Bedeutung für die Erklärung der Entstehungsweise des Grundgebirges. *Bull. Comm. géol. Finl.* no. 6.
- SIMONEN, A., 1960: Pre-Quaternary rocks in Finland. *Bull. Comm. géol. Finl.* no. 191: pp. 1–49.

- SIMONEN, A., and KOUVO, O., 1955: Sandstones in Finland. *Compt. Rend. Soc. géol. Finl.* 28; *Bull. Comm. géol. Finl.* no. 168: pp. 57-88.
- SOBRAL, J. M., 1913: Contributions to the geology of the Nordingrå region. *Diss., Univ. Upsala.*
- SØRENSEN, H. ed., 1961: Symposium on migmatite nomenclature. (Report of the Int. Geol. Congr., XXI Session, Norden, 1960. Part XXVI, Supplem. Vol. Sect. 1-21.)
- SRIRAMADAS, A., 1957: Diagrams for the correlation of unit cell edges and refractive indices with the chemical composition of garnets. *Am. Mineralogist* 42: pp. 294-298.
- STEWART, D. B., and ROSEBOOM, E. H., JR., 1962: Lower Temperature Terminations of the Three-phase Region Plagioclase-Alkali Feldspar-Liquid. *J. Petrology* 3:2: pp. 280-315.
- SUNDIUS, N., 1921: Några frågor rörande våra arkäiska intrusivformationer i mellersta och södra Sverige. *GFF* 43: pp. 548-595.
- 1923: Grythyttfältets geologi. *SGU C* 312.
- 1930: On the Spilitic Rocks. *Geol. Mag.* 67: pp. 1-17.
- 1932: Über den sogenannten Eisenanthophyllit der Eulysite. *SGU C* 374.
- 1944: Orogene Erscheinungen im südwestlichen Schweden. *GFF* 66: pp. 288-294.
- SVEDMARK, E., 1891: Geologiska meddelanden från resor i Dalarne och Helsingland. *GFF* 13: pp. 175-215. (Also published in *SGU C* 147, 1895.)
- 1895: Orsa Finmarks geologi. *GFF* 17: pp. 161-181 and 260-266. (Also published in *SGU C* 147, 1895.)
- TEGENGREN, F., 1911: Undersökningar angående malminmutningarna i närheten af den s. k. inlandsbanan mellan Orsa och Pite älfdal. *SGU C* 234.
- TEGENGREN, F., et al., 1924: Sveriges ädlare malmer och bergverk. *SGU Ca* 17.
- TRÖGER, W. E., 1959: Optische Bestimmung der gesteinsbildenden Minerale. Teil 1. Bestimmungstabellen. 3. Aufl. Stuttgart.
- TUTTLE, O. F., and BOWEN, N. L., 1958: Origin of granite in the light of experimental studies in the system $\text{NaAlSi}_3\text{O}_8$ - KAlSi_3O_8 - SiO_2 - H_2O . *Geol. Soc. Am. Mem.* 74.
- WAHL, W., 1936: Om granitgrupperna och bergskedjeveckningarna i Sverige och Finland. *GFF* 58: pp. 90-101.
- 1947: A composite lava flow from Lounatkorkia, Hogland. *Bull. Comm. géol. Finl.* 140: pp. 287-302.
- WELIN, E., 1966a: Two occurrences of uranium in Sweden - the Los cobalt deposit and the iron ores of the Västervik area. *GFF* 87: pp. 492-508.
- 1966b: The Absolute Time Scale and the Classification of Precambrian Rocks in Sweden. *GFF* 88: pp. 29-33.
- 1966c: Uranium Mineralizations and Age Relationships in the Precambrian Bedrock of central and southeastern Sweden. *GFF* 88: pp. 34-67.
- WELIN, E., and BLOMQVIST, G., 1964: Age Measurements on Radioactive Minerals from Sweden. *GFF* 86: pp. 33-50.
- 1966: Further Age Measurements on Radioactive Minerals from Sweden. *GFF* 88: pp. 3-18.
- WELIN, E., BLOMQVIST, G., and PARWEL, A., 1966: Rb/Sr Whole Rock Age Data on some Swedish Precambrian Rocks. *GFF* 88: pp. 19-28.
- WICKMAN, F. E., BLOMQVIST, G., GEIJER, P., PARWEL, A., VON UBISCH, H., and WELIN, E., 1963: Isotopic constitution of ore lead in Sweden. *Arkiv Mineral. Geol.*, vol. 3: pp. 193-257.
- WINCHELL, A. N., 1961: Elements of Optical Mineralogy. Part II. 4th ed., 4th printing. New York.
- WINKLER, H. G. F., 1967: Die Genese der metamorphen Gesteine. 2. Auflage. Berlin-Heidelberg.

TABLES 1—8

AND

FIGS. 69—71

Table 1 a. Chemical analyses of rocks from the Los-Hamra region. Contents of trace elements (V to Rb₂O) in ppm, otherwise weight percent. A list of the analysed rocks is given on p. 220 ff.

Analysis	1	2	3	4	5	6
SiO ₂	60.2	65.1	73.4	65.3	61.9	61.4
TiO ₂	0.60	0.68	0.59	0.68	0.70	0.72
Al ₂ O ₃	20.6	17.6	12.8	16.0	19.8	19.5
Fe ₂ O ₃	1.69	1.52	1.47	1.79	1.45	1.43
FeO	4.97	3.64	3.18	2.88	4.63	5.35
MnO	0.04	0.04	0.04	0.07	0.06	0.06
MgO	2.3	2.3	1.3	3.1	2.2	2.9
CaO	0.4	0.2	2.0	1.1	0.6	0.5
Na ₂ O	1.0	0.9	1.7	1.7	0.9	1.1
K ₂ O	4.8	3.7	2.5	5.4	4.3	3.9
H ₂ O > 105°	3.4	3.7	0.9	2.3	3.4	2.8
H ₂ O < 105°	n. d.	n. d.	n. d.	0.14	n. d.	0.18
P ₂ O ₅	0.13	0.13	0.13	0.13	0.13	0.18
CO ₂	n. d.	n. d.	n. d.	n. d.	n. d.	n. d.
F	n. d.	n. d.	n. d.	n. d.	n. d.	n. d.
S	n. d.	n. d.	n. d.	n. d.	n. d.	n. d.
B ₂ O ₃	0.040	0.019	0.020	0.005	0.048	0.050
Sum	100.17	99.53	100.03	100.60	100.12	100.07
- 0 for S, F	-	-	-	-	-	-
Corr. sum	100.2	99.5	100.0	100.6	100.1	100.1
V	170	100	70	85	110	160
Cr	60	80	80	100	120	60
Co	20	n. d.	n. d.	n. d.	n. d.	15
Ni	40	30	25	30	15	40
Cu	n. d.	< 10	35	< 10	120	n. d.
Pb	< 10	n. d.	n. d.	n. d.	n. d.	< 10
Zr	150	250	200	200	150	150
SrO	< 100	100	< 100	< 100	< 100	< 100
BaO	1 000	700	400	850	750	1 000
Rb ₂ O	250	270	160	160	220	200

Table 1 a (continued)

Analysis	7	8	9	10	11	12
SiO ₂	61.7	60.5	73.1	72.2	65.0	58.4
TiO ₂	0.66	0.62	0.60	0.63	0.71	0.62
Al ₂ O ₃	18.9	20.0	13.9	13.0	17.7	14.8
Fe ₂ O ₃	1.21	0.89	0.48	1.44	0.67	0.75
FeO	5.60	5.68	2.98	2.86	5.95	10.89
MnO	0.07	0.10	0.05	0.06	0.08	0.16
MgO	2.6	2.5	2.0	2.0	2.7	4.6
CaO	0.4	0.8	0.7	0.6	0.7	4.1
Na ₂ O	1.2	1.5	2.1	1.7	1.5	3.1
K ₂ O	4.2	3.7	3.0	3.7	3.6	0.7
H ₂ O > 105°	3.4	3.2	1.30	1.04	1.34	1.5
H ₂ O < 105°	0.26	0.20	0.10	0.10	0.12	0.18
P ₂ O ₅	0.10	0.10	0.15	0.17	0.14	0.21
CO ₂	n. d.	n. d.	n. d.	n. d.	n. d.	0.07
F	n. d.	n. d.	n. d.	n. d.	n. d.	n. d.
S	n. d.	n. d.	n. d.	n. d.	n. d.	0.02
B ₂ O ₃	0.027	0.027	<0.001	0.001	0.009	≤0.003
Sum	100.33	99.82	100.46	99.50	100.22	100.10
- 0 for S, F	-	-	-	-	-	0.01
Corr. sum	100.3	99.8	100.5	99.5	100.2	100.1
V	150	110	60	60	100	370
Cr	110	115	110	110	110	<10
Co	n. d.	n. d.	n. d.	n. d.	n. d.	n. d.
Ni	50	40	40	50	25	<10
Cu	70	60	15	20	80	220
Pb	n. d.	n. d.	n. d.	n. d.	n. d.	n. d.
Zr	150	100	200	200	200	<100
SrO	<100	160	≤100	≤100	<100	300
BaO	900	900	850	1 100	850	550
Rb ₂ O	220	160	110	110	220	<110

Table 1 a (continued)

Analysis	13	14	15	16	17	18
SiO ₂	59.3	60.3	66.5	63.6	63.4	74.2
TiO ₂	0.96	0.60	0.73	0.71	0.50	0.34
Al ₂ O ₃	17.5	15.1	17.6	18.2	16.3	13.0
Fe ₂ O ₃	1.09	4.95	0.96	2.19	0.70	1.18
FeO	8.30	1.34	4.79	3.56	7.19	1.14
MnO	0.14	0.13	0.04	0.03	0.23	0.02
MgO	2.7	4.3	2.1	2.7	5.1	0.6
CaO	3.6	5.3	0.6	0.5	1.9	0.6
Na ₂ O	3.4	0.4	1.7	1.3	1.7	1.4
K ₂ O	1.3	5.2	4.0	5.8	1.3	5.8
H ₂ O > 105°	0.9	1.9	1.3	0.8	1.53	1.4
H ₂ O < 105°	0.20	0.28	n. d.	0.24	n. d.	0.44
P ₂ O ₅	0.58	0.13	0.10	0.13	0.15	0.07
CO ₂	n. d.	n. d.	n. d.	0.03	n. d.	n. d.
F	n. d.	n. d.	n. d.	n. d.	n. d.	0.12
S	n. d.	n. d.	n. d.	<0.01	n. d.	n. d.
B ₂ O ₃	0.047	0.033	0.062	0.009	<0.001	n. d.
Sum	100.02	99.96	100.48	99.80	100.00	100.31
- 0 for S, F	-	-	-	-	-	0.05
Corr. sum	100.0	100.0	100.5	99.8	100.0	100.3
V	210	130	100	100	320	20
Cr	<10	110	100	100	300	<10
Co	n. d.	n. d.	n. d.	n. d.	n. d.	<5
Ni	<10	35	35	35	80	<5
Cu	320	<10	20	20	160	n. d.
Pb	n. d.	n. d.	n. d.	n. d.	n. d.	<10
Zr	<100	150	200	100	150	200
SrO	160	130	<100	<100	170	<100
BaO	300	1 100	800	1 000	100	600
Rb ₂ O	<110	220	160	220	<110	250

Table 1 a (continued)

Analysis	19	20	21	22	23	24
SiO ₂	76.6	76.0	71.5	70.9	75.5	78.7
TiO ₂	0.28	0.28	0.20	0.53	0.16	0.18
Al ₂ O ₃	11.6	12.2	13.9	13.2	12.2	11.5
Fe ₂ O ₃	1.45	1.00	2.52	2.08	1.01	0.86
FeO	0.89	1.65	0.26	2.06	1.05	0.34
MnO	0.02	0.07	0.01	0.07	0.04	0.01
MgO	0.4	0.9	0.5	0.7	0.6	0.6
CaO	0.5	0.5	0.3	1.8	0.6	0.3
Na ₂ O	2.8	1.5	0.6	2.9	0.8	0.6
K ₂ O	5.3	5.6	9.2	4.7	7.6	6.0
H ₂ O > 105°	0.4	0.8	0.6	0.6	1.0	1.0
H ₂ O < 105°	0.10	0.17	0.18	0.20	0.14	0.25
P ₂ O ₅	0.03	0.05	0.11	0.10	<0.01	0.03
CO ₂	n. d.	n. d.	n. d.	n. d.	n. d.	n. d.
F	0.10	0.10	0.05	n. d.	0.15	0.05
S	n. d.	n. d.	n. d.	n. d.	n. d.	n. d.
B ₂ O ₃	n. d.	n. d.	n. d.	n. d.	n. d.	n. d.
Sum	100.47	100.82	99.93	99.84	100.85	100.42
- 0 for S, F	0.04	0.04	0.02	-	0.06	0.02
Corr. sum	100.4	100.8	99.9	99.8	100.8	100.4
V	<20	<20	<20	30	<10	<20
Cr	<10	20	10	<10	20	20
Co	<5	n. d.	n. d.	n. d.	n. d.	n. d.
Ni	<5	<10	<10	<10	<10	<10
Cu	n. d.	<10	<10	25	<10	<10
Pb	<10	n. d.	n. d.	n. d.	n. d.	n. d.
Zr	300	200	200	200	250	200
SrO	<100	<100	<100	190	≤100	<100
BaO	1 000	1 700	650	1 200	800	450
Rb ₂ O	150	110	220	160	270	220

Table 1 a (continued)

Analysis	25	26	27	28	29	30
SiO ₂	75.6	77.6	48.9	49.8	48.4	49.0
TiO ₂	0.17	0.16	1.06	1.21	0.72	1.00
Al ₂ O ₃	11.9	11.8	16.6	16.1	17.8	16.2
Fe ₂ O ₃	1.68	0.71	4.09	3.96	1.34	7.93
FeO	1.27	1.03	7.13	8.54	7.68	7.54
MnO	0.02	0.01	0.25	0.21	0.17	0.13
MgO	0.7	2.9	7.5	5.7	9.5	6.0
CaO	0.1	0.1	11.2	9.2	10.3	6.9
Na ₂ O	0.3	0.3	2.2	3.2	1.9	4.0
K ₂ O	6.9	2.7	0.5	0.5	0.5	0.6
H ₂ O >105°	1.3	2.4	0.86	1.4	1.4	1.2
H ₂ O <105°	0.28	0.41	n. d.	n. d.	0.16	n. d.
P ₂ O ₅	<0.01	0.06	0.13	0.15	0.08	0.15
CO ₂	n. d.	n. d.	n. d.	n. d.	n. d.	n. d.
F	n. d.	n. d.	n. d.	n. d.	n. d.	n. d.
S	n. d.	n. d.	n. d.	n. d.	n. d.	n. d.
B ₂ O ₃	n. d.	0.010	<0.001	<0.001	n. d.	<0.001
Sum	100.22	100.19	100.42	99.97	99.95	100.65
- 0 for S, F	-	-	-	-	-	-
Corr. sum	100.2	100.2	100.4	100.0	100.0	100.7
V	<20	20	320	290	230	250
Cr	15	<10	300	260	370	110
Co	n. d.	n. d.	40	40	40	30
Ni	<10	15	85	40	150	25
Cu	15	<10	160	100	130	<10
Pb	n. d.	n. d.	n. d.	n. d.	n. d.	n. d.
Zr	300	200	150	150	<100	150
SrO	<100	<100	150	100	270	160
BaO	1 000	250	200	200	200	300
Rb ₂ O	220	160	<110	<110	<110	<110

Table 1 a (continued)

Analysis	31	32	33	34	35	36
SiO ₂	45.2	76.4	76.8	73.5	73.7	72.6
TiO ₂	1.87	0.03	0.20	0.35	0.34	0.43
Al ₂ O ₃	13.6	13.5	12.8	12.5	13.0	12.4
Fe ₂ O ₃	2.10	0.15	0.36	0.40	0.34	1.25
FeO	10.64	1.43	1.58	2.79	2.93	2.77
MnO	0.22	0.03	0.04	0.07	0.10	0.07
MgO	11.5	0.1	0.3	0.4	0.4	0.4
CaO	10.8	0.8	1.0	1.0	1.2	1.5
Na ₂ O	2.0	3.0	3.0	2.7	3.8	2.8
K ₂ O	0.5	4.3	4.1	5.1	2.7	4.7
H ₂ O >105°	1.7	0.47	0.2	1.4	0.9	0.4
H ₂ O <105°	n. d.	0.05	n. d.	0.10	0.18	0.20
P ₂ O ₅	0.17	0.04	0.03	0.06	0.04	0.05
CO ₂	n. d.	n. d.	n. d.	n. d.	n. d.	n. d.
F	n. d.	0.16	0.11	0.06	n. d.	0.05
S	n. d.	n. d.	n. d.	n. d.	n. d.	n. d.
B ₂ O ₃	n. d.	<0.001	0.004	n. d.	n. d.	n. d.
Sum	100.30	100.46	100.52	100.43	99.63	99.62
- 0 for S, F	-	0.07	0.05	0.03	-	0.02
Corr. sum	100.3	100.4	100.5	100.4	99.6	99.6
V	330	<20	<20	<20	<20	<20
Cr	1 200	<10	20	20	10	<10
Co	40	<5	n. d.	n. d.	n. d.	<5
Ni	100	<5	<10	<10	<10	<5
Cu	175	n. d.	15	<10	<10	n. d.
Pb	n. d.	20	n. d.	n. d.	n. d.	20
Zr	100	150	100	200	150	200
SrO	150	100	<100	100	<100	<100
BaO	270	1 300	1 100	1 000	800	1 050
Rb ₂ O	<110	150	110	160	160	100

Table 1 a (continued)

Analysis	37	38	39	40	41	42
SiO ₂	75.1	73.4	77.7	77.2	77.2	77.6
TiO ₂	0.30	0.31	0.07	0.15	0.14	0.18
Al ₂ O ₃	12.4	13.6	12.1	12.2	12.0	11.4
Fe ₂ O ₃	0.90	0.78	0.49	0.16	0.86	1.04
FeO	2.58	1.94	0.75	1.11	0.67	0.53
MnO	0.06	0.05	0.01	0.03	0.02	0.01
MgO	0.3	0.5	0.3	0.6	0.2	0.5
CaO	1.0	1.2	0.2	0.2	0.7	0.2
Na ₂ O	3.1	2.8	3.3	2.9	3.0	2.7
K ₂ O	3.6	4.8	5.2	4.7	5.3	4.4
H ₂ O >105°	0.7	0.9	0.13	0.7	0.5	1.1
H ₂ O <105°	0.30	0.40	0.10	n. d.	0.22	0.16
P ₂ O ₅	0.05	0.06	0.02	0.03	0.02	0.12
CO ₂	n. d.	n. d.	n. d.	n. d.	n. d.	n. d.
F	n. d.	n. d.	0.07	0.04	0.16	n. d.
S	n. d.	n. d.	n. d.	n. d.	n. d.	n. d.
B ₂ O ₃	n. d.	n. d.	<0.001	n. d.	n. d.	n. d.
Sum	100.39	100.74	100.44	100.02	100.99	99.94
- 0 for S, F	-	-	0.03	0.02	0.07	-
Corr. sum	100.4	100.7	100.4	100.0	100.9	99.9
V	<20	<20	<20	<20	<20	<20
Cr	30	30	<10	30	10	10
Co	n. d.	n. d.	n. d.	n. d.	n. d.	n. d.
Ni	<10	<10	<10	<10	<10	<10
Cu	20	20	<10	<10	15	<10
Pb	n. d.	n. d.	n. d.	n. d.	n. d.	n. d.
Zr	250	250	150	100	150	150
SrO	<100	<100	≤100	<100	<100	<100
BaO	800	900	200	850	350	1 700
Rb ₂ O	330	270	270	110	220	<110

Table 1 a (continued)

Analysis	43	44	45	46	47	48
SiO ₂	72.3	71.7	70.9	70.6	71.8	63.4
TiO ₂	0.11	0.42	0.57	0.45	0.39	0.62
Al ₂ O ₃	15.3	13.0	13.3	13.9	13.4	15.7
Fe ₂ O ₃	0.57	0.65	1.98	0.23	0.45	1.43
FeO	0.79	2.65	3.23	3.12	2.79	3.73
MnO	0.05	0.07	0.08	0.05	0.05	0.09
MgO	0.6	1.3	0.9	1.0	0.9	3.0
CaO	2.3	1.8	2.3	2.0	1.8	4.8
Na ₂ O	4.7	4.0	3.1	3.0	3.2	3.1
K ₂ O	2.7	3.0	2.5	4.2	3.9	2.7
H ₂ O > 105°	0.22	0.9	0.9	0.8	0.8	1.5
H ₂ O < 105°	0.06	0.10	0.20	0.10	0.08	0.28
P ₂ O ₅	0.05	0.11	0.12	0.17	0.13	0.17
CO ₂	n. d.	n. d.	n. d.	n. d.	n. d.	n. d.
F	0.03	0.10	n. d.	0.07	0.04	n. d.
S	n. d.	n. d.	n. d.	n. d.	n. d.	n. d.
B ₂ O ₃	<0.001	n. d.	n. d.	n. d.	n. d.	n. d.
Sum	99.78	99.80	100.08	99.69	99.73	100.52
- 0 for S, F	0.01	0.04	-	0.03	0.02	-
Corr. sum	99.8	99.8	100.1	99.7	99.7	100.5
V	<20	50	30	40	40	130
Cr	<10	25	30	40	40	80
Co	<5	n. d.	n. d.	n. d.	n. d.	n. d.
Ni	<5	<10	<10	≤10	<10	35
Cu	n. d.	30	20	20	<10	40
Pb	≤10	n. d.	n. d.	n. d.	n. d.	n. d.
Zr	≤100	100	250	150	150	100
SrO	400	100	200	100	100	620
BaO	950	500	800	1 000	1 200	1 000
Rb ₂ O	<100	110	110	110	110	<110

Table 1 a (continued)

Analysis	49	50	51	52	53	54
SiO ₂	63.3	66.6	67.5	67.1	71.8	73.6
TiO ₂	0.72	0.53	0.53	0.58	0.28	0.17
Al ₂ O ₃	16.8	15.5	15.7	15.2	13.9	13.7
Fe ₂ O ₃	2.25	1.50	1.47	1.29	1.00	0.41
FeO	2.50	1.95	1.74	2.61	1.70	1.62
MnO	0.12	0.09	0.09	0.09	0.05	0.05
MgO	1.5	1.1	1.1	1.2	0.7	0.3
CaO	3.0	2.3	2.4	2.4	1.7	0.8
Na ₂ O	4.1	3.9	3.9	3.5	3.1	3.0
K ₂ O	5.0	5.9	4.5	4.8	5.0	5.4
H ₂ O > 105°	0.66	0.57	0.7	0.65	0.9	0.4
H ₂ O < 105°	0.09	0.13	n. d.	0.06	0.20	0.18
P ₂ O ₅	0.24	0.17	0.17	0.17	0.08	0.08
CO ₂	n. d.	n. d.	n. d.	n. d.	n. d.	n. d.
F	0.13	0.13	0.12	0.13	n. d.	n. d.
S	n. d.	n. d.	n. d.	n. d.	n. d.	n. d.
B ₂ O ₃	<0.001	<0.001	0.001	<0.001	n. d.	n. d.
Sum	100.41	100.37	99.92	99.78	100.41	99.71
- 0 for S, F	0.05	0.05	0.05	0.05	-	-
Corr. sum	100.4	100.3	99.9	99.7	100.4	99.7
V	70	40	50	50	35	<20
Cr	<10	<10	<10	10	30	<10
Co	10	n. d.	n. d.	10	n. d.	n. d.
Ni	10	<10	<10	10	<10	<10
Cu	n. d.	20	30	n. d.	15	13
Pb	20	n. d.	n. d.	20	n. d.	n. d.
Zr	250	200	150	250	150	100
SrO	500	400	420	280	150	140
BaO	1 350	1 200	1 100	1 250	600	700
Rb ₂ O	100	220	160	200	380	330

Table 1 a (continued)

Analysis	55	56	57	58	59	60
SiO ₂	73.3	74.0	50.3	54.3	62.0	62.8
TiO ₂	0.27	0.24	0.85	0.91	0.68	0.65
Al ₂ O ₃	13.7	14.0	16.0	17.3	15.3	15.9
Fe ₂ O ₃	0.65	0.83	5.3	4.56	1.85	3.80
FeO	1.21	0.76	3.6	3.04	3.05	1.38
MnO	0.04	0.05	0.15	0.11	0.09	0.09
MgO	0.4	0.4	6.8	6.1	3.4	2.1
CaO	0.8	0.7	8.9	7.3	3.9	3.9
Na ₂ O	3.0	3.5	2.1	3.0	3.4	3.1
K ₂ O	5.3	5.5	2.8	2.8	4.2	4.3
H ₂ O > 105°	1.0	0.22	2.2	0.7	2.3	1.7
H ₂ O < 105°	0.38	0.20	0.5	0.08	0.28	0.16
P ₂ O ₅	0.05	0.07	0.32	0.34	0.21	0.21
CO ₂	n. d.	n. d.	n. d.	n. d.	n. d.	n. d.
F	n. d.	0.04	n. d.	n. d.	n. d.	n. d.
S	n. d.	n. d.	n. d.	n. d.	n. d.	n. d.
B ₂ O ₃	n. d.	<0.001	n. d.	n. d.	n. d.	n. d.
Sum	100.10	100.51	99.82	100.54	100.66	100.09
- 0 for S, F	-	0.02	-	-	-	-
Corr. sum	100.1	100.5	99.8	100.5	100.7	100.1
V	<20	<20	250	230	130	130
Cr	35	<10	140	130	30	45
Co	n. d.	n. d.	30	25	40	<10
Ni	<10	<10	40	60	10	15
Cu	15	<10	60	n. d.	n. d.	45
Pb	n. d.	n. d.	<10	15	30	n. d.
Zr	200	100	n. d.	200	250	250
SrO	100	100	900	900	450	630
BaO	800	500	1 000	1 050	1 400	1 300
Rb ₂ O	270	270	n. d.	<100	<100	110

Table 1 a (continued)

Analysis	61	62	63	64	65	66
SiO ₂	63.2	72.7	73.7	75.4	73.91	75.9
TiO ₂	0.61	0.28	0.28	0.22	0.30	0.28
Al ₂ O ₃	15.0	14.5	13.4	13.2	13.42	12.5
Fe ₂ O ₃	4.14	0.96	0.88	0.77	1.01	0.81
FeO	0.99	0.58	0.44	0.36	0.45	0.40
MnO	0.10	0.11	0.04	0.05	0.02	0.03
MgO	1.8	0.4	0.2	0.1	0.26	0.3
CaO	3.5	1.0	0.7	0.6	0.96	0.7
Na ₂ O	3.9	4.5	3.7	3.7	3.58	3.3
K ₂ O	5.2	5.1	6.1	5.7	4.88	6.0
H ₂ O > 105°	1.3	0.5	0.5	0.4	0.73	0.5
H ₂ O < 105°	0.27	0.1	0.16	0.13	0.06	0.15
P ₂ O ₅	0.21	0.10	<0.01	0.06	0.00	0.06
CO ₂	n. d.	n. d.	n. d.	n. d.	n. d.	n. d.
F	n. d.	0.07	0.08	0.13	n. d.	0.04
S	n. d.	n. d.	n. d.	n. d.	n. d.	n. d.
B ₂ O ₃	n. d.	n. d.	n. d.	n. d.	n. d.	n. d.
Sum	100.22	100.90	100.18	100.82	99.58	100.97
- 0 for S, F	-	0.03	0.03	0.05	-	0.02
Corr. sum	100.2	100.9	100.2	100.8	99.6	101.0
V	100	<20	<10	<10	<20	<10
Cr	40	20	20	25	30	<10
Co	<10	n. d.	n. d.	n. d.	<10	n. d.
Ni	10	<10	<10	<10	<10	<10
Cu	30	25	<10	<10	15	<10
Pb	n. d.	n. d.	n. d.	n. d.	n. d.	n. d.
Zr	300	200	150	150	200	150
SrO	700	140	100	<100	140	100
BaO	1 400	600	300	300	300	300
Rb ₂ O	220	160	270	270	270	220

Table 1 a (continued)

Analysis	67	68	69	70	71	72
SiO ₂	73.4	75.42	73.38	75.8	64.1	64.4
TiO ₂	0.26	0.27	0.26	0.21	0.59	0.58
Al ₂ O ₃	13.5	13.12	14.34	12.4	17.9	16.9
Fe ₂ O ₃	0.63	1.09	0.60	0.62	1.63	1.28
FeO	0.75	0.36	0.91	0.45	1.27	1.69
MnO	0.05	0.03	0.05	0.06	0.09	0.08
MgO	0.4	0.24	0.21	0.2	0.7	0.7
CaO	1.0	0.36	0.87	0.5	2.3	1.7
Na ₂ O	4.0	3.24	3.60	3.2	4.0	4.5
K ₂ O	5.8	5.12	5.38	6.0	5.5	7.8
H ₂ O > 105°	0.5	0.75	0.54	0.3	1.3	0.5
H ₂ O < 105°	0.17	0.06	0.08	0.10	0.36	0.22
P ₂ O ₅	0.04	n. d.	n. d.	<0.01	0.12	0.17
CO ₂	n. d.	n. d.	n. d.	n. d.	n. d.	n. d.
F	0.09	0.01	0.03	n. d.	n. d.	0.08
S	n. d.	0.06	0.06	n. d.	n. d.	n. d.
B ₂ O ₃	n. d.	n. d.	n. d.	n. d.	n. d.	n. d.
Sum	100.59	100.13	100.31	99.84	99.86	100.60
- 0 for S, F	0.04	0.03	0.04	-	-	0.03
Corr. sum	100.6	100.1	100.3	99.8	99.9	100.6
V	<20	<20	<20	<20	25	<20
Cr	20	20	25	60	30	<10
Co	n. d.	<10	<10	<10	n. d.	<5
Ni	<10	<10	<10	<10	<10	<5
Cu	<10	20	20	≤10	30	n. d.
Pb	n. d.	n. d.	n. d.	n. d.	n. d.	25
Zr	200	300	200	200	400	300
SrO	110	120	120	<100	520	250
BaO	500	250	650	200	3 000	3 000
Rb ₂ O	270	440	220	330	110	100

Table 1 a (continued)

Analysis	73	74	75	76	77	78
SiO ₂	65.7	69.32	78.6	77.4	76.9	73.7
TiO ₂	0.58	0.40	0.14	0.18	0.18	0.08
Al ₂ O ₃	16.4	16.31	11.8	11.9	12.3	14.3
Fe ₂ O ₃	1.55	0.70	0.29	0.23	0.48	0.54
FeO	1.39	1.15	0.20	0.24	0.56	0.57
MnO	0.09	0.05	0.02	0.02	0.05	0.03
MgO	0.7	0.27	0.1	0.1	0.4	0.3
CaO	1.2	1.35	0.3	0.4	0.4	0.5
Na ₂ O	4.4	3.65	3.3	3.7	3.5	3.6
K ₂ O	6.3	5.88	4.8	5.3	5.3	5.6
H ₂ O > 105°	1.1	0.64	0.6	0.5	0.5	0.8
H ₂ O < 105°	0.30	0.08	0.30	0.32	0.15	0.2
P ₂ O ₅	0.10	n. d.	<0.01	0.02	<0.01	0.18
CO ₂	n. d.	n. d.	n. d.	n. d.	n. d.	n. d.
F	0.08	0.14	0.04	0.02	0.08	0.11
S	n. d.	0.04	n. d.	n. d.	n. d.	n. d.
B ₂ O ₃	n. d.	n. d.	n. d.	n. d.	n. d.	n. d.
Sum	99.89	99.98	100.49	100.33	100.80	100.51
- 0 for S, F	0.03	0.08	0.02	0.01	0.03	0.05
Corr. sum	99.9	99.9	100.5	100.3	100.8	100.5
V	20	<20	<20	<20	<10	<20
Cr	<10	20	20	<10	10	<10
Co	<5	<10	<5	n. d.	n. d.	<5
Ni	<5	<10	<5	<10	<10	<5
Cu	n. d.	30	n. d.	<10	<10	n. d.
Pb	20	n. d.	50	n. d.	n. d.	30
Zr	300	250	150	100	100	≤100
SrO	150	190	<100	<100	<100	<100
BaO	850	1 000	<100	250	300	200
Rb ₂ O	100	220	350	270	330	400

Table 1 a (continued)

Analysis	79	80	81	82	83	84
SiO ₂	78.1	75.1	64.5	66.4	65.5	73.9
TiO ₂	0.14	0.21	0.57	0.68	0.69	0.34
Al ₂ O ₃	11.9	12.9	16.0	15.5	15.6	12.7
Fe ₂ O ₃	0.63	0.76	2.46	1.87	1.55	1.18
FeO	0.28	0.67	1.69	1.49	1.75	1.75
MnO	0.02	0.07	0.10	0.10	0.10	0.06
MgO	0.1	0.5	1.4	1.2	0.9	0.5
CaO	0.3	0.6	3.2	2.1	2.4	1.1
Na ₂ O	3.2	3.6	3.8	3.8	4.2	3.0
K ₂ O	5.5	4.9	4.5	5.6	6.4	4.4
H ₂ O > 105°	0.2	1.0	1.2	0.7	1.1	0.8
H ₂ O < 105°	0.04	0.42	0.30	0.27	0.22	0.08
P ₂ O ₅	<0.01	<0.01	0.19	0.22	0.19	0.03
CO ₂	n. d.	n. d.	n. d.	n. d.	n. d.	n. d.
F	0.01	n. d.	n. d.	0.12	0.13	0.19
S	n. d.	n. d.	n. d.	n. d.	n. d.	n. d.
B ₂ O ₃	n. d.	n. d.	n. d.	n. d.	n. d.	n. d.
Sum	100.42	100.73	99.91	100.05	100.73	100.03
- 0 for S, F	0.00	-	-	0.05	0.05	0.08
Corr. sum	100.4	100.7	99.9	100.0	100.7	100.0
V	<20	<20	90	30	30	<20
Cr	20	20	35	10	20	10
Co	n. d.	n. d.	n. d.	n. d.	n. d.	<5
Ni	<10	<10	<10	<10	<10	<5
Cu	<10	15	40	<10	15	n. d.
Pb	n. d.	n. d.	n. d.	n. d.	n. d.	20
Zr	100	150	200	300	250	200
SrO	<100	100	400	300	350	<100
BaO	200	400	1 200	2 200	2 700	650
Rb ₂ O	330	220	220	160	160	250

Table 1 a (continued)

Analysis	85	86	87	88	89	90
SiO ₂	73.44	48.6	48.6	48.6	60.0	63.9
TiO ₂	0.27	2.70	2.10	2.40	1.26	1.21
Al ₂ O ₃	12.50	16.3	16.2	15.8	14.3	13.2
Fe ₂ O ₃	1.12	0.83	1.75	3.49	2.47	1.89
FeO	2.22	11.22	10.12	10.05	6.92	5.38
MnO	0.05	0.25	0.19	0.19	0.19	0.15
MgO	0.43	4.1	5.3	5.7	0.9	1.5
CaO	1.21	9.0	8.3	7.5	3.6	3.0
Na ₂ O	2.86	3.0	2.9	2.7	4.0	4.0
K ₂ O	4.97	1.6	1.6	1.4	4.0	4.6
H ₂ O > 105°	0.68	1.5	2.1	1.1	1.7	1.3
H ₂ O < 105°	0.15	0.10	0.26	0.26	0.42	0.39
P ₂ O ₅	tr.	0.60	0.39	0.39	0.31	0.28
CO ₂	n. d.	n. d.	n. d.	n. d.	n. d.	n. d.
F	n. d.	n. d.	n. d.	n. d.	n. d.	n. d.
S	n. d.	n. d.	n. d.	n. d.	n. d.	n. d.
B ₂ O ₃	n. d.	n. d.	n. d.	n. d.	n. d.	n. d.
Sum	99.90	99.80	99.81	99.58	100.07	100.80
- 0 for S, F	-	-	-	-	-	-
Corr. sum	99.9	99.8	99.8	99.6	100.1	100.8
V	<20	380	220	270	<20	50
Cr	50	60	50	75	<10	<10
Co	<10	30	45	40	10	10
Ni	<10	30	100	70	<5	<5
Cu	20	200	70	100	50	60
Pb	n. d.	<10	n. d.	n. d.	20	15
Zr	250	150	150	200	300	200
SrO	<100	350	340	300	190	150
BaO	1 100	950	700	800	1 400	950
Rb ₂ O	220	<100	110	<110	<100	150

Table 1 b. Cation percentages, anion contents (for 100 cations) and Niggli values for rocks from the Los-Hamra region. Numbers correspond to those of Table 1 a.

Analysis	1	2	3	4	5	6
Si	58.7	64.6	71.0	62.4	60.6	59.8
Ti	0.4	0.5	0.4	0.5	0.5	0.5
Al	23.7	20.6	14.6	18.0	22.9	22.4
Fe ³⁺	1.2	1.1	1.1	1.3	1.1	1.1
Fe ²⁺	4.1	3.0	2.6	2.3	3.8	4.4
Mn	0.0	0.0	0.0	0.1	0.0	0.0
Mg	3.3	3.4	1.9	4.4	3.2	4.2
Ca	0.4	0.2	2.1	1.1	0.6	0.5
Na	1.9	1.7	3.2	3.1	1.7	2.1
K	6.0	4.7	3.1	6.6	5.4	4.8
P	0.1	0.1	0.1	0.1	0.1	0.2
C	—	—	—	—	—	—
B	0.1	0.0	0.0	0.0	0.1	0.1
Sum	99.9	99.9	100.1	99.9	100.0	100.1
O	157	161	173	161	159	160
OH	22	24	6	15	22	18
F	—	—	—	—	—	—
S	—	—	—	—	—	—
Sum	179	185	179	176	181	178
<i>si</i>	236	303	393	271	256	241
<i>qz</i>	+72	+143	+225	+87	+96	+85
<i>al</i>	48	48	40	39	48	45
<i>fm</i>	35	36	31	35	34	39
<i>c</i>	2	1	11	5	3	2
<i>alk</i>	16	15	17	21	15	14
<i>mg</i>	0.39	0.45	0.34	0.55	0.40	0.44
<i>k</i>	0.76	0.73	0.49	0.68	0.76	0.70
<i>ti</i>	1.8	2.4	2.4	2.1	2.2	2.1
<i>h</i>	44	57	16	32	47	37
<i>w</i>	0.23	0.27	0.29	0.36	0.22	0.19
<i>p</i>	0.2	0.3	0.3	0.2	0.2	0.3
<i>co₂</i>	—	—	—	—	—	—
<i>f₂</i>	—	—	—	—	—	—
<i>s</i>	—	—	—	—	—	—
<i>T</i>	+32	+33	+23	+18	+33	+31
<i>t</i>	+30	+32	+12	+13	+30	+29

Table 1 b (continued)

Analysis	7	8	9	10	11	12
Si	60.3	59.1	69.9	69.9	62.3	55.9
Ti	0.5	0.5	0.4	0.5	0.5	0.4
Al	21.8	23.0	15.7	14.8	20.0	16.7
Fe ³⁺	0.9	0.7	0.3	1.0	0.5	0.5
Fe ²⁺	4.6	4.6	2.4	2.3	4.8	8.7
Mn	0.1	0.1	0.0	0.0	0.1	0.1
Mg	3.8	3.6	2.8	2.9	3.9	6.6
Ca	0.4	0.8	0.7	0.6	0.7	4.2
Na	2.3	2.8	3.9	3.2	2.8	5.7
K	5.2	4.6	3.7	4.6	4.4	0.9
P	0.1	0.1	0.1	0.1	0.1	0.2
C	—	—	—	—	—	0.1
B	0.0	0.0	0.0	0.0	0.0	0.0
Sum	100.0	99.9	99.9	99.9	100.1	100.0
O	157	157	171	171	165	157
OH	22	21	8	7	9	10
F	—	—	—	—	—	—
S	—	—	—	—	—	0
Sum	179	178	179	178	174	167
<i>si</i>	247	235	390	384	265	176
<i>qz</i>	+87	+75	+206	+200	+105	+36
<i>al</i>	45	46	44	41	43	26
<i>fm</i>	38	36	31	35	39	50
<i>c</i>	2	3	4	3	3	13
<i>alk</i>	15	15	21	21	15	10
<i>mg</i>	0.41	0.40	0.51	0.46	0.42	0.41
<i>k</i>	0.70	0.62	0.48	0.59	0.61	0.13
<i>ti</i>	2.0	1.8	2.4	2.5	2.2	1.4
<i>h</i>	45	42	23	18	18	15
<i>w</i>	0.16	0.12	0.13	0.31	0.09	0.06
<i>p</i>	0.2	0.2	0.4	0.4	0.2	0.3
<i>co₂</i>	—	—	—	—	—	0.3
<i>f₂</i>	—	—	—	—	—	—
<i>s</i>	—	—	—	—	—	0.1
<i>T</i>	+30	+31	+23	+20	+28	+16
<i>t</i>	+28	+28	+19	+17	+25	+3

Table 1 b (continued)

Analysis	13	14	15	16	17	18
Si	56.4	58.4	63.4	60.6	60.7	71.8
Ti	0.7	0.4	0.5	0.5	0.4	0.2
Al	19.6	17.3	19.8	20.5	18.4	14.8
Fe ³⁺	0.8	3.6	0.7	1.6	0.5	0.9
Fe ²⁺	6.6	1.1	3.8	2.8	5.8	0.9
Mn	0.1	0.1	0.0	0.0	0.2	0.0
Mg	3.8	6.2	3.0	3.8	7.3	0.9
Ca	3.7	5.5	0.6	0.5	2.0	0.6
Na	6.3	0.8	3.1	2.4	3.2	2.6
K	1.6	6.4	4.9	7.1	1.6	7.2
P	0.5	0.1	0.1	0.1	0.1	0.1
C	—	—	—	0.0	—	—
B	0.1	0.1	0.1	0.0	0.0	—
Sum	100.2	100.0	100.0	99.9	100.2	100.0
O	161	160	166	165	163	170
OH	6	12	8	5	10	9
F	—	—	—	—	—	0
S	—	—	—	—	—	—
Sum	167	172	174	170	173	179
<i>si</i>	196	203	288	255	223	460
<i>qz</i>	+40	+51	+116	+75	+87	+236
<i>al</i>	34	30	45	43	34	48
<i>fm</i>	39	38	34	35	50	17
<i>c</i>	13	19	3	2	7	4
<i>alk</i>	14	13	18	20	9	31
<i>mg</i>	0.34	0.56	0.40	0.46	0.53	0.32
<i>k</i>	0.20	0.89	0.61	0.75	0.33	0.73
<i>ti</i>	2.4	1.5	2.4	2.1	1.3	1.6
<i>h</i>	10	21	19	11	18	29
<i>w</i>	0.11	0.77	0.15	0.36	0.08	0.48
<i>p</i>	0.8	0.2	0.2	0.2	0.2	0.2
<i>co₂</i>	—	—	—	0.2	—	—
<i>f₂</i>	—	—	—	—	—	1.2
<i>s</i>	—	—	—	—	—	—
<i>T</i>	+20	+17	+27	+23	+25	+17
<i>t</i>	+7	-2	+24	+21	+18	+13

Table 1 b (continued)

Analysis	19	20	21	22	23	24
Si	72.5	72.5	68.6	67.6	72.3	76.1
Ti	0.2	0.2	0.1	0.4	0.1	0.1
Al	12.9	13.7	15.7	14.8	13.8	13.1
Fe ³⁺	1.0	0.7	1.8	1.5	0.7	0.6
Fe ²⁺	0.7	1.3	0.2	1.6	0.8	0.3
Mn	0.0	0.1	0.0	0.1	0.0	0.0
Mg	0.6	1.3	0.7	1.0	0.9	0.9
Ca	0.5	0.5	0.3	1.8	0.6	0.3
Na	5.1	2.8	1.1	5.4	1.5	1.1
K	6.4	6.8	11.3	5.7	9.3	7.4
P	0.0	0.0	0.1	0.1	0.0	0.0
C	—	—	—	—	—	—
B	—	—	—	—	—	—
Sum	99.9	99.9	99.9	100.0	100.0	99.9
O	173	173	169	169	171	176
OH	3	5	4	4	6	6
F	0	0	0.1	—	0.5	0.2
S	—	—	—	—	—	—
Sum	176	178	173	173	178	182
<i>si</i>	481	467	401	356	471	590
<i>qz</i>	+229	+243	+157	+140	+231	+358
<i>al</i>	43	44	46	39	45	51
<i>fm</i>	15	22	16	22	16	14
<i>c</i>	3	3	2	10	4	2
<i>alk</i>	38	31	36	29	35	33
<i>mg</i>	0.24	0.38	0.26	0.24	0.35	0.49
<i>k</i>	0.55	0.71	0.91	0.52	0.86	0.87
<i>ti</i>	1.3	1.3	0.8	2.0	0.7	1.0
<i>h</i>	8	16	11	10	21	25
<i>w</i>	0.59	0.35	0.90	0.48	0.46	0.70
<i>p</i>	0.1	0.1	0.3	0.2	0.0	0.1
<i>co₂</i>	—	—	—	—	—	—
<i>f₂</i>	1.0	1.0	0.4	—	1.5	0.6
<i>s</i>	—	—	—	—	—	—
<i>T</i>	+5	+13	+10	+10	+10	+18
<i>t</i>	+2	+10	+8	0	+6	+16

Table 1 b (continued)

Analysis	25	26	27	28	29	30
Si	73.7	76.4	45.8	47.3	45.2	46.1
Ti	0.1	0.1	0.7	0.9	0.5	0.7
Al	13.7	13.7	18.3	18.0	19.6	18.0
Fe ³⁺	1.2	0.5	2.9	2.8	0.9	5.6
Fe ²⁺	1.0	0.8	5.6	6.8	6.0	5.9
Mn	0.0	0.0	0.2	0.2	0.1	0.1
Mg	1.0	4.3	10.5	8.1	13.2	8.4
Ca	0.1	0.1	11.2	9.4	10.3	7.0
Na	0.6	0.6	4.0	5.9	3.4	7.3
K	8.6	3.4	0.6	0.6	0.6	0.7
P	0.0	0.0	0.1	0.1	0.1	0.1
C	—	—	—	—	—	—
B	—	0.0	0.0	0.0	—	0.0
Sum	100.0	99.9	99.9	100.1	99.9	99.9
O	172	174	152	151	150	151
OH	8	16	5	9	9	8
F	—	—	—	—	—	—
S	—	—	—	—	—	—
Sum	180	190	157	160	159	159
<i>si</i>	497	525	109	120	107	115
<i>qz</i>	+273	+369	-11	-12	-13	-25
<i>al</i>	46	47	22	23	23	22
<i>fm</i>	22	39	46	45	48	50
<i>c</i>	1	1	27	24	24	17
<i>alk</i>	31	14	5	8	5	10
<i>mg</i>	0.31	0.76	0.55	0.45	0.65	0.42
<i>k</i>	0.94	0.86	0.13	0.09	0.15	0.09
<i>ti</i>	0.8	0.8	1.8	2.2	1.2	1.8
<i>h</i>	29	54	6	11	10	9
<i>w</i>	0.54	0.38	0.34	0.29	0.14	0.49
<i>p</i>	0.0	0.2	0.1	0.2	0.1	0.2
<i>co₂</i>	—	—	—	—	—	—
<i>f₂</i>	—	—	—	—	—	—
<i>s</i>	—	—	—	—	—	—
<i>T</i>	+15	+33	+17	+15	+18	+12
<i>t</i>	+14	+32	-10	-9	-6	-5

Table 1 b (continued)

Analysis	31	32	33	34	35	36
Si	42.4	72.1	72.3	70.2	70.3	69.5
Ti	1.3	0.0	0.1	0.3	0.2	0.3
Al	15.0	15.0	14.2	14.1	14.6	14.0
Fe ³⁺	1.5	0.1	0.3	0.3	0.2	0.9
Fe ²⁺	8.3	1.1	1.2	2.2	2.3	2.2
Mn	0.2	0.0	0.0	0.1	0.1	0.1
Mg	16.1	0.1	0.4	0.6	0.6	0.6
Ca	10.8	0.8	1.0	1.0	1.2	1.5
Na	3.6	5.5	5.5	5.0	7.0	5.2
K	0.6	5.2	4.9	6.2	3.3	5.7
P	0.1	0.0	0.0	0.0	0.0	0.0
C	—	—	—	—	—	—
B	—	0.0	0.0	—	—	—
Sum	99.9	99.9	99.9	100.0	99.8	100.0
O	145	173	174	168	170	170
OH	11	3	1	9	6	3
F	—	0.5	0.3	0.2	—	0.1
S	—	—	—	—	—	—
Sum	156	177	175	177	176	173
<i>si</i>	91	479	474	418	415	392
<i>qz</i>	-29	+239	+238	+186	+195	+168
<i>al</i>	16	50	47	42	43	39
<i>fm</i>	56	9	13	19	19	21
<i>c</i>	23	5	7	6	7	9
<i>alk</i>	5	35	34	33	30	31
<i>mg</i>	0.62	0.10	0.21	0.18	0.18	0.15
<i>k</i>	0.14	0.49	0.47	0.55	0.32	0.52
<i>ti</i>	2.8	0.2	0.9	1.5	1.5	1.8
<i>h</i>	11	10	4	27	17	7
<i>w</i>	0.15	0.08	0.17	0.11	0.09	0.29
<i>p</i>	0.1	0.1	0.1	0.1	0.1	0.1
<i>co₂</i>	—	—	—	—	—	—
<i>f₂</i>	—	1.6	1.1	0.5	—	0.4
<i>s</i>	—	—	—	—	—	—
<i>T</i>	+11	+15	+13	+9	+13	+8
<i>t</i>	-12	+10	+6	+3	+6	-1

Table 1 b (continued)

Analysis	37	38	39	40	41	42
Si	71.5	69.5	72.8	73.2	72.6	74.4
Ti	0.2	0.2	0.1	0.1	0.1	0.1
Al	13.9	15.2	13.4	13.6	13.3	12.9
Fe ³⁺	0.6	0.6	0.3	0.1	0.6	0.7
Fe ²⁺	2.1	1.5	0.6	0.9	0.5	0.4
Mn	0.0	0.0	0.0	0.0	0.0	0.0
Mg	0.4	0.7	0.4	0.8	0.3	0.7
Ca	1.0	1.2	0.2	0.2	0.7	0.2
Na	5.7	5.1	6.0	5.3	5.5	5.0
K	4.4	5.8	6.2	5.7	6.4	5.4
P	0.0	0.0	0.0	0.0	0.0	0.1
C	—	—	—	—	—	—
B	—	—	0.0	—	—	—
Sum	99.8	99.8	100.0	99.9	100.0	99.9
O	172	169	173	172	172	173
OH	4	6	0.8	4	3	7
F	—	—	0.2	0.1	0.5	—
S	—	—	—	—	—	—
Sum	176	175	174	176	176	180
<i>si</i>	442	406	507	508	494	541
<i>qz</i>	+218	+178	+235	+256	+234	+289
<i>al</i>	43	44	47	47	45	47
<i>fm</i>	20	17	9	13	10	14
<i>c</i>	6	7	1	1	5	2
<i>alk</i>	31	32	43	38	40	38
<i>mg</i>	0.13	0.25	0.31	0.46	0.20	0.38
<i>k</i>	0.43	0.53	0.51	0.52	0.54	0.52
<i>ti</i>	1.3	1.3	0.4	0.8	0.7	1.0
<i>b</i>	14	17	3	15	11	26
<i>w</i>	0.24	0.27	0.37	0.11	0.54	0.64
<i>p</i>	0.1	0.1	0.0	0.1	0.0	0.3
<i>co₂</i>	—	—	—	—	—	—
<i>f₂</i>	—	—	0.7	0.4	1.6	—
<i>s</i>	—	—	—	—	—	—
<i>T</i>	+12	+12	+4	+9	+5	+9
<i>t</i>	+6	+5	+3	+8	0	+7

Table 1 b (continued)

Analysis	43	44	45	46	47	48
Si	67.2	67.9	67.9	67.2	68.3	59.9
Ti	0.1	0.3	0.4	0.3	0.3	0.4
Al	16.8	14.5	15.0	15.6	15.0	17.5
Fe ³⁺	0.4	0.5	1.4	0.2	0.3	1.0
Fe ²⁺	0.6	2.1	2.6	2.5	2.2	2.9
Mn	0.0	0.1	0.1	0.0	0.0	0.1
Mg	0.8	1.8	1.3	1.4	1.3	4.2
Ca	2.3	1.8	2.4	2.0	1.8	4.9
Na	8.5	7.3	5.8	5.5	5.9	5.7
K	3.2	3.6	3.1	5.1	4.7	3.3
P	0.0	0.1	0.1	0.1	0.1	0.1
C	—	—	—	—	—	—
B	0.0	—	—	—	—	—
Sum	99.9	100.0	100.1	99.9	99.9	100.0
O	169	167	169	168	168	161
OH	1	6	6	5	5	9
F	0.1	0.3	—	0.2	0.1	—
S	—	—	—	—	—	—
Sum	170	173	175	173	173	170
<i>si</i>	365	357	346	349	369	227
<i>qz</i>	+137	+141	+158	+137	+153	+59
<i>al</i>	46	38	38	40	41	33
<i>fm</i>	10	23	27	21	21	31
<i>c</i>	12	10	12	11	10	18
<i>alk</i>	32	29	22	28	29	17
<i>mg</i>	0.44	0.41	0.24	0.35	0.33	0.51
<i>k</i>	0.27	0.33	0.35	0.48	0.45	0.36
<i>ti</i>	0.4	1.6	2.1	1.7	1.5	1.7
<i>h</i>	4	15	15	13	14	18
<i>w</i>	0.40	0.18	0.36	0.06	0.13	0.26
<i>p</i>	0.1	0.2	0.2	0.4	0.3	0.3
<i>co₂</i>	—	—	—	—	—	—
<i>f₂</i>	0.2	0.8	—	0.6	0.3	—
<i>s</i>	—	—	—	—	—	—
<i>T</i>	+14	+9	+16	+12	+12	+16
<i>t</i>	+2	-1	+4	+1	+2	-2

Table 1 b (continued)

Analysis	49	50	51	52	53	54
Si	58.9	62.0	63.3	63.2	67.8	69.7
Ti	0.5	0.4	0.4	0.4	0.2	0.1
Al	18.4	17.0	17.3	16.9	15.5	15.3
Fe ³⁺	1.6	1.1	1.0	0.9	0.7	0.3
Fe ²⁺	1.9	1.5	1.4	2.1	1.3	1.3
Mn	0.1	0.1	0.1	0.1	0.0	0.0
Mg	2.1	1.5	1.5	1.7	1.0	0.4
Ca	3.0	2.3	2.4	2.4	1.7	0.8
Na	7.4	7.0	7.1	6.4	5.7	5.5
K	5.9	7.0	5.4	5.8	6.0	6.5
P	0.2	0.1	0.1	0.1	0.1	0.1
C	—	—	—	—	—	—
B	0.0	0.0	0.0	0.0	—	—
Sum	100.0	100.0	100.0	100.0	100.0	100.0
O	161	163	164	164	167	170
OH	4	4	4	4	6	3
F	0.4	0.4	0.4	0.4	—	—
S	—	—	—	—	—	—
Sum	165	167	168	168	173	173
<i>si</i>	240	282	297	292	369	422
<i>qz</i>	+32	+54	+81	+80	+141	+178
<i>al</i>	38	39	41	39	42	46
<i>fm</i>	23	19	19	22	17	12
<i>c</i>	12	10	11	11	9	5
<i>alk</i>	27	32	29	28	32	36
<i>mg</i>	0.37	0.37	0.38	0.36	0.32	0.21
<i>k</i>	0.45	0.50	0.43	0.47	0.52	0.54
<i>ti</i>	2.0	1.7	1.7	1.9	1.1	0.7
<i>b</i>	8	8	10	9	15	8
<i>w</i>	0.45	0.41	0.43	0.31	0.35	0.19
<i>p</i>	0.4	0.3	0.3	0.3	0.2	0.2
<i>co₂</i>	—	—	—	—	—	—
<i>f₂</i>	0.8	0.9	0.8	0.9	—	—
<i>s</i>	—	—	—	—	—	—
<i>T</i>	+11	+7	+12	+11	+10	+10
<i>t</i>	-1	-3	+1	0	+1	+5

Table 1 b (continued)

Analysis	55	56	57	58	59	60
Si	69.6	69.0	48.1	50.3	58.5	59.8
Ti	0.2	0.2	0.6	0.6	0.5	0.5
Al	15.3	15.4	18.0	18.9	17.0	17.8
Fe ³⁺	0.5	0.6	3.8	3.2	1.3	2.7
Fe ²⁺	1.0	0.6	2.9	2.4	2.4	1.1
Mn	0.0	0.0	0.1	0.1	0.1	0.1
Mg	0.6	0.6	9.7	8.4	4.8	3.0
Ca	0.8	0.7	9.1	7.2	3.9	4.0
Na	5.5	6.3	3.9	5.4	6.2	5.7
K	6.4	6.5	3.4	3.3	5.1	5.2
P	0.0	0.1	0.3	0.3	0.2	0.2
C	—	—	—	—	—	—
B	—	0.0	—	—	—	—
Sum	99.9	100.0	99.9	100.1	100.0	100.1
O	169	170	149	156	156	160
OH	6	1	14	4	14	11
F	—	0.1	—	—	—	—
S	—	—	—	—	—	—
Sum	175	171	163	160	170	171
<i>si</i>	422	416	126	143	219	237
<i>qz</i>	+178	+160	-14	-5	+35	+49
<i>al</i>	47	46	24	27	32	35
<i>fm</i>	12	11	43	40	32	27
<i>c</i>	5	4	24	21	15	16
<i>alk</i>	36	39	10	12	21	22
<i>mg</i>	0.28	0.31	0.59	0.60	0.56	0.43
<i>k</i>	0.54	0.51	0.47	0.38	0.45	0.48
<i>ti</i>	1.2	1.0	1.6	1.8	1.8	1.8
<i>h</i>	19	4	18	6	27	21
<i>w</i>	0.33	0.50	0.57	0.57	0.35	0.71
<i>p</i>	0.1	0.2	0.3	0.4	0.3	0.3
<i>co₂</i>	—	—	—	—	—	—
<i>f₂</i>	—	0.4	—	—	—	—
<i>s</i>	—	—	—	—	—	—
<i>T</i>	+11	+7	+14	+15	+11	+13
<i>t</i>	+6	+3	-10	-6	-4	-3

Table 1 b (continued)

Analysis	61	62	63	64	65	66
Si	59.5	67.1	69.0	70.2	69.9	70.9
Ti	0.4	0.2	0.2	0.2	0.2	0.2
Al	16.7	15.8	14.8	14.5	15.0	13.8
Fe ³⁺	2.9	0.7	0.6	0.5	0.7	0.6
Fe ²⁺	0.8	0.4	0.3	0.3	0.4	0.3
Mn	0.1	0.1	0.0	0.0	0.0	0.0
Mg	2.5	0.5	0.3	0.1	0.4	0.4
Ca	3.5	1.0	0.7	0.6	1.0	0.7
Na	7.1	8.1	6.7	6.7	6.6	6.0
K	6.2	6.0	7.3	6.8	5.9	7.1
P	0.2	0.1	0.0	0.0	0.0	0.0
C	—	—	—	—	—	—
B	—	—	—	—	—	—
Sum	99.9	100.0	99.9	99.9	100.1	100.0
O	159	167	168	170	169	170
OH	8	3	3	2	5	3
F	—	0.2	0.2	0.4	—	0.1
S	—	—	—	—	—	—
Sum	167	170	171	172	174	173
<i>si</i>	239	380	421	451	433	458
<i>qz</i>	+31	+120	+149	+179	+179	+190
<i>al</i>	33	45	45	47	46	44
<i>fm</i>	25	10	8	6	9	9
<i>c</i>	14	6	4	4	6	5
<i>alk</i>	27	40	43	43	39	42
<i>mg</i>	0.40	0.31	0.22	0.14	0.25	0.31
<i>k</i>	0.47	0.43	0.52	0.50	0.47	0.54
<i>ti</i>	1.7	1.1	1.2	1.0	1.3	1.3
<i>h</i>	16	9	10	8	14	10
<i>w</i>	0.79	0.60	0.64	0.66	0.67	0.65
<i>p</i>	0.3	0.2	0.0	0.1	0.0	0.1
<i>co₂</i>	—	—	—	—	—	—
<i>f₂</i>	—	0.6	0.7	1.2	—	0.4
<i>s</i>	—	—	—	—	—	—
<i>T</i>	+6	+5	+2	+4	+7	+2
<i>t</i>	-8	-1	-2	0	+1	-3

Table 1 b (continued)

Analysis	67	68	69	70	71	72
Si	68.3	71.3	68.7	71.4	60.2	59.1
Ti	0.2	0.2	0.2	0.1	0.4	0.4
Al	14.8	14.6	15.8	13.8	19.8	18.3
Fe ³⁺	0.4	0.8	0.4	0.4	1.2	0.9
Fe ²⁺	0.6	0.3	0.7	0.4	1.0	1.3
Mn	0.0	0.0	0.0	0.0	0.1	0.1
Mg	0.6	0.3	0.3	0.3	1.0	1.0
Ca	1.0	0.4	0.9	0.5	2.3	1.7
Na	7.2	5.9	6.5	5.8	7.3	8.0
K	6.9	6.2	6.4	7.2	6.6	9.1
P	0.0	—	—	0.0	0.1	0.1
C	—	—	—	—	—	—
B	—	—	—	—	—	—
Sum	100.0	100.0	99.9	99.9	100.0	100.0
O	167	171	169	171	160	159
OH	3	5	3	2	8	3
F	0.3	0.0	0.1	—	—	0.2
S	—	0.1	0.1	—	—	—
Sum	170	176	172	173	168	162
<i>si</i>	400	470	410	475	269	262
<i>qz</i>	+136	+210	+155	+203	+45	+10
<i>al</i>	43	48	47	46	44	40
<i>fm</i>	9	9	9	7	14	14
<i>c</i>	6	2	5	3	10	7
<i>alk</i>	41	40	39	43	31	38
<i>mg</i>	0.34	0.24	0.20	0.25	0.31	0.30
<i>k</i>	0.49	0.51	0.50	0.55	0.48	0.53
<i>ti</i>	1.1	1.3	1.1	1.0	1.9	1.8
<i>h</i>	9	16	10	6	18	7
<i>w</i>	0.43	0.73	0.37	0.55	0.54	0.41
<i>p</i>	0.1	—	—	0.0	0.20	0.3
<i>co₂</i>	—	—	—	—	—	—
<i>f₂</i>	0.8	0.1	0.3	—	—	0.5
<i>s</i>	—	0.7	0.6	—	—	—
<i>T</i>	+2	+8	+8	+3	+13	+2
<i>t</i>	-4	+6	+3	0	+3	-5

Table 1 b (continued)

Analysis	73	74	75	76	77	78
Si	61.5	64.9	74.1	72.7	71.9	69.0
Ti	0.4	0.3	0.1	0.1	0.1	0.1
Al	18.1	18.0	13.1	13.2	13.5	15.8
Fe ³⁺	1.1	0.5	0.2	0.2	0.3	0.4
Fe ²⁺	1.1	0.9	0.2	0.2	0.4	0.4
Mn	0.1	0.0	0.0	0.0	0.0	0.0
Mg	1.0	0.4	0.1	0.1	0.6	0.4
Ca	1.2	1.4	0.3	0.4	0.4	0.5
Na	8.0	6.6	6.0	6.7	6.3	6.5
K	7.5	7.0	5.8	6.4	6.3	6.7
P	0.1	—	0.0	0.0	0.0	0.1
C	—	—	—	—	—	—
B	—	—	—	—	—	—
Sum	100.1	100.0	99.9	100.0	99.8	99.9
O	160	165	173	171	171	168
OH	7	4	4	3	3	5
F	0.2	0.4	0.1	0.1	0.2	0.3
S	—	0.1	—	—	—	—
Sum	167	170	177	174	174	173
<i>si</i>	290	342	558	518	483	424
<i>qz</i>	+42	+98	+282	+230	+211	+160
<i>al</i>	43	47	49	47	46	49
<i>fm</i>	15	10	4	4	9	8
<i>c</i>	6	7	2	3	3	3
<i>alk</i>	37	36	44	47	43	41
<i>mg</i>	0.30	0.21	0.27	0.28	0.41	0.33
<i>k</i>	0.49	0.51	0.49	0.49	0.50	0.51
<i>ti</i>	1.9	1.5	0.8	0.9	0.9	0.3
<i>h</i>	16	11	14	11	10	15
<i>w</i>	0.50	0.35	0.56	0.46	0.43	0.46
<i>p</i>	0.2	—	0.0	0.0	0.0	0.4
<i>co₂</i>	—	—	—	—	—	—
<i>f₂</i>	0.6	1.1	0.5	0.2	0.8	1.0
<i>s</i>	—	0.4	—	—	—	—
<i>T</i>	+6	+11	+5	0	+3	+8
<i>t</i>	0	+4	+3	-3	0	+5

Table 1 b (continued)

Analysis	79	80	81	82	83	84
Si	73.2	70.7	60.9	62.3	60.9	70.4
Ti	0.1	0.1	0.4	0.5	0.5	0.2
Al	13.2	14.3	17.8	17.1	17.1	14.3
Fe ³⁺	0.4	0.5	1.7	1.3	1.1	0.8
Fe ²⁺	0.2	0.5	1.3	1.2	1.4	1.4
Mn	0.0	0.1	0.1	0.1	0.1	0.0
Mg	0.1	0.7	2.0	1.7	1.2	0.7
Ca	0.3	0.6	3.2	2.1	2.4	1.1
Na	5.8	6.6	7.0	6.9	7.6	5.5
K	6.6	5.9	5.4	6.7	7.6	5.3
P	0.0	0.0	0.1	0.2	0.1	0.0
C	—	—	—	—	—	—
B	—	—	—	—	—	—
Sum	99.9	100.0	99.9	100.1	100.0	99.7
O	173	169	161	163	160	170
OH	1	6	8	4	7	5
F	0.0	—	—	0.4	0.4	0.6
S	—	—	—	—	—	—
Sum	174	175	169	167	167	176
<i>si</i>	527	447	260	287	273	422
<i>qz</i>	+247	+191	+56	+63	+37	+190
<i>al</i>	47	45	38	39	38	43
<i>fm</i>	6	12	22	20	17	18
<i>c</i>	2	4	14	10	11	7
<i>alk</i>	45	39	26	31	34	33
<i>mg</i>	0.17	0.38	0.38	0.40	0.33	0.24
<i>k</i>	0.53	0.47	0.44	0.49	0.50	0.49
<i>ti</i>	0.7	0.9	1.7	2.2	2.2	1.5
<i>h</i>	5	20	16	10	15	15
<i>w</i>	0.67	0.51	0.57	0.53	0.44	0.38
<i>p</i>	0.0	0.0	0.3	0.4	0.3	0.1
<i>co₂</i>	—	—	—	—	—	—
<i>f₂</i>	0.1	—	—	0.8	0.9	1.7
<i>s</i>	—	—	—	—	—	—
<i>T</i>	+2	+6	+12	+8	+4	+10
<i>t</i>	0	+2	-2	-2	-7	+3

Table 1 b (continued)

Analysis	85	86	87	88	89	90
Si	70.0	46.6	46.7	46.7	57.7	60.4
Ti	0.2	1.9	1.5	1.7	0.9	0.9
Al	14.0	18.4	18.4	17.9	16.2	14.7
Fe ³⁺	0.8	0.6	1.3	2.5	1.8	1.3
Fe ²⁺	1.8	9.0	8.1	8.1	5.6	4.3
Mn	0.0	0.2	0.2	0.2	0.2	0.1
Mg	0.6	5.9	7.6	8.2	1.3	2.1
Ca	1.2	9.3	8.6	7.7	3.7	3.0
Na	5.3	5.6	5.4	5.0	7.5	7.3
K	6.0	2.0	2.0	1.7	4.9	5.5
P	0.0	0.5	0.3	0.3	0.3	0.2
C	—	—	—	—	—	—
B	—	—	—	—	—	—
Sum	99.9	100.0	100.1	100.0	100.1	99.8
O	170	150	148	152	156	159
OH	4	10	13	7	11	8
F	—	—	—	—	—	—
S	—	—	—	—	—	—
Sum	174	160	161	159	167	167
<i>si</i>	408	123	121	120	215	245
<i>qz</i>	+176	-17	-19	-16	+23	+41
<i>al</i>	41	24	24	23	30	30
<i>fm</i>	19	41	44	49	33	32
<i>c</i>	7	24	22	20	14	12
<i>alk</i>	33	10	10	9	23	26
<i>mg</i>	0.19	0.37	0.44	0.43	0.15	0.27
<i>k</i>	0.53	0.26	0.27	0.25	0.40	0.43
<i>ti</i>	1.1	5.1	3.9	4.4	3.4	3.5
<i>h</i>	13	13	17	9	20	17
<i>w</i>	0.31	0.06	0.14	0.24	0.24	0.24
<i>p</i>	0.0	0.6	0.4	0.4	0.5	0.5
<i>co₂</i>	—	—	—	—	—	—
<i>f₂</i>	—	—	—	—	—	—
<i>s</i>	—	—	—	—	—	—
<i>T</i>	+8	+14	+14	+14	+7	+4
<i>t</i>	+1	-10	-8	-6	-7	-8

Table 1 c. Modal (volume percent) analyses and modal estimates of rocks from the Los-Hamra region. In the modal estimates, the following signs have been used: +++++ = main minerals; +++ = essential minerals; ++ = subordinate minerals; + = accessory minerals (cf. p. 13). Numbers correspond to those of Table 1 a.

Analysis	1	2	3	4	5	6
Mineral						
Quartz	++++	++++	++++	++++	++++	++++
Plagioclase ¹⁾	++	++	+++	++	+	+
K-feldspar (perthitic)						
Muscovite (sericite)	+++	++++	+++	++++	+++	+++
Biotite	++	+	+++	+++	+++	+++
Chlorite	++++	+++	++	++	+++	++
Cordierite						+++
Andalusite						+++
Sillimanite						
Epidote group			+	++		
{ Common hornblende { (or actinolite)						
Cumingtonite						
Anthophyllite						
Diopside						
Augite						
Olivine						
Garnet						
Calcite						
Prehnite						
Opaque minerals	+	++	++		+	+
Apatite	+	+	+	+	+	+
Zircon	+	+	+	+	+	+
Sphene + leucoxene	+			—		
Tourmaline	+	+	+	+	+	+
Fluorite						
Rutile						
Plagioclase composition. Figures indicate mol. % anorthite	alb.	alb.	alb.	alb.	alb.	alb.
N ²⁾	—	—	—	—	—	—

1) And secondary epidote + sericite.

2) Number of points counted.

Table 1 c (continued)

Analysis	7	8	9	10	11	12 ³⁾
Mineral						
Quartz	++++	+++	++++	~ 45	~ 40	++++
Plagioclase ¹⁾	+	++	+++	+	~ 20	++
K-feldspar (perthitic)	++		++++	~ 35		
Muscovite (sericite)	+++	+++	++	+	~ 15	+
Biotite	+++	+++	+++	~ 10	~ 20	+++
Chlorite		++			+	
Cordierite	++++		++	~ 5	~ 2	
Andalusite	+++	+++				
Sillimanite						
Epidote group						++
{Common hornblende						++
{(or actinolite)						++
Cummingtonite						++++
Anthophyllite						
Diopside						++
Augite						
Olivine						
Garnet						+
Calcite						+
Prehnite						
Opaque minerals	+	++	+	~ 4	+	+
Apatite	+	+	+	+	+	
Zircon	+	+	+	+	+	
Sphene + leucoxene					+	+
Tourmaline	+	+	+	+	+	
Fluorite						
Rutile						
Plagioclase composition. Figures indicate mol. % anorthite	alb.	~ 10	20	alb.— —olig.	~ 25	olig.
N ²⁾	—	—	—	2180	1611	—

¹⁾ And secondary epidote + sericite.

²⁾ Number of points counted.

³⁾ Very approximate composition (layered rock).

Table 1 c (continued)

Analysis	13 ³⁾	14 ³⁾	15	16	17	18
Mineral						
Quartz	+++	+++	30	49	+++	++++
Plagioclase ¹⁾	++	+	10	2	++++	++
K-feldspar (perthitic)		+++		10		++++
Muscovite (sericite)	+	++	35	4	+	+++
Biotite	++	+++	25	20	+++	+
Chlorite	+	+			++	+
Cordierite	++				++	
Andalusite						
Sillimanite			+	14		
Epidote group	++	+++				+
{ Common hornblende { (or actinolite)	+++	+++				
Cumingtonite	+++					
Anthophyllite	++				+++	
Diopside	+++					
Augite						
Olivine						
Garnet					++	
Calcite						+
Prehnite						
Opaque minerals	+	++	+	+	+	+
Apatite		+	+	+	+	+
Zircon		+	+	+	+	+
Sphene + leucoxene	+	+				+
Tourmaline		+				+
Fluorite						+
Rutile						
Plagioclase composition. Figures indicate mol. % anorthite	~ 40	—	19—25	23—28	~ 33	alb.
N ²⁾	—	—	1841	1492	—	—

1) And secondary epidote + sericite.

2) Number of points counted.

3) Very approximate composition (layered rock).

Table 1 c (continued)

Analysis	19	20	21	22	23	24
Mineral						
Quartz	++++	++++	++++	++++	++++	++++
Plagioclase ¹⁾	+++	+++	++	+++	++(?)	++
K-feldspar (perthitic)	++++	++++	++++	++++	++++	++++
Muscovite (sericite)	++	+++	+++	+	+++	+++
Biotite	++	+++	+	++	+	
Chlorite	+	+		+		
Cordierite						
Andalusite						
Sillimanite						
Epidote group	+	+		+	++	+
{Common hornblende (or actinolite)						
Cummingtonite						
Anthophyllite						
Diopside						
Augite						
Olivine						
Garnet						
Calcite						
Prehnite						
Opaque minerals	+	+	++	++	++	++
Apatite	+	+	+	+		
Zircon	+	+	+	+	+	+
Sphene+leucoxene	+			++		
Tourmaline			+			
Fluorite	+				+	
Rutile						
Plagioclase composition. Figures indicate mol. % anorthite	3	~10	~20	24-33	(alb.)	0
N ²⁾	—	—	—	—	—	—

¹⁾ And secondary epidote + sericite.

²⁾ Number of points counted.

Table 1 c (continued)

Analysis	25	26	27	28	29	30
Mineral						
Quartz	++++	++++	1	+		+
Plagioclase ¹⁾	+(?)		30	35	41	39
K-feldspar (perthitic)	++++					
Muscovite (sericite)	+++	+++	+		+	
Biotite	+++	+++		+	+	
Chlorite	+		+		+	1
Cordierite		} 4)				
Andalusite						
Sillimanite						
Epidote group			3		+	3
{ Common hornblende { (or actinolite)			64	61	57	36
Cummingtonite						
Anthophyllite						
Diopside						
Augite						
Olivine						
Garnet						
Calcite						+
Prehnite				+	+	
Opaque minerals	++		2	3	1	19 ⁵⁾
Apatite		+		+		+
Zircon	+	+				
Sphene+leucoxene	+			+		+
Tourmaline					+	
Fluorite						
Rutile						
Plagioclase composition. Figures indicate mol. % anorthite	(alb.)	—	45	31—37	53—65	~15
N ²⁾	—	—	1790	1496	1530	1394

¹⁾ And secondary epidote + sericite.

²⁾ Number of points counted.

⁴⁾ Completely altered to sericite.

⁵⁾ Magnetite.

Table 1 c (continued)

Analysis	31	32	33	34	35	36
Mineral						
Quartz		++++	++++	++++	++++	++++
Plagioclase ¹⁾	+(?)	+++	+++	+++	++++	+++
K-feldspar (perthitic)		++++	++++	++++	+++	++++
Muscovite (sericite)	+	++	+	+	+	+
Biotite	+	++	++	+++	++	++
Chlorite	+	++	+	++	+	++
Cordierite						
Andalusite						
Sillimanite						
Epidote group	2	+	+	++	+	+
{Common hornblende (or actinolite)	85					++
Cummingtonite						
Anthophyllite						
Diopside	+					
Augite						
Olivine						
Garnet						
Calcite						
Prehnite		+		+		
Opaque minerals	10	+	+	+	+	+
Apatite		+	+	+	+	+
Zircon		+	+	+	+	+
Sphene+leucoxene	+		++		+	++
Tourmaline		+				
Fluorite		+	+		+	
Rutile						
Plagioclase composition. Figures indicate mol. % anorthite	—	11—15	15—20	23—27	12—17	13—17
N ²⁾	725	—	—	—	—	—

1) And secondary epidote + sericite.

2) Number of points counted.

Table 1 c (continued)

Analysis	37	38	39	40	41	42
Mineral						
Quartz	39	++++	35	40	39	++++
Plagioclase ¹⁾	30	+++	32	17	15	+++
K-feldspar (perthitic)	12	++++	31	37	43	++++
Muscovite (sericite)	1	++	+	+	1	++
Biotite	17	+++	2	+	+	
Chlorite	+	+		3	1	++
Cordierite						
Andalusite						
Sillimanite						
Epidote group	+	+	+		+	+
{Common hornblende (or actinolite)						
Cummingtonite						
Anthophyllite						
Diopside						
Augite						
Olivine						
Garnet						
Calcite						
Prehnite						
Opaque minerals	+	+	+	+	+	+
Apatite	+	+		+	+	
Zircon	+	+	+	+	+	+
Sphene+leucoxene				+		+
Tourmaline						+
Fluorite		+	+		+	
Rutile						
Plagioclase composition. Figures indicate mol. % anorthite	16	16—21	12	2	2—9	1
N ²⁾	1350	—	1746	1578	1632	—

¹⁾ And secondary epidote + sericite.

²⁾ Number of points counted.

Table 1 c (continued)

Analysis	43	44	45	46	47	48
Mineral						
Quartz	27	31	38	++++	++++	26
Plagioclase ¹⁾	58	45	38	++++	++++	43
K-feldspar (perthitic)	10	11	7	+++	+++	8
Muscovite (sericite)	+	+	+	++	+	+
Biotite	3	11	15	+++	+++	11
Chlorite	+	1		+	++	+
Cordierite						
Andalusite						
Sillimanite						
Epidote group	+	+	+		+	1
{Common hornblende (or actinolite)			+			9
Cummingtonite						
Anthophyllite						
Diopside						
Augite						
Olivine						
Garnet						
Calcite	+			+	+	+
Prehnite	+					+
Opaque minerals	+	+	+	+	+	+
Apatite	+	+	+		+	+
Zircon		+	+	+	+	+
Sphene + leucosene	+	+	+			1
Tourmaline						
Fluorite						
Rutile	+					
Plagioclase composition. Figures indicate mol. % anorthite	23—27	18—22	17—62	25	23	26—43
N ²⁾	1561	1394	1580	—	—	1700

1) And secondary epidote + sericite.

2) Number of points counted.

Table 1 c (continued)

Analysis	49	50	51	52	53	54
Mineral						
Quartz	~8 ⁶⁾	~17 ⁶⁾	~18 ⁶⁾	~18 ⁶⁾	++++	++++
Plagioclase ¹⁾	++++	++++	++++	++++	++++	++++
K-feldspar (perthitic)	++++	++++	++++	++++	++++	++++
Muscovite (sericite)	+	+	+	+	+	++
Biotite	+++	++	+++	+++	+++	++
Chlorite	++	++	++		+	+
Cordierite						
Andalusite						
Sillimanite						
Epidote group	+	+	+	+	+	
{Common hornblende (or actinolite)	+++	++	++	+++	++	
Cummingtonite						
Anthophyllite						
Diopside						
Augite		+				
Olivine						
Garnet						
Calcite	+	+	+			
Prehnite	+	++	+			
Opaque minerals	++	++	++	++	+	+
Apatite	+	+	+	+	+	+
Zircon	+	+	+	+	+	+
Sphene + leucoxene	++	++	++	++	++	
Tourmaline						+
Fluorite						+
Rutile						
Plagioclase composition. Figures indicate mol. % anorthite	14—27	23—28	15—24	15—35	11—24	5—18
N ²⁾	—	—	—	—	—	—

1) And secondary epidote + sericite.

2) Number of points counted.

6) According to quantitative X-ray powder analysis.

Table 1 c (continued)

Analysis	55	56	57	58	59	60
Mineral						
Quartz	31	++++	+	+	+++	+++
Plagioclase ¹⁾	31	++++	++++7)	++++	++++	++++
K-feldspar (perthitic)	34	++++		++	++++	++++
Muscovite (sericite)	+	+	+	++	+	+
Biotite	1	+++		+		
Chlorite	2	++	++	+	++	++
Cordierite						
Andalusite						
Sillimanite						
Epidote group	+	+	++	+++	+++	+++
{Common hornblende (or actinolite)		++	+	++		
Cummingtonite						
Anthophyllite						
Diopside						
Augite		+	+++	+++		
Olivine						
Garnet						
Calcite				+	+	
Prehnite						
Opaque minerals	+	++	+++	+++	+	++
Apatite	+	+			+	+
Zircon	+	+				
Sphene+leucoxene	+	+	+		++	+
Tourmaline						
Fluorite	+					
Rutile		+				
Plagioclase composition. Figures indicate mol. % anorthite	2—16	7—25	and.	37—65	4	0
N ²⁾	1861	—	—	—	—	—

¹⁾ And secondary epidote + sericite.

²⁾ Number of points counted.

⁷⁾ Phenocrysts strongly saussuritized.

Table 1 c (continued)

Analysis	61	62	63	64	65	66
Mineral						
Quartz	+++	++++	++++	++++	++++	++++
Plagioclase ¹⁾	++++	}++++	}++++	}++++	}++++	}++++
K-feldspar (perthitic)	++++					
Muscovite (sericite)	+					
Biotite		+	+	+	+	+
Chlorite	++	++	+	+	+	+
Cordierite						
Andalusite						
Sillimanite						
Epidote group	+++	++	++	+	++	+
{Common hornblende						
{(or actinolite)	++					
Cumingtonite						
Anthophyllite						
Diopside						
Augite						
Olivine						
Garnet						
Calcite	+				+	
Prehnite						
Opaque minerals	++	+	+	+	+	+
Apatite	+	+	+	+	+	+
Zircon		+	+	+	+	+
Sphene + leucoxene	++	+	+		++	+
Tourmaline						
Fluorite			+	+	+	
Rutile						
Plagioclase composition. Figures indicate mol. % anorthite	alb. (-and.)	1	0	3	alb.	0
N ²⁾	-	-	-	-	-	-

¹⁾ And secondary epidote + sericite.

²⁾ Number of points counted.

Table 1 c (continued)

Analysis	67	68	69	70	71	72
Mineral						
Quartz	++++	++++	++++	++++	+++	+++
Plagioclase ¹⁾	} +++++	} +++++	} +++++	} +++++	} +++++	+++
K-feldspar (perthitic)						+++++
Muscovite (sericite)	+	+	+	+	+	+
Biotite		+				
Chlorite	++		++		++	+++
Cordierite						
Andalusite						
Sillimanite						
Epidote group	++		++	+	++	++
{Common hornblende						
{(or actinolite)						
Cummingtonite						
Anthophyllite						
Diopside						
Augite						
Olivine						
Garnet						
Calcite	+	+	+	+		
Prehnite						
Opaque minerals	+	+	+	+	++	++
Apatite	+	+	+	+	+	+
Zircon	+	+	+	+	+	+
Sphene+leucoxene	+	+	+	+	++	+
Tourmaline						
Fluorite	+		+	+	+	
Rutile						
Plagioclase composition. Figures indicate mol. % anorthite	1	2	1	alb.— —olig.	2	alb.— —and.
N ²⁾	—	—	—	—	—	—

1) And secondary epidote + sericite.

2) Number of points counted.

Table 1 c (continued)

Analysis	73	74	75	76	77	78
Mineral						
Quartz	+++	+++	37	35	31	30
Plagioclase ¹⁾	+++	+++	23	6	13	31
K-feldspar (perthitic)	++++	++++	39	58	55	29
Muscovite (sericite)	+	+	1	+	+	8
Biotite	+	++		+	1	
Chlorite	++	+	+		+	2
Cordierite						
Andalusite						
Sillimanite						
Epidote group	++	+		+	+	
{Common hornblende {(or actinolite)						
Cumingtonite						
Anthophyllite						
Diopside						
Augite						
Olivine						
Garnet						
Calcite						+
Prehnite	+					
Opaque minerals	++	++	+	+	+	+
Apatite	+	+			+	+
Zircon	+	+	+	+	+	+
Sphene + leucoxene	+			+	+	+
Tourmaline						
Fluorite	+			+		+
Rutile						
Plagioclase composition. Figures indicate mol. % anorthite	alb.— —labr.	alb.— —labr.	3	0	alb. (—olig.)	4
N ²⁾	—	—	1463	1741	1664	1990

¹⁾ And secondary epidote + sericite.

²⁾ Number of points counted.

Table 1 c (continued)

Analysis	79	80	81	82	83	84
Mineral						
Quartz	36	30	+++	+++	+++	++++
Plagioclase ¹⁾	1	13	+++	+++	+++	+++
K-feldspar (perthitic)	62	55	++++	++++	++++	++++
Muscovite (sericite)	+	+	+	+	+	+
Biotite	+	+	++			+
Chlorite	+	1	+	++	++	+++
Cordierite						
Andalusite						
Sillimanite						
Epidote group	+		+	++	+	+
{Common hornblende						
{(or actinolite)			++		+	
Cummingtonite						
Anthophyllite						
Diopside						
Augite			+			
Olivine						
Garnet						
Calcite		+				
Prehnite			+		+	
Opaque minerals	+	+	++	++	++	+
Apatite	+	+	+	+	+	+
Zircon	+	+	+	+	+	+
Sphene + leucoxene	+	+	+	+	+	
Tourmaline						
Fluorite				+		
Rutile		+				
Plagioclase composition. Figures indicate mol. % anorthite	alb.	alb.	alb.— —labr.	alb.	alb.— —and.	0
N ²⁾	1744	1622	—	—	—	—

¹⁾ And secondary epidote + sericite.

²⁾ Number of points counted.

Table 1 c (continued)

Analysis	85	86	87	88	89	90
Mineral						
Quartz	++++	2	3	3	11	11
Plagioclase ¹⁾	+++	55	52	57	~ 20	~ 16
K-feldspar (perthitic)	++++	7	3	8	~ 53	~ 52
Muscovite (sericite)	+	+	+	+	+	+
Biotite		5 ⁸⁾	5	4 ⁹⁾	4	4
Chlorite	++		+	3 ⁸⁾		
Cordierite						
Andalusite						
Sillimanite						
Epidote group	+	+	+	+	+	+
{Common hornblende {(or actinolite)		1	14	1	4	10
Cumingtonite						
Anthophyllite						
Diopside						
Augite		18	15	15	4	4
Olivine		4		3		
Garnet						
Calcite						
Prehnite						
Opaque minerals		7	7	6	2	2
Apatite	+	1	+	+	+	+
Zircon	+					+
Sphene + leucoxene	+				+	+
Tourmaline						
Fluorite	+					
Rutile						
Plagioclase composition. Figures indicate mol. % anorthite	3	32—69	20—71	32—69	0—37	0—35
N ²⁾	—	1595	1685	1422	1302	1431

¹⁾ And secondary epidote + sericite.

²⁾ Number of points counted.

⁸⁾ Includes serpentine and talc.

⁹⁾ Includes phlogopite.

List of analysed rocks in Tables 1 a—c. For localities, see Fig. 69 (p. 224) and Plate 1.

1. Slate. Ryggskog slate quarries, 340/312.
2. Phyllite. Västerhocklan, 294/339.
3. Metasiltstone. Västerhocklan, 310/304.
4. Phyllite. Noppikoski, 212/034.
5. Phyllite to mica-schist with chlorite porphyroblasts. Västerhocklan, 309/297. See also Table 6: no. 1.
6. Mica-schist with porphyroblasts of andalusite and cordierite. Västerhocklan, 309/289.
7. Mica-schist, transitional to a hornfels. Kolarsjön, 279/370.
8. Mica-schist. Svartån, 243/298.
9. Hornfels. N. Stensjön, 344/412.
10. Hornfels. Orrtjärnsklinten, 349/417.
11. Argillitic gneiss. Pajkölen, 362/435.
12. Skarn-bearing meta-argillite. Kolarsjön, 273/368. See also Table 3: no. 4.
13. Skarn-bearing meta-argillite. Kolarsjön, 271/365. See also Table 3: no. 6 and Table 4: no. 2.
14. Skarn-bearing meta-argillite. Lillskog, 516/255.
15. Argillitic gneiss (to mica-schist). Storlugnet, 280/268.
16. Sillimanite gneiss. Dåasen, 440/286.
17. Anthophyllite-almandite-cordierite gneiss. Fetingsberg, 464/247. See also Table 3: no. 13 and Table 5: no. 5.
18. Metarhyolite. Ryggskog, 350/309.
19. Metarhyolite. Järpberget, 397/172.
20. Metarhyolite. (Contaminated with meta-argillite.) Risberget, 352/204.
21. Metarhyolite. (Somewhat contaminated with meta-argillite.) Risberget, 348/205.
22. Metarhyolite. Uvberget, 365/224.
23. Metarhyolite. Noppikoski, 209/032.
24. Metarhyolite. Tallsjön, 192/073.
25. Metarhyolite. Sandsjöån, 244/108.
26. Mica-schist (tectonized metarhyolite) with sericitized andalusite and/or cordierite. Sandsjöån, 252/100.
27. Basic, amphibolitic metavolcanite. Lillskog, 523/249.
28. Basic, amphibolitic metavolcanite. Dåasen, 435/329. See also Table 3: no. 23.
29. Basic, amphibolitic metavolcanite (or sub-volcanic intrusion). Romberg, 399/348. See also Table 3: no. 25.
30. Magnetite-rich, basic amphibolitic metavolcanite. Los, 383/308. See also Table 3: no. 24.
31. Basic, amphibolitic metavolcanite. (Metaspilite.) Storkullen, 256/363.
32. Primorogenic granite. Voxnahed, 300/246.

33. Primorogenic granite. Storlugnet, 303/259.
34. Primorogenic granite. Lossjön, 408/300.
35. Primorogenic light granodiorite. Oreälven, 256/030.
36. Primorogenic granite. Storkölen, 503/338.
37. Primorogenic light granodiorite. Rytarklitten, 420/117.
38. Primorogenic granite with scattered microcline augen. Dåasberget, 411/320.
39. Primorogenic granite, fine-grained. Stenhakersberget, 434/244.
40. Primorogenic, quartz-porphyrific and granophyric granite. Laxtjärn, 311/277.
41. Primorogenic granite, fine-grained. Risberget, 359/200.
42. Primorogenic, quartz-porphyrific granite. Oreälven, 229/031.
43. Primorogenic granodiorite. Mickeltjärn, 163/359.
44. Primorogenic granodiorite with scattered microcline augen. Västersjön, 499/214.
45. Primorogenic granodiorite. Storlugnet, 288/267.
46. Primorogenic granodiorite with microcline augen. Nybyn, 480/144.
47. Primorogenic granodiorite with microcline augen. Västersjön, 495/214.
48. Primorogenic dark granodiorite. Hamra, 295/223.
49. Rätan granite, porphyritic. Fågelsjö, 128/370.
50. Rätan granite, porphyritic. Acksjön, 106/418.
51. Rätan granite, porphyritic. Kolarsjön, 266/390.
52. Rätan granite, porphyritic. Gräsberget, 325/444.
53. Rätan granite, porphyritic, weakly schistose. Tjärnbäcksberget, 211/235.
54. Rätan granite, weakly porphyritic to even-grained. Svartån, 240/299.
55. Fine-grained (aplitic) granite in Rätan granite. St. Sjöarberget, 070/377.
56. Granite porphyry in Rätan granite. St. Acksjöberget, 109/452.
57. Dala porphyrite. Korsiberget, 174/166. See also Table 4: no. 14.
58. Dala porphyrite. Börningsberget, 080/304. See also Table 4: no. 13.
59. Dala porphyrite. Tallsjön, 189/075.
60. Dala porphyrite. Oreälven, 178/030.
61. Dala porphyrite. Vassjöån, 187/038.
62. Dala porphyry, poor in phenocrysts. Weakly eutaxitic. Gethelvetet, 142/225.
63. Dala porphyry, poor in phenocrysts. Eutaxitic. Knoppvägen, 169/061.
64. Dala porphyry, poor in phenocrysts. Finnberget, 028/165.
65. Dala porphyry, poor in phenocrysts. Eutaxitic. Älvho, 158/032. (von Eckermann 1936, analysis no. 77.)
66. Dala porphyry, poor in phenocrysts. Eutaxitic. Somewhat recrystallized through dolerite intrusion. Älvho, 150/034.
67. Dala porphyry, poor in phenocrysts. Weakly eutaxitic. Björnsjöknopparna, 078/236.

68. Dala porphyry, poor in phenocrysts. Weakly eutaxitic. Korrisjön, 143/231. Analyst: A. Aaremäe.
69. Dala porphyry, poor in phenocrysts. Eutaxitic. Storsvedberget, 050/314. Analyst: A. Aaremäe.
70. Dala porphyry, poor in phenocrysts. With well developed pseudo-fluidal texture (Fig. 43). Flarksjön, 119/203.
71. Dala porphyry, rich in phenocrysts. With well developed pseudo-fluidal texture. Vassjöån, 173/063.
72. Dala porphyry, rich in phenocrysts. Älvho, 158/036.
73. Dala porphyry, rich in phenocrysts. St. Sundsjöberget, 148/178.
74. Dala porphyry, rich in phenocrysts. Tandhem, 165/233. Analyst: A. Aaremäe.
75. Dala granite, fine-grained. Vässinkoski, 128/031.
76. Dala granite, fine-grained. Långtjärn, 069/225.
77. Dala granite, weakly porphyritic. Finnbergsbron, 048/139.
78. Dala granite, fine-grained. Sandsjön, 198/155.
79. Dala granite, fine- to medium-grained. Naappo, 194/224.
80. Dala granite, medium-grained. County of Jämtland, west of the Los-Hamra region. Lat. 61°57'00" N., long. 14°05'30" E.
81. Dala granite, porphyritic. County of Jämtland, west of the Los-Hamra region. Lat. 61°40'40" N., long. 14°03'30" E.
82. Dala granite, porphyritic. Rutimovuo, 052/150.
83. Dala granite, porphyritic. Finnberget, 025/142.
84. Dala granite, weakly porphyritic. Västbacka, 210/178.
85. Dala granite, weakly porphyritic. V. Råberget, 214/074. (von Eckermann 1936, analysis no. 70.)
86. Dolerite. Naappo, 194/226. See also Table 4: nos. 17 and 23.
87. Dolerite, uralitized. Älvho, 144/031. See also Table 4: no. 18.
88. Dolerite. Gäddtjärn, 062/234. See also Table 4: nos. 19 and 24.
89. Approx. granitic differentiate in dolerite. Pilkalampinoppi, 151/135. See also Table 4: nos. 28 and 32.
90. Approx. granitic differentiate in dolerite. Siikamäki, 146/096. See also Table 4: no. 27.

Table 1 d. Estimated accuracies for the chemical analyses of Table 1 a. See also p. 13.

Elements and oxides	Range	Accuracy
SiO ₂	—	± 2 % of value indicated
TiO ₂	—	± 5 % „ „ „
Al ₂ O ₃	—	± 3 % „ „ „
Fe ₂ O ₃	< 5 %	± 0.1
	> 5 %	± 0.2
FeO	—	± 0.15
MnO	—	± 0.02
MgO	low	± 10 % of value indicated
	high	± 5 % „ „ „
CaO	low	± 10 % „ „ „
	high	± 3 % „ „ „
Na ₂ O	low	± 10 % „ „ „
	high	± 5 % „ „ „
K ₂ O	low	± 10 % „ „ „
	high	± 5 % „ „ „
H ₂ O	—	± 0.2
P ₂ O ₅	—	± 0.02
CO ₂	(< 1 %)	± 10 % of value indicated
F	—	± 0.01
S	—	± 0.02
B ₂ O ₃	low (near 0.001)	± 30 % of value indicated
	high	± 10 % „ „ „
Cr	< 200 ppm	± 20 ppm
	> 200 ppm	± 10 % of value indicated
Co	< 100 ppm	± 10 ppm
	> 100 ppm	± 10 % of value indicated
Ni	< 100 ppm	± 10 ppm
	> 100 ppm	± 10 % of value indicated
V	< 200 ppm	± 20 ppm
	> 200 ppm	± 10 % of value indicated
Cu	< 100 ppm	± 10 ppm
	> 100 ppm	± 10 % of value indicated
BaO	< 500 ppm	± 50 ppm
	> 500 ppm	± 10 % of value indicated
SrO	< 500 ppm	± 50 ppm
	> 500 ppm	± 10 % of value indicated
Zr	—	± 50 ppm
Rb ₂ O	—	± 50 ppm

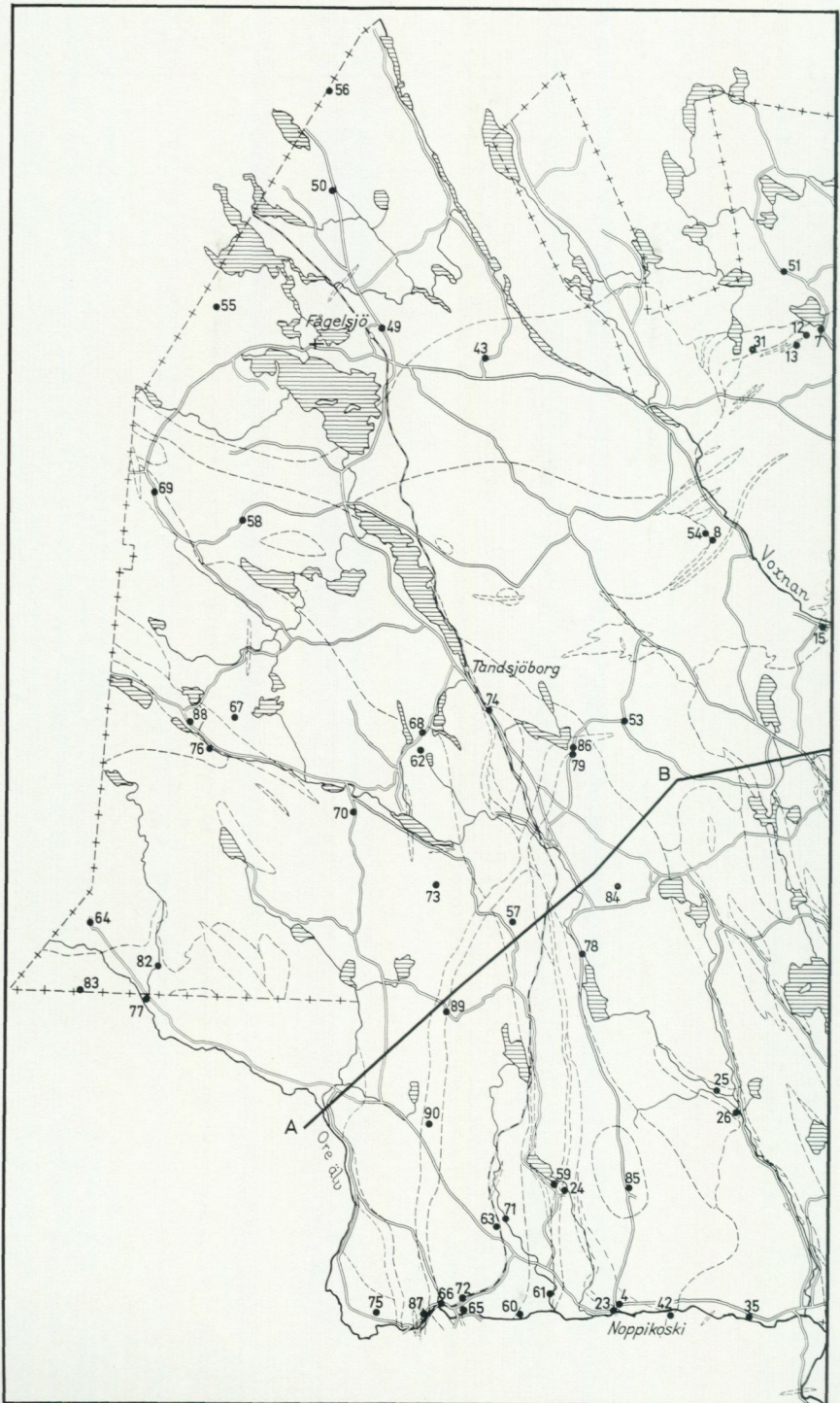
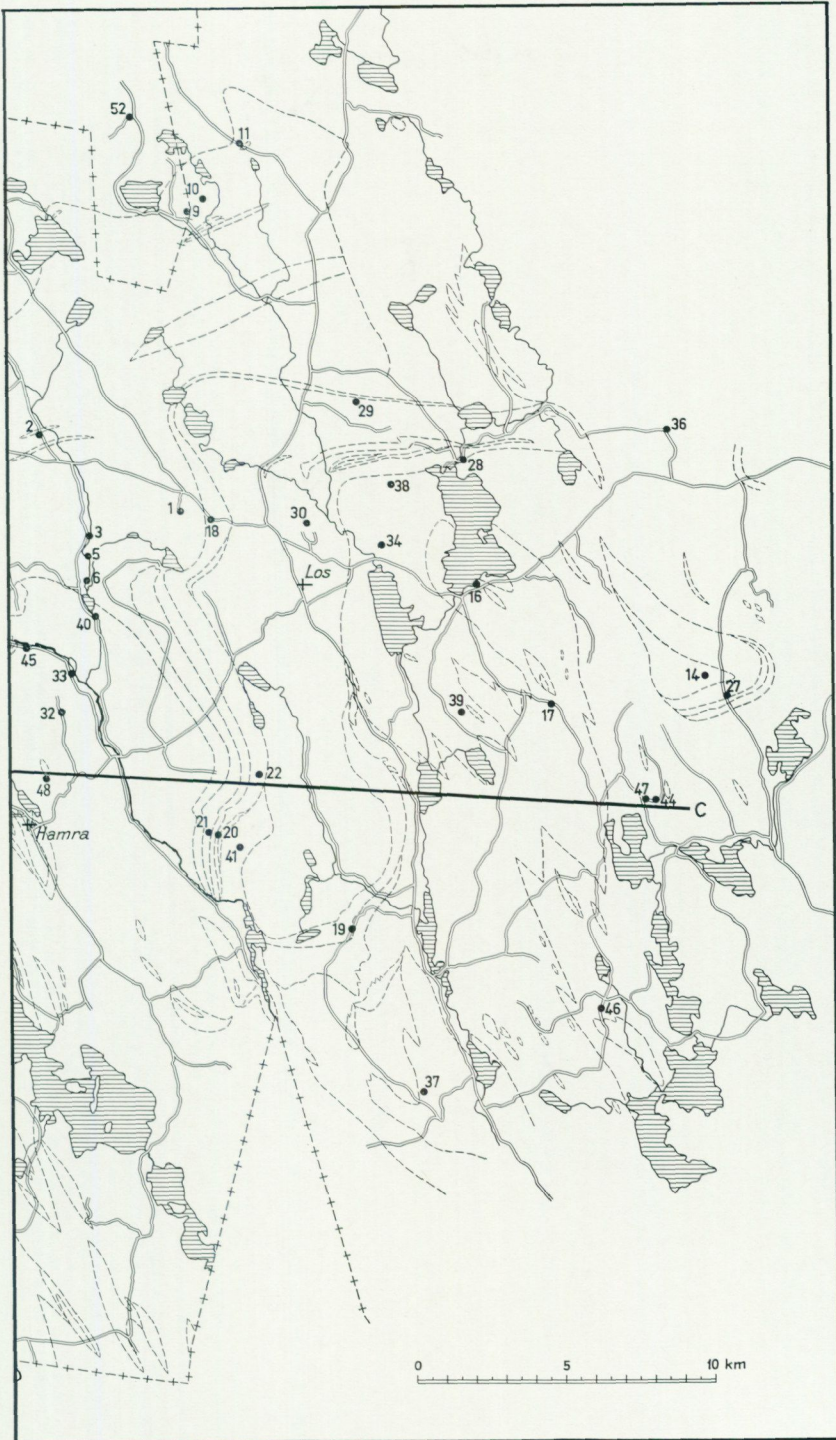


Fig. 69. Localities of sampling for chemical analyses. Numbers correspond to those of Table 1.



The line A-B-C indicates the position of the cross section in Fig. 61.
 (Rock contacts indicated by broken lines, cf. Plate 1.)

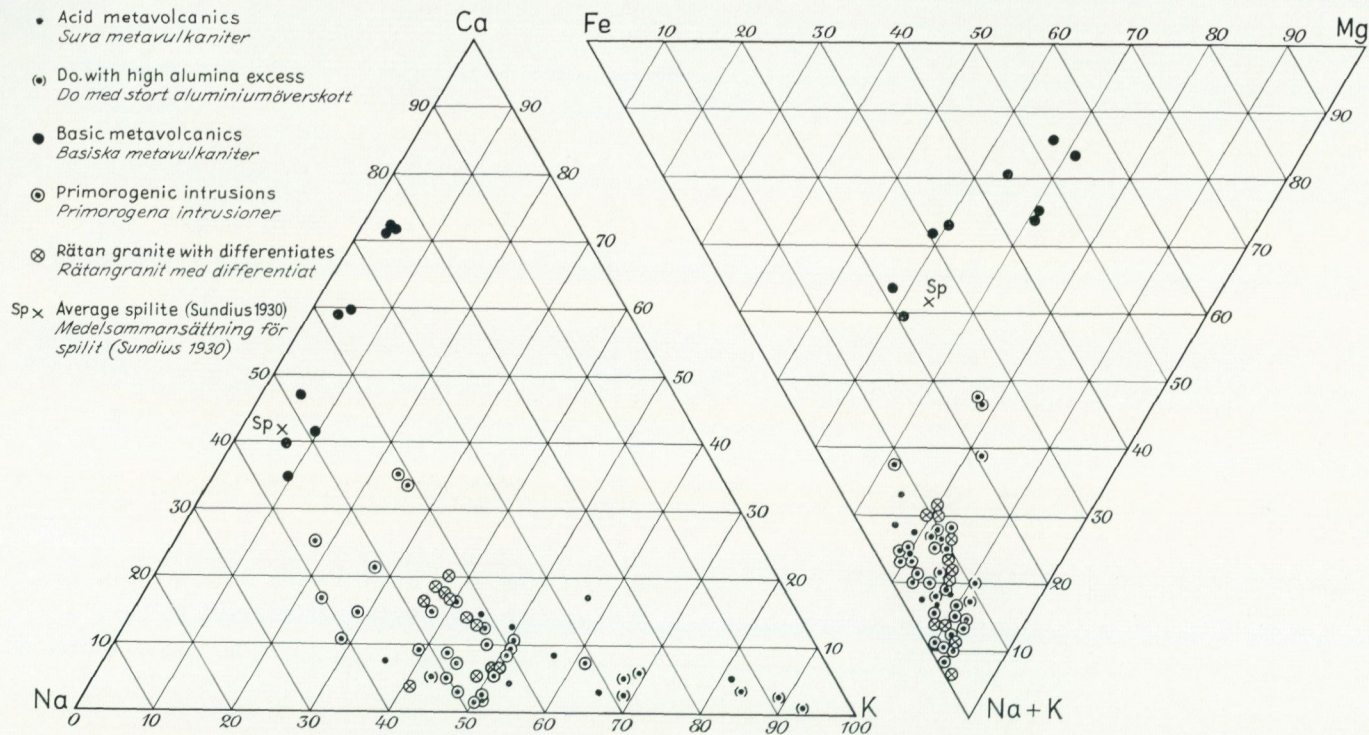


Fig. 70. Ca-Na-K and Fe-Mg-(Na+K) diagrams (atomic proportions) of metavolcanics, primorogenic intrusions and Rätan granite with differentiates. Chemical analyses used for plotting are taken from: this work: nos. 18–25, 27–56; von Eckermann (1936): nos. 31–33, 35–38, 41, 44–48, 50–51, 59–61, 64–65, 73.

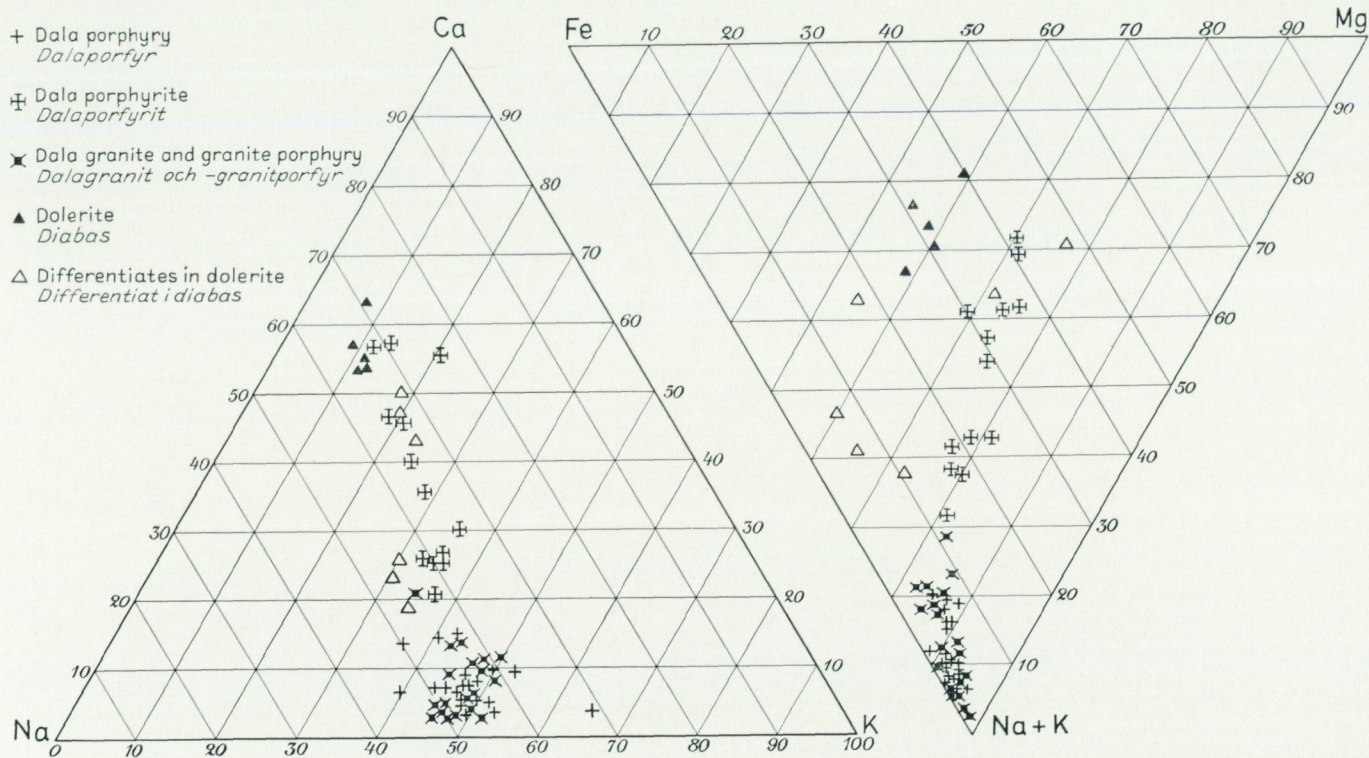


Fig. 71. Ca-Na-K and Fe-Mg-(Na+K) diagrams (atomic proportions) of sub-Jotnian and Jotnian igneous rocks. Chemical analyses used for plotting are taken from: this work: nos. 57-90; von Eckermann (1936): nos. 69-70, 74-79, 81-97, 104, 106-110. (Nos. 70 and 77 correspond to nos. 85 and 65, respectively, of the present work.)

Table 2. Suite index, suite type and nomenclature of volcanics and metavolcanics from the Los-Hamra region. Analyses within brackets are of strongly chemically altered rocks.

Rock	Analysis ¹⁾	Suite index σ (Rittmann 1962 a)	Suite type (Rittmann 1962 a)	Nomenclature (Rittmann 1952)
Acid meta- vol- canics	(18)	1.7	strong Pacific	rhyolite)
	19	2.0	average Pacific	alkali rhyolite
	(20)	1.5	strong Pacific	rhyolite)
	(21)	3.4	weak Pacific	")
	22	2.1	average Pacific	"
	23	2.2	" "	"
	(24)	1.2	strong Pacific	")
	(25)	1.6	" "	")
	E 36	3.0	average Pacific	dark soda rhyolite
	E 37	1.5	strong Pacific	rhyolite
	E 38	1.7	" "	"
	(E 41)	1.1	" "	quartz latite)
	E 59	1.8	" "	rhyolite
E 60	2.5	average Pacific	alkali rhyolite	
(E 61)	1.1	strong Pacific	rhyolite)	
Basic meta- vol- canics	27	1.2	" "	pigeonite-labradorite andesite
	28	2.0	average Pacific	olivine andesite
	29	1.1	strong Pacific	olivine basalt
	30	3.5	weak Pacific	olivine-andesine basalt
	31	2.8	average Pacific	olivine basalt
	E 31	5.6	weak Atlantic	olivine-andesine basalt
	E 32	4.9	transitional Atlantic	olivine andesite
	E 33	2.8	average Pacific	pigeonite andesite
	E 35	1.6	strong Pacific	andesine basalt
Dala porphy- rites	57	3.3	weak Pacific	olivine trachybasalt
	58	3.0	average Pacific	andesine trachybasalt to labradorite trachyandesite
	59	3.0	weak Pacific	dark quartz latite
	60	2.8	average Pacific	quartz latite
	61	4.1	weak Mediterranean	rhyolite
	E 84	3.1	weak Pacific	dark quartz latite
	E 85	3.9	" "	latite
	E 86	4.1	weak Mediterranean	"
	E 87	3.7	weak Pacific	"
	E 88	1.8	average Pacific	labradorite trachyandesite
	E 89	2.7	" "	" "
	E 90	2.8	" "	" "
	E 91	3.7	weak Pacific	pigeonite-labradorite andesite to olivine trachybasalt

Table 2 (continued)

Rock	Analysis ¹⁾	Suite index σ (Rittmann 1962 a)	Suite type (Rittmann 1962 a)	Nomenclature (Rittmann 1952)
Dala por- phyries	62	3.1	weak Pacific	alkali rhyolite
	63	3.1	" "	" "
	64	2.7	average Pacific	" "
	65, E 77	2.3	" "	rhyolite
	66	2.6	" "	alkali rhyolite
	67	3.2	weak Pacific	" "
	68	2.2	average Pacific	rhyolite
	69	2.7	" "	" "
	70	2.6	" "	alkali rhyolite
	71	4.3	weak Mediterranean	rhyolite to quartz latite
	72	7.1	average Mediterranean	alkali trachyte
	73	5.0	weak Mediterranean	" "
	74	3.5	weak Pacific	rhyolite
	(E 74	2.1	average Pacific	")
	E 76	3.0	weak Pacific	alkali rhyolite
	E 78	2.8	average Pacific	rhyolite
	E 79	5.2	weak Mediterranean	alkali trachyte to alkali rhyolite
E 82	5.7	" "	alkali trachyte	
E 83	5.7	" "	trachyte	

¹⁾ Numbers with prefix "E", see von Eckermann (1936).
Otherwise, see the present work, Table 1.

Table 3. Optical data and *mg* values for amphiboles from the Los-Hamra region.

No.	Mineral	Locality (see Plate 1)	n_γ	n_α	$2V_\gamma$ (degrees)	<i>mg</i> ¹⁾
1	Anthophyllite	416/333	1.655	—	75	0.7
2	Cummingtonite	242/311	1.647	—	—	0.8
3	Tremolite	236/256	1.632	—	98	1.0
4	Cummingtonite	273/368	1.678	1.658	81	0.4
5	„	275/370	1.689	1.661	89	0.3
6	„	271/365	1.685	—	90	0.4
7	„	276/371	1.695	—	—	0.3
8	„	269/364	1.678	—	—	0.5
9	Al-anthophyllite	271/365	1.699	—	84	0.3 ²⁾
10	Common hornblende	271/365	1.671	—	—	0.7
11	„ „	269/364	1.681	—	—	0.5
12	Al-anthophyllite	462/228	1.682	1.662	81	0.5
13	„	465/246	1.688	1.668	80	0.4
14	Anthophyllite	401/131	1.660	—	c. 70	0.6
15	Tremolite	227/033	1.638	—	—	0.9
16	Cummingtonite	238/364	1.649	—	(<90)	0.7
17	Actinolite	246/357	1.659	—	—	0.6
18	Grunerite	247/359	1.705	—	94	0.2
19	„	245/357	1.705	—	—	0.2
20	Cummingtonite	246/353	1.703	—	c. 103	0.2
21	Common hornblende	245/357	1.698	—	—	0.3
22	Tremolite	418/331	1.628	—	—	1.0
23	Common hornblende	435/329	1.680	—	123	0.6
24	„ „	383/308	1.662	—	109	0.8
25	„ „	399/348	1.667	—	105	0.7
26	Cummingtonite	393/167	1.658	—	80	0.6
27	„	465/346	1.657	—	71	0.6
28	Anthophyllite	465/346	1.655	—	67	0.7

¹⁾ $mg = \frac{Mg}{Mg+Fe^{2+}}$; Determined from refractive indices (Tröger 1959).

²⁾ Cf. Lundqvist (1962).

Table 4. Optical data and mg values for pyroxenes and olivines from the Los-Hamra region.

No.	Mineral	Locality (see Plate 1)	n_{γ}	$2V_{\gamma}$ (degrees)	$mg^{1)}$
1	Diopside ²⁾	435/333	1.719	60	0.7
2	„	271/365	1.735	58	0.4
3	„	276/371	1.741	57	0.3
4	„	459/219	1.728	57	0.5
5	Olivine	414/331	1.682	90	0.94
6	Diopside	410/331	1.708	58	0.8
7	Olivine	328/161	1.702 ³⁾	89	0.83
8	Diopside	236/256	1.713	57	0.7
9	„	269/372	1.720	55	0.6
10	„	262/365	1.720	57	0.6
11	„	364/434	1.729	56	0.5
12	Ferrohypersthene	301/412	1.737	129	0.4
13	Augite	080/304	1.716	48—57	—
14	„	174/166	1.713	52	—
15	„	203/032	1.727	51	—
16	„	077/176	1.716	54	—
17	„	194/226	1.724	51	—
18	„	144/031	1.719	40—47	—
19	„	062/234	1.718	37—42	—
20	„	093/206	1.721	42	—
21	„	298/149	1.737	43—50	—
22	„	083/259	1.719	41—45	—
23	Olivine	194/226	1.785	109	0.44
24	„	062/234	1.762	104	0.55
25	„	093/206	1.749	100	0.62
26	„	298/149	1.720	96	0.76
27	Augite	146/096	1.740	53	—
28	„	151/135	1.740	48—58	—
29	„	162/168	1.744	49—53	—
30	„	169/075	1.718	53	—
31	„	180/089	1.719	48	—
32	Olivine	151/135	—	c. 125	c. 0.0 ⁴⁾
33	„	162/168	1.852	129	0.1
34	Augite	035/258	1.730	54	—
35	„	080/146	—	c. 57	—
36	Diopside	290/200	1.714	55	0.7

¹⁾ $mg = \frac{Mg}{Mg+Fe^{2+}}$; Determined from refractive indices (Tröger 1959).

²⁾ In this table used as a collective name for the diopside-hedenbergite series.

³⁾ $n_{\alpha} = 1.668$.

⁴⁾ Determined from $2V$.

Table 5. Refractive indices, unit cell edges and chemical composition of garnets from the Los-Hamra region.

No.	Locality (see Plate 1)	n	a ₀ (Å)	Main component(s) of garnet (Sriramadas 1957)
1	276/371	1.812	11.51	almandite
2	c. 518/230 ¹⁾	1.865	11.96	andradite
3	c. 236/262 ¹⁾	1.856	11.97	„
4	275/370	1.815	11.51	almandite
5	465/246	1.800	11.48	„
6	262/365	1.808	11.89	andradite + grossularite
7	364/434	1.775	11.84	grossularite
8	279/269	1.813	11.50	almandite

¹⁾ Boulder from moraine.

Table 6. Optical data for phlogopites and one chlorite from the Los-Hamra region.

No.	Mineral	Locality (see Plate 1)	$\frac{n\gamma + n\beta}{2}$	2V _α	Birefringence
1	Chlorite	309/297	1.630	small	c. 0.004
2	Phlogopite	418/331	1.578	„	—
3	„	344/144	1.597	„	—
4	„	344/144	1.585	„	—
5	„	328/161	1.591	„	—
6	„	350/205	1.580	„	—

Table 7. Composition of perthitic alkali feldspars from the Los-Hamra region.

No.	Rock	Locality (see Plate 1)	Ab (mol.%)	Or (mol.%)	An (mol.%)	Fe ₂ O ₃ (wt.%)	SrO (wt.%)	BaO (wt.%)	Weight % Ab in solid solution with Or. ¹⁾	No. (Table 8)	No. (Table 1)
1	Primorogenic granite	300/246	13	86	1	0.2	0.01	0.3	0	6	32
2	Primorogenic light granodiorite	256/030	17	82	1	0.3	0.02	0.3	0	8	35
3	Pegmatite (migmatite terrain)	235/032	11	89	0	0.6	—	—	0	20	—
4	Do.	287/091	19	80	1	0.2	—	—	0	22	—
5	Rätan granite, phenocrysts	128/370	21	78	1	0.3	—	—	0	29	49
6	Do.	106/418	26	73	1	0.3	0.05	0.3	0	27	50
7	Do.	266/390	20	78	1	0.3	0.06	0.4	0	24	51
8	Pegmatite in Rätan granite	190/426	17	82	0	0.2	—	—	0	30	—
9	Dala porphyry, phenocrysts ²⁾	119/203	34	65	1	0.2	0.03	0.07	c. 0—2	36	70
10	„ „ „ „ ³⁾	158/036	33	65	2	0.5	0.03	0.4	c. 2—3	42	72
11	„ „ „ „ (pink) ³⁾	148/191	37	61	2	0.4	—	—	0	34	—
12	„ „ „ „ (red) ³⁾	150/190	29	70	1	0.7	0.03	0.3	c. 1—2	33 a	—
13	„ „ „ „ ³⁾	165/233	34	64	2	0.2	—	—	c. 3—4	40 a	74
14	„ „ „ ³⁾ , large phenocryst	165/233	35	64	1	0.1	—	—	c. 3	40 b	74
15	Dala granite, phenocrysts	052/150	33	65	2	0.6	0.03	0.5	1	59	82
16	Dala granite	214/074	37	62	1	0.4	—	—	0	50	85
17	Pegmatite in Dala granite	225/125	9	90	1	0.2	—	—	0	64	—
18	Do.	207/178	16	83	1	0.2	—	—	0	65	—
19	Dala granite ⁴⁾	128/031	26	74	—	—	—	—	—	57	75
20	Do. ⁴⁾	048/139	41	59	—	—	—	—	—	58	77
21	Do. ⁴⁾	194/224	47	53	—	—	—	—	—	53	79
22	Do. ⁴⁾	069/225	48	52	—	—	—	—	—	56	76

¹⁾ Determined according to Goldsmith and Laves (1961).

²⁾ Phenocrysts <1/3 of rock volume.

³⁾ Phenocrysts ≥1/3 of rock volume.

⁴⁾ These compositions have been calculated from whole rock chemical and modal analyses, assuming a content of 5 % K-feldspar and 5 % muscovite in the plagioclase.

Table 8. Optical and X-ray data for (perthitic) potash feldspars from different rock types in the Los-Hamra region.

No.	Rock type and locality (For localities, see Plate 1)	Optical data									Triclinicity Δ [$\Delta = 12.5 (d_{131} - d_{1\bar{3}1})$]	Note	No.
		$\alpha' \wedge (001)$ on (010)			$\alpha' \wedge (010)$ on (001)			$2V_{\alpha}$					
		Variation (degrees)	Average (de- grees)	N^{\parallel}	Variation (degrees)	Average (de- grees)	N^{\parallel}	Variation (degrees)	Average (de- grees)	N^{\parallel}			
1	Acid metavolcanics Ryggskog (350/309)	5.0—7.0	6.0	3	1—15	—	12	80—83	81	4	0.93	2) Phenocrysts " Matrix Ignimbrite "flames" Matrix Phenocrysts	1
2	Noppikoski (209/032)	5.0—6.0	5.5	6	3—16	—	9	c. 81—85	c. 83	2	c. 0.9		2
3 a	Risberget (357/211)	4.5—5.5	5.0	5	14.5—16.0	15.5	7	81—84	83	2	—		3 a
3 b	" "	—	—	—	—	—	—	—	—	—	1.0		3 b
4 a	Tallsjön (192/072)	5.5—6.0	6.0	2	0—9	—	10	c. 73—81	c. 76	5	0.9		4 a
4 b	" "	—	—	—	—	—	—	—	—	—	c. 0.9	4 b	
5	Mårdsjön (357/246)	4.5—5.5	5.0	5	c. 5—15	—	10	c. 80—84	c. 82	4	—	5	
6	Primorogenic intru- sions, even-grained Voxnahed (300/246)	4.0—5.5	4.5	5	15.0—17.5	16.5	5	81—86	83	3	0.89		6
7	Risberget (359/200)	4.5—5.0	5.0	5	15.5—16.5	16.0	5	78—82	80	3	0.95		7
8	Oreälven (256/030)	4.5—6.5	5.5	4	15.0—18.5	16.5	5	80—83	82	3	0.94		8
9	Ryttarklitten (420/117)	5.0—7.0	6.0	5	15.0—17.0	15.5	5	83—88	85	3	0.94		9
10	Primorogenic intru- sions, augen-bearing Dåasberget (411/320)	4.0—5.0	4.5	5	15.0—17.0	16.0	5	79—82	81	3	0.94	Augen " " " " " "	10
11	Gällsjön (516/186)	5.0—5.5	5.0	5	15.0—16.5	16.0	5	75—76	75	3	0.93		11
12	Nybyn (480/144)	4.5—5.0	4.5	5	14.5—17.5	16.5	5	84—88	86	3	0.95		12
13	Hornberget (461/177)	4.0—5.0	4.5	5	15.5—17.5	16.5	5	80—84	83	4	0.95		13
14	Kölberg (435/378)	5.0—6.5	5.5	5	15.5—17.0	16.5	6	81—84	83	2	0.93		14
15	Tackåsen (340/033)	4.5—6.5	5.0	5	15.5—17.0	16.5	5	80—82	81	3	0.95		15
16	Långberget (214/259)	4.0—5.0	4.5	10	14.5—17.5	16.5	10	80—81	81	2	0.90		16

17	Serorogenic augen- granite Rensjön (288/095)	4.0—5.5	4.5	5	15.5—17.0	16.0	5	79—86	83	3	0.92	Augen	17
18	Pegmatites of migma- tite terrains Storlugnet (279/269)	5.0—6.0	5.0	5	14.5—19.0	16.5	5	78—80	79	2	0.71		18
19	Ö. Råberget (250/063)	5.0—7.0	6.0	5	14.5—16.0	15.0	7	79—83	81	2	0.87		19
20	Oreälven (235/032)	3.5—6.0	5.0	5	15.5—16.5	16.0	5	83—84	84	2	0.96		20
21	Oreälven (256/030)	4.5—6.5	5.0	5	16.0—17.5	16.5	5	82—85	83	3	0.98		21
22	Rensjön (287/091)	5.0—6.5	5.5	5	15.0—17.5	16.0	5	80—81	80	3	0.84		22
23	Rätan granite Fågelsjö (363/095)	5.0—6.0	5.5	5	14.0—17.0	15.0	5	80—81	80	3	0.93	Phenocrysts	23
24	Kolarsjön (266/390)	4.5—6.0	5.5	5	14.0—17.0	15.5	5	81—82	81	3	0.88	”	24
25	Svartån (215/302)	3.5—5.5	4.5	5	15.5—18.0	16.5	5	81—84	82	3	0.90		25
26	Tjärnbäcksberget (211/235)	5.0—5.5	5.0	5	14.0—17.0	16.0	5	81—82	82	2	0.94	Phenocrysts	26
27	Acksjön (106/418)	4.5—7.0	5.5	5	14.5—16.0	15.5	5	81—86	84	3	0.92	”	27
28	Gräsberget (325/444)	3.5—6.0	4.0	5	15.0—17.0	16.5	5	82—88	84	4	0.93	Phenocrysts + matrix	28
29	Fågelsjö (128/370)	4.0—5.0	4.5	5	15.5—17.5	16.5	5	79—84	81	4	0.92	Phenocrysts	29
30	Pegmatite in Rätan granite Garpmyran (190/426)	5.0—6.5	5.5	5	15.5—18.0	16.5	5	79—83	81	3	0.96		30
31	Fine-grained (aplitic) granite in Rätan granite St. Sjöarberget (070/377)	3.5—5.5	5.0	5	14.5—17.0	15.5	5	82—85	83	3	0.90		31

Table 8 (continued)

No.	Rock type and locality (For localities, see Plate 1)	Optical data									Triclinicity Δ [$\Delta = 12.5 (d_{131} - d_{\bar{1}\bar{3}\bar{1}})$]	Note	No.
		$\alpha' \wedge (001)$ on (010)			$\alpha' \wedge (010)$ on (001)			$2V\alpha$					
		Variation (degrees)	Average (degrees)	N^1	Variation (degrees)	Average (degrees)	N^1	Variation (degrees)	Average (degrees)	N^1			
32	Granite porphyry in Rätan granite St. Acksjöberget (109/452)	4.5—6.0	5.0	5	15.0—16.0	15.5	5	82—86	84	3	0.91	Phenocrysts	32
33 a	Dala porphyries Sundsjön (150/190), red perthite	5.0—7.0	6.0	8	0.0—10.0	—	8	59—69	64	5	0.76	Phenocrysts	33 a
33 b	Sundsjön (150/190), red perthite	—	—	—	—	—	—	—	—	—	c. 0.7—0.8	Phenocrysts + matrix	33 b
34	Sundsjön (148/191), pink perthite	5.0—7.5	5.5	15	0.0—2.0	0.5	12	62—66	65	3	0.79	Phenocrysts	34
35	Pilkalampinoppi (155/138)	6.5—7.5	7.0	5	0.0—1.5	1.0	5	61—64	62	3	0.8	"	35
36	Flarksjön (119/203)	5.0—9.0	7.0	7	0.5—2.0	1.0	5	66—79	(72)	7	≤ 0.9 (strongly varying)	"	36
37	Vässinkoski (138/029)	6.5—9.0	7.5	5	0.0—2.0	1.0	8	64—69	67	3	c. 0.7—0.8	"	37
38	Oreälven (175/030)	7.0—9.0	8.5	5	0.0—1.0	1.0	6	66—71	69	5	0.81	"	38
39	Hornsjön (077/176)	6.5—8.0	7.5	5	0.0—1.0	0.5	5	69—77	73	5	$\leq c. 0.7$	"	39
40 a	Tandhem (165/233)	6.0—8.5	7.0	6	0.0—1.5	0.5	5	58—63	61	4	c. 0.1	"	40 a
40 b	" "	6.0—8.0	7.5	9	0.0—1.5	1.0	5	52—64	(58)	8	c. (0.4—)0.1	Big phenocryst	40 b
41	Knoppvägen (169/061)	6.0—8.0	7.0	6	0.0—5.0	2.0	10	58—65	61	3	c. 0.7	Phenocrysts	41
42	Älvho (158/036)	5.5—9.0	7.0	6	0.0—1.5	0.5	7	68—74	71	3	0.7	"	42
43 a	Finnberget (028/165)	5.5—7.0	6.5	5	1—12	—	10	75—79	77	3	0.84	"	43 a
43 b	" "	—	—	—	—	—	—	—	—	—	c. 0.8	Phenocrysts + matrix	43 b
44	Vassjöån (173/063)	6.0—7.0	6.5	5	0.0—1.0	0.5	5	52—54	53	3	c. 0.1—0.2	Phenocrysts	44
45	Lillhamra (166/206)	5.0—8.0	6.5	5	0.0—2.0	1.0	6	63—65	64	4	c. 0.6	"	45

46	Dala granite porphyry, dike Tallsjöbäcken (202/049)	6.5—8.0	7.0	7	c. 0.5— 2.5	c. 1.5	9	66—72	68	3	c. 0.77	Phenocrysts	46
47	Dala granites Sandsjön (211/120)	5.0—6.5	6.0	5	14.5—16.5	15.5	5	69—81	(77)	6	0.86	Phenocrysts	47
48	Sandsjö (207/195)	5.5—8.5	7.5	9	4.0—14.0	—	11	62—64	63	3	0.78		48
49	„ (210/178)	5.5—8.0	6.5	6	0.0— 1.0	0.5	5	54—70	(63)	3	0.7		49
50	V. Råberget (214/074)	5.0—6.5	6.0	5	2.5—17.5	—	17	60—86	(73)	6	0.86		50
51	Kalleåsen (216/197)	5.0—6.5	5.5	5	1.5—15.5	—	11	66—68	67	3	c. 0.77		51
52	Sandsjöån (212/134)	c. 6.0—9.0	c. 8.0	5	c. 1.0— 2.0	c. 1.5	6	c. 71—74	c. 73	3	0.86		52
53	Naappo (194/224)	8.0—9.0	8.5	6	0.0— 1.0	0.5	5	66—74	69	5	0.80		53
54	Sandsjön (198/155)	c. 6.0—8.5	c. 7.0	5	c. 0 — 3	c. 1.5	6	c. 66—72	c. 69	3	0.78		54
55	Jämtland County (see Table 1: no. 80)	5.5—7.0	6.5	5	0.0— 1.0	0.5	5	53	53	4	0.80		55
56	Gäddtjärn (069/225)	c. 8.0—10.0	c. 9.0	6	c. 0.0— 5.5	c. 2.0	8	c. 66—77	(c. 72)	5	0.88		56
57	Vässinkoski (128/031)	c. 8.5—9.5	c. 9.0	5	c. 0.0— 4.0	c. 1.5	7	c. 63—75	(c. 67)	4	0.88		57
58	Finnbergsbron (048/139)	6.0—7.5	7.0	5	2 —17	—	10	55—71	(64)	6	0.79		58
59	Rutimovuo (052/150)	6.5—7.5	7.0	5	0.0— 2.5	1.0	8	58—72	(65)	4	c. 0.7	Phenocrysts	59
60	Finnberget (025/142)	5.0—7.0	6.0	5	0.0— 0.5	0.0	6	51—69	(59)	5	c. 0.6—0.7	„	60
61	Palomäki (071/153)	6.0—8.0	7.0	7	0.5— 1.5	1.0	6	63—76	(69)	6	0.80	„	61
62	Pegmatites in Dala granite Sandsjön (211/120)	6.0—6.5	6.0	5	15.0—17.0	16.5	5	77—79	78	2	0.77		62
63	Sandsjöån (227/122)	5.5—6.5	6.0	5	0.5—17.5	—	12	76—78	77	3	0.75		63
64	Sandsjöån (225/125)	4.5—7.5	6.0	6	12.5—16.0	14.0	8	76—78	77	3	0.85		64
65	Sandsjö (207/178)	5.5—6.5	6.0	6	0.0— 3.0	1.0	5	c. 80—81	c. 81	2	0.8		65

Table 8 (continued)

No.	Rock type and locality (For localities, see Plate 1)	Optical data									Triclinicity Δ [$\Delta = 12.5 (d_{131} - d_{\bar{1}\bar{3}\bar{1}})$]	Note	No.
		$\alpha' \wedge (001)$ on (010)			$\alpha' \wedge (010)$ on (001)			$2V_{\alpha}$					
		Variation (degrees)	Average (degrees)	N ¹⁾	Variation (degrees)	Average (degrees)	N ¹⁾	Variation (degrees)	Average (degrees)	N ¹⁾			
66	Aplite in Dala granite Sandsjö (207/195)	6.0—7.0	6.5	6	1.0—9.0	—	7	65—72	69	3	0.81		66
67	Dala granite, pebble in Jotnian conglomerate St. Gönsjön (039/250) ³⁾	c. 5.0—6.5	c. 5.5	8	c. 0.0—6.0	c. 1.5	7	c. 57—66	c. 63	3	0.75		67
68	Dala granite, fragment in breccia horizon in Dala porphyrite Korsiberget (175/174)	c. 6.0—8.5	c. 7.5	5	c. 0.0—1.5	c. 0.5	5	c. 44—59	(c. 53)	4	c. 0.6—0.7		68
69	Approx. granitic differentiates in dolerite Siikamäki (146/096)	c. 9.0—10.0	c. 9.5	6	c. 0.0—2.5	c. 1.5	5	54—58	56	2	c. 0.7—0.8		69
70	Pikkalampinoppi (151/135)	8.5—10.5	9.5	5	0.0—1.0	0.5	5	61—65	63	3	0.8		70
71	Aplitic dike in dolerite St. Gönsjön (035/258)	—	—	—	—	—	—	67—68	68	2	0.86		71

1) N = number of determinations.

2) Optical measurements on phenocrysts, triclinicity determined for phenocrysts and matrix.

3) From moraine boulder of Jotnian conglomerate.

INDEX

- Abukuma-type facies series 157
 Accessories 13
 Accuracy of measurement 12, 13, 146, 147, 223
 Acid metavolcanics 44, 47-51, 54, 145, 151, 160, 226
 Acid primorogenic intrusions 60-64
 Ackelamsberget 134
 Acksjöberget, St. 75
 Acksjön (Fågelsjö) 158
 Acksjön (Nybyn) 14
 Actinolite 38, 230
 Adularia 156
 Aeromagnetic maps 137
 Age determination 71, 161
 Age determination (potassium-argon method) 143, 157-159, 161, 164
 Age determination (rubidium-strontium method) 159, 161, 164, 165
 Age determination (uranium-lead method) 132, 133, 157-159, 161, 164, 165
 Agglomerate 53, 77, 78, 89, 92-94
 Ahkiolampi 26
 Albite (in perthite) 145-156
 Albite rims 60, 64, 73
 Alkali amphibole 40
 Alkali feldspar 145-156, 233-238
 Alkaline dolerite 91
 Almandite 24, 28, 32, 33, 46, 64, 68, 232
 Almesåkra 121
 Almesåkra formation 164, 165
 Alpine orogeny 160
 Älvdalen 79, 95
 Älvho 86, 95, 97, 102, 111, 140, 143
 Amphibolite 38, 51-58, 132, 133, 144, 158, 179, 180, 194, 195, 209, 210, 226
 Amphibolite facies 31, 157, 163
 Amphodelite 38
 Amygdaloidal texture 52, 53, 56, 89, 93, 132
 Amygdule 52, 53, 56, 89
 Anatectic magma 159, 160
 Anatexis 159
 Andalusite 16-19, 23, 36, 51, 115, 118, 138, 143, 163
 Andesite 57
 Andradite 25, 26, 56, 232
 Ängratörn 141
 Anorthite 38, 46
 Anorthoclase 156
 Anthophyllite 18, 23, 27, 28, 31-33, 40, 51, 57, 134, 230
 Anthophyllite-cordierite gneiss 18, 33, 51
 Anthophyllite gneiss 32, 33, 177, 192, 207
 Anticline 136

- Anti-rapakivi texture 73, 116
Apatite 38, 67, 68, 109
Aplite 66-68, 70, 74-76, 117, 118, 157, 184, 199, 214
Aplite granite 66-68
Archean complex 8
Argillite gneiss 21, 23, 24, 31-33, 66-68, 176, 177, 191, 192, 206, 207
Argillitic gneiss, see argillite gneiss
Argon loss 158, 164
Arkose 36, 44, 77, 88, 122, 123, 157
Arsenic 132
Arsenopyrite 131, 132
Åsby dolerite 121, 123, 124, 164
Ash flow tuff 103
Assimilation 49, 63-65, 67, 100, 115, 118, 130
Atlantic suite type 57
Augen 32, 58, 60, 61, 64, 66, 69-73, 75, 158
Augen-granite 61, 71, 160
Augite 73, 90, 91, 100, 124, 129, 231
Aureole, see contact aureole
Authigenic minerals 164
Axial angle (potash feldspar) 146, 148, 149, 152, 154-156
Axinite 45
Axiolitic texture 48, 103
- Banding 30, 39, 42-45, 58, 78, 106-108, 131, 140
Barium 21, 30, 50, 51, 63, 75, 76, 92, 110, 147, 148
Baryte 132
Basal breccia 78, 84-88, 121, 139
Basal conglomerate 78, 84, 86, 88, 121, 139
Basal layers of the Dala volcanics 77, 79-88, 139, 163
Basalt 57, 165
Basement 88
Basic intrusions 52
Basic metatuff 38, 54, 131
Basic metatuffite 52, 58
Basic metavolcanics, see amphibolite
Basiska urgraniter 59
Bedding 15, 25, 28, 32, 34, 39, 41, 45, 52, 58, 78-80, 112, 113, 134, 135, 137, 139, 140, 144
Bergslagen 9, 26, 29
Biotite 17, 138
Biotite isograd 15, 157
Biotite-schist 133
Bismuth 132
Bismuthinite 132
Björkberg 8, 43-45
Björna 158
Blastopelitic texture 15, 22
Blastosammittic texture 35
Blue quartz 51

- Blyberg porphyry 95
Bohus granite 143
Börningsberget 89, 91, 134
Boron 20, 21, 23
Brännberget 23, 47
Breccia 21, 22, 34, 44, 49, 53-55, 68-70, 77-79, 83-88, 91-94, 106, 108, 109,
111-114, 121, 131, 134, 139, 141, 142
Brecciation, see breccia
Bredvad porphyry 79, 95, 98
Bygget 39, 47, 52, 56, 69
Bytownite 46, 133
- Calcareous sandstone 37
Calcite 37-39, 44, 55, 56, 91, 117, 131, 132, 134
Calcium in alkali feldspar 147
Caledonides 137, 143
Canyon 140
Carbonate 37-39, 44
Cataclasis 71, 74, 117, 119, 140-142
Cavity filling 105
Chalcedony 79, 82-84, 88, 122
Chalcocite 91, 132, 134
Chalcopyrite 73, 131-134
Chemical analysis 13, 21-25, 30, 31, 33, 38, 40, 46, 50, 57, 63, 65, 76, 83, 91, 92,
106, 108-111, 120, 129, 130, 147, 156, 175-204, 226, 227, 233
Chemical analysis (sampling localities) 224, 225
Chert 41
Chloanthite 132
Chlorite 15-17, 43, 44, 57, 58, 138, 232
Chlorite-schist 133
Chondrodite 38, 43
Chromium 57
Clinopyroxene 55, 73, 75, 90, 91, 100, 117, 124, 129, 231
Cobalt 8, 11, 130-133, 142
Cobalt deposit 8
Cobalt mineralization 133, 142
Cobalt mines 8, 11, 130, 132, 142
Cobalt ore 132
Cobaltite 132
Collapsed pumice 48, 103
Common hornblende 29, 30, 40, 45, 46, 55-57, 61, 133, 230
Common hornblende, alteration of 57
Composite dike 91
Conglomerate 11, 24, 34, 45, 54, 77-79, 84, 86, 88, 89, 92-94, 114, 121, 122,
124, 139, 162
Contact aureole 16, 22, 69, 74
Contact metamorphism 16, 22, 23, 58, 124
Contact metasomatism 45
Contamination 50, 130
Coordinate system 13

- Copper 51, 131–134, 142
Copper mineralization 134, 142
Copper mines 51, 130, 131, 134
Cordierite 16–19, 22–24, 28, 30–33, 36, 51, 67, 68, 134, 138, 163
Cordierite-andalusite quartzite 36
Cordierite-anthophyllite gneiss 18, 33, 51
Cordierite-sillimanite quartzite 36
Corrosion 58, 73, 82, 98–100, 115–117, 128
Corrosion embayment 49, 61, 99, 116, 118
Corundum 101
Cretaceous 159
Cross-bedding 79, 122, 135, 136
Cross-hatching 36, 145
Cryptoperthite 149–151
Crystalline limestone 8, 9, 37–39
Crystalline schist 38
Crystallization differentiation 63, 65, 92, 111, 165
Cummingtonite 22, 27–30, 37, 57, 230
Cycle 160, 161
- Dåasberget 18, 24–26, 38, 41–45, 61, 136
Dåasen 14, 24, 31, 36, 136, 137
Dåasen granite 9
Dal formation 143, 164
Dala granite 70, 76, 77, 93, 94, 98, 108–111, 114–120, 133, 141, 142, 156, 160, 187–189, 202–204, 217–219, 227
Dala granite, fragments of 93, 98, 114
Dala granite, pebbles of 94, 114
Dala-Härdal granite 77
Dala porphyrite 76–79, 84, 88–92, 108–110, 121, 134, 139, 160, 184, 185, 199, 200, 214, 215, 227
Dala porphyry 76–79, 93–111, 139, 140, 160, 185–187, 200–202, 215–217, 227
Dala porphyry, phenocryst-poor 95, 96, 185, 186, 200, 201, 215, 216
Dala porphyry, phenocryst-rich 95, 96, 186, 187, 201, 202, 216, 217
Dala sandstone 76–78, 121–123
Dala Sandstone Formation 14, 121–123, 156
Dala Series 10
Dala volcanics 8, 76, 78, 144
Dala Volcanics Formation 14, 77–114, 156, 162
Dalarna 121, 164
Dalecarlia 121, 164
Decussate texture 16, 19, 25, 28, 55
Degree of metamorphism 157
Denudation 11, 163
Denudation surface 11
Diabantite 15
Differentiate 74–76, 128–130, 227
Differentiation 58, 59, 70, 89, 91, 92, 95, 108, 109, 120, 129, 130, 148
Diffraction curves 153
Digerberg sandstone 77, 89

- Digerberg sediments 11
 Dike 66, 67, 69, 75, 91, 118, 119, 121, 123–126, 129, 140, 141, 143, 162
 Diopside 25, 29–31, 38, 43, 45, 46, 56, 133, 231
 Diopside-hedenbergite series 25
 Diorite (sub-Jotnian) 91
 Dip slope 144
 Discordant bedding 34
 Dolerite 91, 121, 123–130, 139, 141, 143, 156, 164, 165, 189, 204, 219, 227
 Dolomite 37–39, 43, 44
- Elfdalgesteine 8
 Epidote 36, 45, 56, 91, 134
 Epidote quartzite 36
 Epidotization 124
 Essential minerals 13
 Eulysite 38, 46, 47
 Eulysitic iron ores 47
 Eutaxitic structure 79, 84, 93–95, 102, 103, 105, 106
 Excavation 18, 22, 26, 43
 Exsolution 146, 147, 155
 Extinction angle 146, 149–152
- Facing of beds 80, 135, 136
 Fahlerz 132
 Fault, see faulting
 Faulting 25, 52, 77, 78, 131, 134, 135, 138, 140, 141, 143, 158, 159, 163, 165
 Faxen 33
 Fayalite 46, 47, 129
 Feldspar-quartzite 157
 Ferrohortonolite 129
 Ferrohypersthene 57, 58, 231
 Fetingsberg 31, 61, 137
 Fetingsklacken 32, 33
 Filipstad granite 23
 Film perthite 19, 22, 31, 72, 146
 Flames 48, 49, 78, 79, 86, 95, 97, 101–104, 106, 139, 140
 Flarksjön 96, 101, 106–109, 112
 Flattening 103, 105
 Fluoborite 45
 Fluorite 67, 79, 118, 133
 Foam lava 106
 Fold, see folding
 Fold axis 136–138, 141
 Fold hinge 135, 137
 Folding 10, 17, 42, 106, 107, 131, 134, 136–139, 156, 157
 Forsterite 43
 Fresh-water argillite 20, 21
- Gabbro (sub-Jotnian) 91
 Gäddtjärn 128

- Galena 131, 132
 Garberg granite 115
 Garnet 13, 25, 26, 28, 29, 31, 45, 46, 56, 67, 68, 118, 133, 232
 Garnet skarn 38
 Garpmyran 75
 Gävle 121
 Gävleborg County, mapping of 11
 Geosyncline 138, 139, 157, 159
 Geosyncline of central Norrland 157
 Gersdorffite 132
 Glass-shard texture 48, 92, 93, 101, 103, 111–113
 Glassy texture 101
 Glomeroporphyritic texture 99
 Gneiss 30–33
 Gold 131
 Gothian cycle 160, 161
 Gothian era 161
 Gothian orogeny 160–162
 Graben 139, 159, 165
 Graded bedding 112
 Granåsen 114
 Granite facies 158, 159
 Granite (in dolerite) 128–130, 189, 204, 219, 227
 Granite porphyry 74, 75, 91, 184, 199, 214, 227
 Granitic composition 59–61, 63, 74, 120
 Granitization 159
 Granoblastic texture 20, 22, 48
 Granodiorite 59, 61, 63–65, 71, 74, 180–182, 195–197, 210–212
 Granophyre 59, 61, 62, 72, 75, 98, 102, 103, 105, 114, 115, 117–119, 128, 129
 Granophyric texture, see granophyre
 Graphic texture 36, 73
 Graphite 21, 22, 32, 36, 37, 133
 Graphite phyllite 21, 22, 133
 Gråtbäck 140, 163
 Great Basin District 159
 Greenalite 30, 40, 47
 Greenschist facies 157
 Greywacke, see metagreywacke
 Grossularite 38, 56, 232
 Grottan 140
 Grunerite 27, 28, 39–41, 46, 230
 Gryssjön, Ned. 114, 119, 123, 141, 145
 Grythytte syncline 157
- Hälleflinta 8, 26, 27
 Hammarkesen 36
 Hamra 8, 14, 65, 133, 142
 Hamrånge 135
 Hamravallen, Öv. 25, 26, 45, 46, 61, 141
 Härjedalen 121

- Härnö formation 138, 157
 Härnö granite 68, 158
 Hästberget 16, 20, 30
 Heavy mineral layers 35
 Hedbäcken 31
 Hematite 25, 29, 44, 46, 79, 117, 132, 134, 141
 Hematite pigmentation 147–149
 Hiatus 76, 163
 Hogland 88
 Hoglandian 10
 Högsvedberget 137
 Hornberget 64, 65
 Hornblende-hornfels facies 16, 74
 Hornfels 21–24, 30, 74, 146, 176, 191, 206
 Horst 139, 140, 143
 Humite minerals 43, 45
 Hydrothermal activity 77, 124
 Hydrothermal deposition 87
 Hydrothermal leaching 88
- Ice movement, direction of 24, 143
 Ignimbrite 48, 49, 78, 79, 86, 95, 97, 99, 101–106, 111, 112, 159, 160
 Ilmenite 127, 128, 131
 Imbrication 139
 Inclusion, see xenolith
 Indonesia 160
 Intermediära urgraniter 59
 Intermediate primorogenic intrusions 59, 64–66
 Intraformational conglomerate 11
 Inverse zoning 55
 Iron anthophyllite 46
 Iron-formation 40
 Iron mine 46
 Iron ore 11, 39–47, 141
 Isoclinal folding 136
- Jämtland County 123
 Järna granite 159, 163
 Järpberget 53
 Jasper 41, 82, 86, 94, 122
 Jaspilite 34, 37, 41, 45
 Johannisberg 23
 Jointing 73, 124
 Jotnian 10, 11, 76, 77, 120, 121
 Jotnian complex 120–130, 156, 163–165
- Kårböle 72, 158
 Karlsbad twinning 72
 Karlsberg 30
 Karlshamn granite 161

- Keratophyre 20, 27
 Kivanhoberget 43
 Kolarsjöbäcken 18
 Kolarsjön 16, 24, 27–30, 40, 52, 56, 69, 72
 Kopparberg County 77–79, 89, 91, 94, 113, 121, 123, 129, 130, 134, 143, 161, 163
 Korpmäki 140, 163
 Korrissjön 105
 Korsiberget 93, 144
 Kroksjön 129
 Krokvattnet 16, 52
 Kuttermäki 61
 Kvarnån 141
 Kvarnberg 18, 33, 36, 51, 61, 135
- Lake Superior iron ores 40, 41
 Lakisberget 18, 46, 51
 Lakisberget mine 18
 Långberget 61, 71, 73, 141
 Lången, Öv. 64
 Late-kinematic 66
 Late-orogenic 66
 Lava 53, 88, 89
 Laxtjärn 16, 61, 62, 67, 138
 Lead 131, 143
 Lead isotopes 159
 Lead mineralization 143
 Leksand 162
 Lepidoblastic texture 15, 17, 19, 22, 26, 31, 138
 Leptite 9, 26
 Leptite formation 27
 Lillhamra 141, 145
 Lillskog 24–26, 34, 36, 45, 47, 52, 58, 135–137, 141
 Limestone 8, 9, 37–39
 Lineation 64, 136–138, 141
 Lithic sandstone 88, 122, 123
 Ljusdal granite 72
 Loån 142
 Loftahammar granite 162
 Los 8, 11, 33, 47, 51, 53, 56, 130, 132, 135, 137, 142, 157
 Los Formation 13, 156, 157
 Lossjön 47, 61, 136, 138, 142
 Lower Dala series 77, 88, 161–163
 Lower Loos Series 9, 142
 Ludwigite 45
- Magma temperature (Råtan granite) 74
 Magnetic maps 12, 135, 137
 Magnetite 8, 18, 28, 29, 32, 33, 39–46, 51, 54, 55, 57, 127, 131, 133
 Magnetite deposit 8, 11, 39–46
 Magnetite quartzite 28, 29

- Main minerals 13
Malachite 91, 134
Malånäs 156
Mälaren 121
Malmbäck conglomerate 162
Malungshed 58
Manganese 40, 46, 47
Mansjö granite 9
Mansjöberget 8, 37, 38, 46, 47, 137
Mantle, see mantling
Mantling 58, 64, 72, 73, 99, 115, 116, 128
Marcasite 131-133
Marginal facies 60-62, 69, 70, 117, 138
Marine argillite 20, 21
Marl 27
Masugnsbyn 40, 47
Mechanism of ignimbrite eruptions 105
Mediterranean suite type 89, 108
Meta-arenite 33-37
Meta-argillite 14-33, 74, 162, 163
Meta-arkose, see arkose
Metagreywacke 14, 27, 138, 157
Metamorphic differentiation 27
Metamorphic grade 157
Metarhyolite 21, 44, 47-51, 54, 82, 84, 86, 134, 136, 163, 177-179, 192-194, 207-209, 226
Metasiltstone 19-21, 24, 27, 32, 175, 190, 205
Metasomatism 18, 27, 33, 44-46, 51, 65, 69, 71, 158
Metaspilite 39, 52, 55-57, 226
Metatect 32
Miarolitic cavities 117
Mica-schist 15-19, 21, 23, 30, 44, 51, 61, 134, 138, 140-143, 175, 176, 179, 190, 191, 194, 205, 206, 209
Mica-schist, tectonic 21, 51, 61, 134, 179, 194, 209
Microbrecciation 106
Microcline 145-156
Microcline augen, see augen
Micropoikilitic texture 48, 49, 90, 101, 119
Microscopic determination 12, 146
Migmatite 32, 38, 60, 61, 64-66, 138, 157, 162
Migmatization, see migmatite
Mining pit 44, 51, 132, 133
Miogeosynclinal 157
Mixing of magmas 92
Modal analysis 32, 205-219
Modal estimate 13
Molybdenite 75
Monzonite 128-130
Mora 113

- Moraine boulders, observations of 12, 24, 26, 38, 53, 54, 56, 65, 69–71, 81, 91, 93, 94, 102, 106–109, 112, 113, 117, 121
- Morphology 143–145
- Mortar structure 71, 141, 142
- Mud-cracks 80, 81, 122
- Muhos 121
- Murchisonite cleavage 145
- Muscovite 67, 69, 83
- Mylonitization 140, 141
- Myrmekite 60, 64, 73, 117
- Naappo 127
- Naggen quartzite 161
- Native bismuth 132
- Nätsjö copper mines 130, 131
- Nätsjön 73
- Needle quartz 102
- Nematoblastic texture 25, 26, 28, 55
- Niccolite 132
- Nickel 8, 131–133
- Nickeliferous pyrrhotite 8
- Nickelglance 132
- Non-clastic quartzite 36, 37
- Noppikoski 8, 15, 30, 33–36, 47, 48, 61, 77, 82, 86, 135, 136, 138, 139, 143, 155, 157, 158, 163
- Noppi Series 9, 10
- Nordingrå 76, 121, 129, 144, 164
- Normal zoning 55, 65, 73, 90, 99, 124, 129
- Norrbotten 47
- Nöungen 65
- Nybyn 64
- Öje dolerite 121, 143, 164
- Öjungen, L. 140, 141
- Old Archaean 9
- Olivine 41, 43, 90, 127, 129, 231
- Olofstorp 38, 39
- Opal 88, 122
- Ophitic texture 124, 127
- Optical data 230–232
- Order-disorder 149
- Oreälven 37, 62, 79, 91, 95, 125, 126, 140, 143, 158
- Ornamental stone 95
- Örnberget (Korsilampi) 95, 144
- Örnberget (Los) 54
- Orogenic complex 13, 134, 156
- Orrok porphyry 95
- Orsa Finnmark 7, 8
- Orthoclase 145–156
- Orthopyroxene 46, 57, 74, 231

- Orthopyroxene subfacies 58
 Össjön 23, 67, 69
 Östergården 57
 Overflowing glowing clouds 103
 Overthrust 143
- Pacific suite type 50, 57, 89, 108
 Pajala 40, 47
 Pajaso 43
 Pajkölen 23, 56, 67, 69, 138
 Paragneiss 32
 Pectinate texture 48, 103
 Pegmatite 38, 66–68, 70, 75, 117, 118, 133, 138, 142, 157, 158, 163
 Peneplain 142, 159
 Peridotite 38, 47
 Persberg 23
 Perthite 19, 22, 31, 72, 111, 145–156, 233–238
 Petrochemical calculations 13
 Phanerozoic ignimbrites 48, 103, 105, 159
 Phenoclast 19, 20, 92
 Phlogopite 38, 41–44, 232
 Phyllite 15, 16, 21, 22, 30, 58, 133, 144, 155, 157, 158, 175, 190, 205
 Piedmontite 36
 Pilkalampinoppi 111, 145
 Pisolith 112, 113
 Pitchblende 132
 Pleistocene 159
 Pliocene 159
 Poikilitic texture 15, 17, 19, 23, 44, 48, 51, 55, 57, 58, 64, 70, 75, 98, 117, 119
 Porphyritic texture 47, 49, 52, 59, 61, 62, 64, 70, 78, 89–91, 94, 96–98, 100, 101, 114–119, 129
 Porphyroblast 15–19, 23, 32, 57, 61, 64, 66, 69, 72, 75, 98
 Position, indication of 13
 Post-magmatic activity 77, 148, 155
 Post-orogenic complex 14, 134, 156
 Potash feldspar 145–156, 233–238
 Potash feldspar-cordierite hornfels facies 23, 58, 74, 157
 Precipitate of silica 28, 34, 36
 Pressure solution 122, 123
 Primorogenic granite 16, 17, 44, 47, 59–63, 67, 71, 163, 180, 181, 195, 196, 210, 211, 226
 Primorogenic granodiorite 59, 61, 64, 65, 71, 180–182, 195–197, 210–212, 226
 Primorogenic intrusions 52, 58–65, 138, 156, 157, 160, 226
 Prospecting 11, 130
 Protoclastic deformation 117
 Pseudo-fluidal structure 48, 140, 144
 Pseudo-fluidal texture 48, 100–102, 104–106, 111
 Pumice 48, 103, 112
 Pyrite 75, 91, 124, 131–133
 Pyroclastic texture 77, 82, 83, 106, 113

- Pyroxene gneiss 38, 46
Pyrrhotite 8, 21, 22, 28, 75, 131-134
- Quarry 15, 38
Quartz 15, 29, 51, 106, 117, 131-134, 141
Quartz diorite 59, 65
Quartz dolerite 91, 143
Quartz latite 89
Quartz porphyry 47-51, 88
Quartz syenite 120
Quartzite 24, 28, 29, 33-37, 44, 77, 79, 84, 134, 142, 144, 160-163
Quartzite breccia 68, 83, 84
Quartzite conglomerate 34, 86, 88
Quartzite sandstone 33-37
- Råberget, Ö. 34, 163
Råberget, V. 118
Ragunda 76, 144
Räkaklitt 141
Rämsberg 161
Randomly disordered structures 155
Rännås porphyry 95
Rapakivi granite 76, 120, 145, 159
Rapakivi texture 72, 99, 116
Rapakivi weathering 73
Råtan granite 8, 10, 14, 16, 18, 22, 28, 56-58, 61, 64, 66, 67, 69-76, 114, 136-142, 148, 156, 158, 159, 163, 183, 198, 213, 226
Reduction patches 122
Refractive indices 12, 230-232
Regeneration 72
Relief 144
Rensjön 67, 68
Replacement 88, 120
Retrograde alteration 24, 58
Revsund granite 139, 158, 163
Rheoignimbrite 106, 111
Rhyolite 89, 92, 95. See also metarhyolite
Ripple-marks 15, 80, 81, 122
Risåsen 21, 22, 27-30, 34, 37-41, 47, 133
Risberget 30, 36, 44, 45, 49, 61, 135
Risberg granite 9
Rock crystal 79
Rödön 76
Romberg 15, 52, 136
Rubidium 21, 50, 51, 75, 76, 92, 110
Rullbo 8, 15, 22, 47, 69, 70, 133, 142
Russia 159
Rutimovuo 116
Ryggskog 15, 34, 35, 49, 136, 157
Ryttarklitten 60

- Sandsjö 69, 73, 115, 119, 141
Sandsjöån 47, 51, 57, 114, 141, 145
Sandsjöberget 79, 83, 84
Sandstone 77, 79, 80, 82, 84, 88, 121–123, 165
Särna dolerite 121
Satakunta 121
Sättnässjön 71
Scapolite 38
Scarp 144
Schist 77
Schistosity 60, 64, 71, 134, 135, 137–139, 141, 157, 163
Scoriaceous structure 52, 55, 56
Sedimentary iron ore 40, 41, 45, 47
Selingen 47, 51, 57, 135, 140, 141
Separation 147
Sericitization 84, 86, 87
Serorogenic alteration 60, 63, 66, 156
Serorogenic aplite granite 66–68
Serorogenic granite 65, 66, 68–70, 138, 157, 158
Serorogenic intrusions 66–69, 156, 160
Serpentine 41, 44, 127
Shale 121
Shear zone 57, 131, 134, 137
Shearing 24, 119, 139, 142
Siderite 30, 40
Silica 34, 36, 47, 87, 88
Silicification 50, 77, 79, 84, 86–88
Sill 165
Sillakorvamäki, St. 104
Silleråsen 30
Sillimanite 18, 23, 31, 36, 61, 137
Sillimanite gneiss 31, 146, 177, 192, 207
Sillimanite quartzite 36
Siltstone 77, 79, 83, 86, 88, 121
Siltstone gneiss 32
Silver 131
Silverknoppen 78, 106
Sjöändan 69
Skarn 9, 24, 25, 28, 29, 38–47, 55, 56, 133
Skarn minerals, see skarn
Skarn schlieren 23–25, 27, 30, 31, 56
Skarn-bearing conglomerate 34
Skarn-bearing meta-argillite 21, 24–31, 33, 176, 177, 191, 192, 206, 207
Skarn-bearing quartzite 34, 36
Skellefte granite 68
Skrälldalen 141
Slate 15, 21, 144, 157, 175, 190, 205
Slaty cleavage 15
Småland granite 161, 162
Småland porphyry 160, 161

- Småland-Värmland granites 160, 162, 163
Smaltite 132
Södermanland County 129
Sörberget 47, 48
Spessartite 46
Sphalerite 131, 132
Sphene 8, 73, 123
Sphene granite 8
Spherulite 82, 101, 103, 104
Spilite, see metaspilite
Spinel 38
Spotty schist 17
Ställsten 134
Ställstensberget 51, 134
Statistical analysis 120
Stensjön, N. 66, 69, 70
Stockholm granite 68
Storfaxberget 58
Storhamrasjön 67
Storkullen 22
Storkvarnberget 52
Storlugnet 15, 36, 59, 64, 66, 68
Stratigraphy 78, 79, 134-143, 157
String perthite 31, 146
Strontium 30, 75, 76, 92, 109, 110, 147, 148
Structure 10, 134-143
Sub-doleritic texture 124
Subgreywacke 157
Sub-Jotnian 10, 11, 76, 77, 120, 121
Sub-Jotnian complex 76-120, 156, 163-165
Sub-Jotnian igneous activity 159, 160
Sub-Loos Series 9, 142
Submicroscopic twinning 149, 152
Sub-ophitic texture 124
Subordinate minerals 13
Subvolcanic intrusions 52
Suite index 13, 228, 229
Suite type 13, 50, 89, 108, 228, 229
Sulphide deposit 8, 11, 130-134
Sulphide impregnation 57, 91
Sulphur 132
Sundsjön 79, 96, 98, 118
Sura urgraniter 59, 60
Suursaari 88
Svartälven 121
Svartån 16, 70, 74, 133
Svartåvallen 69, 73
Svecofennian era 161
Svecofennian orogeny 158-160
Svecofennian period 161

- Svecofennides 157
 Sveconorwegian regeneration 161
 Svensbo 32
 Synclinal hinge 137, 141
 Syncline 38, 47, 52, 135, 137, 157
 Synkinematic 58
- Tackåsen 60
 Tallberget, St. 54
 Tallsjöbäcken 34, 114, 119
 Tallsjön 15, 30, 49, 79–82, 84–87, 91, 124, 139
 Talus breccia 9, 88, 142
 Tandhem 105, 118, 119
 Tandsjöborg 15
 Tandsjöhallan 58, 69
 Tandsjön 69, 73, 79, 139, 141, 145
 Tectonic breccia 141, 142
 Tectonic line 140–143
 Tectonic model 138
 Tectonic movement 71
 Tectonic zone 10, 51, 57, 61, 74, 122, 138, 140–143, 145
 Tectonics 10, 134–143
 Tenskog 16, 18, 33, 36, 47, 51, 52, 57, 68, 134, 135, 137, 142
 Tertiary 143, 159
 Tilting 77, 134, 139, 163
 Titanomagnetite 127, 128
 Tjädermyråsen 83
 Toreskär 114, 117
 Tourmaline 15, 17, 19, 21–24, 31, 35, 57, 67, 68
 Trace elements 20, 21, 30, 33, 50, 57, 63, 65, 76, 92, 108–110, 130
 Trachybasalt 89, 92
 Trachyte 95
 Trachytic texture 90
 Trehörningsjö 158
 Tremolite 26, 36, 37, 41–45, 230
 Triclinicity 146, 152–156
 Triclinization 145, 155
 Tridymite, pseudomorphs after 102
 Tuff 77, 79, 83, 88, 89, 92–94, 111–113
 Tuff breccia 88
 Tuff texture 26, 83
 Tuffite 77, 78, 83, 89, 92–94, 111–113
 Tufflava 106, 111
 Tunnel 124–126, 140
 Tuscany 159, 160
 Twinning (albite) 117, 146
 Twinning (chondrodite) 43
 Twinning (grunerite) 40
 Twinning (potash feldspar) 72, 122, 145, 149, 151, 152, 155, 156

- Unconformity 8-11, 78, 86, 139, 162, 163
Uplift 95, 143
Upper Archaean 9
Upper Dala series 77, 162
Upper Loos Series 9
Uraninite 132
Uranium 132
Urgraniter 59
Utö 27, 156
- Vallåsen 30
Vallknopparna 95
Vanadium 20, 21
Vänge granite 60
Vapour-phase minerals 105
Värmland granites 162
Vassjöån 83, 100, 111
Vassjön, St. 92-95
Västerbotten County 158
Västerhocklan 10, 15-17, 19
Västernorrland County 158
Västernsjön 65, 137
Västervik 161, 162
Vein perthite 72, 145
Vein quartz 29, 84, 131, 134
Veined gneiss 32
Vesuvianite 38, 56
Vetlanda 161, 162
Viborg rapakivi 88
Viscous flow (in Dala porphyry) 106
Vitreous texture 95, 96
Volcanic breccia 49, 53-55, 89, 91-94, 111, 134
Volumetric analyses 12
Voxnan 7, 15, 142
- Way-up structure 34, 135
Weathering 36, 86-88, 122, 163
Welded tuff 103, 105
Welding 105
Whetstone 15
Wollastonite 38
- Xenolith 58, 59, 65, 69, 70, 97, 98, 111, 114, 115
- Yellowstone Park 159
- Zinc 131
Zircon 109
Zirconium 76, 109, 110

- Zoning (amygdules) 53
- Zoning (augite) 90, 124, 129
- Zoning (breccia fragments) 86–88
- Zoning (ignimbrite flames) 103
- Zoning (microcline) 72, 145
- Zoning (pisoliths) 112, 113
- Zoning (plagioclase) 55, 60, 65, 73, 90, 99, 115, 124, 129
- Zoning (skarn) 29

PRIS 25 KRONOR

Distribution
SVENSKA REPRODUKTIONS AB
FACK VÄLLINGBY 1

Växjö 1968 C. Davidsons Boktr. AB

Printed in Sweden